50
copies

NATIONAL AERONAUTICS AND SPACE ADMINISTRATION

Technical Report 32-1086

Surveyor II Mission Report

Mission Description and Performance

JET PROPULSION LABORATORY
CALIFORNIA INSTITUTE OF TECHNOLOGY
PASADENA, CALIFORNIA

April 1, 1967

NATIONAL AERONAUTICS AND SPACE ADMINISTRATION

Technical Report 32-1086

Surveyor II Mission Report

Mission Description and Performance

Approved by:

Howard H. Haglund
Surveyor *Project Manager*

JET PROPULSION LABORATORY
CALIFORNIA INSTITUTE OF TECHNOLOGY
PASADENA, CALIFORNIA

April 1, 1967

TECHNICAL REPORT 32-1086

Prepared Under Contract No. NAS 7-100
National Aeronautics & Space Administration

Preface

This document constitutes the Project Mission Report on *Surveyor II*, the second in a series of unmanned missions designed to soft-land on the lunar surface. The report consists of a technical description and an evaluation of engineering results of the systems utilized in the *Surveyor II* mission. Contributions from the major systems which support the Project were used in preparation of the report.

The report for this mission consists of a single volume only. Premature termination of the *Surveyor II* mission precluded the obtaining of scientific data and results which would normally be presented as separate parts of each Mission Report.

Contents

Contents (contd)

Tables

Contents (contd)

Tables (contd)

Figures

Contents (contd)

Figures (contd)

Contents (contd)

Figures (contd)

Contents (contd)

Figures (contd)

Abstract

Surveyor II, the second of a series of unmanned missions designed to soft-land on the moon, was launched from Cape Kennedy, Florida, on September 20, 1966. After a nominal launch phase and accurate injection into lunar transfer trajectory, a normal transit phase was achieved until execution of midcourse velocity correction, when one of the three vernier engines failed to fire, causing unbalanced thrust. A spacecraft tumbling condition resulted which could not be corrected either by use of the cold-gas jet system or repeated firings of the vernier engines. The unstable condition caused premature termination of the mission and prevented attainment of the flight objectives, for which a soft-landing was prerequisite. A thorough investigation by a specially appointed Failure Review Board has not disclosed a specific cause for the failure. A technical description of the mission and an evaluation of engineering data obtained are presented herein.

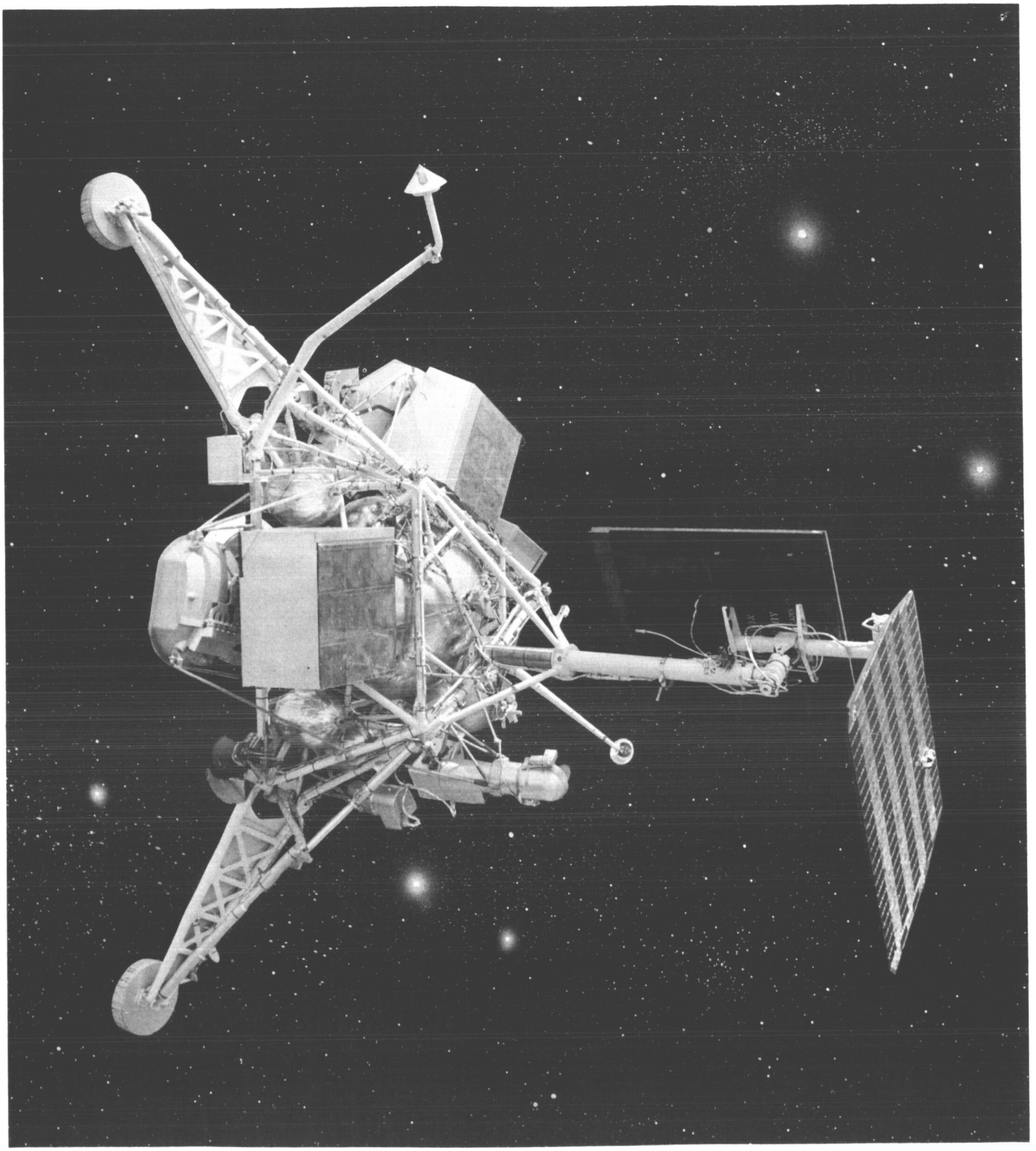

I. Introduction

Surveyor II was launched from Cape Kennedy, Florida, at 12:31:59.824 GMT on September 20, 1966. The launch vehicle provided a very satisfactory injection into lunar transfer trajectory, and a nominal mission was achieved until initiation of midcourse correction thrusting. During midcourse thrusting, one of the three vernier engines did not fire and spacecraft moment control was lost. A spacecraft tumbling condition resulted which could not be corrected either by activation of the cold-gas jet system or by repeated attempts to fire the vernier engines. In the unstable mode, spacecraft power was insufficient to complete the transit phase. The mission was terminated when loss of spacecraft signal occurred at 09:35:00 GMT on September 22, 1966, about 30 sec after a final command was sent that fired the retro motor. A thorough investigation by a formally appointed Failure Review Board has not disclosed a specific failure mode.

A. Surveyor Project Objectives

Surveyor is one of two unmanned lunar exploration projects currently being conducted by the National Aeronautics and Space Administration. The other, *Lunar Orbiter*, is providing medium- and high-resolution photographs over broad areas to aid in site selection for the *Surveyor* and *Apollo* landing programs.

The overall objectives of the *Surveyor* Project are:

1. To accomplish successful soft landings on the moon as demonstrated by operations of the spacecraft subsequent to landing.
2. To provide basic data in support of *Apollo*.
3. To perform operations on the lunar surface which will contribute new scientific knowledge about the moon and provide further information in support of *Apollo*.

Prior to the initial *Surveyor* mission (*Surveyor I*) it was planned to utilize the first four *Surveyor* spacecraft to satisfy Project Objective 1 above, and to utilize the following three spacecraft to satisfy Objective 2. Preliminary design was under way for follow-on spacecraft, in addition to the first seven, which would carry special scientific instruments to satisfy Objective 3. However, advantage has been taken of the highly successful *Surveyor I* mission, which satisfied Objectives 1 and 2 (for one possible *Apollo* landing site) and contributed significantly to the attainment of Objective 3, to accelerate the attainment of Objective 3 and also shorten the total program.

To this end, the follow-on missions have been cancelled and a plan is being implemented to incorporate on the remaining missions the most desirable scientific instruments that can be added without major alterations in Project schedule. The *Surveyor II* mission was unaffected by this redirection; the third mission is the earliest upon which it may be possible to incorporate additional scientific equipment.

On the *Surveyor II* mission, attainment of any of the Project Objectives was precluded by the spacecraft tumbling condition that ensued from the attempted midcourse correction maneuver.

B. Project Description

The *Surveyor* Project is managed by the Jet Propulsion Laboratory for the NASA Office of Space Science and Applications. The Project is supported by four major administrative and functional elements or systems: Launch Vehicle System, Spacecraft System, Tracking and Data Acquisition System (T&DA), and Mission Operations System (MOS). In addition to overall project management, JPL has been assigned the management responsibility for the Spacecraft, Tracking and Data Acquisition, and Mission Operations Systems. NASA/Lewis Research Center (LeRC) has been assigned responsibility for the *Atlas/Centaur* launch vehicle system.

1. Launch Vehicle System

Atlas/Centaur launch vehicle development began as an Advanced Research Projects Agency program for synchronous-orbit missions. In 1958, General Dynamics/Convair was given the contract to modify the *Atlas* first stage and develop the *Centaur* upper stage, and Pratt & Whitney was given the contract to develop the high-impulse LH_2/LO_2 engines for the *Centaur* stage.

The Kennedy Space Center, Unmanned Launch Operations branch, working with LeRC, is assigned the *Centaur* launch operations responsibility. The *Centaur* vehicle utilizes Launch Complex 36, which consists of two launch pads (A and B) connected to a common blockhouse. The blockhouse has separate control consoles for each of the pads. Pad 36A was utilized for the *Surveyor II* mission.

The launch of *Atlas/Centaur* AC-7 on the *Surveyor II* mission was the second operational use of an *Atlas/Centaur* vehicle, the first having been the successful flight of AC-10 on the *Surveyor I* mission. Both *Surveyor* missions utilized the "direct ascent" mode, wherein the *Centaur* second stage provided only one continuous burn to achieve injection into the desired lunar transfer trajectory. Eight R&D flight tests were conducted in the *Centaur* vehicle program prior to the *Surveyor II* mission. The final *Centaur* development flight (AC-9), conducted on October 26, 1966, subsequent to the *Surveyor II* mission, successfully demonstrated capability to launch via "parking orbit" ascent trajectories. The parking orbit ascent mode, involving a second burn of the *Centaur* stage (after a coast in parking orbit), will be utilized on the next mission and on all but one of the remaining missions.

2. Spacecraft System

The *Surveyor* spacecraft weight of about 2200 lb and overall dimensions were established in accordance with the *Atlas/Centaur* vehicle capabilities. Three major features, first demonstrated on the *Ranger* missions, were incorporated in the *Surveyor* spacecraft system: fully attitude-stabilized spacecraft, earth-directed high-gain antenna, and the midcourse maneuver. Demonstration of TV communication at lunar distances is another *Ranger* achievement which has been of value to *Surveyor* and the other lunar programs. In addition, the *Surveyor* spacecraft utilizes several new features associated with the complex terminal phase of flight and soft-landing: throttleable vernier rockets with solid-propellant main retromotor; extremely sensitive velocity- and altitude-sensing radars, and an automatic closed-loop guidance and control system. The demonstration of these devices on *Surveyor* missions is a direct benefit to the *Apollo* program, which will employ similar techniques. Design, fabrication, and test operations of the *Surveyor* spacecraft are performed by Hughes Aircraft Company under the technical direction of JPL.

3. Tracking and Data Acquisition System

The T&DA system provides the tracking and communications link between the spacecraft and the Mission Operations System. For *Surveyor* missions, the T&DA system uses the facilities of: (1) the Air Force Eastern Test Range for tracking and telemetry of the spacecraft and vehicle during the launch phase, (2) the Deep Space Network for precision tracking, communications, data transmission and processing, and computing, and (3) the Manned Space Flight Network and the World-Wide Communications Network (NASCOM), both of which are operated by Goddard Space Flight Center.

The critical flight maneuvers and most picture-taking operations on *Surveyor* missions are commanded and

recorded by the Deep Space Station at Goldstone, California (DSS 11), during its view periods. Other stations which provided prime support for the *Surveyor II* mission were DSS 42, near Canberra, Australia, DSS 51, at Johannesburg, South Africa, and DSS 72, at Ascension Island; at Cape Kennedy, DSS 71 provided support during prelaunch and launch operations. In addition, backup support was provided by DSS 61, near Madrid, Spain, and DSS 12 and 14 (with a 210-ft antenna), Goldstone, California.

4. Mission Operations System

The Mission Operations System essentially controls the spacecraft from launch through termination of the mission. In carrying out this function, the MOS constantly evaluates the spacecraft performance and prepares and issues appropriate commands. The MOS is supported in its activities by the T&DA system as well as special hardware provided exclusively for the *Surveyor* Project and referred to as mission-dependent equipment. Included in this category are the Command and Data Handling Consoles installed in the DSS's, the Television Ground Data Handling System, and other special display equipment.

C. Mission Objectives

The specific objectives of each *Surveyor* mission are denoted as "flight objectives." For *Surveyor II* the flight objectives were specified in two categories: primary and secondary.

(1) Primary Flight Objectives:

a. Accomplish a soft landing on the moon at a site east of the *Surveyor I* landing point.

b. Demonstrate the capability of the spacecraft to soft-land on the moon with an oblique approach angle not greater than approximately 25 deg.

c. Obtain post-landing television pictures and touchdown dynamics, radar reflectivity, and thermal data of the lunar surface.

(2) Secondary Flight Objective:

a. Demonstrate the capability of DSS 72 to support future *Surveyor* missions.

The early part of the *Surveyor II* mission was carried out as planned with the full capability of meeting all of the above objectives. However, the primary flight objectives could not be achieved owing to the spacecraft tumbling condition which developed after the midcourse maneuver was commanded. The secondary objective was met, with DSS 72 providing useful data during gaps between the view periods of other DSIF prime stations.

D. Mission Summary

Surveyor II was launched with *Atlas/Centaur* AC-7 from Pad 36A at Cape Kennedy. Because of holds called during the countdown to overcome launch vehicle problems, liftoff was delayed until the end of the first planned launch window, at 12:31:59.824 GMT on September 20, 1966. Following a nominal direct-ascent boost phase, the spacecraft was very accurately injected into a lunar transfer trajectory. The uncorrected lunar impact point was within 150 km of the prelaunch aiming point.

Deep Space Station 72, at Ascension, was the first DSIF station to achieve one-way lock. Received data confirmed the satisfactory condition of the spacecraft and the successful completion of the automatic post-injection events such as sun acquisition and solar panel deployment. As planned, DSS 51 was the first station to establish two-way lock and exercise control of the spacecraft by command.

For approximately the first 16½ hr of flight, a nominal mission was achieved, including Canopus star acquisition. When the three vernier engines were commanded on for midcourse velocity correction, which lasted 9.8 sec (as preset by earth-based command), Vernier Engine 3 failed to provide thrust, causing the spacecraft to tumble at a rate of about 1.22 rev/sec.

The nitrogen gas-jet system, which is normally enabled during and after the midcourse velocity correction, operated for several minutes to stabilize the spacecraft. Although the spin rate was reduced to 0.97 rev/sec, the gas-jet system was inhibited after about 60% of the gas had been expended, and it became evident that the remaining gas supply was insufficient to stop the spinning.

Since the spacecraft was rotating in such a way that energy could not be obtained from the solar panels, the only source of electrical power was the spacecraft batteries. Steps were therefore taken to conserve power. Nevertheless, stored spacecraft power was insufficient to complete the lunar transit.

During the remaining life of the spacecraft, a total of 39 attempts were made to overcome the vernier engine problem by firing the engines for short periods, ranging from 0.2 to 2.5 sec and finally, for 21.5 sec. Vernier Engine 3 did not respond to any of these attempts. However, thrust was delivered by the other two verniers in each firing, and the spacecraft finally reached a spin rate of 2.3 deg/sec.

About 28.5 hr after the attempted midcourse correction, when very little battery power remained, a final sequence was commanded which fired the main retro motor and Vernier Engines 1 and 2. The spacecraft signal was lost about 30 sec after main retro ignition, bringing the *Surveyor II* mission to an end.

The entire Mission Operations System and Deep Space Network responded well to the unexpected difficulties which developed in the mission and provided the Project with tracking and telemetry data as well as the command function until mission termination.

A Failure Review Board was appointed consisting of representatives from JPL, NASA Office of Space Science and Applications, HAC, and Reaction Motors Division of Thiokol. A thorough investigation conducted by the Board has not revealed the exact cause of the *Surveyor II* spacecraft failure. However, as a result of the detailed investigation, a number of recommendations have been made relative to the spacecraft system to assure against a similar failure as well as to provide better diagnostic data on future missions.

II. Space Vehicle Preparations and Launch Operations

The *Surveyor II* spacecraft was assembled and subjected to flight-acceptance testing at the Hughes Aircraft Corporation facility, El Segundo, California. After completion of these tests it was shipped to the Air Force Eastern Test Range (AFETR), Cape Kennedy, on the Super Guppy cargo aircraft, arriving on July 19, 1966. The *Atlas/Centaur* launch vehicle stages were airlifted to AFETR after undergoing testing in the Combined Systems Test Stand (CSTS) at San Diego. Prelaunch assembly, checkout, and systems tests were accomplished successfully at AFETR, and the space vehicle was launched on September 20, 1966 at 12:31:59.824 GMT, near the end of the first scheduled launch window.

A. Spacecraft Assembly and Testing

Tests and operations on each spacecraft are conducted by a test team and data analysis team which work with the spacecraft throughout the period from the beginning of testing until launch. The test equipment used to control and monitor the spacecraft system performance at all test facilities includes (1) a system test equipment assembly (STEA) containing equipment for testing each of the spacecraft subsystems, (2) a command and data handling console (CDC) similar to the units located at each of the DSIF stations (see Section VI) for receiving telemetry and TV data and sending commands, and (3) a computer data system (CDS) for automatic monitoring of the spacecraft system. Automatic monitoring capability is necessary because of the large number of telemetered data points and high sampling frequency of most of the *Surveyor* telemetry modes. The CDS provides the following features to aid the data analysis personnel in evaluating the spacecraft performance:

(1) Digital magnetic tape recording of all input data.

(2) Suppression of nonchanging data. Only data points which reflect a change are printed on display devices.

(3) Alarm limit capability. Critical telemetry functions are monitored for out-of-tolerance indications which would be damaging to the spacecraft. An audible alarm sounds if these limits are exceeded.

(4) Request message. In the event that telemetry data is desired for evaluation, a print of requested data is provided.

The *Surveyor II* spacecraft (SC-2) was initially assembled December 8, 1964 and then passed through the following test phases:

1. Spacecraft Ambient Testing

The ambient testing phase consists of group tests, initial system checkout, and mission sequence tests. In the initial systems checkout, each subsystem is tested for compatibility and calibration with other subsystems, and a systems readiness test is performed for initial system operational verification. The primary objectives of the mission sequence tests are to obtain system performance characteristics under ambient conditions and in the electromagnetic environment expected on the launch pad and in flight prior to separation from the *Centaur*.

After the group tests and initial system checkout, three mission sequences were completed on the *Surveyor II* spacecraft. The last of these was a plugs-out run approaching flight configuration with simulated electromagnetic environment. A period of extensive rework and preparation for solar-thermal-vacuum testing followed these ambient tests.

2. Solar-Thermal-Vacuum (STV) Testing

The STV sequence of tests is conducted to verify proper spacecraft performance in simulated missions at various solar intensities and a vacuum environment. In these tests, as well as the vibration test phase which follows, the propellant tanks are loaded with "referee" fluids to simulate flight weight and thermal characteristics.

The *Surveyor II* spacecraft began the STV sequence of tests in the solar-vacuum chamber in mid-April 1966. The first sequence, run at 87% of nominal sun intensity, was successful except for a major compartment overheating problem and failure of the battery case, which damaged the structure of Compartment A and Transmitter B. The second sequence, run at 112% solar intensity, was aborted when improper operation of two thermal control switches in Compartment A again caused compartment overheating. After correction of the thermal control problem, the test at 112% solar intensity was repeated and all systems were normal until the terminal descent phase, when problems were encountered which involved a short in the flight control sensor group (FCSG), improper transmission of telemetry data by the central signal processor (CSP), and a Canopus tracker malfunction. Following repair of the FCSG and CSP plus installation of a new gyro package and Canopus tracker, the sequence at 112% solar intensity was performed with no mission critical problems. The third sequence, conducted in the plugs-out configuration at 100% solar intensity, was successful up to terminal descent, when the boost-regulator (BR) failed. The BR failure stopped the spacecraft telemetry and command systems, preventing commands from turning off the radar altimeter and doppler velocity sensor (RADVS) and resulted in RADVS overheating. Repair consisted of replacing the BR and parts of the RADVS. A final 20-hr STV run was performed to flight-qualify the system with the new BR and RADVS. This run was successful, and the spacecraft was removed from the vacuum chamber and preparations for vibration testing were initiated.

3. System Vibration Testing

Vibration tests are conducted in the three orthogonal axes of the spacecraft to verify proper operation after exposure to a simulated launch-phase vibration environment. For these tests the spacecraft is placed in the launch configuration, with legs and omniantennas in the folded position. In addition, a vernier engine vibration test is conducted, with vibration input at the vernier engine mounting points, to simulate the environment during the midcourse maneuver and terminal descent phases of flight.

The *Surveyor II* vibration test phase began on June 29, 1966. The spacecraft was moved to the vibration test facility and progressed through three axes of vibration test, with no problems until the final test, during which the shaker system delivered a severe transient pulse causing a high shock load of short duration to be received by the spacecraft. Resulting damage was a partial breakage of the retro rocket mountings and two antenna and solar panel positioner (A/SPP) snubbers. The damage was repaired and the Z-axis vibration was repeated to complete the test phase on July 10. The vernier engine vibration and "buzz" tests were successfully completed on July 13, 1966. An unrelated RADVS crystal detector failure was found during the vernier engine vibration phase. This detector was replaced on the spacecraft and then vibrated by a "sting" drive and functionally tested to validate the installation. This completed all system testing at El Segundo and, after preparation, *Surveyor II* was shipped to Cape Kennedy via the Super Guppy cargo aircraft on July 18, 1966.

B. Launch Vehicle Combined Systems Testing

Following successful completion of factory acceptance testing of each stage, the *Atlas* was installed in the CSTS

at San Diego, California, on April 27, 1966; the *Centaur* was installed in the CSTS on May 5, 1966. Test sequences in the CSTS culminated in the vehicle Compatibility Composite Test on May 25. Test data evaluation was completed on June 1, 1966. Minor hardware modifications were completed and the *Atlas* was shipped by air to AFETR on June 18, followed by the nose fairing and interstage adapter on June 21 and the *Centaur* on June 24, 1966.

C. Launch Operations at AFETR

The major operations performed at AFETR after arrival of the launch vehicle and the spacecraft are listed in Table II-1.

1. Initial Preparations

The *Atlas* and *Centaur* stages of AC-7 were erected on June 22 and June 29, respectively, and proceeded through component, system, and ground support equipment (GSE) compatibility checks with no significant problems. Guidance/autopilot testing, the last major airborne system test before spacecraft mating, was satisfactorily completed on August 5.

The spacecraft arrived at AFETR on July 19 and proceeded through receiving inspection and spacecraft assembly. Performance Verification Tests (PVT) 1 through 4 and calibration of the TV system were performed with only minor anomalies occurring.

On August 2, 1966, the spacecraft was transported to the Explosive Safe Facility (ESF), where it was prepared for its first trip to the launch pad. Preparations included (1) installation of a dummy retro rocket and altitude marking radar (AMR), (2) installation of leg and omni-antenna squib mufflers, (3) mating of the spacecraft with the *Centaur* forward adapter, (4) flight level pressurization of the attitude control and propulsion system tanks, (5) encapsulation of the spacecraft within the nose fairing (Fig. II-1), and (6) performance of a spacecraft System Readiness Test (SRT).

Surveyor II was transported to launch pad 36A and mated with the *Centaur* on August 9, 1966.

Table II-1. Major operations at Cape Kennedy

Operation	Location	Date completed, 1966
AC-7[a] erection	Launch Complex 36A	June 29
SC-2[b] inspection, reassembly, and initial testing	Building AO	August 3
SC-2 preparation for on-pad testing; encapsulation and spacecraft System Readiness Test	Explosive Safe Facility (ESF)	August 8
SC-2 mate to *Centaur*	Launch Complex 36A	August 9
DSS-71/SC-2 compatibility test	Launch Complex 36A	August 11
AC-7 Propellant Tanking Test;	Launch Complex 36A	August 11
AC-7/SC-2 Joint Flight Acceptance Composite Test (J-FACT)	Launch Complex 36A	August 16
SC-2 demate	Launch Complex 36A	August 16
SC-2 decapsulation, depressurization, removal of J-FACT items, and alignment checks	Explosive Safe Facility	August 21
SC-2 final preparation: RADVS ranging test, vernier propulsion phasing, mission sequence test, and TV photogrammetric calibration	Building AO	August 30
AC-7 Flight Acceptance Composite Test (without SC-2)	Launch Complex 36A	September 8
SC-2 propellant loading, pressurization, and weight and balance checks	Explosive Safe Facility	September 14
AC-7 Composite Readiness Test (CRT)	Launch Complex 36A	September 14
SC-2 final encapsulation and spacecraft SRT	Explosive Safe Facility	September 15
SC-2 remate to *Centaur*	Launch Complex 36A	September 16
Launch	Launch Complex 36A	September 20

[a] *Atlas/Centaur* vehicle designation.
[b] *Surveyor II* spacecraft designation.

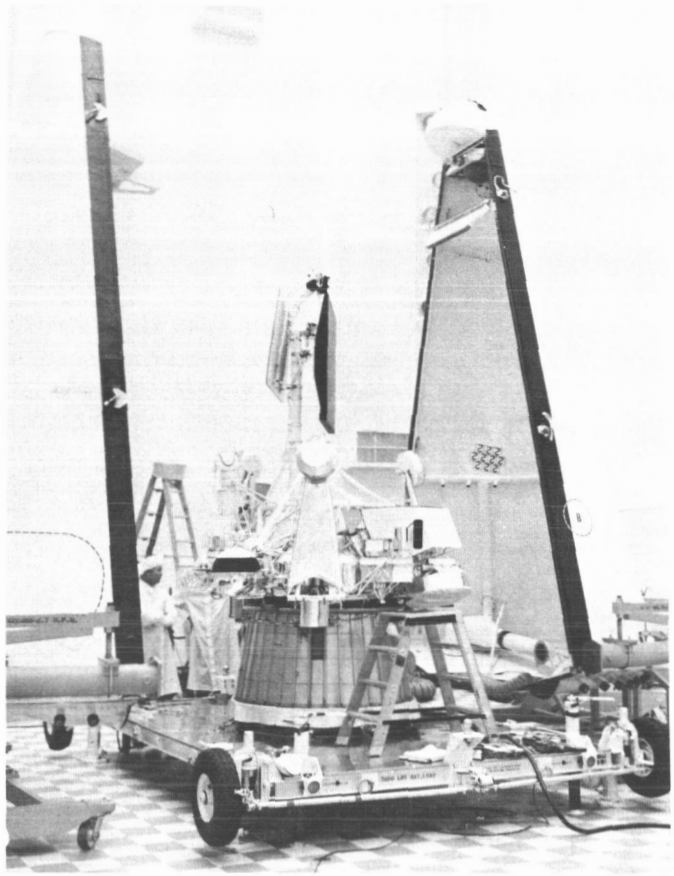

Fig. II-1. *Surveyor II* spacecraft prepared for encapsulation

2. Propellant Tanking Test and Joint Flight Acceptance Composite Test (J-FACT)

After the spacecraft was mated with the *Centaur*, a series of tests were performed to verify proper operation with the blockhouse equipment and the RF air link between the launch pad and Building AO. All control of the spacecraft except for external power and some monitor functions is at Building AO. On August 9 an SRT and practice countdown were performed, and on August 10 and 11 a compatibility test between the spacecraft and DSS 71 at Cape Kennedy was successfully accomplished. During this test a frequency shift problem was observed when the spacecraft transmitter frequency was transferred from wide-band to narrow-band mode. Tests on SC-3* demonstrated that a generic drift problem exists but that the condition was acceptable.

*Serial designation for *Surveyor* spacecraft scheduled for next *Surveyor* mission.

The spacecraft next participated in the launch vehicle Propellant Tanking Test. During this test the launch vehicle is completely tanked with propellants, the launch pad stand is moved back, and the complete vehicle is exposed to off- and on-board RF sources as in the launch countdown. No RF interference problems were noted.

J-FACT was performed on August 16, with the spacecraft operating in the actual prelaunch environment. This test culminated in the simulation of launch events through spacecraft separation. A predicted failure mode (first seen on SC-3) was observed when the auto deploy logic was not enabled with the *Centaur* command for "transmitter to high power." The problem was traced to diode stray capacitance which turns off the deployment logic flip-flop. The decision was made to disable the diode deploy logic and command on the deploy logic prior to launch.

The spacecraft temperature was maintained constant during the entire on-pad period to permit accurate pressure decay measurements of the vernier propulsion system and attitude control system.

3. Final Flight Preparations

Following demate from the *Centaur*, the spacecraft was moved back to the ESF, where it was decapsulated and depressurized. During depressurization a system pressure calibration was performed on the helium and nitrogen pressure transducers. The dummy retro, AMR, and battery were removed and alignment was completed at the ESF. On August 21, the spacecraft was transferred back to the Spacecraft Checkout Facility for the performance of PVT 5, which consisted of a number of special tests such as the RADVS ranging vernier propulsion system phasing, and the final Mission Sequence Test in the plugs-out configuration. A special photogrammetric calibration of the television subsystem was also performed at this time to improve the accuracy of view angle calibration. This would permit more accurate mapping of surface features on the moon.

On August 31 the spacecraft was moved back to the ESF for final preparations, including propellant loading, final weight, balance and alignment checks, and performance of the PVT 6 test series. Some thermal surfaces were damaged during propellant loading and required rework. Propellant fumes entrapped in the protective bag attacked the thermal finish, particularly around Landing Leg 3. Individual steps of PVT 6 test sequence were phased with the final preparations to verify flight readiness.

The final weight, balance, and alignment checks were conducted after loading of the vernier system propellants and installation of the main retro motor. A problem was encountered in alignment when the A/SPP was stepped. The A/SPP polar axis missed steps in a certain sector of its travel. Analysis indicated that the unit probably had not degraded but that the test fixture subjected the unit to unusual loading which could not occur in the mission. The unit was accepted for flight on this basis.

After the spacecraft was mated to the *Centaur* adapter, the helium and nitrogen tanks were brought to flight pressures, the spacecraft was encapsulated, and a final SRT was performed on September 15. On September 16, the spacecraft was moved to the launch pad and mated to the *Centaur*.

An *Atlas/Centaur* FACT was performed on September 8 with only one anomaly occurring. The FACT countdown was conducted in a routine manner until *T*-5 min, at which time a hold was called because of an indication of excessive *Centaur* inverter temperature. The problem was found to be within the transducer recorder; it was corrected, and the count was resumed after a hold of 1 min.

The launch vehicle CRT, the last multiple systems test prior to spacecraft mating and launch countdown, was conducted on September 14 and proved the launch readiness of all *Atlas* and *Centaur* electrical and RF systems. No abnormal deviations of test events were noted.

4. Countdown and Launch

Final spacecraft and launch vehicle checks began immediately after spacecraft mating on September 16. After a spacecraft SRT was performed, the retro motor safe-and-arm check was performed. Following installation of the launch vehicle ordnance devices, the pyrotechnic circuits were checked and launch readiness tests were started. *Atlas* fuel tanking and *Centaur* hydrogen peroxide loading were accomplished on September 17. During launch vehicle checkout operations on September 19 (launch day minus 1), *Centaur* engine feedback traces did not appear normal. Troubleshooting isolated the problem to the aerospace ground equipment (AGE) demodulator in the instrumentation circuit. The *Atlas* telemetry package and its accessory were replaced because of improper operation of the commutator.

The final spacecraft SRT began at 19:16 EST on September 19 at a countdown time of *T*-615 min and was completed at *T*-430 min.

At *T*-260 min, activation of the *Atlas* telemetry battery resulted in a low open-circuit voltage, which reflected a decaying trend. A spare battery was installed, activated, and successfully load tested with no impact on the count.

After service tower removal at approximately *T*-120 min, a weak signal strength was recorded for spacecraft Receiver B. First evaluation of this anomaly attributed the problem to a poor RF link caused by the tower removal. (Later, during Canopus acquisition maneuvers, it was confirmed that the signal was indeed low all across the antenna pattern. Subsequent checks disclosed that an AGC shift had occurred between final spacecraft encapsulation and arrival at the launch pad. This problem is also discussed in Section VI-C, Mission Operations Chronology.)

The countdown proceeded without interruption to *T*-90 min (04:01 EST), when a scheduled 70-min hold was started. The spacecraft system joined the launch vehicle countdown during this period. The count was resumed at 05:11 EST and proceeded as planned to *T*-5 min, when a second scheduled hold of 15 min was started. This hold was extended an additional 7 min to investigate an apparent low temperature indication within the *Centaur* hydrogen peroxide engine system. The temperature was determined to be correct; the count resumed at 06:58 EST and proceeded down to *T*-115 sec, when it was necessary to hold and recycle to *T*-5 min. This hold was called because the *Atlas* liquid oxygen (LO_2) boil-off valve did not close at the start of the flight pressurization sequence and the proper pressure could not be reached. During the investigation of the problem, the *Atlas* was pressure-cycled several times, with the LO_2 boil-off valve closing properly each time. It was then decided to resume count as soon as the *Atlas* LO_2 supply, which had fallen below the acceptable level, could be replenished. At this time it was discovered that the automatic LO_2 topping system was not operating properly, and manual operation was employed. After a hold of 26 min, the count was picked up at 07:27 EST, although the *Atlas* LO_2 was still below the proper level, because the launch window for the day closed at 07:32. The flight level was reached at approximately *T*-3 min, and the count continued down to liftoff (Fig. II-2), which occurred at 07:31:59.824 EST (12:31:59.824 GMT), September 20, 1966. The flight azimuth was 114.361 deg.

The countdown included a total of 85 min of planned, built-in holds — one of 70-min duration at *T*-90 min, and a second of 15-min duration at *T*-5 min. AC-7/SC-2 consumed a total hold time of 118 min. The launch window

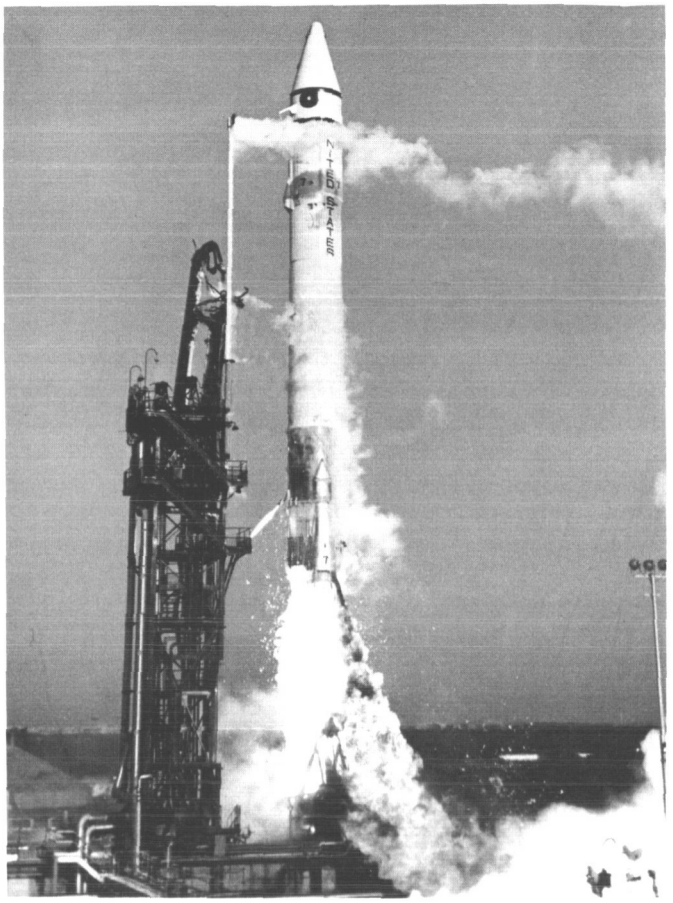

Fig. II-2. *Atlas/Centaur* AC-7 launching *Surveyor II*

for September 20 extended from 06:56 to 07:32 EST, providing a duration of 36 min. A countdown time summary is shown in Table II-2.

The general performance of GSE was satisfactory throughout the launch countdown. Commercial power failed at $T + 60$ sec, and a Cape-wide loss was experienced for approximately 5 sec. Except for some loss of optical coverage, the power loss did not cause any significant problems, since most facilities were operating from critical or generator power.

With the exception of an anomaly in the *Centaur* telemetry system, all systems performed normally throughout the launch, and the spacecraft was injected into an accurate lunar trajectory. The anomaly in the telemetry system was a failure to receive spacecraft vibration data from three of five accelerometers. The powered flight sequence of events and launch vehicle performance are described in Section III.

Table II-2. *Surveyor II* countdown time summary

Event	Countdown time	EST
		(September 19)
Started spccecraft SRT	T-615 min	19:16
Comp'eted spacecraft SRT	T-430 min	22:21
		(September 20)
Started launch veh'cle countdown	T-300 min	00:31
Started 70-min built-in hold (BIH)	T-90 min	04:01
Spacecraft joined launch vehicle coun:down	T-90 min	04:35
End BIH; resumed countdown	T-90 min	05:11
Started 15-min BIH	T-5 min	06:36
BIH extended	T-5 min	06:51
Resumed countdown	T-5 min	06:58
Hold; recycled to T-5 min	T-115 sec	07:01
Resumed countdown	T-5 min	07:27
Liftoff	T-0 min	07:31:59.824

The atmospheric conditions on launch day were favorable. Surface winds were 6 to 12 knots from 190 deg, with unrestricted visibility of 10 miles. Surface temperature was 79°F, with relative humidity of 93% and a dewpoint of 77°F. Sea level atmospheric pressure was 29.900 in. Cloud cover consisted of 0.10 cumulus at 1,400 ft, 0.10 altocumulus at 11,000 ft, and 0.5 cirrus at an unknown altitude. Maximum winds aloft were reported to be 63 ft/sec from 225 to 245 deg at 23,000 ft altitude, with a decrease to 50 ft/sec at 60,000 ft. The maximum expected shear parameter was 4 ft/sec per thousand feet of altitude.

D. Launch Phase Real-Time Mission Analysis

The launch windows which were finally established for the September 1966 launch period are shown in Fig. II-3. Launching on days prior to September 20 was not acceptable because touchdown at the desired lunar landing site would have occurred in darkness (prior to sunrise). The "performance constraint" was based upon a requirement on the *Surveyor II* mission that there be a minimum excess *Centaur* propellant weight of 235 lb to cover 3-sigma launch vehicle performance dispersions. This represents an increase from the value of 175 lb used for the *Surveyor I* mission to provide additional protection against the uncertainties associated with the determination of performance dispersions. The "post-MECO* tracking constraint" was based upon the Class I

*Main engine cutoff.

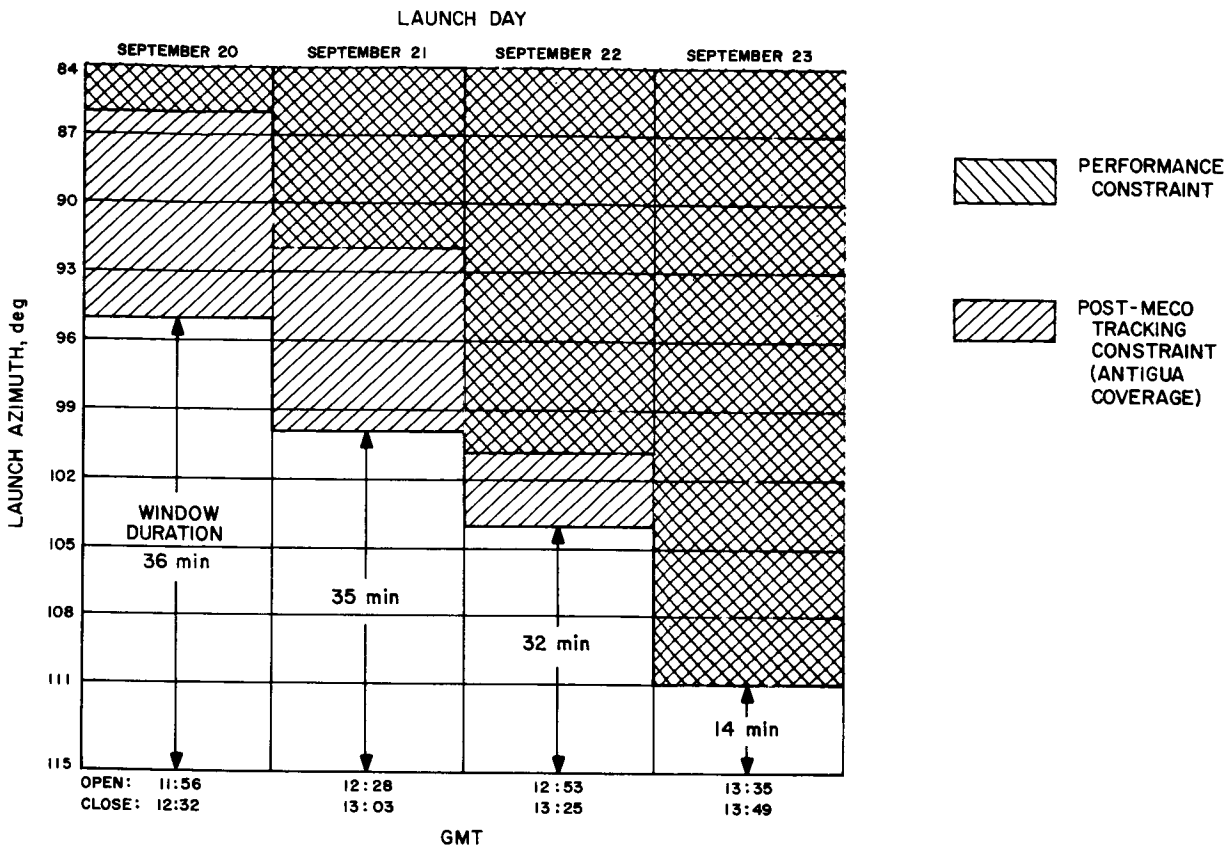

Fig. II-3. Final *Surveyor II* launch window design for September 1966

requirement (see Section V) for 60 sec of post-MECO radar tracking data for which it was considered important to have Antigua coverage. Station coverage capability for the launch phase of the *Surveyor II* mission is presented in Section V.

1. Countdown to Launch

During countdown operations, those factors acting to constrain the launch window or period were continually evaluated by the Launch Phase Mission Analyst. The Mission Director was advised of these evaluations for consideration in the launch or hold decision.

Several temporary problems occurred relative to the Tracking and Data Acquisition (T&DA) facilities during the countdown. These problems included the following: (1) interruptions were experienced in the teletype circuits to DSS 42 and 72 and in the voice circuits to DSS 51 and 72; (2) a marginal condition developed in the high-speed data line to DSS 72; (3) Bermuda and Trinidad radars were inoperative temporarily owing to elevation encoder and coherent memory filter problems, respectively; (4) RF propagation fade interfered with the transmission links with Range Instrumentation Ship (RIS) *Coastal Crusader;* and (5) a heavy storm near Canberra threatened DSS 42. The Mission Director was advised that none of these problems constituted a *hold* condition, and the T&DA system was in a *go* condition at liftoff.

2. Launch to DSN Acquisition

During the launch-to-DSN-acquisition phase of flight, the occurrence of "mark" events was reported in real time by the AFETR and MSFN, followed later with a report of the times at which they occurred. The small deviations of the mark times from nominal were judged to be well within the 3-sigma dispersions. The *Centaur* burn time was about 2.5 sec longer than expected; however, similarly longer *Centaur* burn times had been experienced on previous flights. Consequently, the powered flight was considered to be quite normal.

Launch vehicle telemetry was retransmitted to Cape Kennedy in real-time from all stations down to Antigua until the spacecraft transmitter was switched to high power, at which time the spacecraft S-band data was

sent up the subcable and real-time retransmission of launch vehicle data was ceased. Reports of the real-time analysis of launch vehicle data indicated a nominal powered flight. The normality of powered flight was confirmed by reports of nominal acquisition times by each of the tracking stations.

Four minutes after MECO, the AFETR real-time computer system (RTCS) at Cape Kennedy had computed the first orbit based on Antigua radar data. This orbit, considered a "fair" fit, further indicated a nominal powered flight and injection into a satisfactory lunar transfer orbit. There were reports, however, which indicated the slight possibility that spacecraft separation had not been normal. It was reported that Trinidad, which is capable of tracking more than one object, did not see separation. Also, the intermittent data from Ascension and Pretoria was thought possibly to have been caused by a tumbling vehicle. This concern was proved unfounded when it was learned that unfavorable aspect angles may have prevented Trinidad from observing separation, and near-real-time voice reports on the *Centaur* roll, pitch, and yaw rate gyros confirmed that a stable vehicle had been observed by Ascension.

III. Launch Vehicle System

The *Surveyor* spacecraft was injected into its lunar transit trajectory by a General Dynamics *Atlas/Centaur* vehicle (AC-7). The vehicle was launched on a "direct ascent" powered flight from Launch Complex 36A of the AFETR at Cape Kennedy, Florida. This was the second operational flight of an *Atlas/Centaur* vehicle, the first having been the successful flight of AC-10 on the *Surveyor I* mission. AC-10 and AC-7 were identical in all essential respects except for the use of 1000-lb-thrust vernier engines on the AC-7 *Atlas* stage. Later-model vernier engines, rated at 670-lb thrust, were used on AC-10, which was assembled after AC-7.

The *Atlas/Centaur* vehicle with the *Surveyor* spacecraft encapsulated in the nose fairing is 113 ft long and weighs 303,000 lb at liftoff (2-in. rise). The basic diameter of the vehicle is a constant 10 ft from the aft end to the base of the conical section of the nose fairing. The configuration of the completely assembled vehicle is illustrated in Fig. III-1. Both the *Atlas* first stage and *Centaur* second stage utilize thin-wall, pressurized, main propellant tank sections of monocoque construction to provide primary structural integrity and support for all vehicle systems. The first and second stages are joined by an interstage adapter section of conventional sheet and stringer design. The clamshell nose fairing is constructed of laminated fiberglass over a fiberglass honeycomb core and attaches to the forward end of the *Centaur* cylindrical tank section.

A. *Atlas* Stage

The first stage of the *Atlas/Centaur* vehicle is a modified version of the *Atlas D* used on many previous NASA and Air Force missions such as *Ranger, Mariner,* and *OGO*. The *Atlas* propulsion system burns RP-1 kerosene and liquid oxygen in each of its five engines to provide a total liftoff thrust of approximately 388,000 lb. The individual sea-level thrust ratings of the engines are: two booster engines at 165,000 lb each; one sustainer engine at 57,000 lb; and two vernier engines at 1000 lb each. The *Atlas* can be considered a 1½-stage vehicle because the "booster section," weighing 6000 lb and consisting of the two booster engines together with the booster turbo pumps and other equipment located in the aft section, is jettisoned after about 2.5 min of flight. The sustainer and vernier engines continue to burn until propellant depletion. A mercury manometer propellant utilization system is used to control mixture ratio for the purpose of minimizing propellant residuals at *Atlas* burnout.

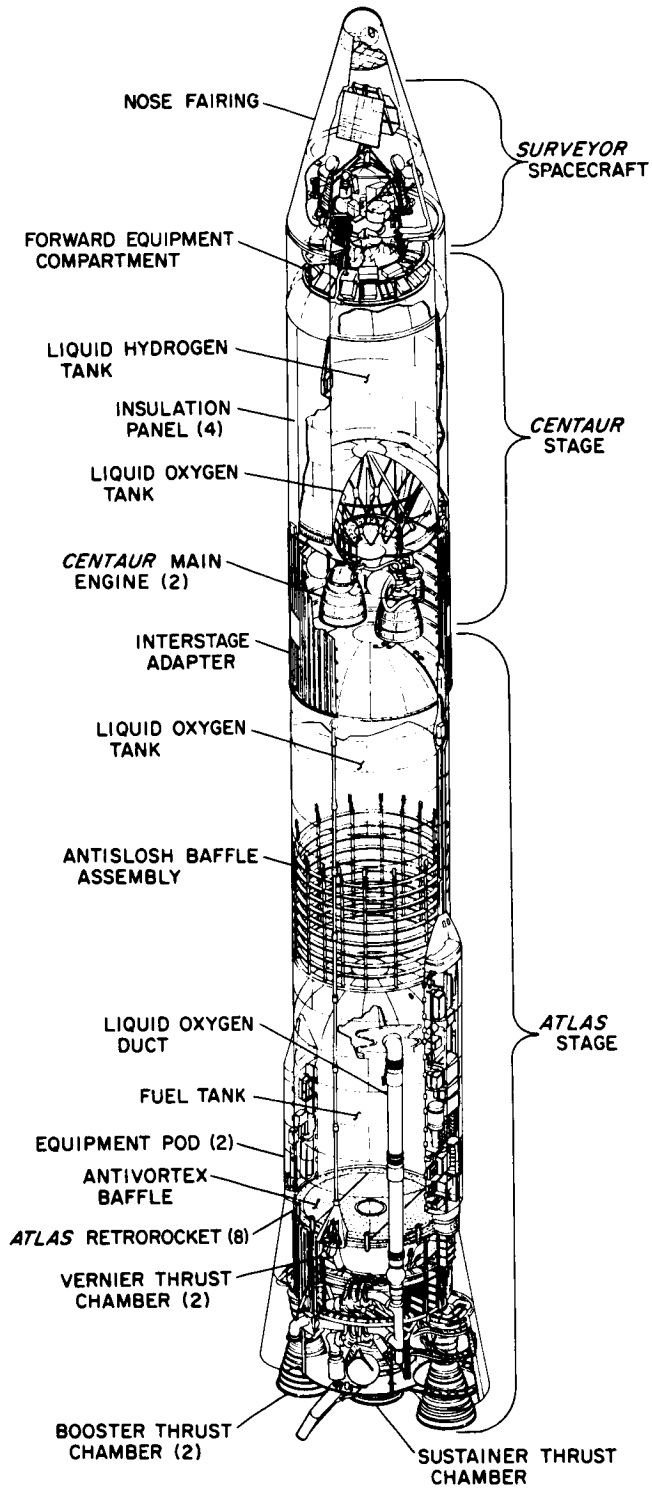

Fig. III-1. *Atlas/Centaur/Surveyor* space vehicle configuration

Flight control of the first stage is accomplished by the *Atlas* autopilot, which contains displacement gyros for attitude reference, rate gyros for response damping, and a programmer to control flight sequencing until *Atlas/Centaur* separation. After booster jettison, the *Atlas* autopilot also is fed steering commands from the all-inertial guidance set located in the *Centaur* stage. Vehicle attitude and steering control are achieved by the coordinated gimballing of the five thrust chambers in response to autopilot signals.

The *Atlas* contains a single VHF telemetry system which transmits data on 108 first-stage measurements until *Atlas* separation. The system operates on a frequency of 229.9 mc over two antennas mounted on opposite sides of the vehicle at the forward ends of the equipment pods. Redundant range-safety command receivers and a single destructor unit are employed on the *Atlas* to provide the Range Safety Officer with means of terminating the flight by initiating engine cutoff and destroying the vehicle. The system is inactive after normal *Atlas* staging occurs. The AZUSA tracking system has been deleted from the *Atlas* for *Surveyor* missions, leaving only the C-band tracking system on the *Centaur* stage.

B. *Centaur* Stage

The *Centaur* second stage is the first vehicle to utilize liquid hydrogen/liquid oxygen, high-specific-impulse propellants. The cryogenic propellants require special insulation to be used for the forward, aft, and intermediate bulkheads as well as the cylindrical walls of the tanks. The cylindrical tank section is thermally insulated by four jettisonable insulation panels having built-in fairings to accommodate antennas, conduits, and other tank protrusions. The insulation panel hinges were redesigned for AC-10 to overcome a deployment control problem which had been suspected on vehicle development flights AC-6 and AC-8. Most of the *Centaur* electronic equipment packages are mounted on the forward tank bulkhead in a compartment which is air-conditioned prior to liftoff.

The *Centaur* is powered by two constant-thrust engines rated at 433-sec specific impulse and 15,000 lb thrust each in vacuum. Each engine can be gimballed to provide control in pitch, yaw, and roll. Propellant is fed from each of the tanks to the engines by boost pumps driven by hydrogen peroxide turbines. In addition, each engine contains integral "boot-strap" pumps driven by hydrogen propellant, which is also used for regenerative cooling of the thrust chambers. A propellant utilization system is used on the *Centaur* stage to achieve minimum residual of one propellant at depletion of the other. The system controls the mixture ratio valves as a continuous

function of propellant in the tanks by means of tank probes and an error ratio detector. The nominal oxygen/hydrogen mixture ratio is 5:1 by weight.

The second-stage all-inertial guidance system contains an on-board computer which provides vehicle steering commands after jettison of the *Atlas* booster section. The *Centaur* guidance signals are fed to the *Atlas* autopilot until *Atlas* sustainer engine cutoff and to the *Centaur* autopilot after *Centaur* main engine ignition. Platform gyro drifts are compensated for by the guidance system computer, which is programmed to set the torquing signals to zero during flight. The *Centaur* autopilot system provides the primary control functions required for vehicle stabilization during powered flight, execution of guidance system steering commands, and attitude orientation following the powered phase of flight. In addition, the autopilot system employs an electromechanical timer to control the sequence of programmed events during the *Centaur* phase of flight, including a series of commands required to be sent to the spacecraft prior to spacecraft separation.

The *Centaur* reaction control system provides thrust to control the vehicle after powered flight. For small corrections in yaw, pitch, and roll attitude control, the system utilizes six individually controlled, fixed-axes, constant-thrust, hydrogen peroxide reaction engines. These engines are mounted in clusters of three, 180 deg apart on the periphery of the main propellant tanks at the interstage adapter separation plane. Each cluster contains one 6-lb-thrust engine for pitch control and two 3.5-lb-thrust engines for yaw and roll control. In addition, four 50-lb-thrust hydrogen peroxide engines are installed on the aft bulkhead, with thrust axes parallel with the vehicle axis. These engines are for use during retromaneuver and for executing larger attitude corrections if necessary.

The *Centaur* stage utilizes a VHF telemetry system with a single antenna transmitting through the nose fairing cylindrical section on a frequency of 225.7 mc. The telemetry system provides data on 149 measurements from transducers located throughout the second stage and spacecraft interface area as well as a spacecraft composite signal from the spacecraft central signal processor.

Redundant range safety command receivers are employed on the *Centaur*, together with shaped charge destruct units for the second stage and spacecraft. This provides the Range Safety Officer with means to terminate the flight by initiating *Centaur* main engine cutoff and destroying the vehicle and spacecraft retrorocket. The system can be safed by ground command, which is normally transmitted by the Range Safety Officer when the vehicle has reached injection energy.

A waiver has been obtained for *Surveyor* missions to permit elimination of the inadvertent separation system, which was designed to provide for the automatic destruction of the *Centaur* and spacecraft in the event of premature spacecraft separation.

A C-band tracking system is contained on the *Centaur* which includes a light-weight transponder, circulator, power divider, and two antennas located under the insulation panels. The C-band radar transponder provides real-time position and velocity data for the Range Safety Instantaneous Impact Predictor as well as data for use in guidance and trajectory analysis.

C. Launch Vehicle/Spacecraft Interface

The general arrangement of the *Surveyor/Centaur* interface is illustrated in Fig. III-2. The spacecraft is completely encapsulated within a nose fairing/adapter system in the final assembly bay of the Explosive Safe Facility prior to being moved to the launch pad. This encapsulation provides protection for the spacecraft from the environment before launch as well as from aerodynamic loads during ascent.

The spacecraft is first attached to the forward section of a two-piece, conical adapter system of aluminum sheet and stringer design by means of three latch mechanisms, each containing a dual-squib pin puller. The following equipment is located on the forward adapter: three separation spring assemblies each containing a linear potentiometer for monitoring separation; a 52-pin electrical connector with a pyrotechnic separation mechanism; three pedestals for the spacecraft-mounted separation sensing and arming devices; a shaped-charge destruct assembly directed toward the spacecraft retromotor; an accelerometer for monitoring lateral vibration at the separation plane; and a diaphragm to provide a thermal seal and to prevent contamination from passing to the spacecraft compartment from the *Centaur* forward equipment compartment.

The low-drag nose fairing is an RF-transparent, clamshell configuration consisting of four sections fabricated of laminated fiberglass cloth faces and honeycomb fiberglass core material. Two half-cone forward sections are brought together over the spacecraft mounted on the forward adapter. An annular thermal bulkhead between

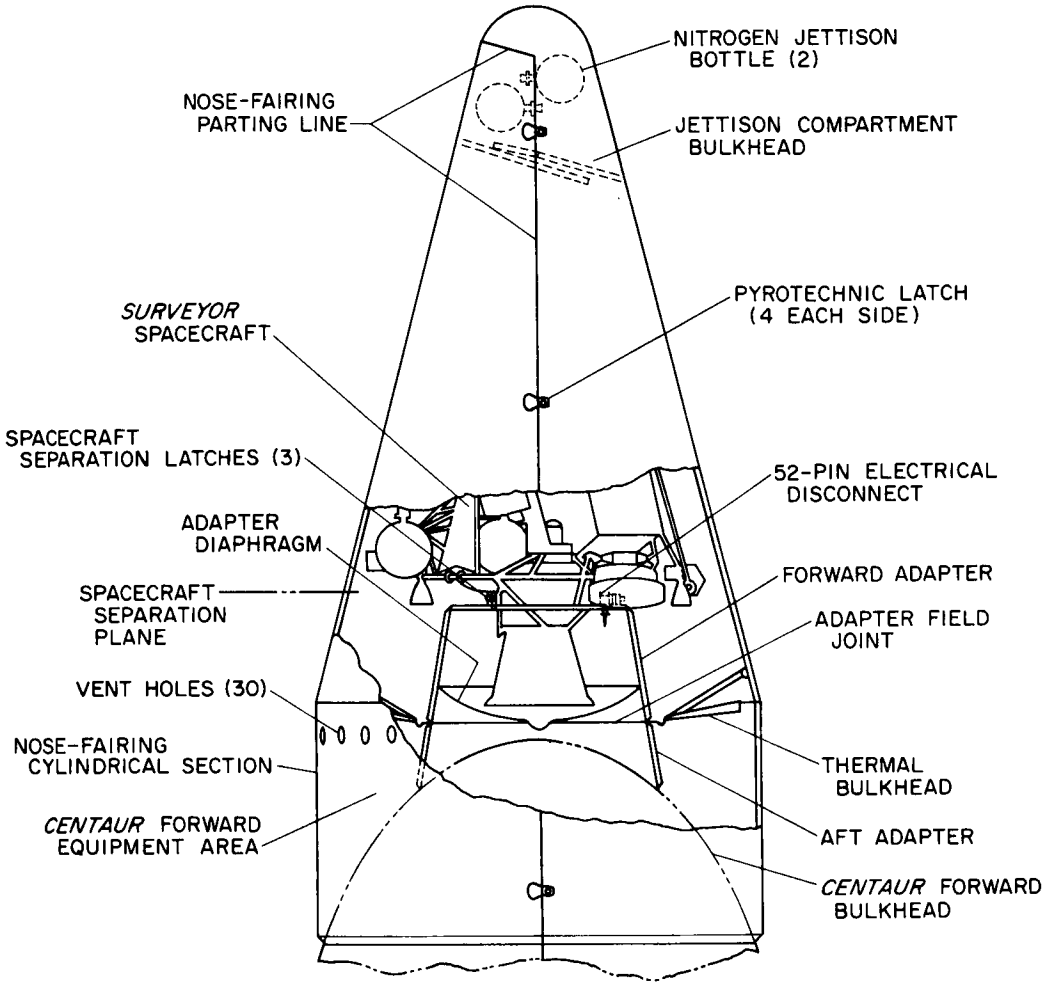

Fig. III-2. *Surveyor/Centaur* interface configuration

the adapter and base of the conical section completes encapsulation of the spacecraft.

The encapsulated spacecraft assembly is mated to the *Centaur* at a flange field joint requiring 72 bolts between the forward and aft adapter sections. The remaining two half-cylindrical sections of the nose fairing are attached to the forward end of the *Centaur* tank around the equipment compartment prior to mating of the spacecraft. Doors in the cylindrical sections provide access to the adapter field joint. The electrical leads from the forward adapter are carried through three field connectors and routed across the aft adapter to the *Centaur* umbilical connectors and to the *Centaur* programmer and telemetry units.

Special distribution ducts are built into the nose fairing and forward adapter to provide air conditioning of the spacecraft cavity after encapsulation and until liftoff. Seals are provided at the joints to prevent shroud leakage except out through vent holes in the cylindrical section.

The entire nose fairing is designed to be ejected by separation of two clamshell pieces, each consisting of a conical and cylindrical section. Four pyrotechnic pin-puller latches are used on each side of the nose fairing to carry the tension loads between the fairing halves. A bolted connection, with a flexible linear-shaped charge for separation, transmits loads between the nose fairing and *Centaur* tank. A nitrogen bottle is mounted in each half of the nose fairing near the forward end to supply gas for cold gas jets to force the panels apart. Hinge fittings are located at the base of each fairing half to control ejection, which occurs under vehicle acceleration of approximately 1 *g*.

D. Vehicle Flight Sequence of Events

All vehicle flight events occurred as programmed at near nominal times with no anomalies. Predicted and actual times for the vehicle flight sequence of events are included in Table A-1 of Appendix A. Figure III-3 illustrates the major nominal events. Following is a brief description of the vehicle flight sequence of events with all times referenced to liftoff (2 in. rise) unless otherwise noted.

1. *Atlas* Booster Phase of Flight

Hypergolic ignition of all five *Atlas* engines was initiated 2 sec before liftoff. Vehicle liftoff occurred at 12:31:59.824 GMT on September 20, 1966, only 8.5 sec prior to closing of the launch window. The launcher mechanism is designed to begin a controlled release of the vehicle when all engines have reached nearly full thrust. At 2 sec after liftoff, the vehicle began a 13-sec programmed roll from the fixed launcher azimuth setting of 105 deg to the desired launch azimuth of 114.36 deg. The programmed pitchover of the vehicle began 15 sec after liftoff and lasted until booster engine cutoff (BECO).

The vehicle reached Mach 1 at 58 sec and maximum aerodynamic loading occurred at 75.7 sec. During the booster phase of flight the booster engines were gimballed for pitch, yaw, and roll control, and the vernier engines were active in roll control only while the sustainer engine was centered.

At 142.2 sec, BECO was initiated by a signal from the *Centaur* guidance system when vehicle acceleration equalled 5.76 g (expected value: 5.7 ± 0.08 g). At 3.1 sec after BECO, with the booster and sustainer engines centered, the booster section was jettisoned by release of pneumatically operated latches.

2. *Atlas* Sustainer Phase of Flight

At BECO + 8 sec the *Centaur* guidance system was enabled to provide steering commands for the *Atlas* sustainer phase of flight. During this phase the sustainer engine was gimballed for pitch and yaw control, while the verniers were active in roll. The *Centaur* insulation panels were jettisoned by firing shaped charges at 176.0 sec at an altitude of approximately 50.5 nm where the aerodynamic heating rate was rapidly decreasing. At 201.9 sec, squibs were fired to unlatch the clamshell nose fairing, which was jettisoned 1.0 sec later by means of nitrogen gas thruster jets activated by pyrotechnic valves.

Other programmed events which occurred during the sustainer phase of flight were: the unlocking of the *Centaur* hydrogen-tank vent valve to permit venting as required to relieve hydrogen boiloff pressure; starting of the *Centaur* boost pumps 43 sec prior to *Centaur* main engine ignition (MEIG); and locking of the *Centaur* oxygen-tank vent valve followed by oxygen-tank pressurization.

Sustainer and vernier engine cutoff (SECO and VECO) occurred at 235.1 sec as a result of fuel depletion with oxidizer depletion imminent. Oxidizer depletion with fuel depletion imminent was the predicted cutoff mode. If cutoff had been as predicted, shutdown would have begun with an exponential thrust decay phase of about 5-sec duration due to low oxidizer inlet pressure to the turbopump and resulting loss in turbopump performance. Then, final fast shutdown by propellant valve closure would have been initiated by actuation of a switch when fuel manifold pressure dropped to 625 psi. In the predicted mode, reduction in fuel manifold pressure is caused by reduction in speed of the turbopump, which also utilizes the main fuel and oxidizer propellants. On this flight, only about 2 sec of exponential decay occurred, due to decay in oxidizer inlet pressure to the turbopump, before fast shutdown was initiated by the uncovering of a fuel depletion sensor located near the bottom of the fuel tank.

Separation of the *Atlas* from the *Centaur* occurred 1.9 sec after SECO by firing of shaped charges at the forward end of the interstage adapter. This was followed by ignition of eight retrorockets located at the aft end of the *Atlas* tank section to back the *Atlas*, together with the interstage adapter, away from the *Centaur*.

3. *Centaur* Phase of Flight Through Spacecraft Separation

The *Centaur* main engines were ignited 9.6 sec after *Atlas/Centaur* separation and burned for 439.7 sec, or until 686.25 sec. Main engine cutoff (MECO) was commanded by the guidance system when the desired injection conditions were reached. At main engine cutoff, the hydrogen peroxide engines were enabled for attitude stabilization.

During the 66.3-sec period between MECO and spacecraft separation, the following signals were transmitted to the spacecraft from the *Centaur* programmer: extend spacecraft landing gear; unlock spacecraft omniantennas; turn on spacecraft transmitter high power. An arming

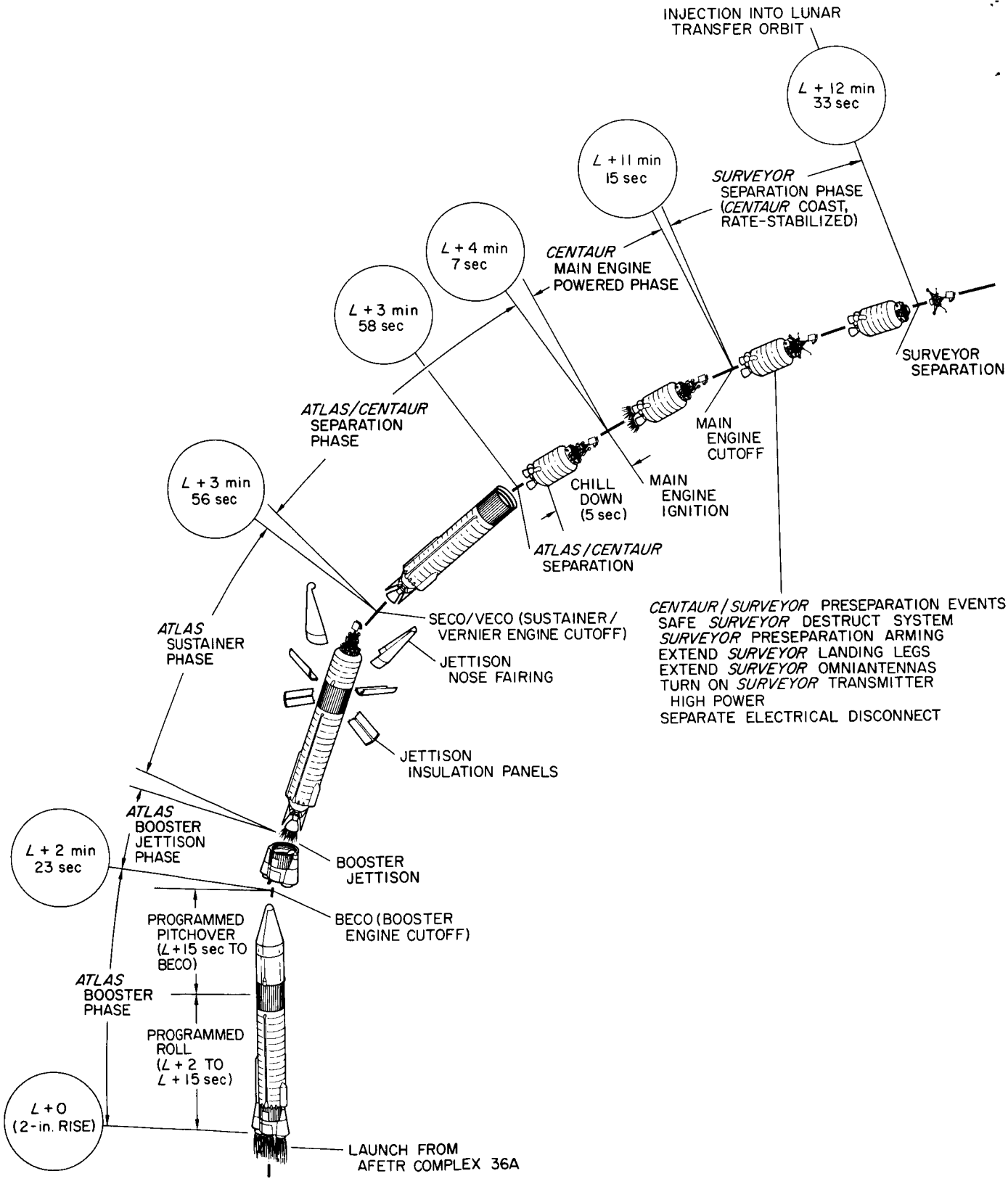

Fig. III-3. Launch phase nominal events

signal also was provided by the *Centaur* during this period to enable the spacecraft to act on the preseparation commands.

The *Centaur* commanded separation of the spacecraft electrical disconnect 5.5 sec before spacecraft separation, which was initiated at 752.6 sec. The *Centaur* attitude-control engines were disabled for 5 sec during spacecraft separation in order to minimize vehicle turning moments.

4. Centaur Retromaneuver

At 5 sec after spacecraft separation, the *Centaur* began a turnaround maneuver using the attitude-control engines to point the aft end of the stage in the direction of the flight path. Four sec after the *Centaur* had reached the mid-point of the turn and while continuing the turn, two of the 50-lb-thrust hydrogen peroxide engines were fired for a period of 20 sec to provide initial lateral separation of the *Centaur* from the spacecraft. At 240 sec after separation, the propellant blowdown phase of the *Centaur* retromaneuver was initiated by opening the hydrogen and oxygen prestart valves. Oxygen was vented through the engine nozzles while hydrogen discharged through vent tubes. Propellant blowdown was terminated after 250 sec by closing the prestart valves. At the same time (1242.9 sec) the *Centaur* power change-over switch was energized to turn off all power except telemetry and C-band beacon.

E. Performance

The *Atlas/Centaur* AC-7 vehicle performance was near nominal, providing a very satisfactory powered flight phase and accurate injection of the *Surveyor II* spacecraft into the prescribed lunar transfer trajectory.

1. Guidance and Flight Control

Performance of the guidance system was excellent as evidenced by the projected miss distance of the injected spacecraft of only about 142 km from the prelaunch aiming point. (Refer to Section VII for a presentation of vehicle guidance accuracy results in terms of equivalent midcourse velocity correction.)

The guidance system discrete commands (BECO, SECO backup, and MECO) were issued well within system tolerance. When guidance steering was enabled from BECO+8 until SECO and again from main engine ignition (MEIG)+4 sec until MECO, the initial attitude errors (maximum 6 deg nose up and 3 deg nose right) were quickly nulled, after which the vehicle was held in close alignment with the commanded steering vector.

Autopilot performance was satisfactory throughout the flight, with proper initiation of programmed events and control of vehicle stability. Vehicle transients at liftoff were similar to those occurring on previous *Centaur* flights and were quickly damped following autopilot activation at 42-in. motion. Vehicle disturbances during the balance of the flight were at or below the expected levels based on previous flights, except for a brief but high roll transient occurring about 5 sec after booster jettison and an unexplained high roll torque during the first 8 sec of the *Centaur* turn-around maneuver.

The *Centaur* reaction control system apparently performed properly, maintaining vehicle control throughout the entire post-MECO and retromaneuver period, when the system was active. Hydrogen peroxide engine duty cycles averaged less than 2%.

2. Propulsion and Propellant Utilization

Both *Atlas* and *Centaur* propulsion systems operated satisfactorily throughout the flight. As has occurred on previous flights, the *Centaur* engines burned longer than expected (about 3 sec), but this was a relatively small deviation in relation to the allowable dispersion.

All vehicle propellant systems performed properly. The *Atlas* propellant utilization (PU) system controlled propellants to effect nearly simultaneously depletion at SECO with fuel depletion shutdown. This resulted in minimum propellant residuals above the pump inlets.

The *Centaur* PU system also performed well, controlling the calculated unbalance of propellants at MECO to 33 lb of liquid hydrogen. Comparing this to the predicted value of 15 lb residual hydrogen indicates a *Centaur* PU system error of 18 lb excess hydrogen. The Centaur "burnable" residuals were calculated to be 131 lb oxygen and 59 lb hydrogen, which could have provided an additional burn time of about 2.3 sec at normal engine flow rates until theoretical oxygen depletion. The predicted values for burnable residuals were 205 lb oxygen and 56 lb hydrogen for a completely nominal flight.

3. Pneumatics, Hydraulics, and Electrical Power

Pressure stability and regulation were satisfactory in both the *Atlas* and *Centaur* hydraulic and pneumatic

circuits, and propellant tank pressures were maintained within the required limits to assure structural integrity.

Performance of vehicle electrical power systems, including range safety power supplies, was normal throughout the flight except for somewhat higher than expected current demands on the *Centaur* electrical system commencing with squib firing for spacecraft separation. Postflight investigation and simulation tests indicate that the abnormal power demands were probably due to a faulty thermal relay in the squib firing circuit. The thermal relays are designed to remove power to the squibs after squib firing because of the high probability that the squibs will develop short circuits when fired. On this flight, it is believed the leads to one of the thermal relays were shorted because of a design defect.

4. Telemetry, Tracking, and Range Safety Command

In general, the *Atlas* and *Centaur* instrumentation and telemetry systems functioned satisfactorily. However, some instrumentation anomalies occurred, including failure of three of the five accelerometers located at the spacecraft/adapter interface to provide vibration data. Cause for the failure to obtain vibration output from the three accelerometers is presently believed to be due to faulty harness connections between the transducers and amplifiers. *Atlas* signal dropout (for 138 millisec) and *Centaur* signal degradation occurred as expected at booster jettison. Some radio frequency interference (RFI) was noted on a few of the *Centaur* telemetry channels until nose fairing separation, when the RFI pattern presumably changed. Cause for the RFI is unknown since protective shielding had been added to the telemetry system design following detection of RFI susceptibility during the AC-6 development flight prelaunch checkout.

Performance of the *Atlas* and *Centaur* range safety command systems was satisfactory. At 9.9 sec after MECO, a range safety command to disable the destruct system was sent from Antigua and properly executed.

5. Vehicle Loads and Environment

All vehicle loads were within expected ranges. Aerodynamic bending loads were well within vehicle capability and less than the predicted values, based upon wind sounding data obtained two hours before launch.

In general, the vibration profile of the AC-7 vehicle appeared to be similar to that of preceding *Centaur* flights. However, the AC-7 vibration environment cannot be as well established because of the failure of three of the five accelerometers installed in the vicinity of the *Centaur/Surveyor* interface. The only high-frequency accelerometer on a continuous telemetry channel was among the three from which useful telemetry output was not obtained. The only unusual oscillation observed was a high roll rate of 4.3 deg/sec (peak to peak) which occurred 5.3 sec after booster jettison (0.4 sec after *Centaur* guidance enable). (See Section IV-A for a discussion of spacecraft launch phase vibration environment.)

Special transducers were installed at the base of the *Atlas* stage on this flight and the previous flight of AC-8 to obtain data for improvement of the base pressure model which is used for trajectory design. Data from this flight indicated generally lower base pressure levels than obtained for the AC-8 flight.

The *Surveyor* compartment pressure dropped in a normal manner from atmospheric to essentially zero at $L + 107$ sec.

6. Separation and Retro Maneuver Systems

All vehicle separation systems functioned normally, although the magnitude of high-frequency transients associated with shaped charge firing is not well determined owing to missing accelerometer data.

Booster section jettison occurred as planned under sustainer engine pitch and yaw attitude control. Relatively high roll and yaw transient rates occurred as a result of this event.

Proper separation of all four insulation panels was confirmed by indications received from four breakwires, one of which was attached to each panel near a hinge arm. Only low transient rates were imparted to the vehicle as a result of this event, providing further evidence of the improvement afforded by the redesigned panel hinges first flown on AC-10.

Normal separation of the nose-fairing was verified by indications from disconnect wires which were utilized for the first time on this flight. These were incorporated in the pullaway electrical connectors of each fairing half. As expected, there was no indication of pressure buildup in the spacecraft compartment at nose-fairing thruster bottle actuation.

Atlas/Centaur separation occurred as planned. Telemetry data indicated all eight *Atlas* retro rockets fired. The

pitch rate gyros indicated no vehicle rotation in the critical pitch plane during this separation event.

At spacecraft separation, all three pyrotechnic release latches actuated within 1 millisec of each other. Data from the extensometers indicated that the three spring assemblies extended normally, producing a spacecraft separation rate of about 1 ft/sec. Residual *Centaur* rotation at separation was 0.19 deg/sec as determined from *Centaur* gyro data. No angular motion between the spacecraft and *Centaur* could be detected from the three extensometers traces, which show that spring stroke vs time was identical for the springs.

The *Centaur* retromaneuver was executed as planned. Five hours after spacecraft separation, the distance between the *Centaur* and spacecraft had increased to 730 km, which is well in excess of the required minimum separation of 336 km at that time. The *Centaur* closest approach to the moon was 5,675 km.

IV. Surveyor Spacecraft

The *Surveyor II* spacecraft was to have flown a flight profile quite similar to that flown on *Surveyor I*. The *Surveyor II* primary flight objectives were (1) to soft-land on the lunar surface at a site east of the *Surveyor I* landing point (0.00 deg latitude and 0.67 deg west longitude in Sinus Medii), (2) to demonstrate the capability of the spacecraft to land with an oblique approach angle not greater than 25 deg (predicted approach angle was 23 deg from the vertical), (3) to transmit post-landing television pictures, and (4) to obtain touchdown dynamics, radar reflectivity, and lunar surface thermal data. To these ends, the *Surveyor II* spacecraft performed the early phases of the mission up to midcourse as planned. During execution of the midcourse maneuver, one vernier engine failed to fire, resulting in a spacecraft tumbling condition which prevented attainment of planned mission objectives. The third vernier engine also failed to ignite during each of 39 post-midcourse attempts to fire the vernier engines.

The *Surveyor II* spacecraft failure was thoroughly investigated by a formally appointed Failure Review Board. Although this investigation did not disclose a specific cause for the failure, many recommendations have been made by the Board to provide on future missions a greater assurance of spacecraft flight readiness and better preflight and in-flight diagnostic data.

A. Spacecraft System

In the *Surveyor* spacecraft design, the primary objective was to maximize the probability of successful spacecraft operation within the basic limitations imposed by launch vehicle capabilities, the extent of knowledge of transit and lunar environments, and the current technological state of the art. In keeping with this primary objective, design policies were established which (1) minimized spacecraft complexity by placing responsibility for mission control and decision-making on earth-based equipment wherever possible, (2) provided the capability of transmitting a large number of different data channels from the spacecraft, (3) included provisions for accommodating a large number of individual commands from the earth, and (4) made all subsystems as autonomous as practicable.

Figure IV-1 illustrates the *Surveyor* spacecraft in the cruise mode and identifies many of the major components. A simplified functional block diagram of the spacecraft system is shown in Figure IV-2. The spacecraft design is discussed briefly in this section and in greater detail in the subsystem sections which follow. A detailed configuration drawing of the spacecraft is contained in Appendix B. The configuration of the *Surveyor* spacecraft is dictated by the selection of a tripod landing gear with three foldable landing legs for the soft landing.

1. Spacecraft Coordinate System

The spacecraft coordinate system (Fig. IV-3) is an orthogonal, right-hand Cartesian system. Figure IV-4 shows the spacecraft motion about its coordinate axes relative to the celestial references. The cone angle of the earth is the angle between the sun vector and the earth vector as seen from the spacecraft. The clock angle of the earth is measured in a plane perpendicular to the sun vector from the projection of the star Canopus vector to the projection of the earth vector in the plane. The

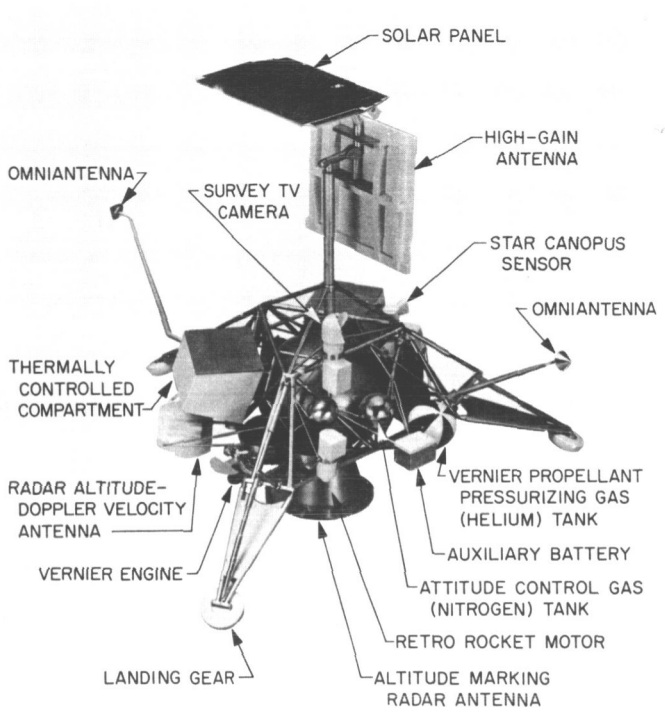

Fig. IV-1. *Surveyor II* spacecraft in cruise mode

spacecraft coordinate system may be related to the cone and the clock angle coordinate system, provided sun and Canopus lock-on has been achieved. In this case the spacecraft minus Z-axis is directed toward the sun, and the minus *X*-axis is coincident with the projection of the Canopus vector in the plane perpendicular to the direction of the sun.

2. Spacecraft Mass Properties

Surveyor II weighed 2203.67 lb at launch, with a final predicted touchdown weight of 644.07 lb nominal. Center of gravity of the vehicle is kept low to obtain stability over a wide range of landing conditions. Center-of-gravity limits after *Surveyor/Centaur* separation for midcourse and retro maneuvers are constrained by the attitude correction capabilities of the flight control and vernier engine subsystems during retrorocket burning. Limits of travel of the vertical center of gravity in the touchdown configuration are designed to landing site assumptions and approach angle requirements so that the spacecraft will not topple when landing.

3. Structures and Mechanisms

The structures and mechanisms subsystem provides basic structural support (including touchdown stabilization), mechanical actuation, thermal protection, and electronic packaging and cabling. A tubular aluminum spaceframe is utilized for basic structural support. Three landing leg assemblies and crushable blocks for lunar landing are attached to the spaceframe. Other mechanisms provided are the high-gain antenna and solar panel positioner (A/SPP), two omniantenna mechanisms, a separation sensing and arming device, the secondary sun sensor, and pyrotechnic devices. Two compartments incorporating special insulation and thermal switches are provided for thermal protection of critical spacecraft components.

4. Thermal Control

Thermal control of equipment over the extreme temperature range of the lunar surface ($+260$ *to* $-260°$F) is accomplished by a combination of passive, semipassive, and active methods including the use of heaters controlled by ground command. The design represents the latest state of the art in the application of structural and thermal design principles to lightweight spacecraft. Units that require critical thermal control are the approach and survey television cameras, altitude marking radar, Compartments A and B, and vernier engine propellant tanks and lines.

5. Electrical Power

The electrical power subsystem is designed to generate, store, convert, and distribute electrical energy. A single solar panel is utilized which is capable of generating continuous unregulated power at 90 to 55 w, depending upon environmental temperature and incidence angle of solar radiation. Peak unregulated power capability is limited to 1000 w by the two spacecraft batteries (main and auxiliary). The initial energy storage of the subsystem is 4400 w-hr. Only one battery, the main battery, can be recharged, to an energy storage of 3520 w-hr. The batteries determine the unregulated power voltage and are designed to sustain a voltage between 17.5 and 27.5 v, with a nominal value of 22 v. The unregulated power is distributed to the loads via an unregulated bus.

Regulated power is provided by a boost regulator at 29 v, controlled to 1% for the flight control and "nonessential" loads and to 2% for the "essential" loads. The maximum regulated power capability of the boost regulator is 270 w.

6. Propulsion

The propulsion subsystem supplies thrust force during the midcourse correction and terminal descent phases of

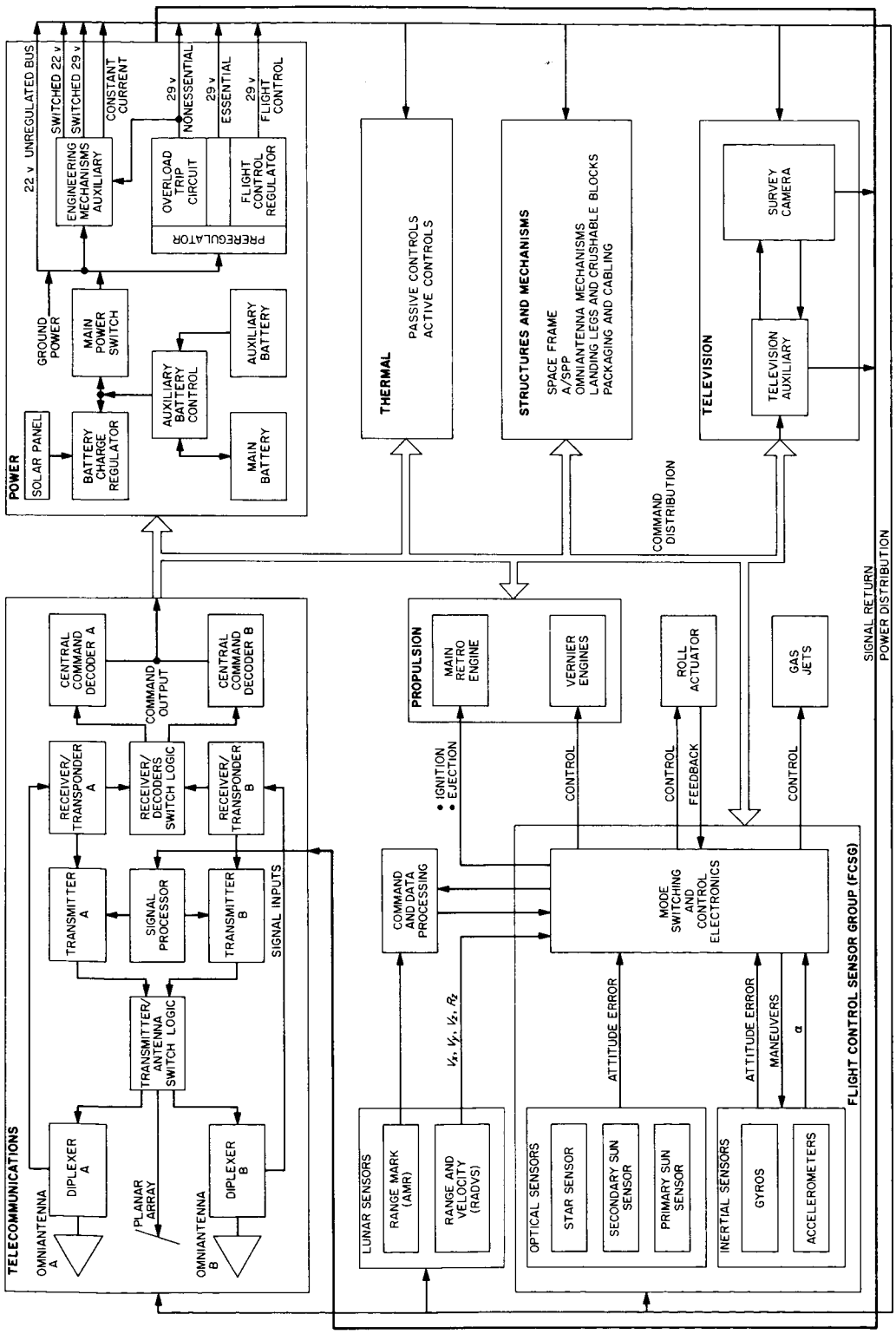

Fig. IV-2. Simplified spacecraft functional block diagram

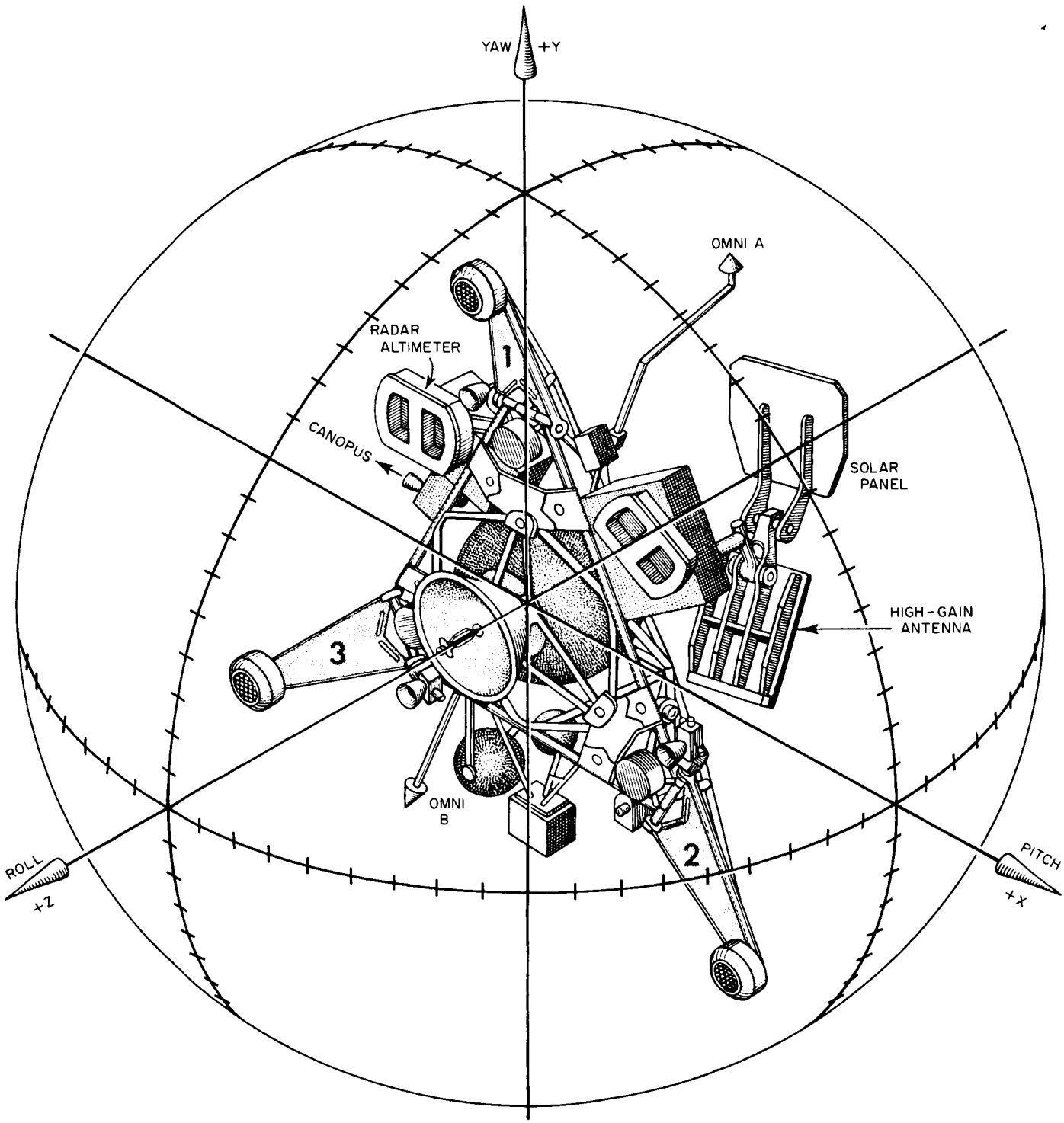

Fig. IV-3. Spacecraft coordinate system

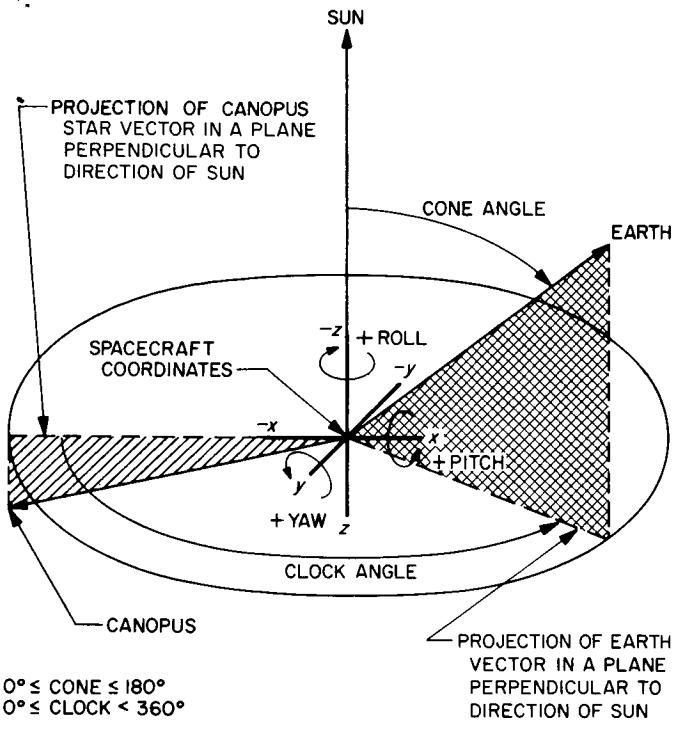

Fig. IV-4. Spacecraft coordinates relative to celestial references

the mission. The propulsion subsystem, consisting of a bipropellant vernier engine system and a solid-propellant main retrorocket motor, is controlled by the flight control system through preprogrammed maneuvers, commands from earth, and maneuvers initiated by flight control sensor signals.

The three thrust chambers of the vernier engine subsystem supply the thrust forces for midcourse maneuver velocity vector correction, attitude control during main retrorocket burning, and velocity vector and attitude control during terminal descent. The thrust of each vernier engine can be throttled over a range of 30 to 104 lb.

The main retrorocket, which performs the major portion of the deceleration of the spacecraft during lunar landing maneuver, is a spherical, solid-propellant motor with partially-submerged nozzle to minimize overall length.

7. Flight Control

The purpose of the flight control subsystem is to control spacecraft flight parameters throughout the transit portion of the mission. Flight control uses three forms of reference to perform its function. These are celestial sensors, inertial sensors, and radar sensors. The outputs of each of these sensors are utilized by analog electronics to create thrust commands for operation of attitude gas jets and the spacecraft vernier and main retro propulsion systems. Flight control requires ground commands for initiation of various sequences and performance of "manual" operations. Flight control programming initiates and controls other sequences.

The celestial sensors allow the spacecraft to be locked to a specific orientation defined by the vectors to the sun and the star Canopus and the angle between them. Initial search and acquisition of the sun is accomplished by the secondary sun sensor. The primary sun sensor then maintains the orientation with the sun line.

Of the inertial sensors, integrating gyros are used to maintain spacecraft orientation inertially when the celestial references are not available. Accelerometers measure the thrust levels of the spacecraft propulsion systems during midcourse correction and terminal descent phases.

The attitude gas jets are cold gas (nitrogen) reaction devices for control of the orientation of spacecraft attitude in all three axes during coast phases of the flight. They are installed in opposing pairs near the ends of the three landing legs. The three vernier engines provide thrust, which can be varied over a wide range, for midcourse correction of the spacecraft velocity vector and controlled descent to the lunar surface. A roll actuator tilts the thrust axis of Vernier Engine 1 away from the spacecraft roll axis for attitude and roll control during thrust phases of flight when the attitude gas jets are not effective. The main retro motor is utilized to remove the major portion of the spacecraft approach velocity during terminal descent.

8. Radar

Two radar systems are employed by the *Surveyor* spacecraft. An altitude marking radar (AMR) provides a mark signal to initiate the main retro sequence. In addition, a radar altimeter and doppler velocity sensor (RADVS) functions in the flight control subsystem to provide three-axis velocity, range, and altitude mark signals for flight control during the main retro and vernier phases of terminal descent. The RADVS consists of a doppler velocity sensor, which computes velocity along each of the spacecraft *X*, *Y*, and *Z* axes, and a radar altimeter, which computes slant range from 50,000 ft to 14 ft and generates *1000-ft mark* and *14-ft mark* signals.

Table IV-1. Content of telemetry signals from spacecraft

Data mode	Source	Significance	Number of points sampled	Form	Comments
Commutator Mode 1	Flight control, propulsion	Provides data required for midcourse maneuver and preretro terminal maneuver	100	Digital	Modes 1, 2, 3, and 4 used one at a time on command per Standard Sequence of Events (SSE)
Commutator Mode 2	Flight control, propulsion, approach TV, AMR, RADVS	Provides data required for retro descent	100	Digital	
Commutator Mode 3	Inertial guidance, approach TV, AMR, RADVS, vernier engines	Provides data required for vernier descent	50	Digital	
Commutator Mode 4	Temperatures, power status, telecommunications	Provides data required for miscellaneous transit and lunar surface operations	100	Digital	
Cruise phase commutator Mode 5	Flight control, power status, temperature	Provides data required during cruise mode to determine general spacecraft status	120	Digital	Used on command per SSE
Thrust phase commutator Mode 6	Flight control, power status, AMR, RADVS, vernier engine conditions	Provides data required for backup of Modes 1, 2, and 3 during thrusting maneuvers	120	Digital	Used on command per SSE
TV commutator Mode 7	TV survey camera	Provides frame identification while survey TV is operating	16	Digital	Frame ID alternates with analog video signals
Vibration data	Launch phase accelerometers	Indicates vibration during launch phase	4	Analog	Transmitted over Centaur telemetry link only
	Post-DSIF acquisition phase accelerometers	Designed to indicate vibration from main retro motor and vernier engine firings and mechanical shock during landing	4	Analog	Installed but not used on *Surveyors I* and *II*
Shock absorber data	Strain gages	Measures strain on landing gear due to landing shock	3	Analog	
Gyro speed	Inertial guidance unit	Indicates angular rate of gyro spin motors	3	Analog	Samples are pitch, roll, and yaw axes on command per SSE

9. Telecommunications

The spacecraft telecommunications subsystem provides for (1) receiving and processing commands from earth, (2) providing angle tracking and one- or two-way doppler data for orbit determination, and (3) processing and transmitting spacecraft telemetry data.

Continuous command capability is assured by two identical receivers which remain on throughout the life of the spacecraft and operate in conjunction with two omniantennas and two command decoders through switching logics.

Operation of a receiver in conjunction with a transmitter through a transponder interconnection provides a phase-coherent system for doppler tracking of the spacecraft during transit and after touchdown. Two identical transponder interconnections (Receiver/Transponder A and Receiver/Transponder B) are provided for redundancy. Transmitter B with Receiver/Transponder B is the transponder system normally operated during transit.

Data signals from transducers located throughout the spacecraft are received and prepared for telemetry transmission by signal processing equipment which performs commutation, analog-to-digital conversion, and pulse-code and amplitude-to-frequency modulation functions. Most of the data signals are divided into six groups ("commutator modes") for commutation by two commutators located within the telecommunications signal processor. (An additional commutator is located within the television auxiliary for processing television frame identification data.) The content of each commutator mode has been selected to provide essential data during particular phases of the mission (Table IV-1). Other signals, such as strain gage data which is required continuously over brief intervals, are applied directly to subcarrier oscillators.

Summing amplifiers are used to combine the output of any one commutator mode with continuous data. The composite signal from the signal processor, or television data from the television auxiliary, is sent over one of the two spacecraft transmitters. The commutators can be operated at five different rates (4400, 1100, 550, 137.5, and 17.2 bits/sec) and the transmitters at two different power levels (10 w or 100 mw). In addition, switching permits each of the transmitters to be operated with any one of the three spacecraft antennas (two omniantennas and a planar array) at either the high or low power level. Selection of data mode(s), data rate, transmitter power, and transmitter-antenna combination is made by ground command. A data rate is selected for each mission phase which will provide sufficient signal strength at the DSIF station to maintain the telemetry error rate within satisfactory limits. The high-gain antenna (planar array) is utilized for efficient transmission of video data. The *Surveyor II* data mode/rate profile is shown in Fig. IV-5.

10. Television

The *Surveyor II* television subsystem included a downward pointing camera for terminal descent photographs, a survey camera for photographs from the lunar surface, and a television auxiliary for final decoding of commands and processing of video and frame identification data for transmission by either of the spacecraft transmitters. The standard sequence of events (SSE) did not call for operation of the approach camera on the *Surveyor II* mission because it was desired to minimize spacecraft operational requirements during the complex and critical terminal descent phase. The survey camera is designed for post-landing operation to provide photographs of the lunar surface panorama, portions of the spacecraft, and the lunar sky. Photographs may be obtained in either of two modes: a 200-line mode for relatively slow transmission over an omniantenna or a 600-line mode for more efficient transmission over the planar array.

11. Instrumentation

Transducers are located throughout the spacecraft system to provide signals that are relayed to the DSIF stations by the telecommunication subsystem. These signals are used primarily to assess the condition and performance of the spacecraft. Some of the measurements also provide data useful in deriving knowledge of certain characteristics of the lunar surface.

In most cases the individual subsystems provide the transducers and basic signal conditioning required for data related to their equipment. All the instrumentation signals provided for the *Surveyor II* spacecraft are summarized by category and responsible subsystem in Table IV-2.

All of the temperature transducers are resistance-type units except for three microdiode bridge amplifier assemblies used in the television subsystem.

The voltage (signals) and position (electronic switches) measurements consist largely of signals from the command and control circuits.

Table IV-2. Spacecraft instrumentation

	Structures, mechanisms, and thermal control	Electrical power	Propulsion	Flight control	Radar	Telecommunication	Television	Total
Temperature	33	5	16	9	7	2	6	78
Pressure			2	2				4
Position (potentiometers)	7						6	13
Position (mechanical switches)	10	3						13
Position (electrical switches)				31	14	9	6	60
Current		18				2		20
Voltage (power)		6				2	1	9
Voltage (signals)				14	6	8		28
Strain gages	3		3					6
Accelerometers	8			1				9
Inertial sensors (gyro speed)				3				3
RF power						2		2
Optical				9				9

A strain gage is mounted on each of the vernier engine brackets to measure thrust and on each of the three landing leg shock absorbers to monitor touchdown dynamics.

The flight control accelerometer is mounted on the retro motor case to verify motor ignition and provide gross retro performance data. Of the remaining eight accelerometers, four are designed to provide data on the vibration environment during launch phase and four are designed to provide data on the dynamic response of spacecraft elements to flight events which occur after spacecraft separation. Only data from the retro motor accelerometer and launch phase accelerometers has been telemetered on *Surveyor* missions to date.

Additional discussion of instrumentation is included with the individual subsystem descriptions.

12. Terminal Maneuver and Descent Phase Design

The system design for automatic terminal descent, which has been developed and used for the first time in the *Surveyor* program, is described here to illustrate the critical functions required to be performed by several of the subsystems.

a. Terminal descent sequence. The terminal phase begins with the preretro attitude maneuvers (Fig. IV-6). These maneuvers are commanded from earth to reposition the attitude of the spacecraft from the coast phase sun-star reference such that the expected direction of the retro thrust vector will be aligned with respect to the spacecraft velocity vector. Following completion of the attitude maneuvers, the AMR is activated. It has been preset to generate a *mark* signal when the slant range to the lunar surface is 60 miles nominal. A backup *mark* signal, delayed a short interval after the AMR *mark* should occur, is transmitted to the spacecraft to initiate the automatic sequence in the event the AMR *mark* is not generated. A delay between the *altitude mark* and main retro motor ignition has been preset in the flight control programmer by ground command. Vernier engine ignition is automatically initiated 1.1 sec prior to main retro ignition.

During the main retro phase, spacecraft attitude is maintained in the inertial direction established at the end of the preretro maneuvers by differential throttle control of the vernier engines while maintaining the total vernier thrust at the midthrust level. The main retro burns at essentially constant thrust for about 40 sec, after which the thrust starts to decay. This tailoff is detected by an inertial switch which increases vernier thrust to the high level and initiates a programmed time delay of about 12 sec, after which the main retro motor case is

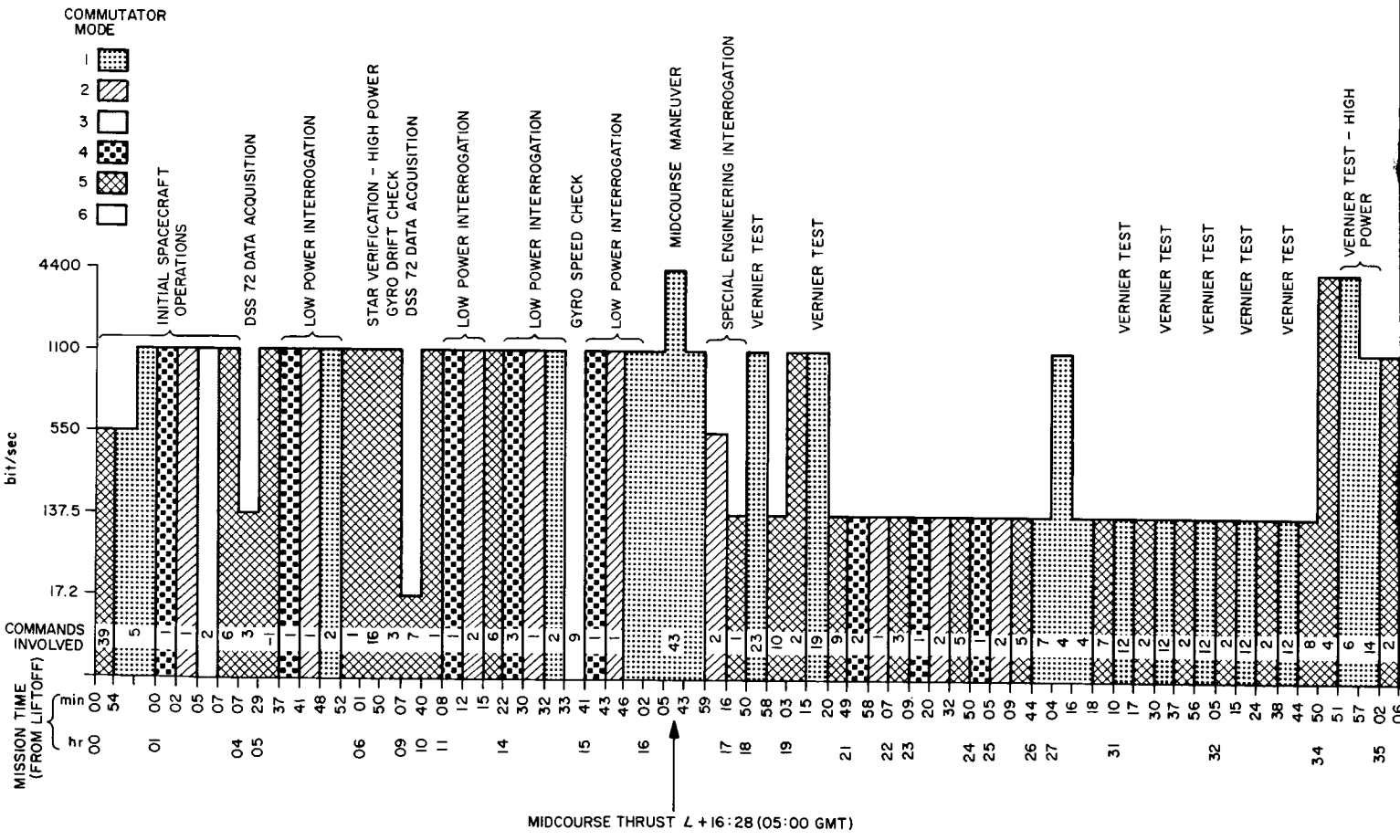
COMMUTATOR MODE
1
2
3
4
5
6
4400
1100
550
137.5
17.2
bit/sec
COMMANDS INVOLVED
MISSION TIME (FROM LIFTOFF)
min
hr
INITIAL SPACECRAFT OPERATIONS
DSS 72 DATA ACQUISITION
LOW POWER INTERROGATION
STAR VERIFICATION - HIGH POWER
GYRO DRIFT CHECK
DSS 72 DATA ACQUISITION
LOW POWER INTERROGATION
LOW POWER INTERROGATION
GYRO SPEED CHECK
LOW POWER INTERROGATION
MIDCOURSE MANEUVER
SPECIAL ENGINEERING INTERROGATION
VERNIER TEST
VERNIER TEST
VERNIER TEST
VERNIER TEST
VERNIER TEST
VERNIER TEST
VERNIER TEST - HIGH POWER
MIDCOURSE THRUST L + 16:28 (05:00 GMT)

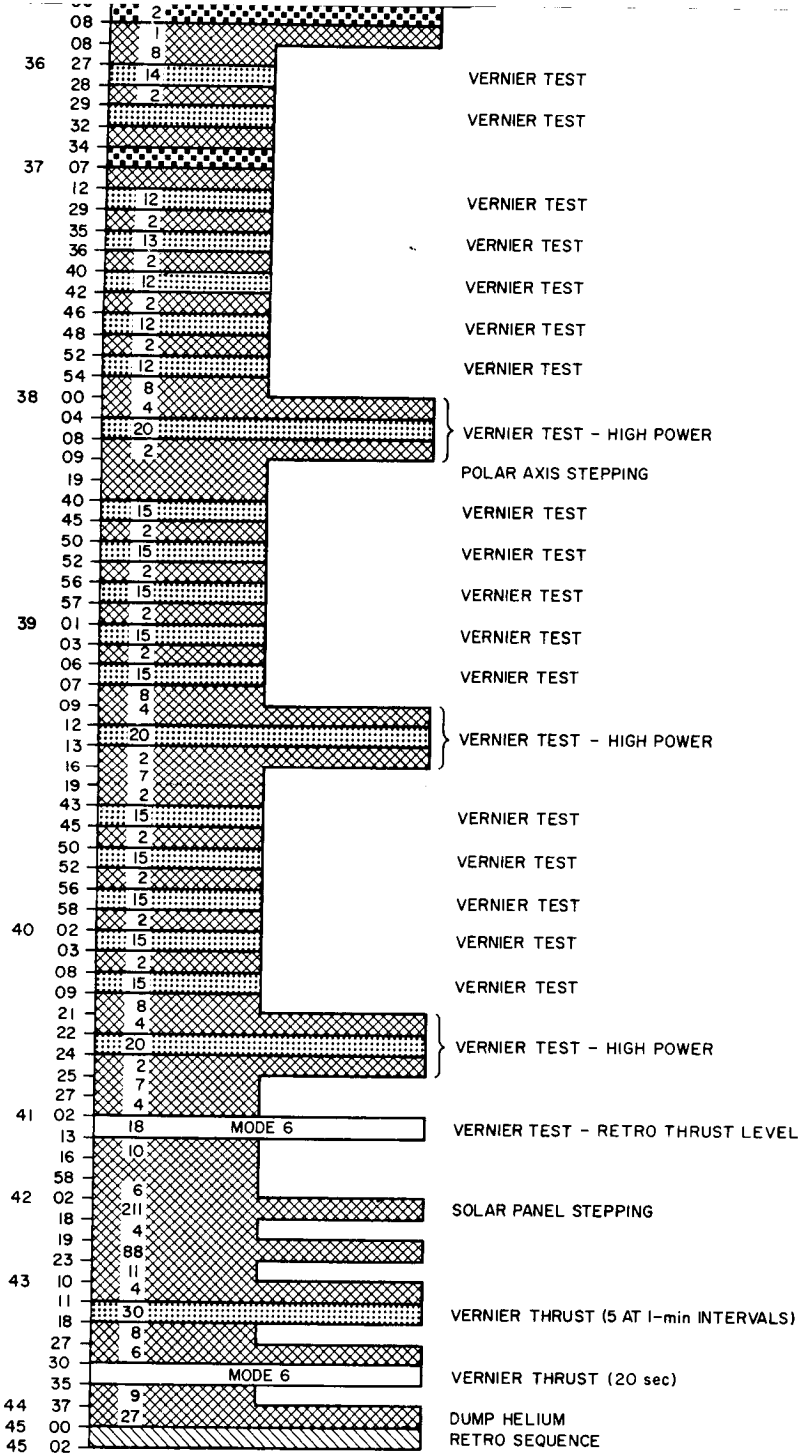

Fig. IV-5. *Surveyor II* data mode/rate profile

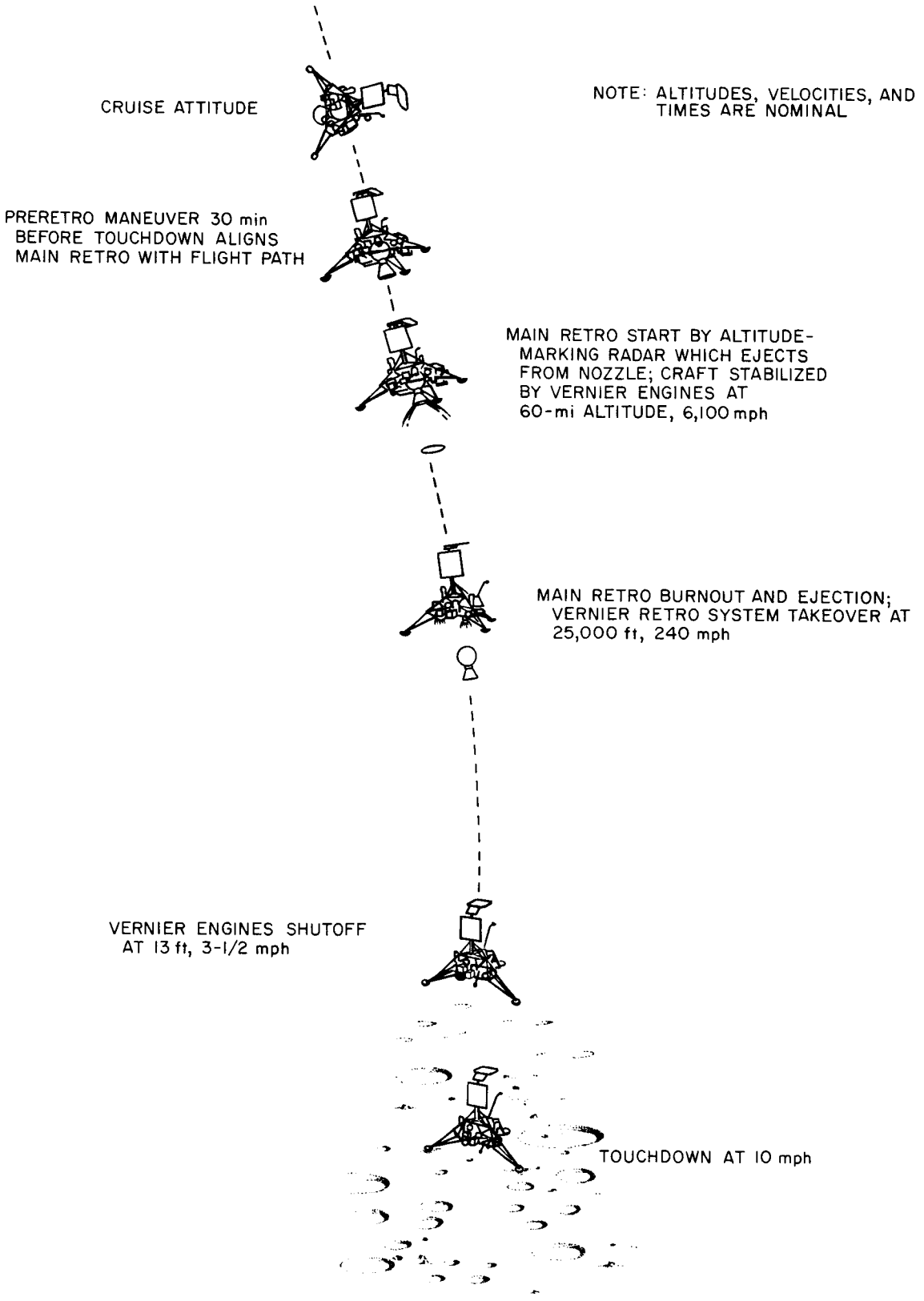

Fig. IV-6. Terminal descent nominal events

ejected. The main retro phase removes more than 95% of the spacecraft velocity and puts the spacecraft position, velocity, and attitude relative to the lunar surface within the capability of the final, vernier phase.

The vernier phase generally begins at altitudes between 10,000 and 50,000 ft and velocities in the range of 100 to 700 ft/sec. This wide range of vernier-phase initial conditions exist because of statistical variations in parameters which affect main retro burnout. About 2 sec after separation of the main retro case, vernier thrust is reduced and controlled to produce a constant spacecraft deceleration of 0.9 lunar *g*, as sensed by an axially oriented accelerometer. The spacecraft attitude is held in the preretro position until the doppler velocity sensor locks onto the lunar surface (Fig. IV-7). The thrust axis is then aligned and maintained to the spacecraft velocity vector throughout the remainder of the descent until the terminal sequence is initiated (when the attitude is again held inertially fixed). With the thrust axis maintained in alignment with the velocity vector, the spacecraft makes a "gravity turn," wherein gravity tends to force the flight path towards the vertical as the spacecraft decelerates.

The vehicle descends at 0.9 lunar *g* until the radars sense that the "descent contour" has been reached (Fig. IV-8). This contour corresponds, in the vertical case, to descent at a constant deceleration. The vernier thrust is commanded such that the vehicle follows the descent contour until shortly before touchdown, when the terminal sequence is initiated. Nominally, the terminal sequence consists of a constant-velocity descent from 40 to 13 ft at 5 ft/sec, followed by a free fall from 13 ft, resulting in touchdown at approximately 13 ft/sec.

b. Terminal descent design constraints. Constraints on the allowable main retro motor burnout conditions are of major importance in *Surveyor* terminal descent design.

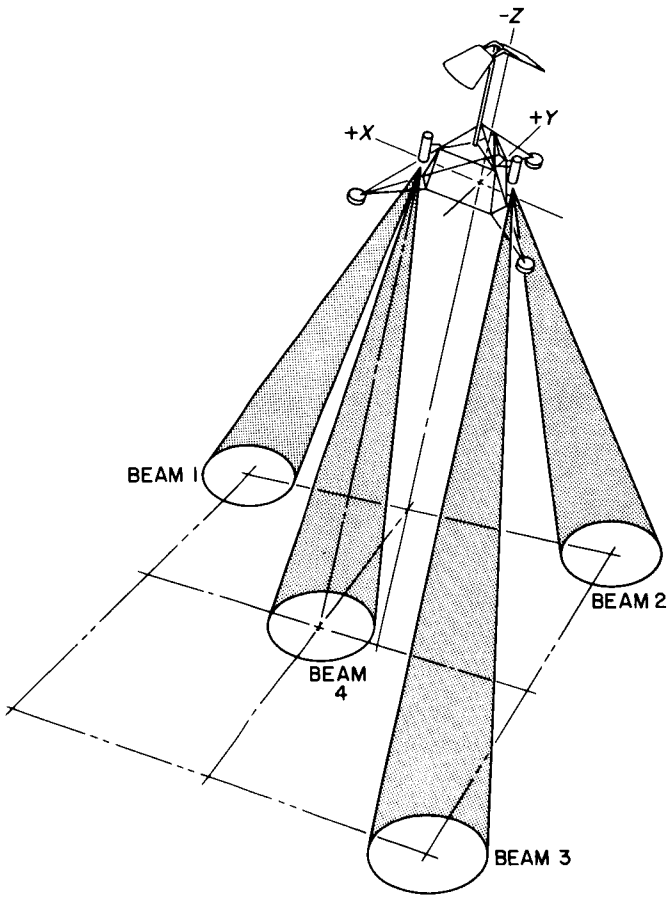

Fig. IV-7. RADVS beam orientation

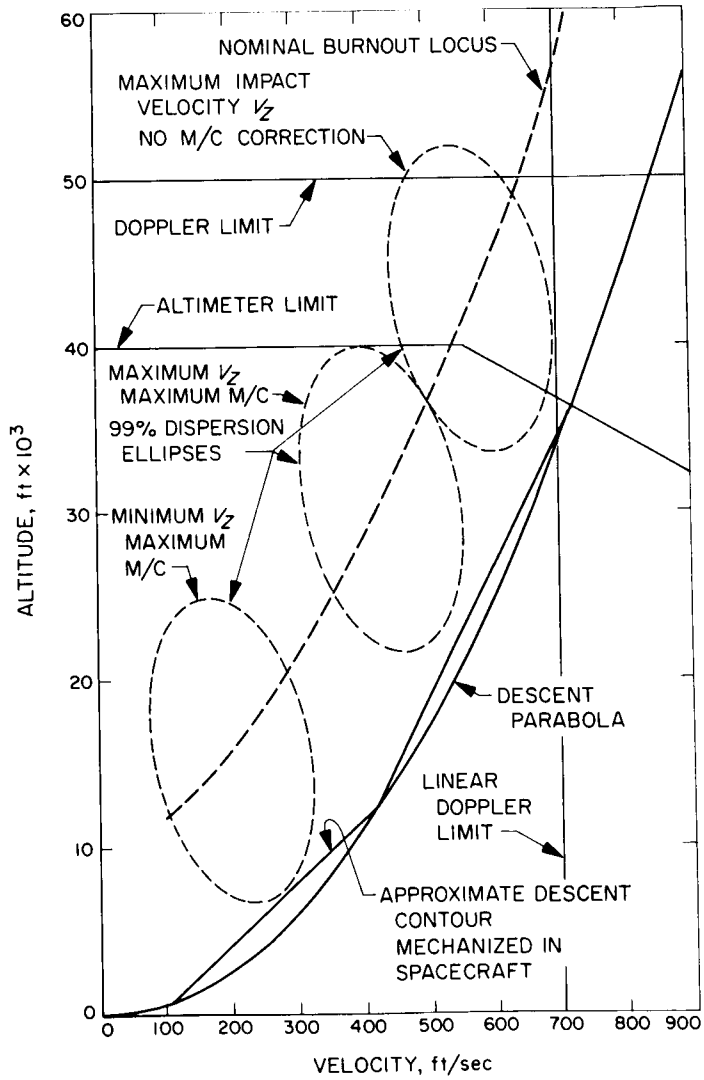

Fig. IV-8. Altitude velocity diagram

RADVS operational limitations contribute to constraints on the main retro burnout conditions. Linear operation of the doppler velocity sensor is expected for slant ranges below 50,000 ft and for velocities below 700 ft/sec. The altimeter limit is between 30,000 and 40,000 ft, depending on velocity. These constraints are illustrated in the range-velocity plane of Fig. IV-8.

The allowable main retro burnout region is further restricted by the maximum thrust capability of the vernier engine system. To accurately control the final descent, the minimum thrust must be less than the least possible landed weight (lunar gravity) of the vehicle. The result is a minimum thrust of 90 lb. This in turn constrains the maximum vernier thrust to 312 lb because of the limited range of throttle control which is possible.

Descent at the maximum thrust to touchdown defines a curve in the range-velocity plane below which main retro burnout cannot be allowed to occur. Actually, since the vernier engines are also used for attitude stabilization by differential thrust control, it is necessary to allow some margin from the maximum thrust level. Furthermore, since it is more convenient to sense deceleration than thrust, the vernier phase of terminal descent is performed at nearly constant deceleration rather than at constant thrust. Therefore, maximum thrust will be utilized only at the start of the vernier phase.

The maximum vernier phase deceleration defines a parabola in the altitude-velocity plane. For vertical descents at least, this curve defines the minimum altitude at which main retro burnout is permitted to occur with a resulting soft landing. This parabola is indicated in Fig. IV-8. (For ease of spacecraft mechanization, the parabola is approximated by a descent contour consisting of straight-line segments.)

Main retro burnout must occur sufficiently above the descent contour to allow time to align the thrust axis with the velocity vector before the trajectory intersects the contour. Thus, a "nominal burnout locus" (also shown in Fig. IV-8) is established which allows for altitude dispersions plus an alignment time which depends on the maximum angle between the flight path and roll axis at burnout.

The allowable burnout region having been defined, the size of the main retro motor and ignition altitude are determined such that burnout will occur within that region.

In order to establish the maximum propellant requirements for the vernier system, it is necessary to consider dispersions in main retro burnout conditions as well as midcourse maneuver fuel expenditures. The principal sources of main retro burnout velocity dispersion are the imperfect alignment of the vehicle prior to main retro ignition and the variability of the total impulse. In the case of a vertical descent, these variations cause dispersions of the type shown in Fig. IV-8, where the ellipse defines a region within which burnout will occur with probability 0.99. The design chosen provides enough fuel so that, given a maximum midcourse correction, the probability of not running out is at least 0.99.

The spacecraft landing gear is designed to withstand a horizontal component of the landing velocity. The horizontal component of the landing velocity is nominally zero. However, dispersions arise primarily because of the following two factors:

(1) Measurement error in the doppler system resulting in a velocity error normal to the thrust axis.

(2) Nonvertical attitude due to: (a) termination of the "gravity turn" at a finite velocity, and (b) attitude control system noise sources.

Since the attitude at the beginning of the constant-velocity descent is inertially held until vernier engine cutoff, these errors give rise to a significant lateral velocity at touchdown.

13. Design Changes

Table IV-3 presents a summary of notable differences in design between the *Surveyors I* and *II*.

14. Spacecraft Reliability

The prelaunch reliability estimate for the *Surveyor II* spacecraft was 0.66 for the flight and landing mission, assuming successful injection. The estimate was based on systems test data. Owing to the number of unit changes on the spacecraft, the reliability estimate is considered generic to *Surveyor II* rather than descriptive of the exact *Surveyor II* spacecraft configuration. Figure IV-9 shows the history of reliability estimates for *Surveyor II* during its system test phases. The detail reliability estimates for flight and landing are listed in Table IV-4. For comparative purposes, *Surveyor I* estimates are also shown.

Table IV-3. Notable differences between *Surveyors I and II*

Item	Description
Boost regulator (BR) overload trip circuit (OTC)	In *Surveyor I* the OTC in the BR was disabled because it would trip during normal operation. The *Surveyor II* BR has a redesigned OTC which does not trip during normal operation
Auto solar panel deploy logic enable	In *Surveyor I* the auto solar panel deploy logic was "enabled" by command prior to launch. In *Surveyor II* a diode was added in the harness to "enable" the auto solar panel deploy logic with the same signal from *Centaur* which causes the transmitter to switch to high power. (Solar panel deployment in both cases is initiated at separation.)
Filter chokes on input to signal processing equipment, and filter on A/D Converter No. 2 nulling amplifier in the command signal processor	Both of these design improvements were to eliminate the large variation in temperature readouts that were present on *Surveyor I* telemetry
Telemetry of flight control (FC) return signal	In *Surveyor II* the FC return signal is telemetered so that the varying harness voltage drops can be accounted for to provide more accurate data on such signals as range and velocity
A/SPP pin pullers	The A/SPP pin puller modules were redesigned to simplify installation at AFETR
A/SPP drive motors	All of the *Surveyor II* drive motors on the A/SPP have roller detents instead of the ball detents used in all but the roll axis on *Surveyor I*. This is a design improvement
Omniantenna latch and release mechanism	The *Surveyor II* release mechanisms for Omniantennas A and B were redesigned to prevent the deployment problem which occurred in flight on *Surveyor I*. The clevis opening was broadened and a kickout spring was added
Command assignments	The engineering mechanism auxiliary (EMA) on *Surveyor II* was modified to double up on the functions of two of the commands so that two command channels were available for fuel and oxidizer dump
Boost regulator FC regulator filter	The *Surveyor II* boost regulator has a new filter on the FC regulator to eliminate the oscillations which would sometimes occur and cause an overload on the shunt regulator
Velocity components $V_\perp$ and $V_\parallel$ gains in flight control sensor group (FCSG)	The $V_\perp$ and $V_\parallel$ radar attitude loop gains were reduced in *Surveyor II* to eliminate a potential instability problem at velocities greater than 535 fps
Auxiliary battery paint pattern	*Surveyor I* auxiliary battery experienced low temperature
Solder splash in signal processing equipment	All units were modified to eliminate a solder splash problem (except the spare central command decoder)
RADVS sidelobe rejection logic	Two resistors in the signal data converter were removed in order to lower the point at which the sidelobe signals are rejected from 28 to 25 db
Canopus sensor sun reference filter change	*Surveyor I* had a Canopus sensor sun filter with a reduction of 50% (filter factor of 1.5) to compensate for any possible fogging of Canopus sensor window, in accordance with recent measurements of Canopus brightness at Tucson. For *Surveyor II* the filter factor was reduced from 1.5 to 1.2 because the fogging problem did not materialize at the Canopus sensor temperature of 79°F for the *Surveyor I* flight
Canopus sensor window	The O-rings on the Canopus sensor window were changed in an effort to prevent possible fogging of the Canopus sensor filter
A/SPP pulse duration	The battery charge-regulator was changed to reduce the A/SPP stepping current pulse duration from 65 to 40 millisec. This change reduced the power dissipation in the battery charge regulator and in the A/SPP drive motors

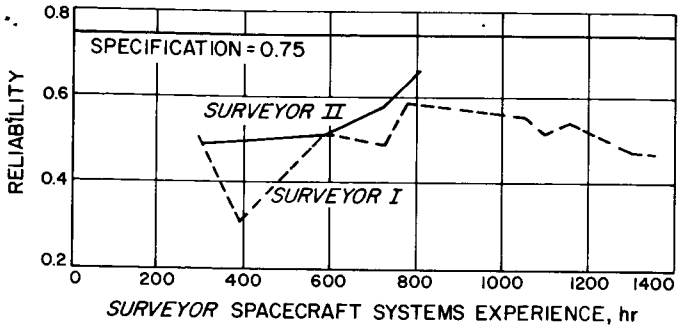

Fig. IV-9. *Surveyor II* reliability estimates

Table IV-4. *Surveyor* spacecraft reliability (flight and landing)

Subsystem	*Surveyor I*	*Surveyor II*
Telecommunications	0.922	0.941
Vehicle mechanisms	0.854	0.865
Propulsion	0.991	0.991
Electrical power	0.866	0.938
Flight controls	0.954	0.930
Subsystems net	0.645	0.704
System interaction reliability factor	0.788	0.930
Spacecraft reliability	(0.645) (0.788) = 0.51	(0.704) (0.930) = 0.66

The primary source of data for reliability estimates is the time and cycle information experienced by *Surveyor II* units during systems tests. Data from *Surveyor I* test and flight experience was included where there were no significant design differences between the units. In general, a failure is considered relevant if it could occur during a mission. Relevance of failures is based on a joint reliability/systems engineering decision.

15. Spacecraft System Performance

The *Surveyor II* spacecraft system performed well during the mission until initiation of vernier engine thrusting for the midcourse velocity correction. Table IV-5 provides a summary listing of spacecraft anomalies including the midcourse correction failure. None of the anomalies which occurred prior to the midcourse maneuver had a significant effect on the mission; however, failure of Vernier Engine 3 to provide midcourse thrust resulted in failure of the mission. (See Mission Operations Chronology (Section VI-C) for a description of spacecraft flight events.)

Table IV-5. Spacecraft anomalies

Anomaly	Effect on mission
1. Two launch phase accelerometer channels did not function properly	None. Telemetry data from third accelerometer, located on the *Centaur* side of the separation plane, was also abnormal
2. The flight control function reverted to inertial mode from rate mode 35 sec prior to separation of the spacecraft from the *Centaur*	None. The flight control was automatically placed back into the rate mode at separation (normal operation)
3. Vernier Line 2 heater was full on	None
4. During Canopus star mapping, star-lock signal was not observed when Canopus was in the field of view	None. Intentional high-gain setting of Canopus sensor, to compensate for possible window fogging, removed the capability of automatic star lock-on. Manual lock-on was executed successfully
5. Receiver B signal strength was observed to be lower than predicted after service tower removal during countdown and during star verification prior to Canopus acquisition	None. Subsequent inflight calibration of this telemetry channel indicated that the premission calibration of signal strength vs the AGC reading was in error
6. Helium transducer pressure indicated approximately a 500-psi zero shift in reading	None
7. Vernier Engine 3 did not respond properly to the vernier engine ignition command for midcourse correction. Subsequent attempts to obtain normal Engine 3 thrusting were all unsuccessful	Caused the spacecraft to tumble, preventing completion of a standard mission

During the boost phase of flight, the *Surveyor* spacecraft is subjected to a variable vibration environment consisting of acoustically induced random vibration and the transient response to discrete flight events. The *Surveyor II* space vehicle was instrumented with five accelerometers in order to obtain information on this vibration environment. The location and orientation of these accelerometers in the launch vehicle/spacecraft

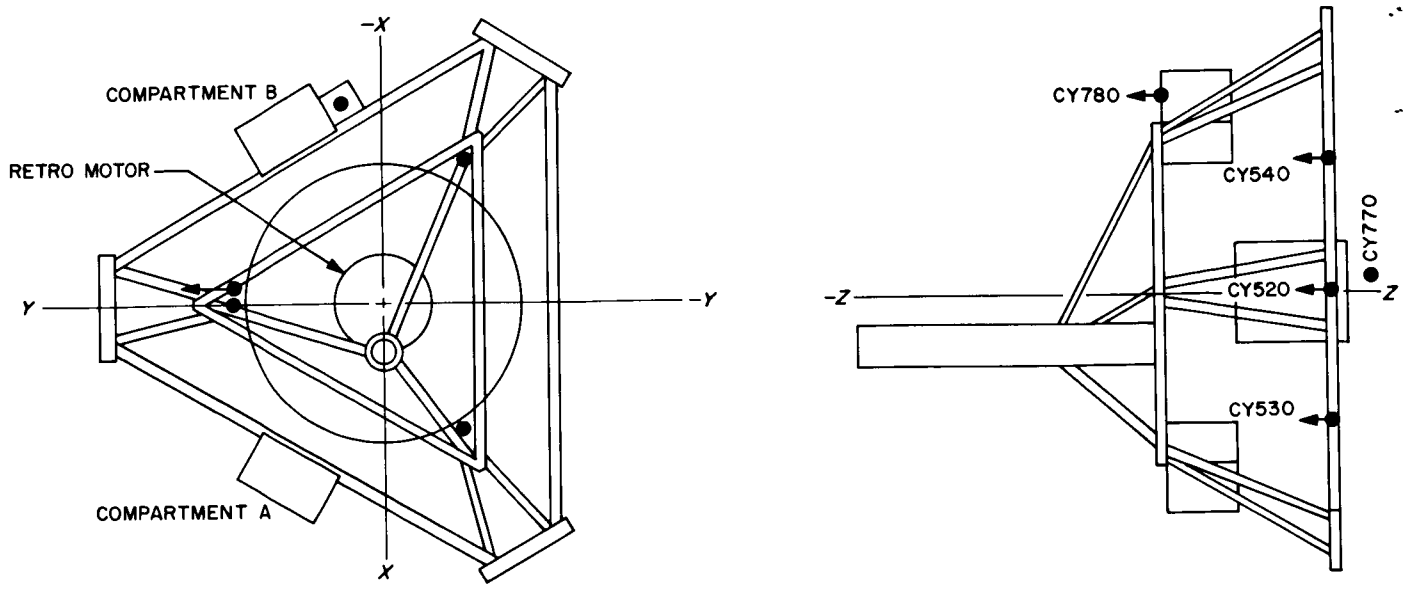

TRANSDUCER	LOCATION	RANGE, g	FREQUENCY RANGE, cps	REMARKS
CY520	SPACECRAFT, NEAR ADAPTER ATTACH POINT 1	±10	2-2500	CONTINUOUS
CY530	SPACECRAFT, NEAR ADAPTER ATTACH POINT 2	±10	2-1260	COMMUTATED
CY540	SPACECRAFT, NEAR ADAPTER ATTACH POINT 3	±10	2-1260	COMMUTATED
CY770	ADAPTER, NEAR SPACECRAFT ATTACH POINT 1	±10	2-1260	COMMUTATED
CY780	SPACECRAFT, IN FCSG	±10	2-1260	COMMUTATED

Fig. IV-10. Launch-phase accelerometer location

interface area are shown in Fig. IV-10. The Z-axis accelerometer CY520 output was telemetered continuously; the other four accelerometers were telemetered on a commutated channel.

Improper output was received from three (CY520, CY530, and CY770) of the five transducers (see also Section III for discussion of this anomaly). At this time it is believed that failure to obtain vibration output from the three accelerometers was due to faulty harnesses between the transducers and amplifiers. Output from the two transducers from which normal data was received was commutated with the output from two of the anomalous accelerometers. Therefore, valid data was provided for less than half the flight time and most of the transients were not recorded. In addition, since the two accelerometers from which good data was received were both in the Z-direction, no lateral-axis vibration data was obtained. Typical data is shown in Table IV-6 for those events which were recorded and may be compared with the *Surveyor I* flight data. The 95 percentile (approximately 2σ high) estimate of the vibration power spectral density (over the frequency bandwidth 100-1500 cps) at *Surveyor II* liftoff is 0.011 g^2/cps. The corresponding specification value is 0.0145 g^2/cps.

Shortly before spacecraft separation, a minor anomaly occurred when the flight control subsystem switched from rate to inertial mode. However, at separation from the *Centaur*, the flight control subsystem was automatically returned to the rate mode.

Star verification and acquisition sequence was nominal, except that it was necessary to achieve Canopus lock-on

Table IV-6. *Surveyor II* vibration levels during launch phase

Event and accelerometer	Maximum zero-to-peak acceleration, g[a]	
	Surveyor II	*Surveyor I*
Liftoff		
CY540	1.5	2
CY780	1.5	1
BECO		
CY780	1.5	[b]
Shroud separation		
CY780	1.25	[b]

[a]As recorded within the frequency bandwidth of 6 to 600 cps.
[b]Not measured on *Surveyor I* because of accelerometer data commutation.

by ground command rather than automatically with the spacecraft in cruise mode. During the star mapping sequence, some difficulty was experienced in readily identifying the celestial bodies because of earth and moon reflections entering the star sensor.

Telemetry data received during the star acquisition sequence indicated an apparent decrease in sensitivity of Receiver B of approximately 18 db below the predicted value. A degradation of 16 db in Receiver B sensitivity (i.e., a receiver malfunction) would have precluded the possibility of retaining two-way lock during the midcourse attitude maneuvers and thrusting sequence. A weak Receiver B signal level had also been noted during countdown operations (see Section II). However, a first evaluation of this anomaly had attributed the problem to a poor RF link due to service tower removal. Subsequent in-flight calibration of this telemetery channel indicated that the premission calibration of signal strength vs the AGC reading was in error. Midcourse maneuver was done in two-way lock, with the bit rate at 1100 rather than 550 bit/sec, since sufficient margin was predicted throughout the midcourse sequence.

When the command to ignite the three vernier engines was sent to the spacecraft as part of the standard midcourse velocity correction sequence, Vernier Engine 3 did not respond properly. The thrust provided by Vernier Engines 1 and 2 resulted in a spinning of the spacecraft at approximately 1.22 rev/sec. An initial attempt to halt the spinning, with the cold gas jets being controlled by the flight control subsystem operating in the rate mode, was terminated when approximately 60% of the available gas supply was required to reduce the spin rate to approximately 0.97 rev/sec, thereby indicating that the available gas supply would not be sufficient to stop the spacecraft rotation. Because the spacecraft was spinning about an axis such that the sun was not in the upper hemisphere of the vehicle, the solar panel was not illuminated, and the main and auxiliary batteries were the only spacecraft power sources from this point in the mission. Subsequent attempts (39 in all) to obtain normal firing of Vernier Engine 3 were unsuccessful and resulted in the spacecraft rotational rate being increased to a maximum of 2.43 rev/sec. With the available power decreasing steadily, it was decided to fire the main retro motor. Communication with the spacecraft was lost approximately 30 sec following ignition of the retro motor. The spacecraft spin rate profile is shown in Fig. IV-11.

16. *Surveyor II* Failure Review Board Summary and Recommendations

A Failure Review Board (FRB) was convened at JPL to review events surrounding the *Surveyor II* spacecraft failure and, if possible, to determine its cause. Membership of the FRB consisted of representatives from JPL, HAC, Reaction Motors Division of Thiokol, and NASA Offices of Space Science and Applications. As a result of extensive review and analysis of the available flight data pertaining to the performance of the vernier propulsion system during each thrusting period, the FRB has concluded that:

(1) Engine 3 never ignited.

(2) Engines 1 and 2 operated inconsistently during some firings following midcourse, if not also during midcourse itself.

Noted examples of performance inconsistencies obtained from analyses of thrust-command, thermal-response, and strain-gage data for the three engines are:

(1) There is no evidence of oxidizer flow to Engine 3 during midcourse, but there is evidence of possible oxidizer flow for 2.0-sec or longer firings following midcourse—all of insufficient quantity to support combustion.

(2) Engine 1 may have failed to ignite on any 0.2-sec commanded impulses, except for Firing 10. (Vernier engine firings are numbered consecutively beginning with the first post-midcourse firing.) This firing yielded a temperature response equivalent to that for the 2-sec or longer firings for some yet-unexplained reason. The extrapolated peak temperature for Engine 1 on Firing 26 is approximately 4 times as high as temperature responses observed

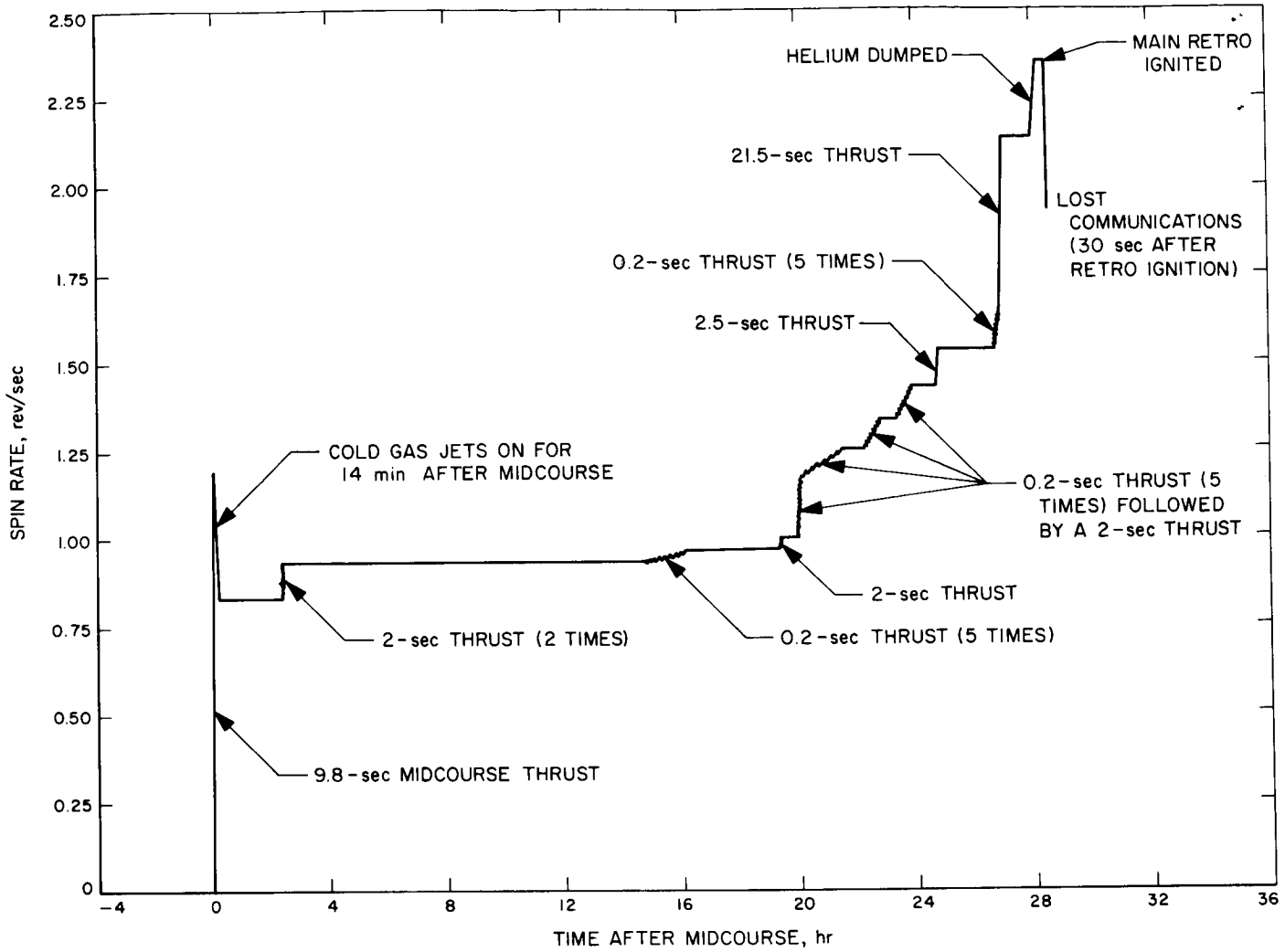

Fig. IV-11. *Surveyor II* spin rate profile

for firings of equivalent commanded duration. Consistent with this excessive temperature rise, Engine 1 flight strain gage data appears to indicate a shutdown delayed on the order of 2.5 sec beyond the shutoff command.

Oxidizer pressure data plotted from this could result in an interpretation of Firing 26 as a "normal" shutdown, the elevated temperature being a probable consequence of an "oxidizer-rich" propellant mixture. While this latter interpretation cannot be totally discounted, a preponderance of judgment supports the theory of a delayed shutdown.

(3) Engine 2 apparently ignited on all of the 0.2-sec impulses. Between 2-sec Firings 1 and 8, the extrapolated peak temperature rise underwent a factor of 3 increase, currently attributable to some unexplained performance variability.

On Firing 39 (21.5-sec duration), Engine 2 appeared to have exhibited a significantly higher than expected temperature for the commanded minimum thrust.

The above examples show the range of performance variability for Engines 1 and 2, as opposed to the sustained restriction to oxidizer flow apparently exhibited for Engine 3.

In conducting the failure investigation, the FRB has tried to identify and evaluate all possible failure modes which could account for the *Surveyor II* failure. A number of failure modes (for TCA's, tanks, lines, etc., of the VPS) have been explored and dispositioned as unlikely in accordance with interpretations of flight data. A serious handicap to this evaluation and dispositioning process

has been the lack of adequate telemetry indicative of VPS performance, particularly during thrusting periods. Certain data critical to the analyses are noisy and/or ambiguous, requiring interpretations and extrapolations which have not always netted agreements between analysts. Lack of adequate signatures of several critical data channels had also contributed to the uncertainty.

One of the problems of the FRB was to determine from the current and voltage telemetry precisely what current was drawn by the solenoid-operated valves (SOV) during vernier thrusting periods. It has been demonstrated through analysis and tests that improper electrical signals to the engine SOV solenoids could result in malfunctioning of the three vernier engines. The limiting sampling rate and noise or ripple on the telemetry channel resulted in uncertainty in the data. A significant portion of the time and energy of the committee was devoted to a study of the data, yet the FRB has been unable to support the hypothesis of an electrical failure.

The FRB has been unable to determine the precise cause of the failure. The position taken by the FRB is that it cannot postulate and support a most-probable single cause of failure—although one may exist. Since no single-failure mode has been established, the Board must leave open the possibility of multiple occurrences, possibly directly linked to a prime failure.

In recognition of failure possibilities remaining open in several areas, the FRB has recommended specific corrective actions for each suspect area without prejudice. These recommendations are contained in Appendix C. They extend to several elements of the VPS, electrical power system, and flight control; they cover design changes, improved test procedures, and reassignments of telemetry channels to provide better preflight and in-flight diagnostics.

To the extent that improved diagnostic tests (including the demonstration of electrical performance margins) can be incorporated, a higher assurance of spacecraft flight readiness should result, providing a measure of insurance against a similar type of failure in future flights.

B. Structures and Mechanisms

The vehicle and mechanisms subsystem provides support, alignment, thermal protection, electrical interconnection, mechanical actuation, and touchdown stabilization for the spacecraft and its components. The subsystem includes the basic spaceframe, landing gear mechanism, crushable blocks, omnidirectional antenna mechanisms, antenna/solar panel positioner (A/SPP), pyrotechnic devices, electronic packaging and cabling, thermal compartments, thermal switches, separation sensing and arming device, and secondary sun sensor.

1. Spaceframe and Substructure

The spaceframe, constructed of thin-wall aluminum tubing, is the basic structure of the spacecraft. The substructure is used to provide attachment between some subsystems and the spaceframe. The landing legs and crushable blocks, the retrorocket engine, the *Centaur* interconnect structure, the vernier propulsion engines and tanks, and the A/SPP attach directly to the spaceframe. The substructure is used for the thermal compartments, TV subsystem, auxiliary battery, RADVS antennas, flight control sensor group, attitude control nitrogen tank, and the vernier system helium tank.

Gyro data and linear potentiometer data indicated that the separation of the spacecraft from the *Centaur* adapter occurred as predicted without physical contact of one body with the other after initiation of separation. (Also see Section III for discussion of spacecraft separation.)

The spacecraft structure survived the boost,cruise and midcourse phases as well as numerous attempts to start Vernier Engine 3. The vibration accelerations were significant only during the boost phase.

2. Landing Gear and Crushable Blocks

The three landing-leg mechanisms are each made up of a landing leg, an intermediate A-frame, a shock absorber, a footpad, a locking strut, and a position potentiometer (Fig. IV-12).

The shock absorber, intermediate A-frame, and telescoping lock strut are interconnected to the spaceframe for folded stowage in the nose shroud. Torsion springs at the leg hinge extend the legs when the squib-actuated pin pullers are operated by *Centaur* or earth command. The hydraulic shock absorber compresses with landing load. The shock absorbers, foot pads, and crushable blocks are designed to absorb the landing shock. After landing, the shock absorbers are locked in place by squib-actuated pin locks.

The legs opened and locked in the landing position when the *Centaur* gave the command. This was verified by the potentiometers and the locking strut microswitches.

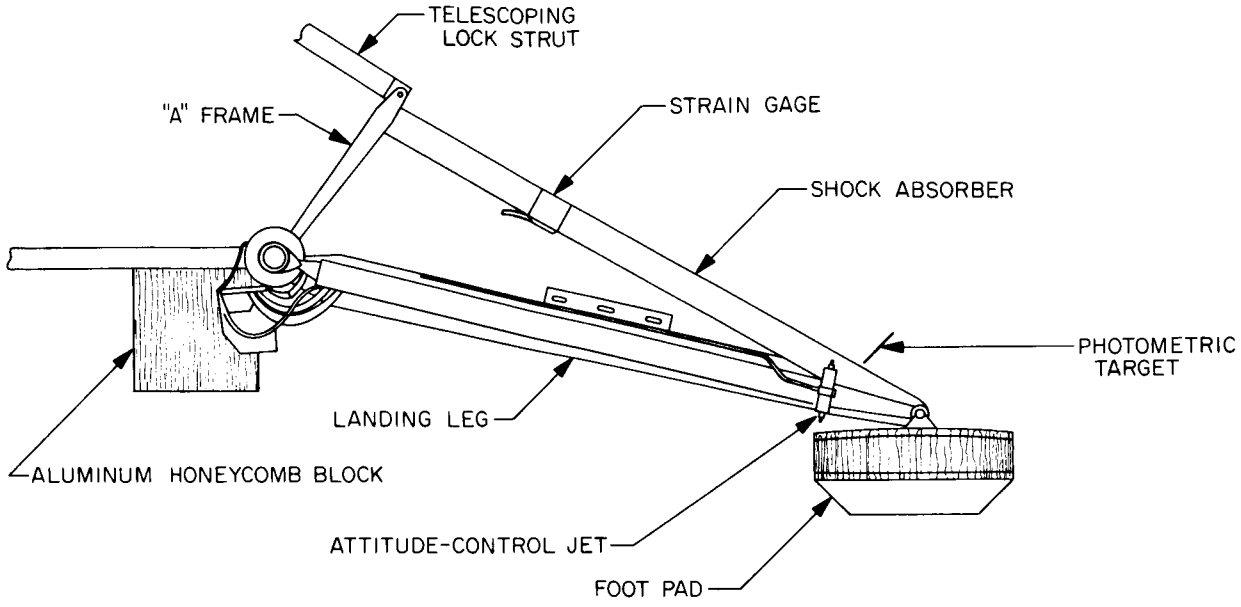

Fig. IV-12. Landing leg assembly

3. Omnidirectional Antennas

The omnidirectional antennas are mounted on the ends of folding booms hinged to the spaceframe. Pins retain the booms in the stowed position. Squib-actuated pin pullers release the booms by *Centaur* or earth command, and torsion springs deploy the antennas. The booms are then locked in position.

The omniantenna booms were extended by *Centaur* command, and both antennas were locked in the landing or transit position as indicated by the telemetry.

4. Antenna and Solar Panel Positioner (A/SPP)

The A/SPP supports and positions the high-gain planar array antenna and solar panel. The planar array antenna and solar panel have four axes of rotation: roll, polar, solar, and elevation (Fig. IV-13). Stepping motors rotate the axes in either direction in response to commands from earth or during automatic deployment following *Centaur*/spacecraft separation. This freedom of movement permits orienting the planar array antenna toward the earth and the solar panel toward the sun.

The solar axis is locked in a vertical position for stowage in the nose shroud. After launch, the solar panel is positioned parallel to the spacecraft X axis. The A/SPP remains locked in this position until after touchdown, at which time the roll, solar, and elevation axes are released. Potentiometers on each axis are read to indicate A/SPP orientation. Each command from earth gives ⅛ degree of rotation in the roll, solar, and elevation axes and 1/16 degree in the polar axis.

The A/SPP operated as expected during the mission. After the shroud was ejected, the roll and solar axes moved to their transit positions.

5. Thermal Compartments

Two thermal compartments (A and B) house thermally sensitive electronic items. Equipment in the compartments is mounted on thermal trays that distribute heat

Table IV-7. Thermal compartment component installation

Compartment A	Compartment B
Receivers (2)	Central command decoder
Transmitters (2)	Boost regulator
Main battery	Central signal processor
Battery charge regulator	Signal processing auxiliary
Engineering mechanisms auxiliary	Engineering signal processor
Television auxiliary	Low data rate auxiliary
Thermal control and heater assembly	Thermal control and heater assembly
Auxiliary battery control	Auxiliary engineering signal processor

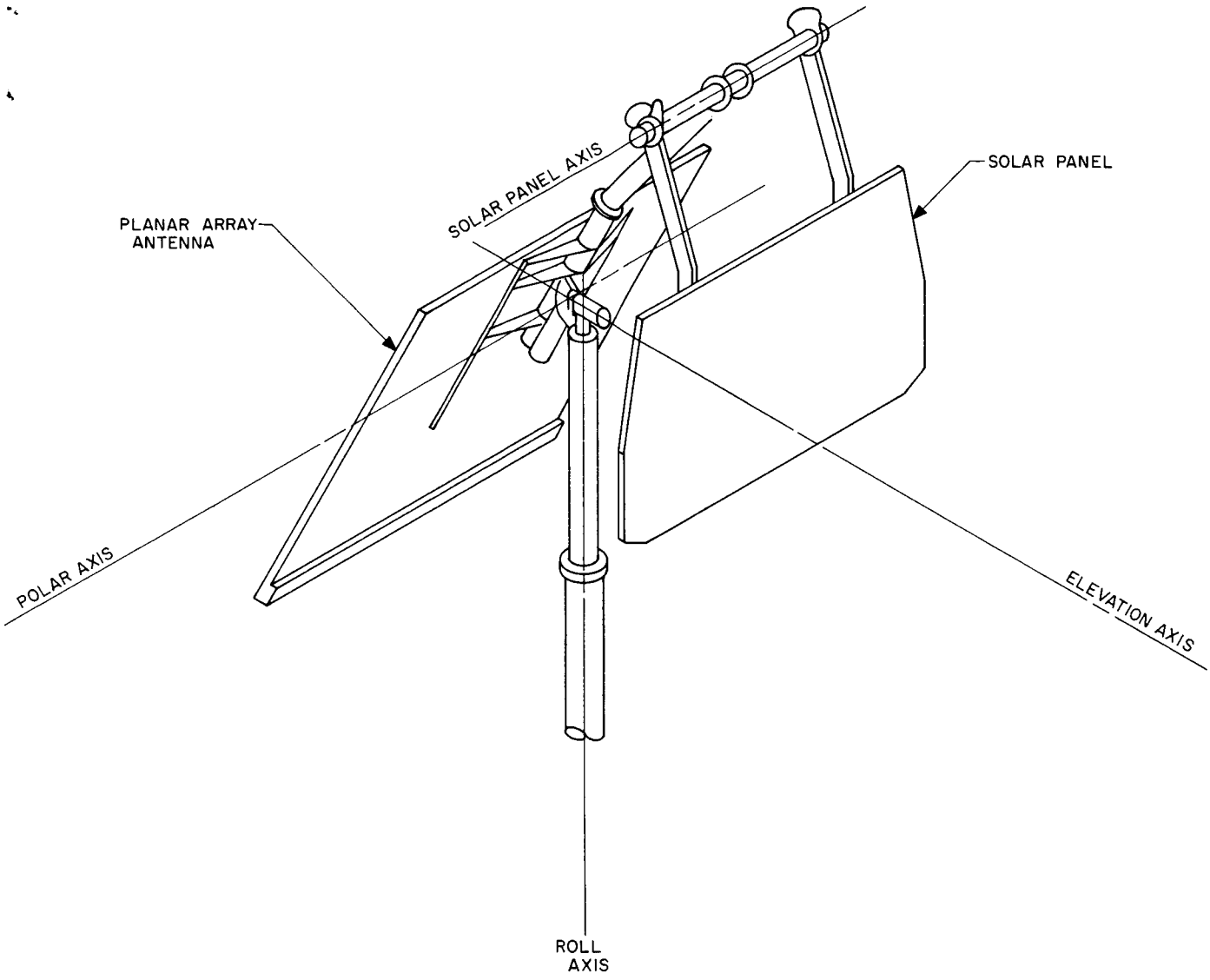

Fig. IV-13. Antenna/solar panel configuration

throughout the compartments. An insulating blanket, consisting of 75 sheets of 0.25-mil-thick aluminized mylar, is installed between the inner shell and the outer protective cover of the compartments. Compartment design employs thermal switches which are capable of varying the thermal conductance between the inner compartment and the external radiating surface. The thermal switches maintain thermal tray temperature below +125°F. Each compartment contains a thermal control and heater assembly to maintain the temperature of the thermal tray above a specified temperature (above 40°F for Compartment A and above 0°F for Compartment B). The thermal control and heater assembly is capable of automatic operation, or may be turned on or off by earth command. Components located within the compartments are identified in Table IV-7.

6. Thermal Switch

The thermal switch is a thermal-mechanical device which varies the conductive path between an external radiation surface and the top of the compartment (Fig. IV-14). The switch is made up of two contact surfaces which are ground to within one wavelength of being optically flat. One surface is then coated with a conforming substance to form an intimate contact with the mating surface. The contact actuation is accomplished by four bimetallic elements located at the base of the switch.

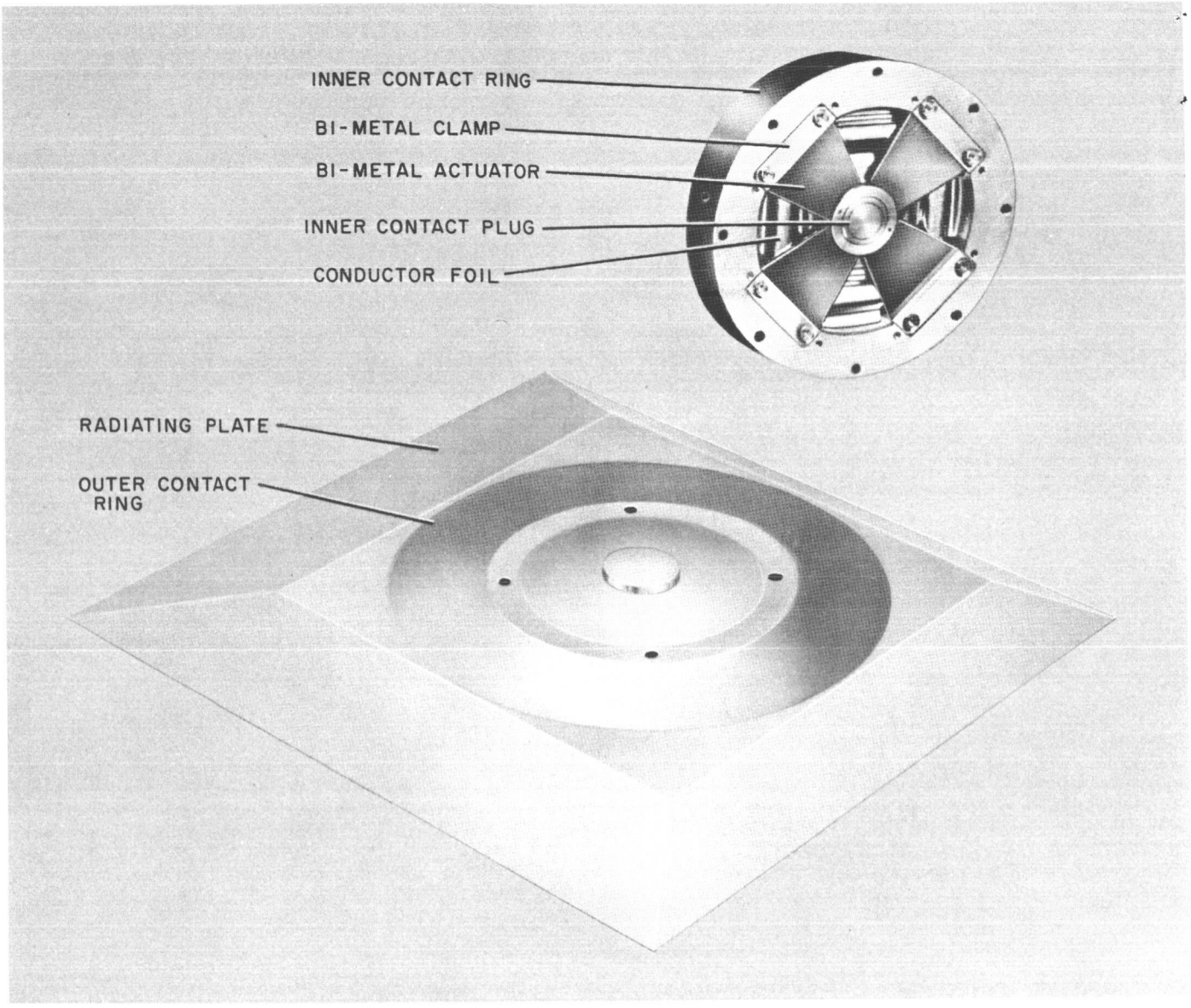

Fig. IV-14. Thermal switch

These elements are connected mechanically to the top of the compartment so that the compartment temperature controls the switch actuation. The switches are identical, but are adjusted to open at three different temperatures: 65, 50 and 40°F.

The external radiator surface is such that it absorbs only 12% of the solar energy incident on it and radiates 74% of the heat energy conducted to its surface. When the switch is closed and the compartment is hot, the switch loses its heat energy to space. When the compartment gets cold, the switch contacts open about 0.020 in., thereby opening the heat-conductive path to the radiator and thus reducing the heat loss through the switch to almost zero.

The thermal switches kept the electronics at or below the maximum temperature at all times during the flight.

7. Pyrotechnic Devices

The pyrotechnic devices installed on *Surveyor II* are indicated in Table IV-8. All the squibs used in these devices are electrically initiated, hot-bridgewire, gas-generating devices. Qualification tests for flight squibs included demonstration of reliability at a firing current

Table IV-8. Pyrotechnic devices

Type	Location and use	Quantity of devices	Quantity of squibs	Command source
Pin pullers	Lock and release Omniantennas A and B	2	2	*Centaur* programmer
Pin pullers	Lock and release landing legs	3	3	*Centaur* programmer
Pin pullers	Lock and release planar antenna and solar panel	7	7	Separation sensing and arming device and ground station
Pin puller	Lock and release vernier thrust chamber No. 1	1	1	Ground station
Separation nuts	Retro rocket attach and release	3	6	Flight control subsystem
Valve	Helium gas release and dump	1	2	Ground station
Pyro switches	EMA board No. 4, RADVS power on and off	4	4	Ground station and flight control subsystem
Initiator squibs	Safe and arm assembly retrorocket initiators	1	2	Flight control subsystem
Locking plungers	Landing leg, shock absorber locks	3	3	Ground station
		25	30	

level of 4 or 4.5 amp. "No Fire" tests were conducted at a 1-amp or 1-w level for 5 min. Electrical power required to initiate pyrotechnic devices is furnished by the spacecraft main battery. Power distribution is through 19.0- and 9.5-amp constant-current generators in the engineering mechanism auxiliary (EMA).

All scheduled pyrotechnic devices functioned normally upon command. Mechanical operation of locks, valves, switches, and plunger, actuated by squibs, was indicated on telemetry signals as part of the spacecraft engineering measurement data.

8. Electronic Packaging and Cabling

The electronic assemblies for *Surveyor II* provided mechanical support for electronic components in order to insure proper operation throughout the various environmental conditions to which they were exposed during the mission. The assemblies (or control items) were constructed utilizing sheet metal structure, sandwich-type etched circuit board chassis with two-sided circuitry, plated through holes, and/or bifurcated terminals. Each control item, in general, consists of only a single functional subsystem and is located either in or out of the two thermally controlled compartments, depending on the temperature sensitivity of the particular subsystem. Electrical interconnection is accomplished primarily through the main spacecraft harness. The cabling system is constructed utilizing a light-weight, minimum-bulk, and abrasion-resistant wire which is an extruded teflon having a dip coating of modified polyimide.

C. Thermal Control

The thermal control subsystem is designed to provide acceptable thermal environments for all components during all phases of spacecraft operation. Spacecraft items with close temperature tolerances were grouped together in thermally controlled compartments. Those items with wide temperature tolerances were thermally decoupled from the compartments. The thermal design fits the "basic bus" concept in that the design was conceived to require minimum thermal design changes for future missions. Monitoring of the performance of the spacecraft thermal design is done by 74 temperature sensors which are distributed throughout the spacecraft as follows:

Flight control	6
Mechanisms	3
Radar	6
Electrical power	3
Transmitters	2
Approach TV	1
Survey TV	2
Vehicle structure	25
Propulsion	15
Engineering payload	11

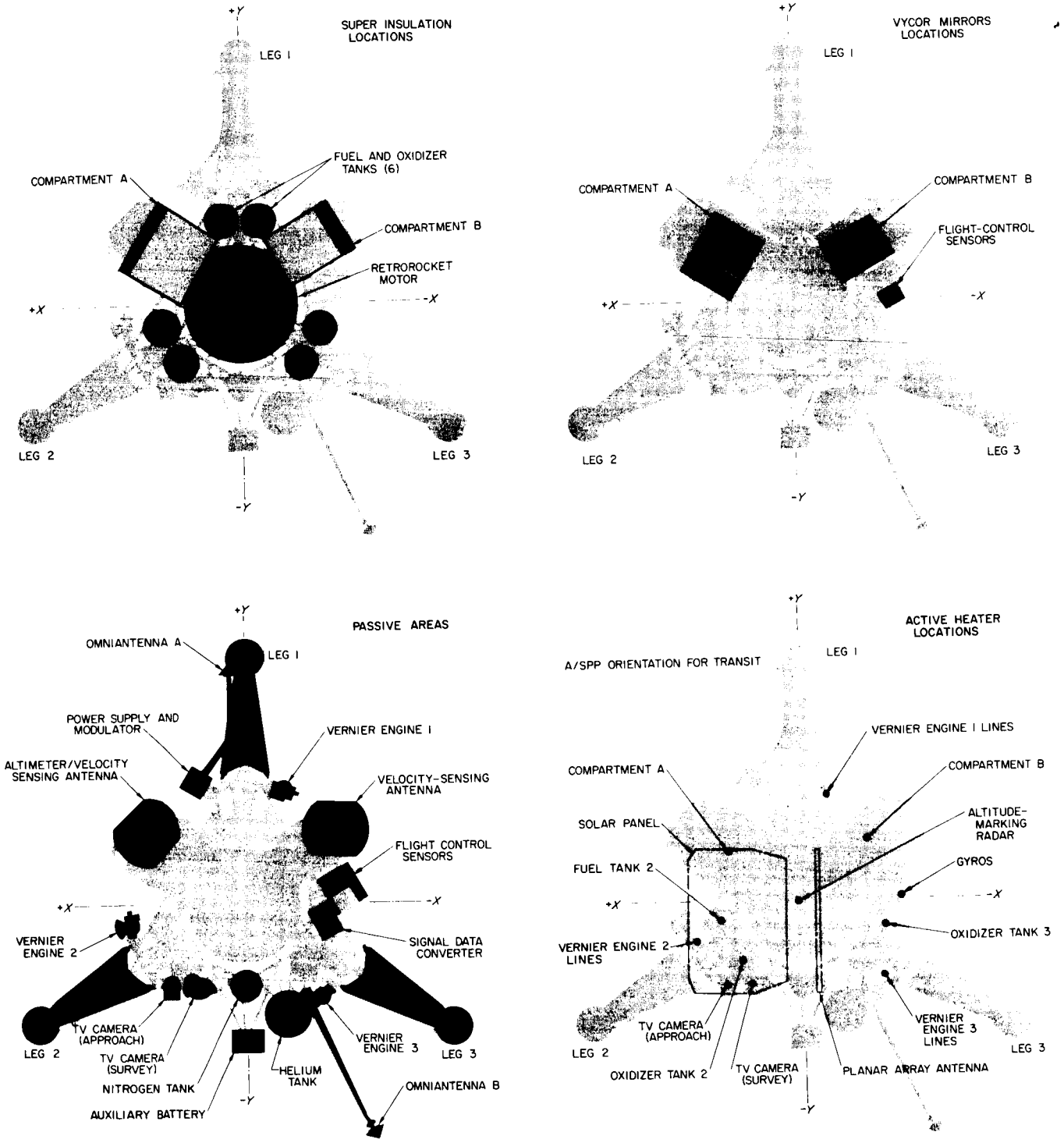

Fig. IV-15. Thermal design

The spacecraft thermal control subsystem is designed to function in the space environment, both in transit and on the lunar surface. Extremes in the environment as well as mission requirements on various pieces of the spacecraft have led to a variety of methods of thermal control. The spacecraft thermal control design is based upon the absorption, generation, conduction, and radiation of heat. Figure IV-15 shows those areas of the spacecraft serviced by different thermal designs.

The radiative properties of the external surfaces of major items are controlled by using paints, by polishing, and by using various other surface treatments. Reflecting mirrors are used to direct sunlight to certain components. In cases where the required radiative isolation cannot be achieved by surface finishes or treatments, the major item is covered with an insulating blanket composed of multiple-sheet aluminized mylar. This type of thermal control is called "passive" control.

The major items whose survival or operating temperature requirements cannot be achieved by surface finishing or insulation alone use heaters that are located within the unit. These heaters can be operated by external command, thermostatic actuation, or both. The thermal control design of those units using auxiliary heaters also includes the use of surface finishing and insulating blankets to optimize heater effectiveness and to minimize the electrical energy required. Heaters are considered "active control."

Items of electronic equipment whose temperature requirements cannot be met by the above techniques are located in thermally controlled compartments (A and B). Each compartment is enclosed by a shell covering the bottom and four sides and contains a structural tray on which the electronic equipment is mounted. The top of each compartment is equipped with a number of temperature-actuated switches (9 in Compartment A and 6 in Compartment B). These switches, which are attached to the top of the tray, vary the thermal conductance between the tray and the outer radiator surfaces, thereby varying the heat-dissipation capability of the compartments. When the tray temperature increases, heat transfer across the switch increases. During the lunar night, the switch opens, decreasing the conductance between the tray and the radiators to a very low value in order to conserve heat. When dissipation of heat from the electronic equipment is not sufficient to maintain the required minimum tray temperature, a heater on the tray supplies the necessary heat. The switches are considered "semi-active."

Examples of units which are controlled by active, semi-active, or passive means are shown in Fig. IV-15.

The thermal performance of the spacecraft up to midcourse was completely as expected with one exception. Vernier Line 2 heater was apparently on, although the line temperature continued to drop. It is estimated that the line temperature would have been close to the minimum operating limit of 0°F at the start of thermal descent.

A change had been made in the auxiliary battery paint pattern because of the low temperature experienced on *Surveyor I*. Auxiliary battery temperature was as desired on *Surveyor II*.

After the midcourse failure, the spacecraft temperatures stabilized at a new equilibrium and did not change much thereafter. Compartment A stabilized at approximately 75°F, Compartment B at 53°F, and flight control units at slightly above normal cruise temperatures until the flight control subsystem was turned off. All other parts of the spacecraft stabilized at or stayed within their operational temperature limits, except for the RADVS SDC and the shock absorbers. Thus, even in a highly nonstandard orientation, the thermal control subsystem continued to allow most spacecraft operations.

Appendix D shows graphically the temperature history of the major spacecraft components.

D. Electrical Power

The electrical power subsystem is designed to generate, store, convert, and distribute electrical energy. A block diagram of the subsystem is shown in Fig. IV-16. The subsystem derives its energy from the solar panel and the spacecraft battery system. The solar panel converts solar radiation energy into electrical energy. Solar panel power capability is affected by temperature and the incidence of solar radiation and varies from 90 to 55 w.

The spacecraft battery system consists of a main battery and an auxiliary battery. The main battery is a secondary or rechargeable battery; the auxiliary battery is a primary or nonrechargeable battery.

The batteries provide about 4090 w during transit, the balance of the energy being supplied by the solar panel. The maximum storage capacity of the main battery is 180 amp-hr; that of the auxiliary battery is 50 amp-hr.

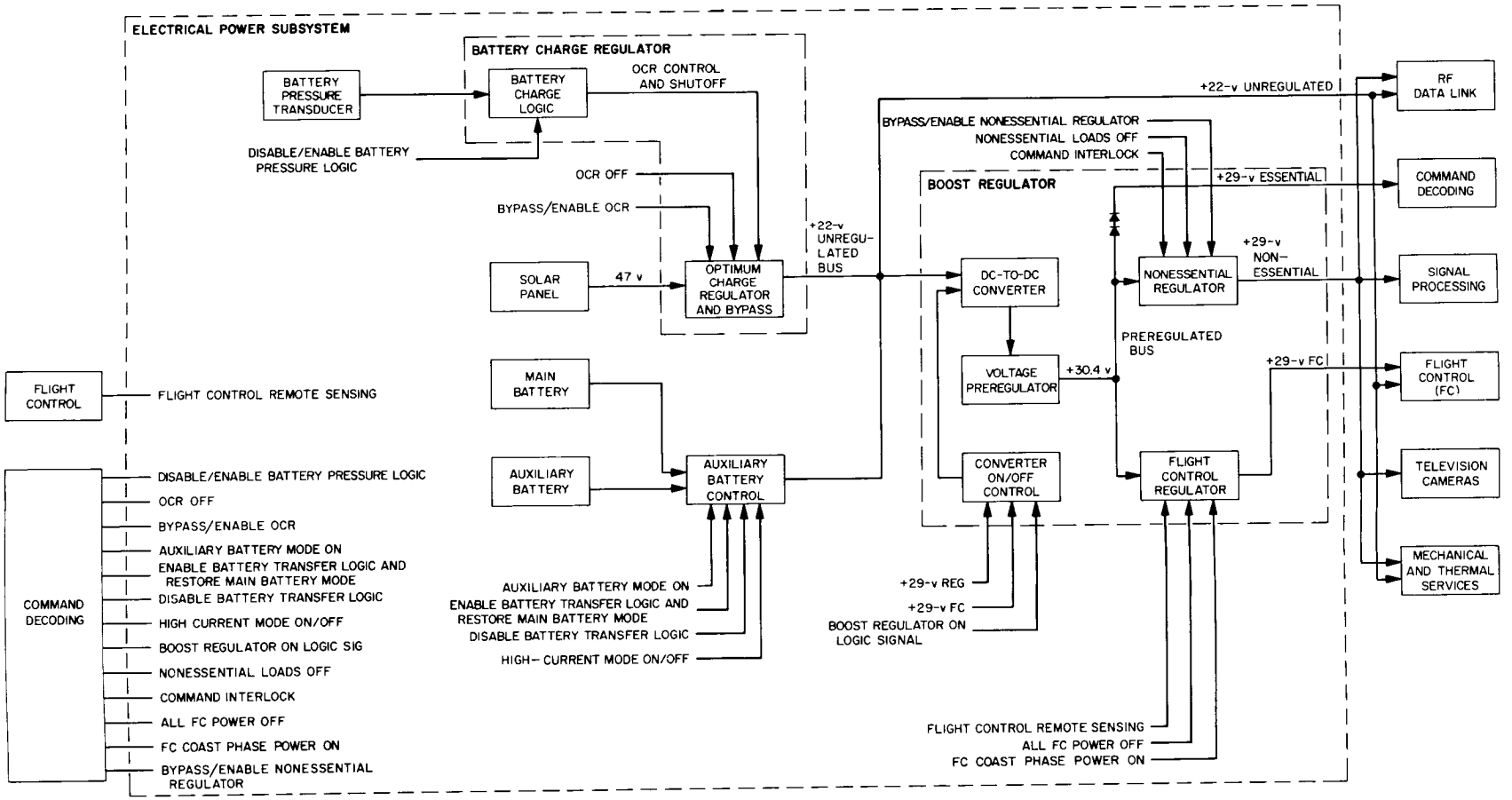

Fig. IV-16. Simplified electrical power functional block diagram

Table IV-9. Comparison of predicted vs actual values

Phase	Battery discharge current, amps		Regulated current, amps		OCR output current, amps		Unregulated current, amps	
	Predicted	Actual	Predicted	Actual	Predicted	Actual	Predicted	Actual
High power after separation and sun acquisition	5.7	5.37	4.60	4.62	3.06	3.22	0.85	0.76
First coast phase	1.61	1.77	2.29	2.45	3.14	3.18	0.86	0.72
Second coast phase	1.6	1.85	2.31	2.38	3.14	3.15	0.86	0.80

The selection of battery operation mode is determined by the auxiliary battery control (ABC). There are three modes of battery operation: main battery mode, auxiliary battery mode, and high-current mode. In the main battery mode only the main battery is connected to the unregulated bus. This is the nominal configuration. In the auxiliary battery mode the main battery is connected to the unregulated bus through a series diode while the auxiliary battery is directly connected. In the high-current mode both the main and auxiliary batteries are connected to the unregulated bus without the series diode. The battery modes are changed by earth commands except that the ABC automatically switches to auxiliary battery mode from main battery mode in case of main battery failure. This automatic function can be disabled by earth command.

The four modes of solar panel operation are controlled by the battery charge regulator (BCR). In the *on* mode the optimum charge regulator (OCR) tracks the volt-ampere characteristic curve of the solar panel and hunts about the maximum power point. In the OCR *off* mode the solar panel output is switched off. This mode is intended to prevent overcharging of the main battery by the solar panel. In the OCR *bypass* mode the solar panel is connected directly to the unregulated bus. This mode is used in case of OCR failure. In the *trickle charge* mode the main battery charging current is controlled by its terminal voltage. Three BCR modes, excluding the *trickle charge* mode, are controlled by earth commands.

The OCR *off* and *trickle charge* modes are automatically controlled by the battery charge logic (BCL) circuitry. When the main battery terminal voltage exceeds 27.5 v or its manifold pressure exceeds 65 psia, the BCR goes automatically to the *off* mode. The *trickle charge* mode is automatically enabled when the main battery terminal voltage reaches 27.3 v. The BCL can be disabled by earth command.

Current from the BCR and spacecraft batteries is distributed to the unregulated loads and the boost regulator (BR) via the unregulated bus. The voltage on the unregulated bus can vary between 17.5 and 27.5 v, with a nominal value of 22 v. The BR converts the unregulated bus voltage to 29.0 v $\pm 1\%$ and supplies the regulated loads. The preregulator supplies a regulated 30.4 v dc to the preregulated bus. The essential loads are fed by the preregulated bus through two series diodes. The diodes drop the preregulated bus voltage of 30.4 v to the essential bus voltage of 29.0 v. The preregulated bus also feeds the flight control regulator and the nonessential regulator, which in turn feeds the flight control and nonessential busses. These regulators can be turned on and off by earth commands. The nonessential regulator has a bypass mode of operation which connects the preregulated bus directly to the nonessential bus. This mode is used if the nonessential regulator fails.

The power subsystem operated normally throughout the mission. Table IV-9 verifies that telemetered parameters were in close agreement with the predicted values.

During the post-injection coast phase the average regulated load was 2.45 amp (Fig. IV-17), with an average BR efficiency of 77.4%, and the average unregulated current was 0.72 amp (Fig. IV-18). Comparable time period predictions indicate that the regulated load should be 2.29 amp and the unregulated current 0.80 to 0.83 amp. During low-power transmitter interrogation, the regulated output was approximately 100 to 150 ma higher than predicted. During high-power transmitter interrogation, this current was as predicted.

For the above mission period, the average (OCR) output current was 3.22 amp (Fig. IV-19), which agrees closely with test data. The average solar panel output current was 1.83 amp (Fig. IV-20) at an average voltage of 48.2 (Fig. IV-21). The overall OCR efficiency was about 81%. The OCR solar panel combination supplied an average of 68% of the total system electrical loads, with the battery providing the remaining 32% of the load.

Battery pressure stabilized during this period to 15 psi (Fig. IV-22) at a steady-state battery temperature of 99°F, both measurements falling well within the normal safe operating limits. Main battery terminal voltage and discharge current are shown in Figs. IV-23 and IV-24. The auxiliary battery voltage history is shown in Fig. IV-25. Figures IV-26, IV-27, and IV-28 show the BR preregulator, 29-v nonessential, and unregulated bus voltages vs mission time.

Following midcourse, the power system operated normally for the life of the spacecraft. The batteries provided the total spacecraft power from midcourse to the end of the mission. Figure IV-29 shows actual vs predicted battery energy consumption for the entire mission. The solar panel alignment was such that it did not receive any radiation from the sun. Under these conditions the solar panel could not provide power to the spacecraft.

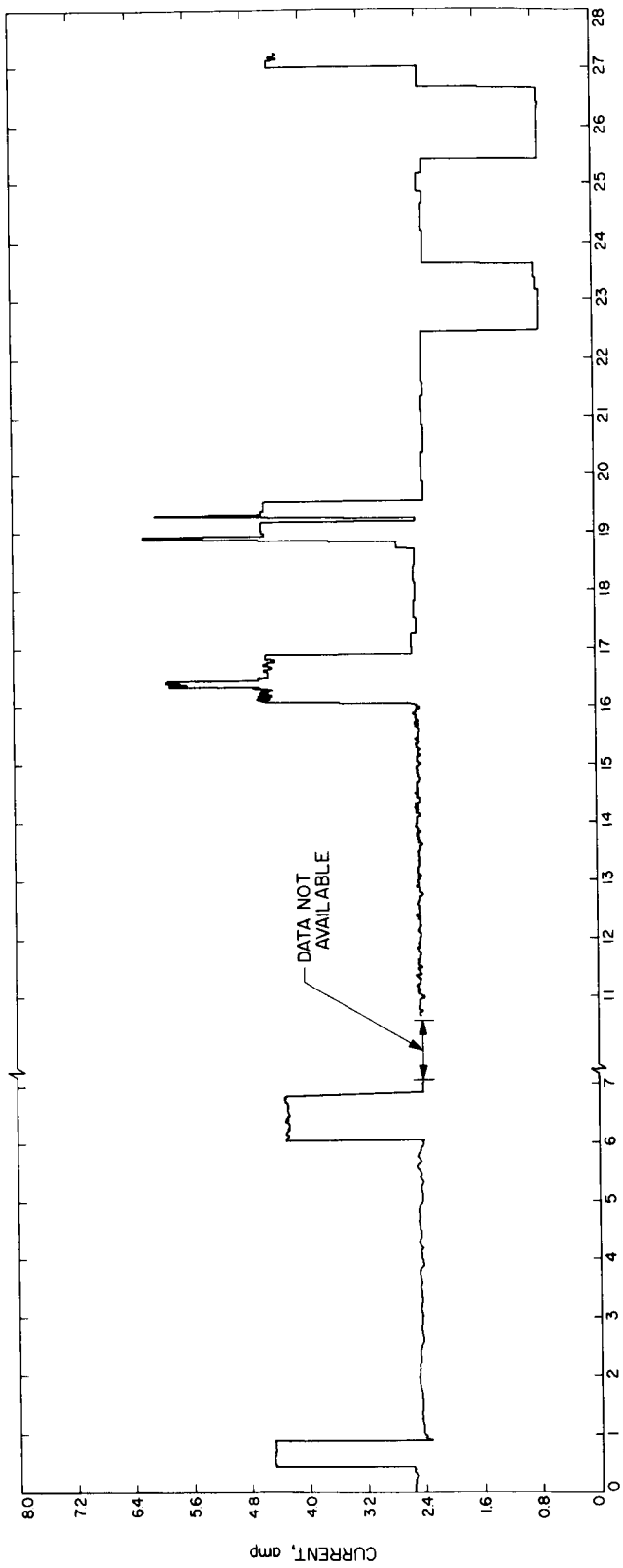

Fig. IV-17. Regulated output current

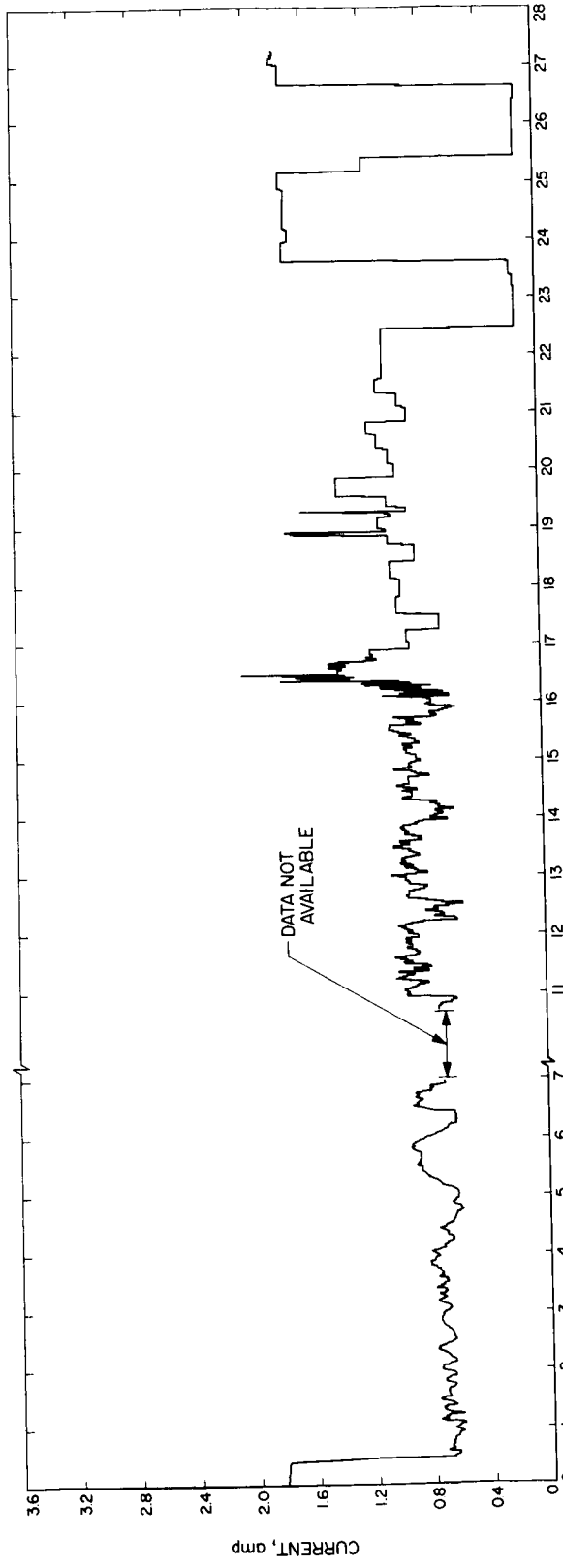

Fig. IV-18. Unregulated output current

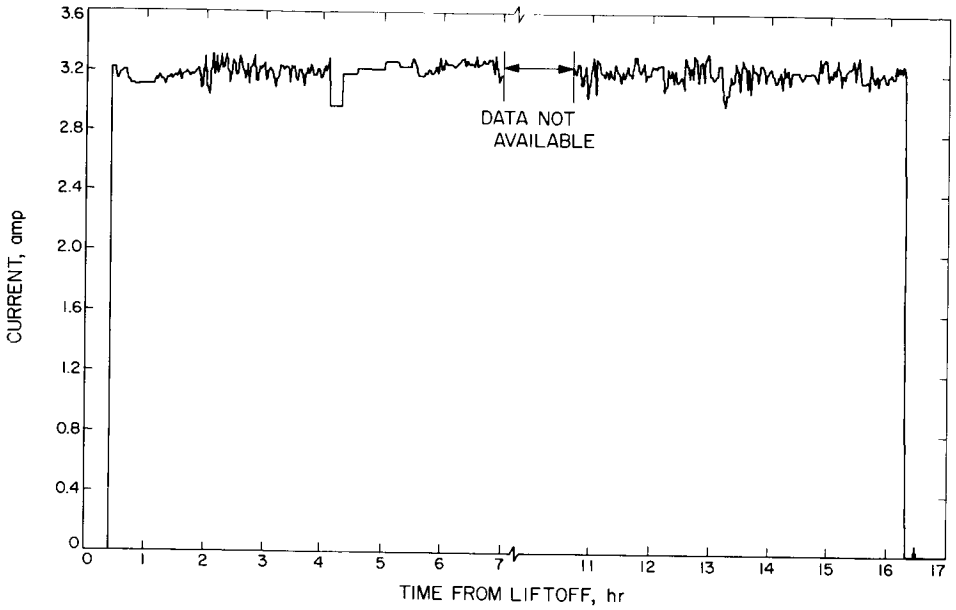

Fig. IV-19. OCR output current

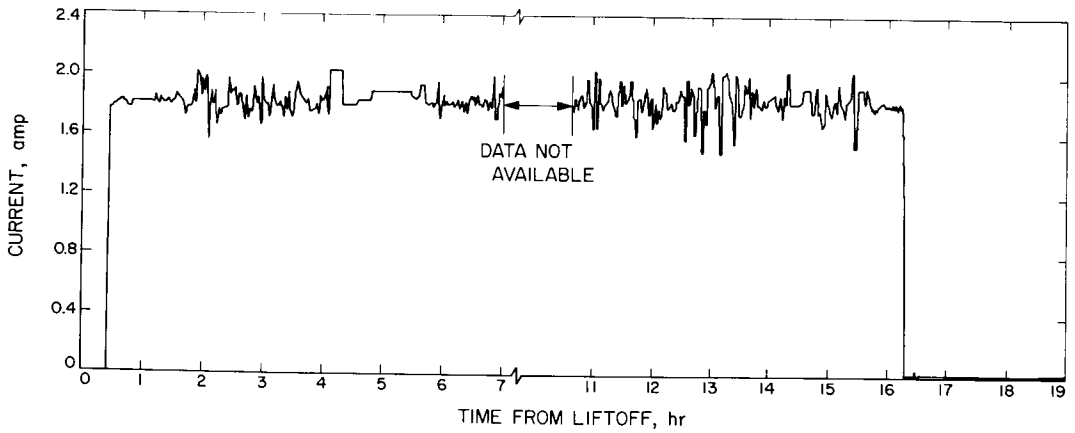

Fig. IV-20. Solar cell array current

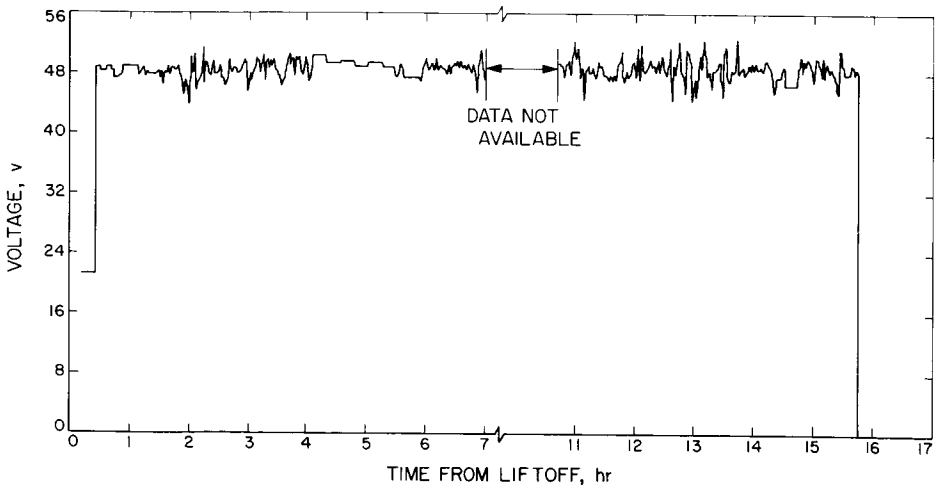

Fig. IV-21. Solar cell array voltage

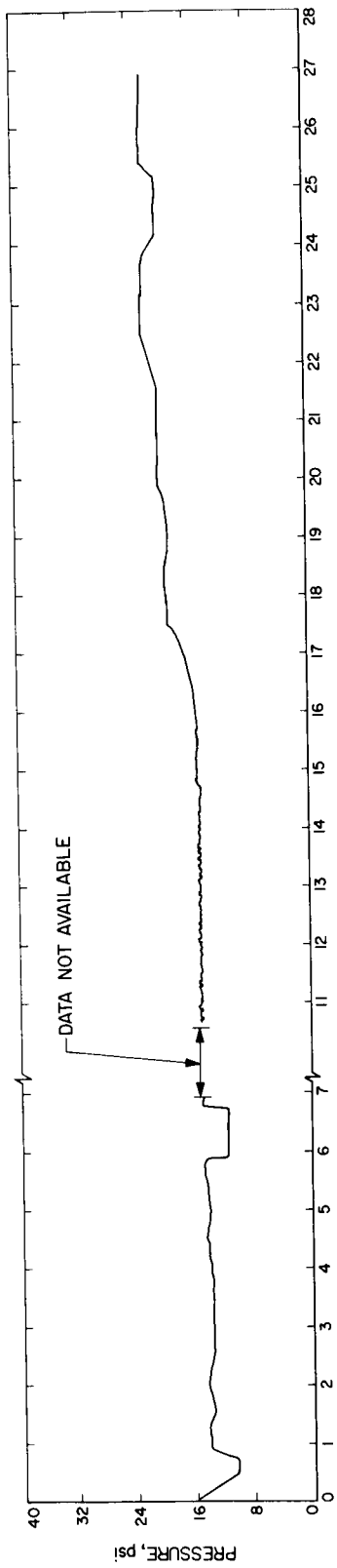

Fig. IV-22. Main battery manifold pressure

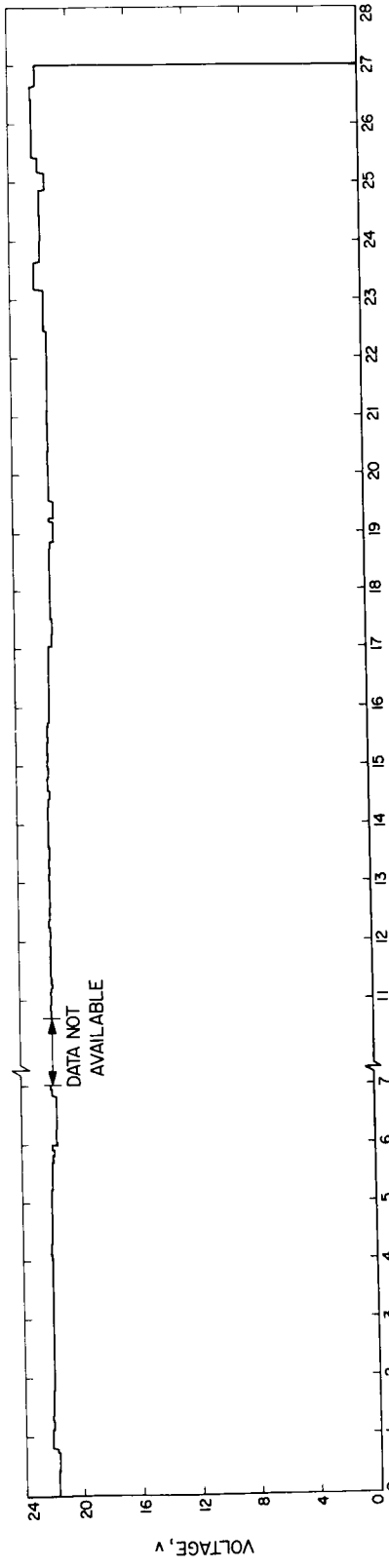

Fig. IV-23. Main battery voltage

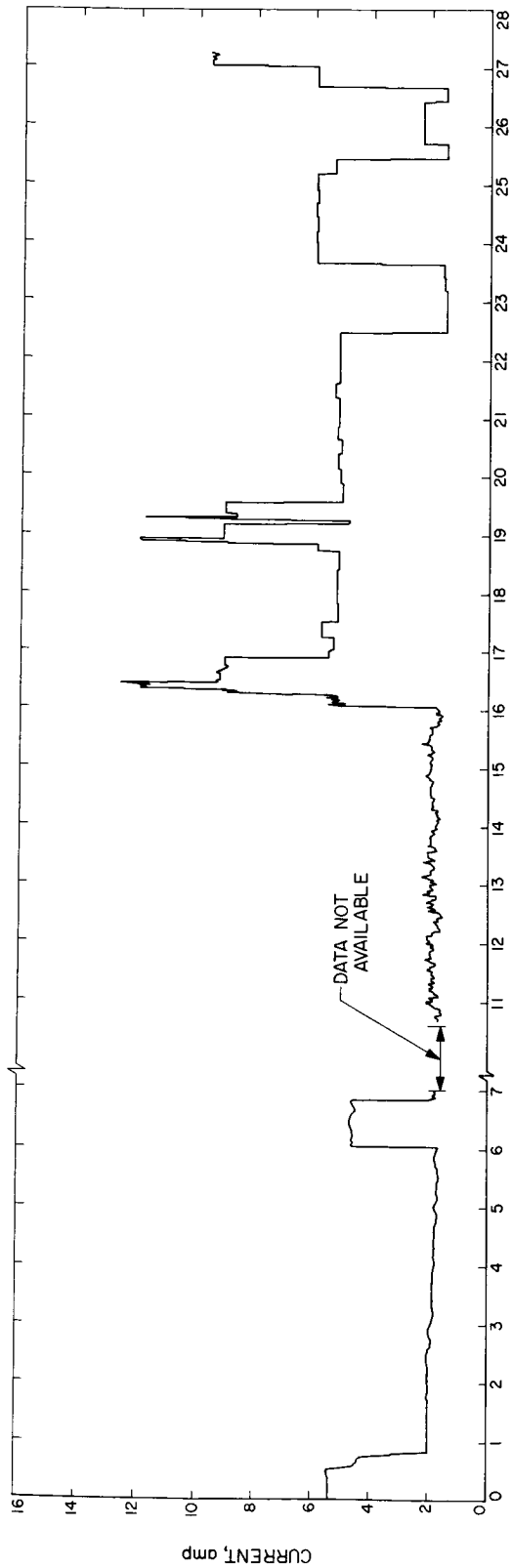

Fig. IV-24. Main battery discharge current

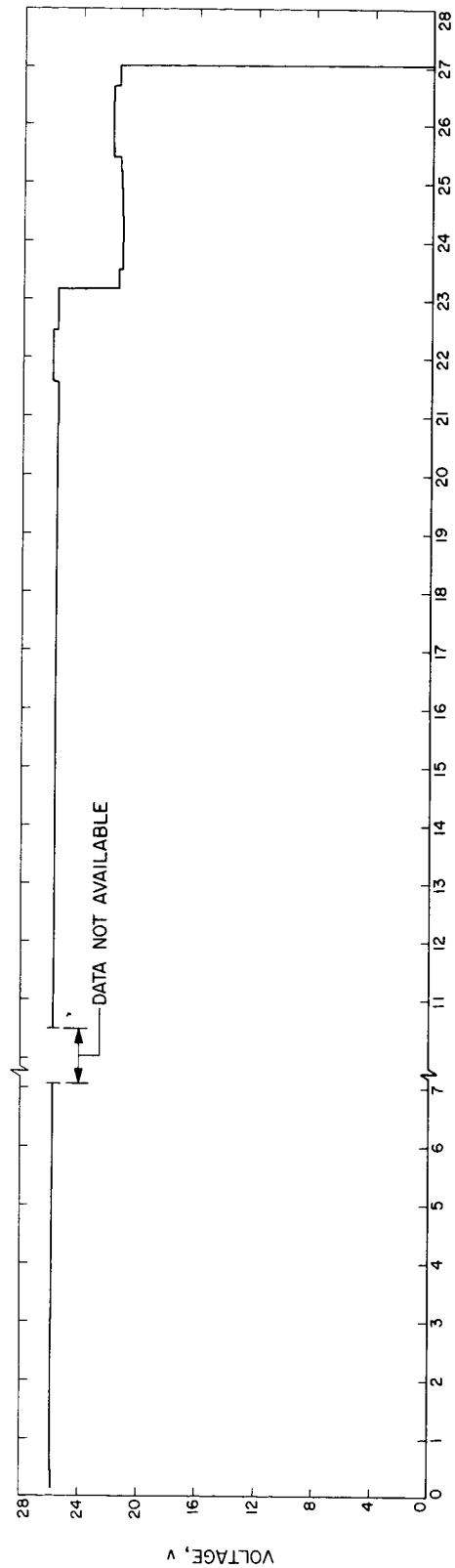

Fig. IV-25. Auxiliary battery voltage

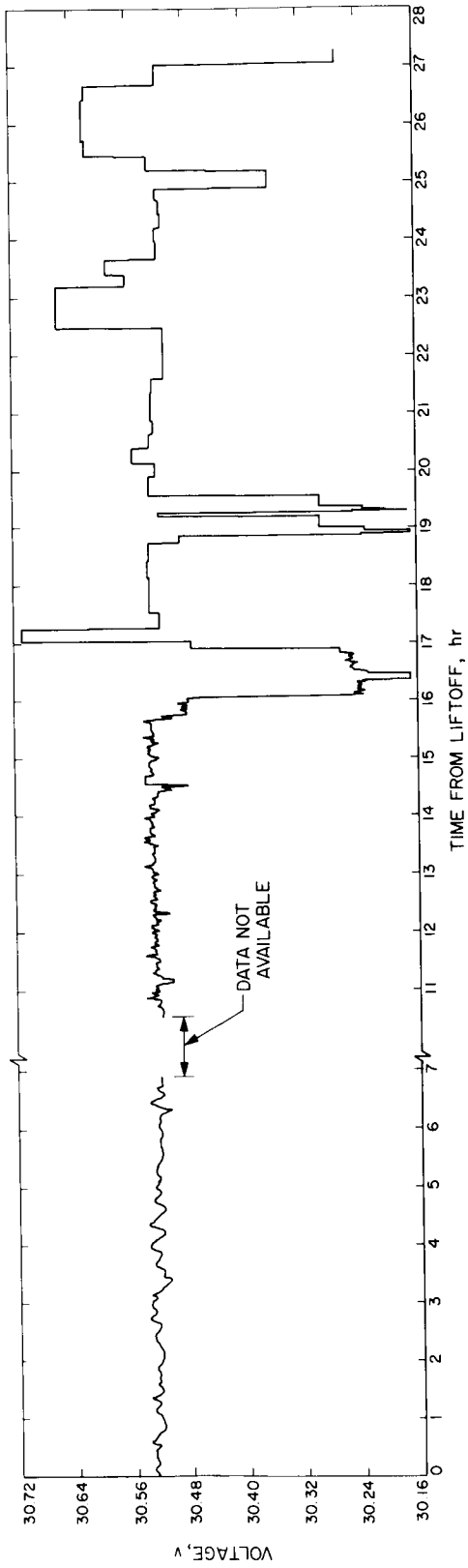

Fig. IV-26. BR preregulator voltage

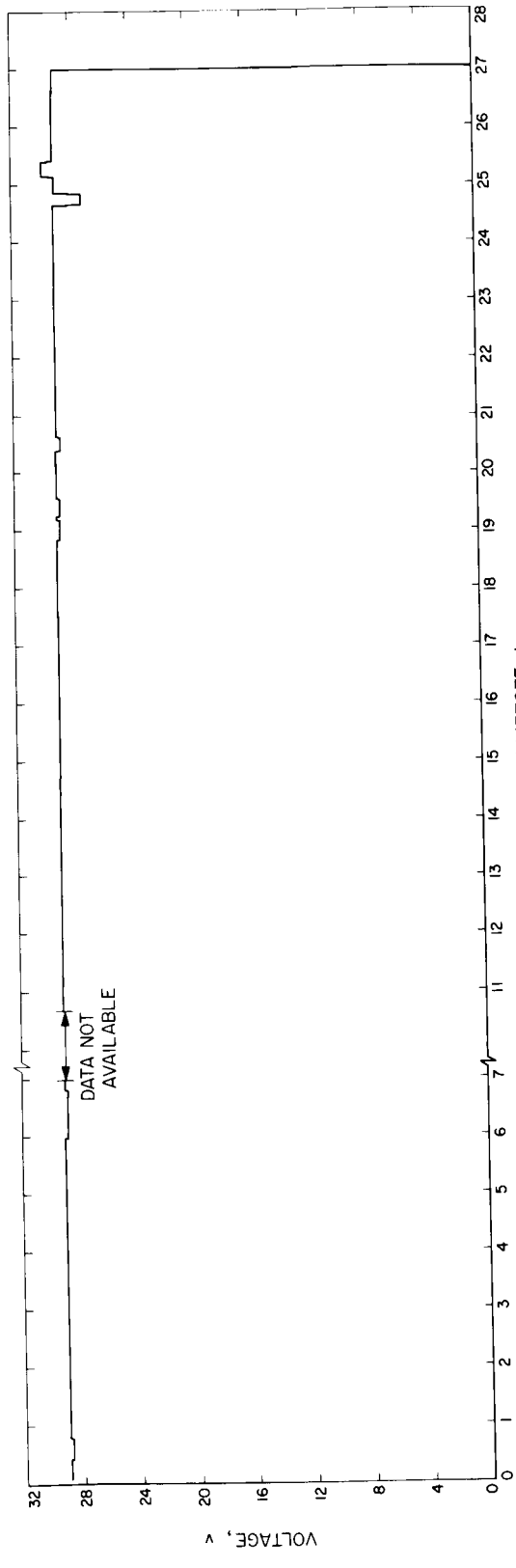

Fig. IV-27. 29-v nonessential voltage

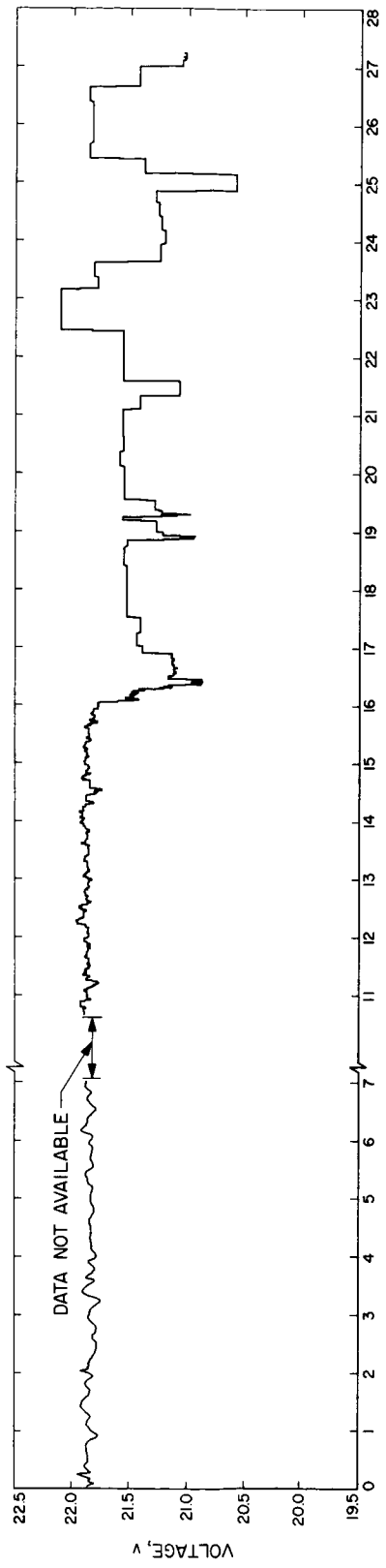

Fig. IV-28. Unregulated bus voltage

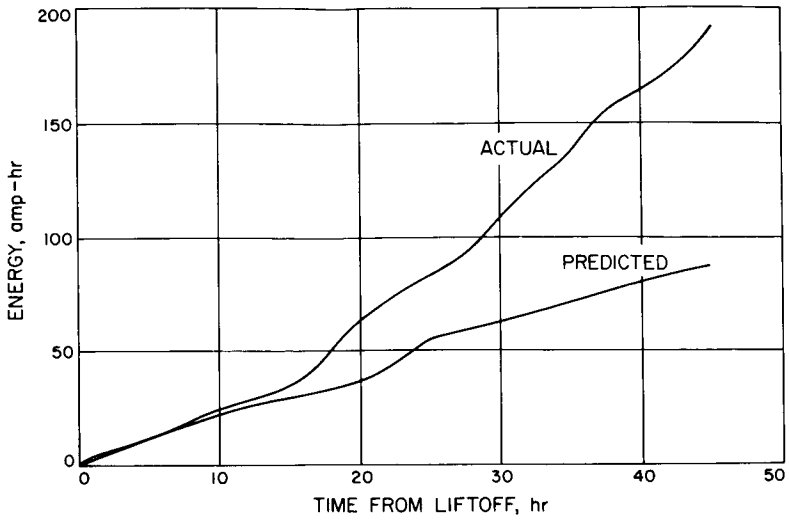

Fig. IV-29. Actual vs predicted battery energy consumption

E. Propulsion

The propulsion subsystem supplies thrust force during the midcourse correction and terminal descent phases of the mission. The propulsion subsystem consists of a vernier engine system and a solid-propulsion main retrorocket motor. The propulsion subsystem is controlled by the flight control system through preprogrammed maneuvers, commands from earth, and maneuvers initiated by flight control sensor signals.

1. Vernier Propulsion

The vernier propulsion subsystem supplies the thrust forces for midcourse maneuver velocity vector correction, attitude control during main retrorocket motor burning, and velocity vector and attitude control during terminal descent. The vernier engine system consists of three thrust chamber assemblies and a propellant feed system. The feed system is composed of three fuel tanks, three oxidizer tanks, a high-pressure helium tank, propellant lines, and valves for system arming, operation, and deactivation.

Fuel and oxidizer are contained in six tanks of equal volume with one pair of tanks for each engine. Each tank contains a Teflon expulsion bladder to permit complete and positive expulsion and to assure propellant control under zero-g conditions. The oxidizer is nitrogen tetroxide (N_2O_4) with 10% by weight nitric oxide (NO) to depress the freezing point. The fuel is monomethyl hydrazine monohydrate (72 MMH • 28 H_2O). Fuel and oxidizer ignite hypergolically when mixed in the thrust chamber. The total usable propellant load is 178.3 lb. The arrangement of the tanks on the spaceframe is illustrated in Fig. IV-30. Propellant freezing or overheating is prevented by a combination of active and passive thermal controls, utilizing surface coatings, multilayered blankets, and electrical and solar heating. The propellant tanks are thermally isolated from a spaceframe to insure that the spacecraft structure will not function as a heat source or as a heat sink.

Propellant tank pressurization is provided by the helium tank and valve assembly (Fig. IV-31). The high-pressure helium is released to the propellant tanks by activating a squib-actuated helium release valve. A single-stage regulator maintains the propellant tank pressure at 730 psi. Helium relief valves relieve excess pressure from the propellant tanks in the event of a helium pressure regulator malfunction.

The thrust chambers (Fig. IV-32) are located near the hinge points of the three landing legs on the bottom of the main spaceframe. The moment arm of each engine is about 38 in. Engine 1 can be rotated ± 6 deg about an axis in the spacecraft X-Y plane for spacecraft roll control. Engine 1 roll actuator is unlocked after boost. Engines 2 and 3 are not movable. The thrust of each engine (which is monitored by strain gages installed on each engine mounting bracket) can be throttled over a range of 30 to 104 lb. The specific impulse varies with engine thrust.

Prior to launch the vernier propulsion system propellant tanks are loaded with a nominal 109 lb of oxidizer and 75 lb of fuel. The propellant tanks are then pressurized

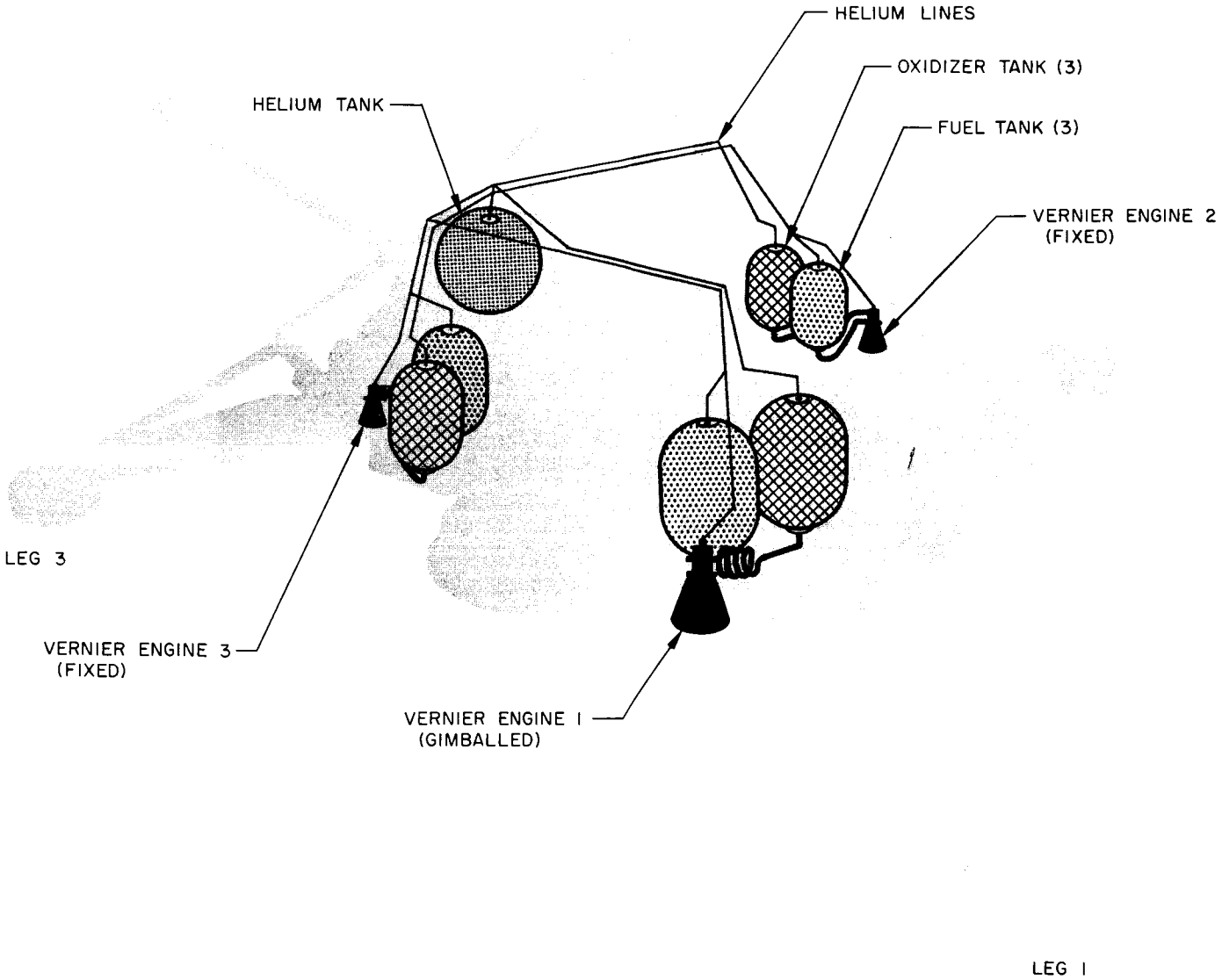

Fig. IV-30. Vernier propulsion system installation

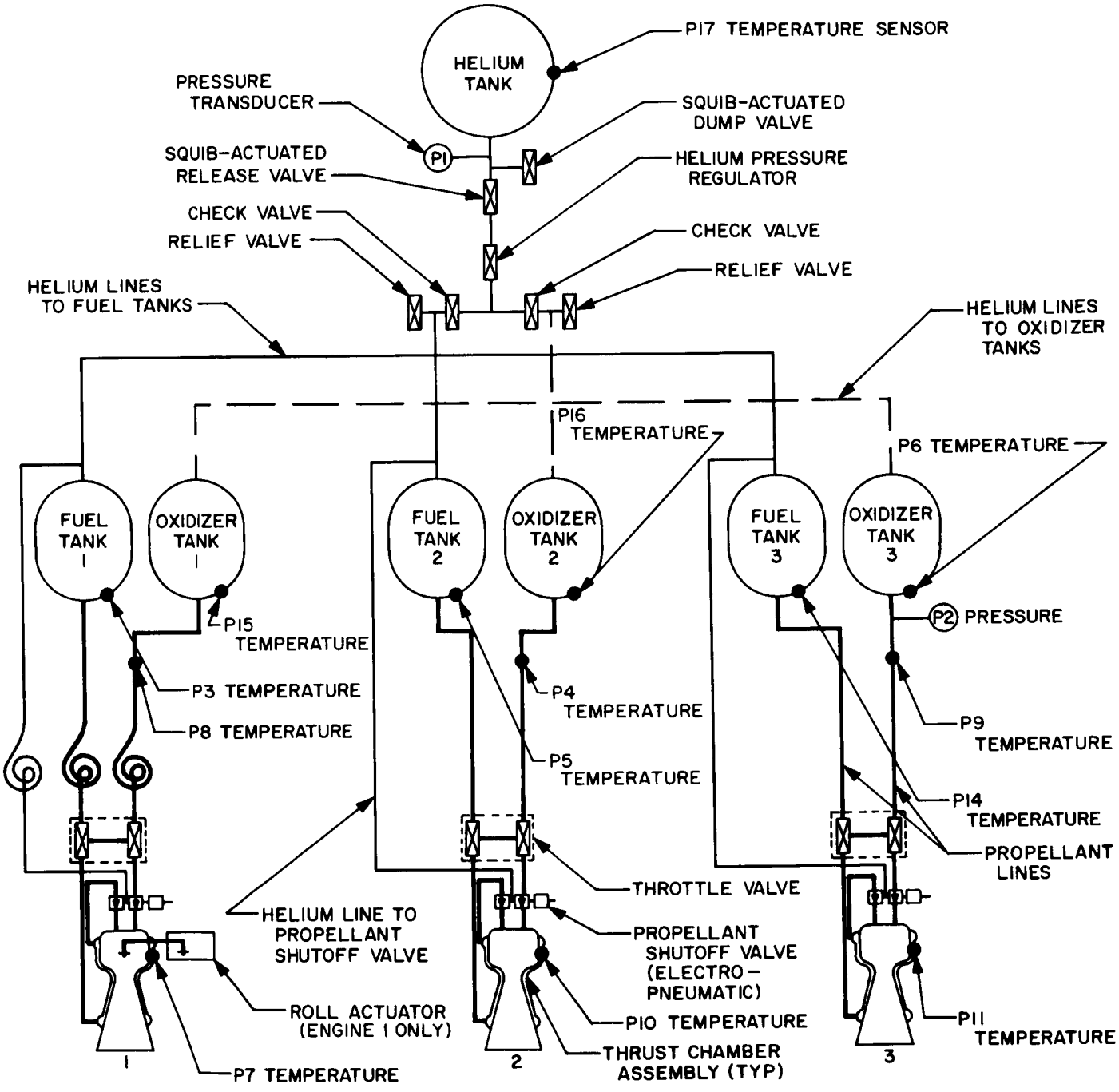

Fig. IV-31. Vernier propulsion system schematic showing locations of pressure and temperature sensors

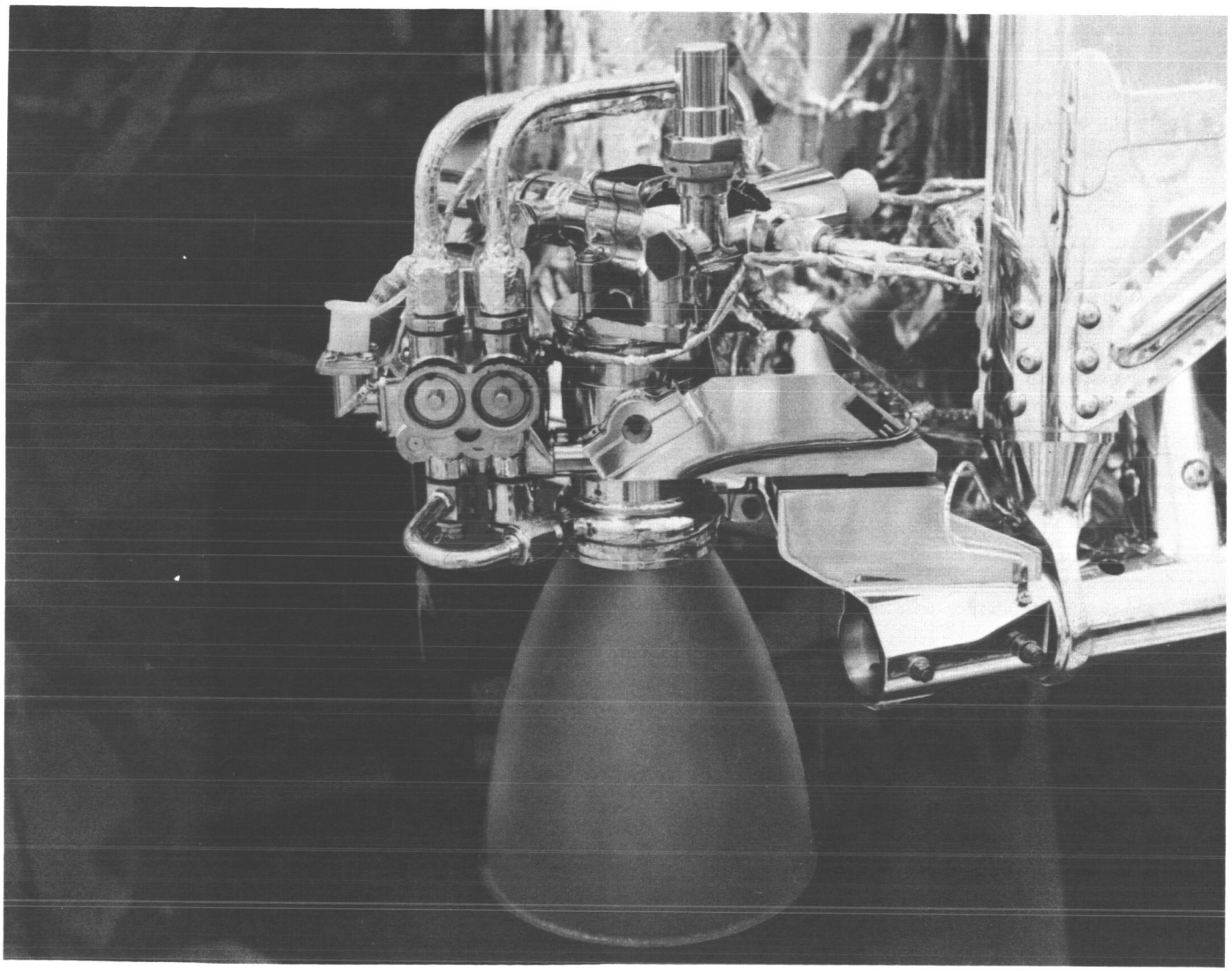

Fig. IV-32. Vernier engine thrust chamber

to 300 psi pad pressure of helium. The high-pressure helium tank is pressurized to a nominal 5175 psi. The vernier system remains in this condition through launch until 7 min before midcourse firing, at which time a squib in the helium release valve is fired. This allows the helium regulator to pressurize the propellant tanks to their nominal working pressure of 730 psi. At midcourse the vernier system is given a command which turns on all three vernier engines to a thrust level equal to 0.1 g for a specified time depending upon the correction desired. After the midcourse maneuver the system remains in the fully pressurized state until the terminal descent sequence. For the terminal descent operation, the vernier engines are ignited 1 sec before the main retro motor fires. During main retro burn, the vernier engines provide attitude control. At the end of main retro burn, the vernier engines are programmed to full thrust to facilitate the retro separation. The vernier engines are then throttled to give an optimum range/velocity profile descent. At approximately 13 ft above the lunar surface, the engines are shut down and the spacecraft free-falls to the lunar surface.

In addition to the pressure and temperature sensors shown in Fig. IV-31, the vernier propulsion system was instrumented with strain gages on each of the engine mounting brackets. During midcourse firing, the strain gages at Engines 1 and 2 indicated thrust levels of approximately the same magnitude as commanded thrust, while the strain gage at Engine 3 indicated essentially no thrust (Fig. IV-33). In fact, the resulting tumbling of the spacecraft verified that Engine 3 did not fire.

Out of several equally probable malfunctions which could be postulated on the basis of real-time data observation, the only type which offered the possibility of correction during the remaining flight time was that involving a "sticking" component in the vernier engine assembly. Therefore, the remainder of the flight was devoted primarily to pulsing and firing the vernier engines and obtaining diagnostic telemetry data.

In support of the *Surveyor II* Failure Review Board (FRB) investigation, a thorough analysis of all available data and a program of simulation tests of various possible conditions have been conducted to determine the most probable causes of the failure. The exact cause of failure has not been determined. (The FRB summary and recommendations are discussed in Section IV-A.)

During the period from launch to midcourse, all of the telemetered propulsion system data indicated normal

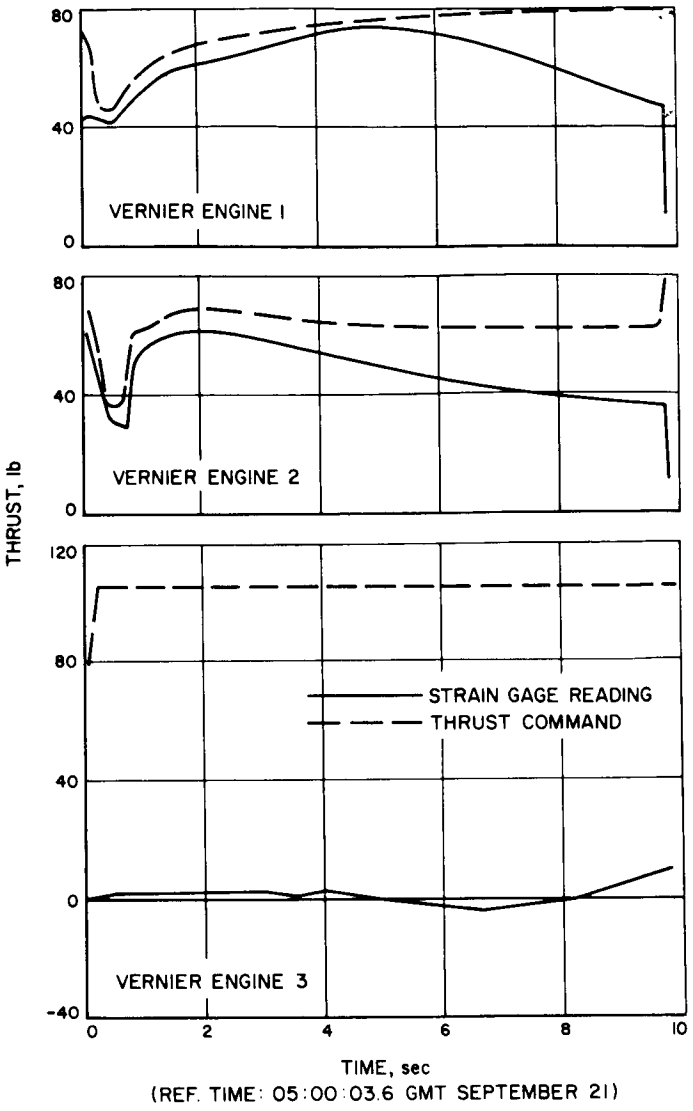

Fig. IV-33. Strain gages and thrust command signals at midcourse

operation, with two minor exceptions—a low temperature on the oxidizer line to Engine 2, and an unexpectedly large drop in helium supply pressure when the release valve was actuated to pressurize the propellant feed system. The two observed anomalies, however, were not related to the subsequent failure to obtain ignition at Engine 3 during the midcourse firing.

Temperature histories of the propulsion subsystem components are shown in Appendix D (Figs. D-6 and D-7). Locations of temperature sensors on the vernier system are shown in Fig. IV-31, and on the main retrorocket in Fig. IV-34. During the period from launch to

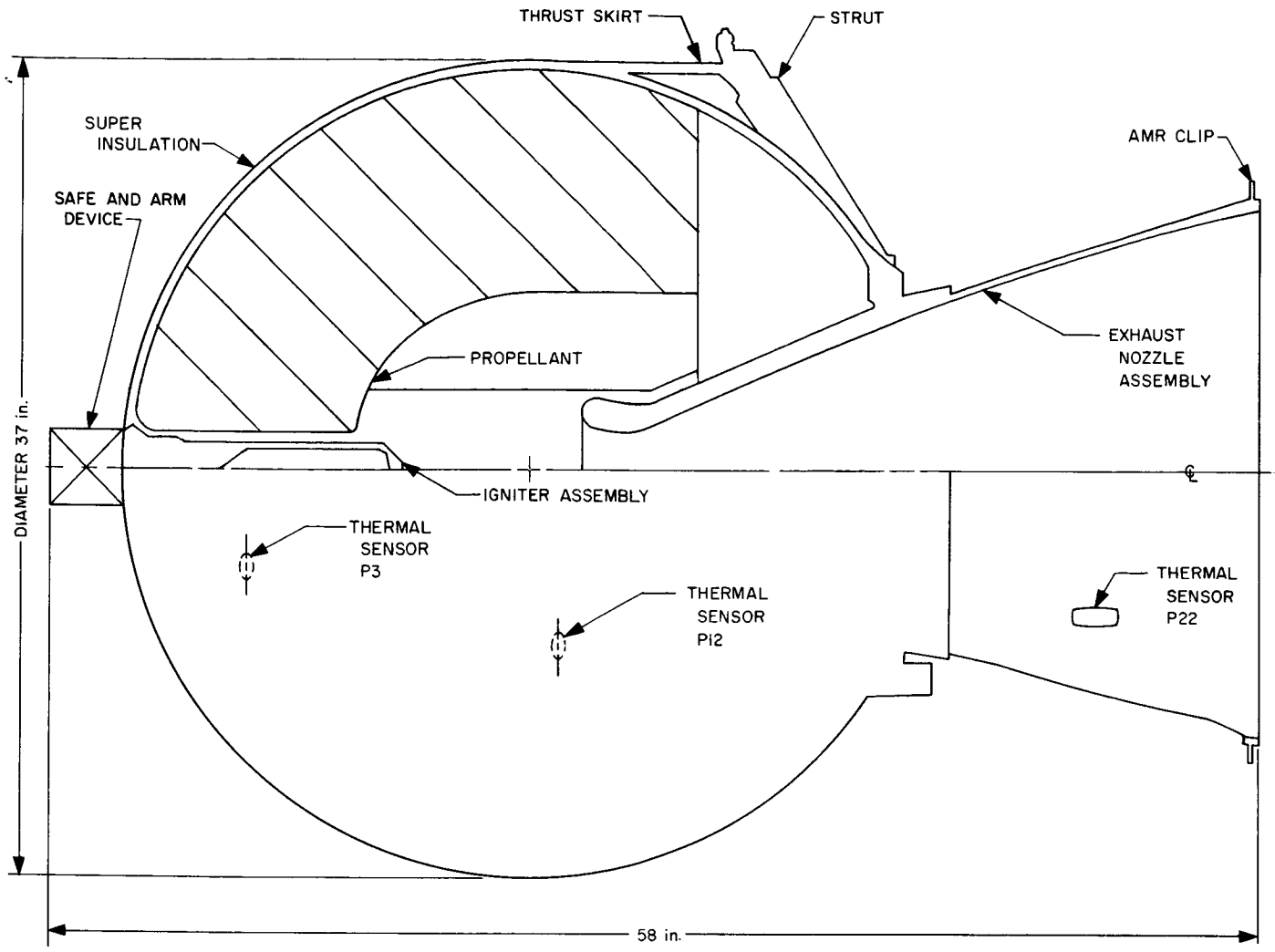

Fig. IV-34. Main retrorocket motor

midcourse, the temperatures of all propulsion components were within their prediction bands except the temperature of Oxidizer Line 2. Post-flight analysis of this anomaly indicates that, although the line heater thermostat was closed, the heater was apparently defective.

Figure IV-35 shows the history of the gas pressure measured at the helium tank and the history of the oxidizer pressure measured at Tank 3. Since there are check valves between the fuel and oxidizer helium pressurization manifolds (see Fig. IV-31), the fuel pressure may differ from the oxidizer pressure. In the present spacecraft design, no measurement of fuel pressure is provided.

The squib-actuated helium release valve was actuated 7 min before midcourse to provide full operating pressure to the propellant feed system. The oxidizer pressure rose to its expected level within 2 sec, and during that 2-sec period the indicated helium tank pressure dropped 735 psi. Pressurization of the helium lines and normal ullage volume of the tanks should have resulted in a supply pressure drop of only about 225 psi.

When the midcourse failure occurred, it was hypothesized that Fuel Tank 3 might have been empty, which would explain the abnormal drop of helium tank pressure. This hypothesis, however, was refuted by the temperature measurements on the fuel tank, which indicated a thermal history characteristic of a fully loaded tank.

Post-flight analysis of point-by-point telemetry data (Fig. IV-36) has revealed that the indicated helium tank

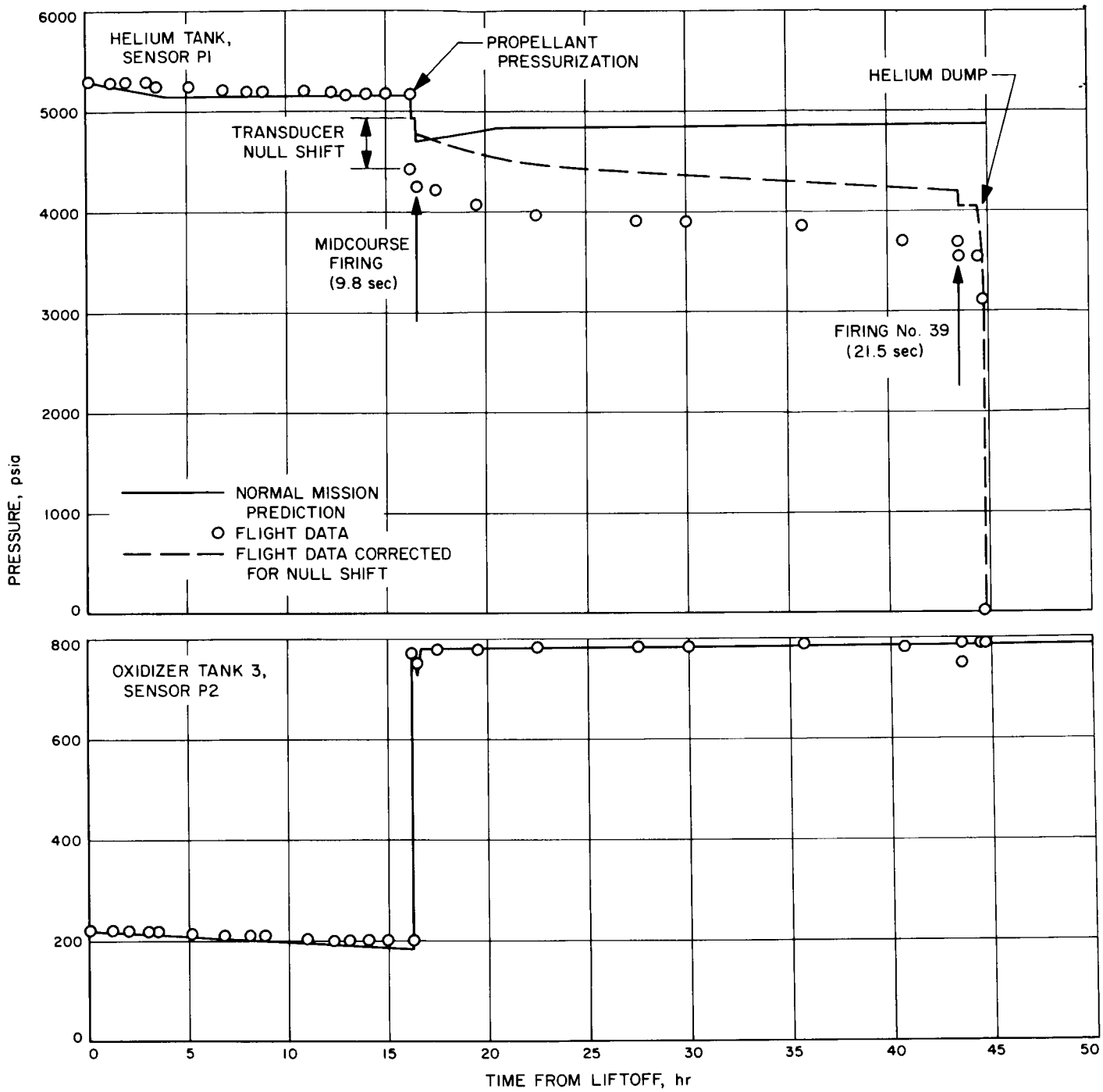

Fig. IV-35. Helium-tank and propellant-tank pressures vs time

pressure fell 530 psi in less than 0.25 sec after firing of the release valve squib. During the next 1½ sec, an additional drop of 205 psi occurred; this rate of supply pressure reduction is characteristic for filling the normal ullage volume and helium lines. It has been concluded that the extreme shock load imposed by the release valve squib caused a shift of −500 to −530 psi in the null reading of the helium tank pressure transducer. Transducer null shifts associated with activation of squib-actuated helium valves had been observed twice during

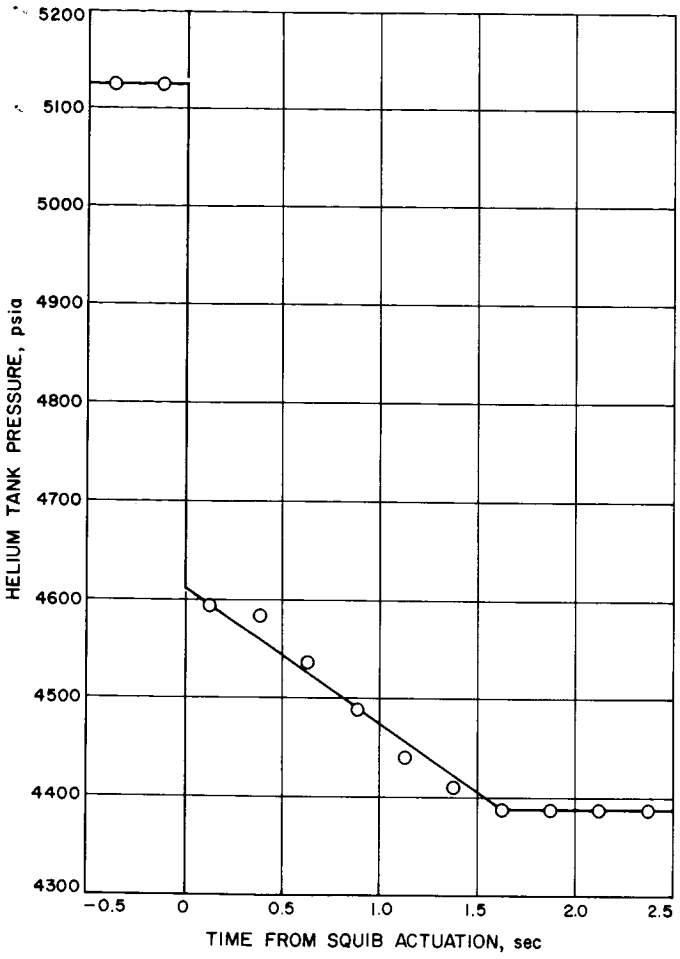

Fig. IV-36. High-resolution plot of helium supply pressure during propellant pressurization

qualification testing of the vernier propulsion system, but in those cases the magnitude of shift was smaller: −180 psi in the T-2 drop test program and +150 psi in the S-7 type-approval program.

The reduction in helium tank pressure which was observed at midcourse (Fig. IV-35) is consistent with 9.8 sec of propellant usage from at least four tanks but not consistent with usage from six tanks.

The observed helium tank pressure history subsequent to midcourse is consistent with the corresponding temperature history of the helium tank (Appendix D). The departure of the helium tank temperature history from the normal-mission prediction after midcourse suggests that spacecraft tumbling caused the helium tank to be shaded more often than it would have been with nominal transit orientation.

The oxidizer pressure history indicates that the helium regulator was operating within specification tolerances* through the mission.

2. Main Retrorocket Motor

The main retrorocket, which performs the major portion of the deceleration of the spacecraft during terminal descent, is a spherical, solid-propellant unit with a partially submerged nozzle to minimize overall length (Fig. IV-34). The motor utilizes a carboxyl/terminated polyhydrocarbon composite-type propellant and conventional grain geometry.

The motor case is attached at three points on the main spaceframe near the landing leg hinges, with explosive nut disconnects for post-burnout ejection. Friction clips around the nozzle flange provide attachment points for the altitude marking radar (AMR). The retrorocket, including the thermal insulating blankets, weighs approximately 1395 lb. This total includes about 1250 lb of propellant. The thermal control design of the retrorocket motor is completely passive, depending on its own thermal capacity and an insulating blanket (21 layers of aluminized mylar plus a cover of aluminized Teflon). The prelaunch temperature of the unit is 70 ±5°F. At terminal maneuver, when the motor is ignited, the propellant will have cooled to a thermal gradient with a bulk average temperature of about 50 to 55°F.

The AMR normally triggers the terminal maneuver sequence. When the retro firing sequence is initiated, the retrorocket gas pressure ejects the AMR. The motor operates at a thrust level of 8,000 to 10,000 lb for approximately 39 sec at an average propellant temperature of 50°F.

The thermal sensors on the main retro motor case closely followed the predicted values from launch until the attempted midcourse correction at launch plus 16 hr. Following the midcourse attempt, temperature deviations due to the tumbling motion of the spacecraft were noted. The upper case temperature continued to decrease at a slightly higher than predicted rate. The lower case temperature increased from 60°F at midcourse to about 72°F when the retro was ignited at launch plus 45 hr. Bulk temperature of the retro motor was estimated to be about 70°F at retro ignition.

*Specification requirements are: operating pressure, 700 to 755 psi; regulator lockup pressure, 795 psi maximum.

The retro motor was ignited while the spacecraft was tumbling at approximately 2.3 rev/sec. Retro ignition and burning were verified for approximately 32 sec after which time all data was lost. Evaluation of spacecraft accelerometer data indicates that the retro motor ignited and burned normally until all data was lost. Because of the tumbling nature of the spacecraft and termination of data, no information was obtained on retro impulse, thrust alignment, center of gravity, tailoff, or separation characteristics.

F. Flight Control

The flight control subsystem is designed to (1) acquire and maintain spacecraft orientation with respect to the sun and the star Canopus, (2) orient the spacecraft for a mid-mission trajectory error correction, (3) execute an incremental velocity change and maintain spacecraft stability during midcourse correction and terminal descent, (4) execute a lunar terminal orientation, and (5) in conjunction with a radar system (RADVS), a solid-propellant retro motor, and three liquid-propellant (vernier) engines, soft-land (at a nominal touchdown velocity of 14 ft/sec) the spacecraft on the lunar surface.

The flight control subsystem consists of the appropriate electronic equipment associated with a Canopus star sensor (roll), primary sun sensors (pitch and yaw) for spacecraft attitude in pitch, yaw, and roll during cruise, an acquisition sensor for initial sun acquisition, three gyros (pitch, yaw, and roll) for rate stabilization and inertial control, and a ± 0.75-g precision accelerometer for midcourse velocity control and acceleration control during the terminal descent.

The control electronics process the reference sensor outputs, earth-based commands, and the flight control programmer and decoder outputs to generate the necessary control signals for use by the vehicle control elements. A simplified flight control functional diagram appears in Fig. IV-37. The vehicle control elements consist of the attitude-control gas-jet activation valves, the vernier engine thrust level control valves and gimbal

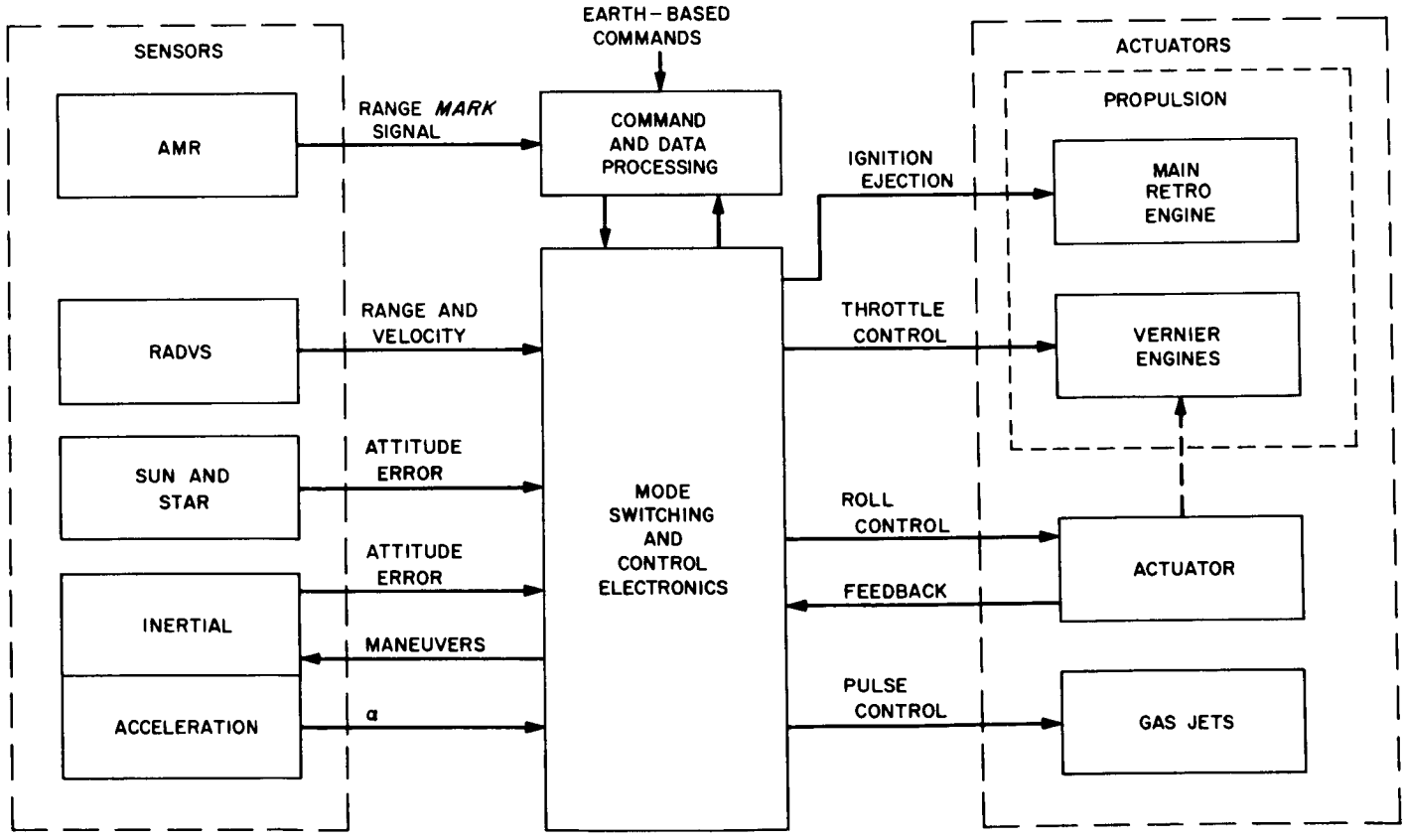

Fig. IV-37. Simplified flight control functional diagram

actuator, and the main retro motor ignitor and separation pyrotechnics.

The gas-jet attitude control system is a cold gas system using nitrogen as a propellant. This system consists of a gas supply system and three pairs of solenoid-valve-operated gas jets interconnected with tubing (see Fig. IV-38). The nitrogen supply tank is initially charged to a nominal pressure of 4600 psia. Pressure to the gas jets is controlled to 40 ± 2 psia by a regulator.

Spacecraft attitude, acceleration, and velocity are controlled as required by various "control loops" throughout the coast and thrust phases of flight, as shown in Table IV-10. Stabilization of the spacecraft tipoff rates after *Centaur* separation is achieved through the use of rate feedback gyro control (rate mode). After rate capture, an inertial mode is achieved by switching to position feedback gyro control.

Because of the long duration of the transit phase and the small unavoidable drift error of the gyros, a celestial reference is used to continuously update the inertially controlled attitude of the spacecraft.

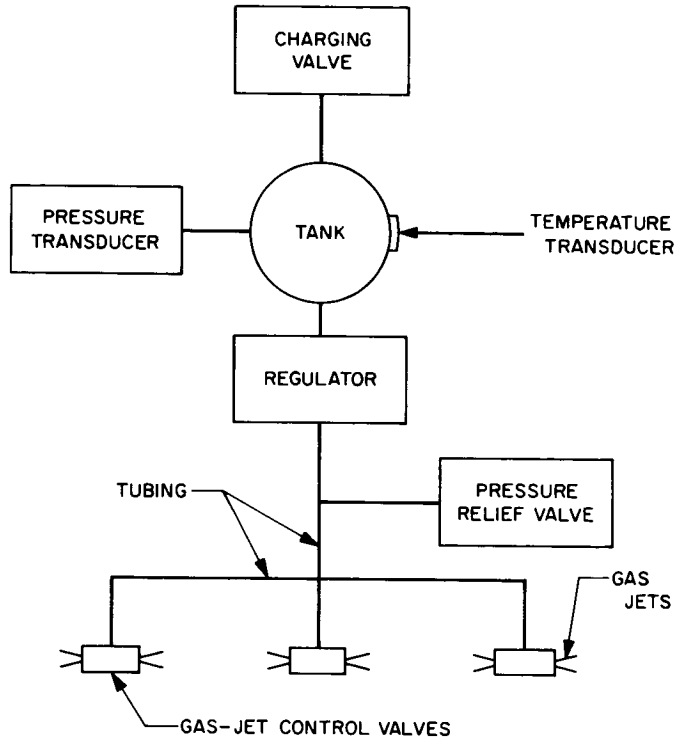

Fig. IV-38. Gas-jet attitude control system block diagram

Table IV-10. Flight control modes

Control loop	Flight phase	Modes	Remarks
Attitude control loop			
Pitch and yaw	Coast	Rate Inertial Celestial	Gas jet matrix signals
	Thrust	Inertial Lunar radar	Vernier engine matrix signals
Roll	Coast	Rate Inertial Celestial	Leg 1 gas jet signals
	Thrust	Inertial	Vernier Engine 1 gimbal command
Acceleration control loop			
Thrust axis	Thrust (midcourse) Thrust (terminal descent)	Inertial (with accelerometer) Inertial (with accelerometer)	Nominal 3.22 ft/sec^2 Minimum 4.77 ft/sec^2 Maximum 12.56 ft/sec^2
Velocity control loop			
Thrust axis	Thrust	Lunar radar	Command segment signals to 43 ft altitude Constant 5 ft/sec velocity signals to 14 ft altitude
Lateral axis	Thrust	Lunar radar	Lateral/angular conversion signals

The celestial references (Fig. IV-4), the sun and the star Canopus, are acquired and maintained after the spacecraft separates from the *Centaur* stage and after automatic deployment of the solar panel. The sun is first acquired by the acquisition sun sensor during a spacecraft roll maneuver which is automatically initiated at completion of solar panel deployment. The 10-deg wide by 196-deg fan-shaped field of view of the acqusition sun sensor includes the Z-axis and is centered about the *X*-axis. The roll command is terminated after initial sun acquisition, and a yaw command is initiated which allows the narrow-view primary sun sensor to acquire and lock on the sun. Automatic Canopus acquisition and lock-on are normally achieved after initiation of a roll command from earth. This occurs because the Canopus sensor angle is preset with respect to the primary sun sensor prior to launch for each mission. Star mapping for Canopus verification is achieved by commanding the spacecraft to roll while maintaining sun lock. A secondary sun sensor, mounted on the solar panel, provides a backup for manual acquisition of the sun if the automatic sequence fails.

The transit phase is performed with the spacecraft in the celestial-referenced mode except for the initial rate-stabilization, midcourse, and terminal descent maneuvers. The midcourse and main retro orientation maneuvers are achieved in the inertial mode. Acceleration control is used for controlling the magnitude of the midcourse velocity increment. During the interval from retro case separation to initiation of radar velocity control, acceleration control is used to control the descent along the spacecraft thrust axis, and velocity control is used for pitch and yaw control to align the spacecraft thrust axis with the velocity vector.

The lunar reference is first established by a signal from an AMR subsystem when the spacecraft is nominally 60 miles above the lunar surface. (Refer to Section IV-G for discussion of radar control during the standard terminal descent phase.)

1. Launch Phase

At launch, with the spacecraft in the 550-bit/sec mode, the gyro temperatures were as follows: roll, 172.3°F; pitch, 170.2°F; and yaw, 172.0°F. (In the 1100-bit/sec mode, the gyro temperatures would read about 8°F higher.) The gyro temperatures stabilized about 1 hr 35 min after liftoff and remained stabilized until flight control power was first turned off about 22 hr after launch for post-midcourse vernier engine firings.

The gas-jet attitude control system contained a charge of 4.5 lb of nitrogen gas based upon a prelaunch pressure of 4586 psig at 79.74°F.

An anomaly occurred 35 sec prior to spacecraft separation from the *Centaur* (simultaneously with the *legs extend* signal) when the flight control reverted to inertial mode from rate mode. The flight control was automatically returned to rate mode at separation.

Separation of the spacecraft from the *Centaur* appeared normal. Direct analysis of the spacecraft gyro outputs was hindered because of an initial position offset of the pitch and yaw gyros of approximately 4 deg (due to the 35-sec abnormal inertial mode operation) at the time that rate mode was initiated by electrical disconnect (5.5 sec prior to spacecraft separation).

An analysis of spacecraft separation is continuing which uses a 6-degrees-of-freedom analog simulation. Initial conditions (*Centaur* residual rates) are programmed in, and body tipoff rates are simulated by applying short-duration external torques. Analog gyro outputs for various body tipoff rates are correlated with the telemetered spacecraft gyro outputs. Preliminary results of this analysis indicate the pitch and yaw tipoff rates to have been less than 0.5 deg/sec and well within the capability of the attitude control system (also refer to Section III).

2. Sun Acquisition

Telemetered data indicated that the automatic sun acquisition occurred properly. Upon completion of solar panel deployment, the spacecraft performed a negative roll for 72 deg until the acquisition sun sensor became illuminated. The spacecraft then stopped and started a positive yaw turn. The spacecraft continued to yaw for 16 deg before the primary sun sensor indicated sun lock-on. The sun acquisition and lock-on sequence took about 3 min.

3. Star Acquisition

Six hours after launch, *cruise mode, manual delay mode,* and *positive angle maneuver* commands were sent to the spacecraft to initiate the star mapping sequence. These commands were followed by the *sun and roll* command to start the actual roll maneuver in a positive direction at a rate of 0.5 deg/sec.

Earthshine had been indicated by a high-intensity signal from the star sensor after the sun was acquired

(reflected light entering within ±35 deg of the star sensor's line of sight will yield a star intensity indication). Based on that indication, it was surmised that the roll angle of Canopus, with respect to the star sensor's line of sight before starting the star mapping roll, was either −60 or −120 deg. The analog traces of the *star angle* and *star intensity* signals recorded during the roll indicated only three distinguishable stars plus a 20-deg-wide low-intensity signal (identified as the moon) and a 48-deg-wide variable-high-intensity signal (identified as the earth). The angular spacing of the signals was compared with the previously calculated star, earth, and moon angles, thus permitting positive identification of Canopus and other stars. Subsequent analysis of bulk printer data identified a fourth star that was not distinguishable on the analog recording because of analog dropouts and noise. Because of the small number of identifiable stars and the variable-intensity indications from the moon and earth, it was decided to perform a second complete revolution for star mapping prior to acquiring Canopus. The first 360-deg map was made using Omniantenna B, while the second map and acquisition were made using Omniantenna A.

Both the *star angle* and *star intensity* signals appeared normal when the sensor rolled past the stars Ras Alhague, Shaula, Canopus, and Zeta C Majoris. When rolling past the moon and earth the *star angle* signal was very erratic about a zero value. The *star intensity* signal increased uniformly when rolling past the moon, but was high and varying when rolling past the earth with its varying surface brightness.

Prior to launch, a sun filter having 20% increased filtering action was installed. This provided the star sensor with a dimmer sun signal, which was expected to permit 20% increased star intensity values. A comparison of actual indicated intensities vs predicted intensities is given in Table IV-11. This comparison indicates either that the sensitivity of the intensity signal was increased more than the planned 20% or that star brightness in space is only known to within about 20%.

No *Canopus lock-on* signal was received when the sensor rolled past Canopus. Therefore, it was necessary to use the *manual lock-on* command to lock on Canopus. A *cruise mode* command was sent at the time Canopus was in the field of view during the third revolution. Spacecraft roll was stopped over 2 deg past the center of the field of view. The subsequent *manual lock-on* command caused the roll error angle to null to zero in approximately 40 sec. Since Canopus did not yield a usable *lock-on* signal, credence is given to the suggestion that the sensitivity of the intensity signal was indeed increased more than the planned 20%. However, it is also possible that Canopus appears brighter in space than predicted.

Table IV-11. Star angles and intensities: indicated vs predicted

Roll angle, deg	Source	Angle from Canopus, deg		Relative intensity	
		Indicated	Predicted	Indicated	Predicted
0	(Start of roll)	First star mapping roll			
100.0	Ras Alhague	−140.0	−139.5	0.971	0.86
135.6	Moon	−104.4	−102.7	1.142	—
150.5	Shaula	−89.5	−89.7	1.430	1.56
240.0	Canopus	0	0	4.995	5.00
262.5	Zeta C Majoris	+22.5	+22.7	0.854	0.72
325.2	Earth	+85.2	+85.0	4.916	—
		Second star mapping roll			
460.0	Ras Alhague	+220.0	+220.5	0.976	0.86
496.2	Moon	+256.2	+257.3	1.127	—
510.5	Shaula	+270.5	+270.3	1.372	1.56
600.0	Canopus	0	0	4.995	5.00
622.5	Zeta C Majoris	+22.5	+22.7	0.844	0.72
684.6	Earth	+84.6	+85.0	4.936	—
		Canopus acquisition roll			
820.0	Ras Alhague	+220.0	+220.5	0.937	0.86
857.4	Moon	+257.4	+257.3	1.137	—
870.5	Shaula	+270.5	+270.3	1.352	1.56
960.0	Canopus	0	0	4.995	5.00
—	No Star	—	—	0.77	0.66

The Canopus sensor was modified to solve a window fogging problem which occurred during early solar-thermal-vacuum (STV) tesing. The thermal paint pattern on the sun shade was changed to increase the sensor temperature, and silicone grease was removed from gaskets to reduce the possibility of contamination. A comparison of the Canopus sensor temperatures of *Surveyors I* and *II* just prior to the midcourse velocity correction indicates that the Canopus sensor temperature was 84.7°F

for *Surveyor II* compared to a temperature of 78°F for *Surveyor I*. There was no evidence of any window fogging of *Surveyor II*.

4. Gyro Drift and Limit Cycle Dead Bands—Cruise Mode

A single gyro drift check was made on September 20 between 19:26:24 (about 7 hr after launch) and 21:35:22 GMT. Drift checks are necessary to ascertain whether a correction factor needs to be included in the premidcourse and terminal maneuver computations to correct for excessive gyro drift. The drift rates were nominal as follows (in deg/hr): pitch, +0.25; yaw, +1.0; roll, −0.79.

The peak-to-peak single-axis optical deadband measurements based upon the data were as follows (in deg): pitch, 0.25; yaw, 0.35; and roll, 0.5.

5. Premidcourse Maneuvers

The premidcourse attitude maneuvers (+75.4 deg roll and +110.6 deg yaw) were accomplished satisfactorily. The alternate or backup maneuvers in the event the spacecraft would not roll were a pitch of −111.1 deg and a yaw of +13.7 deg. In the event that the spacecraft would not yaw, the maneuvers were an additional roll of −89.9 deg followed by a pitch of −110.5 deg.

6. Midcourse Velocity Correction

When midcourse thrusting was commanded at 05:00:02 GMT on September 21, Vernier Engine 3 failed to ignite and the spacecraft tumbled, saturating the gyro error signals, which indicated a minus pitch, plus yaw, and minus roll. After termination of midcourse thrusting, the pitch and yaw gyro error signals varied from plus to minus with a period of about 13 sec until rate mode was commanded *on*, at which time the signals returned to their original saturated positions of minus pitch, plus yaw, and minus roll. The gas-jet amplifiers were not inhibited immediately after thrust termination because it was believed that the tumble rate might be small enough for the gas-jet attitude control system to dampen it out without using an excessive amount of nitrogen. The telecommunications analyst later estimated the maximum tumble rate to be approximately 1.22 rev/sec (a period less than 1 sec) based upon DSIF AGC data. When it became obvious that the gas system would not be able to remove the angular rates, the gas jet amplifiers were inhibited at 05:14:29, with an estimated 2.16 lb of nitrogen remaining and a spacecraft tumble rate of approximately 0.97 rev/sec. Table IV-12 shows the expected and actual nitrogen consumption during the mission as derived from pressure and temperature data.

If it is assumed that the acceleration amplifier was saturated (−14.3-dc difference based on *Surveyor II* test

Table IV-12. Nitrogen gas consumption

Time, GMT	Event	N_2 pressure, psig	N_2 temperature, °F	N_2 remaining, lb	Actual N_2 usage		Expected N_2 usage
					For event	Cumulative total	
September 20							
10:35	Prelaunch	4586	80.0	4.50	0	0	0
13:02:58	Rate stabilization and sun acquisition	4480	77.4	4.45	0.05	0.05	0.100
19:24:58	Canopus acquisition	4100	47.3	4.44	0.01	0.06	0.159
September 21							
04:00:00	Cruise	3970	40.2	4.42	0.02	0.08	0.182
05:14:29	Gas jets inhibited						
06:09:47	Attitude maneuver and midcourse thrusting	1630	6.8	2.16	2.26	2.34	0.288
10:13:37	Post-midcourse	1760	36.7	2.16	0	2.34	

data) and the pitch and yaw shaping amplifier was also saturated (11.04-dc difference) almost immediately after the start of vernier ignition, then the vernier engine thrust level commands may be calculated as follows using nominal vernier amplifier gains:

Engine 1

+150 ma due to acceleration error
−175 ma due to pitch gyro error
+ 64 ma due to yaw gyro error

+ 39 ma

Engine 2

+150 ma due to acceleration error
+ 36 ma due to pitch gyro error
−192 ma due to yaw gyro error

− 6 ma

Engine 3

+150 ma due to acceleration error
+148 ma due to pitch gyro error
+127 ma due to yaw gyro error

+ 80 ma (maximum capability of vernier amplifier)

These values correspond to approximately 85 lb of thrust on Engine 1 and 65 lb on Engine 2. The low output of the acceleration amplifier during midcourse was expected in view of the fact that not enough engine thrust was being generated to achieve the 0.1 *g* being commanded. During all subsequent firings, the output of the acceleration amplifier always indicated high, presumably because of the tumbling effect on the accelerometer.

7. Post-Midcourse Attempts to Ignite Vernier Engine 3

Two attempts were made to ignite Engine 3, beginning at 07:28:27 while the spacecraft was in the normal midcourse velocity correction mode. The engine burn time was 2.0 sec in each case. Vernier Engines 1 and 2 ignited normally, but no indication that Engine 3 ignited was received from the strain-gage telemetry signal, the temperature sensor, or the pitch and yaw gyro error signals.

Next, the vernier engines were commanded on five times in succession, for 0.2 sec every 5 min, followed by a 2.0-sec thrust period. This sequence was performed five times. After the fifth sequence, a 2.5-sec burst was made at the high thrust levels normally used to assist in separating the retro engine after burnout. In order to obtain the desired thrust levels, which occur only between retro engine burnout and delayed burnout, without causing retro ejection, it was necessary to set the retro burnout and retro eject latches high, with thrust phase power off.

Following another sequence of five 0.2-sec firings starting at 07:44:56, a final attempt was made to open the fuel pressure regulator valve by commanding high thrust for 20 sec. The gas jets were enabled as part of this command sequence. The calculated vernier engine thrust commands for this test were as follows:

Engine 1

+ 48 ma due to high thrust command
−175 ma due to pitch gyro
+ 64 ma due to yaw gyro

− 63 ma

Engine 2

+ 48 ma due to high thrust command
+ 36 ma due to pitch gyro
−192 ma due to yaw gyro

− 80 ma (maximum capability of vernier amplifier)

Engine 3

+ 48 ma due to thrust command
+148 ma due to pitch gyro
+127 ma due to yaw gyro

+ 80 ma (maximum capability of vernier amplifier)

The difference between the calculated command for Vernier Engine 1 and the actual can be accounted for by the expected variation in shaping amplifier saturation voltages. The ranges of differential saturation voltages for *Surveyor II* are shown below:

Acceleration amplifier, +15.43 and −14.27 v

Pitch shaping amplifier, +10.63 to +16.88 and −11.04 to −16.77 v

Yaw shaping amplifier, +10.84 to +16.72 and −11.04 to −17.10 v

8. Retro Ignition

At retro ignition (09:34:28.65 on September 22), the indicated thrust level rose from 7.14 to 10.27 *g* and

remained nominally at that level until 09:34:48, at which time the indicated acceleration began increasing until 09:35:00, at which time the acceleration was 11.72 *g*. Shortly thereafter all spacecraft contact was lost. The estimated spin rate at time of data loss was 1.85 rev/sec.

G. Radar

Two radar devices, the altitude marking radar (AMR) and the radar altimeter and doppler velocity sensor (RADVS), are employed on the *Surveyor* spacecraft for use during the terminal descent phase.

1. Altitude Marking Radar

The AMR (Fig. IV-39) is a pulse-type fixed-range measuring radar which provides a *mark* signal at a slant range from the lunar surface that can be preset between 52 and 70 miles. The *mark* signal is used by the flight control subsystem to initiate the automatic operations for spacecraft terminal descent.

The AMR operates at a frequency of 9.3 gc. The mark range is obtained by use of dual-channel video gating (early and late gate signals). The early and late gates are adjacent at the preset range (60 miles for *Surveyor II*) so that, as the spacecraft approaches the lunar surface, the video return becomes equally distributed between these two gates. When the main lobe return is of equal magnitude in both gates and of such an amplitude to overcome a preset bias, the *mark* signal is generated and initiates the automatic operations for spacecraft terminal descent.

The AMR mounts in the retro rocket nozzle and is retained by friction clasps around the nozzle flange with spring washers between the AMR and the flange. When the retro rocket is ignited, the gas generated by the ignitor develops sufficient pressure to eject the AMR from the nozzle. The AMR draws power from 22 vdc through a breakaway plug that also carries input commands, the output *mark* signal, and telemetry information.

The AMR was not turned on during the *Surveyor II* mission. Temperatures were normal during the flight

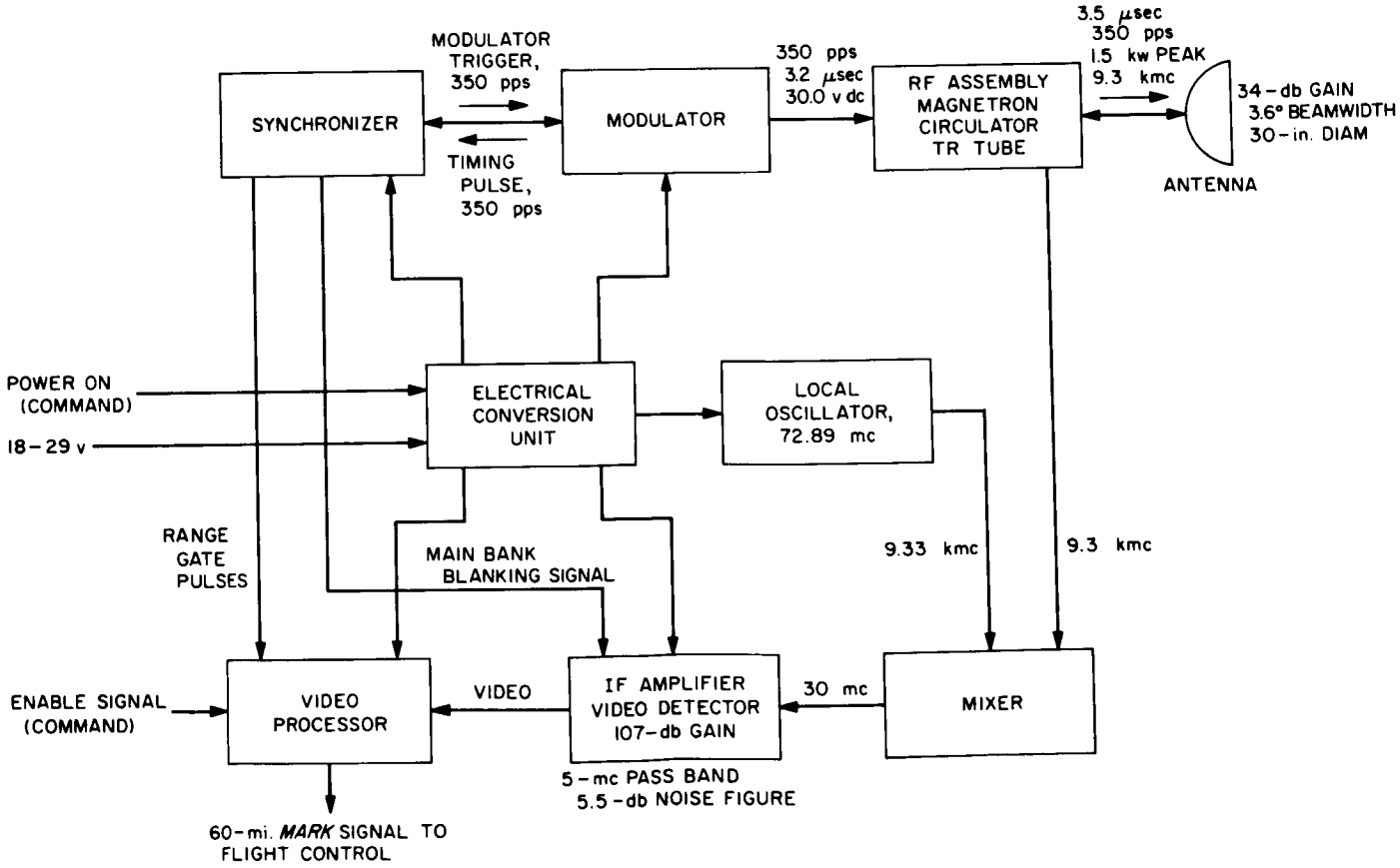

Fig. IV-39. Altitude marking radar functional diagram

except after tumbling. The antenna then received increased thermal radiation from the sun and the temperature at the edge of the antenna increased to +155°F (normal temperature is −185°F).

2. Radar Altimeter and Doppler Velocity Sensor

The RADVS (Fig. IV-40) functions in the flight control subsystem to provide three-axis velocity, range, and altitude mark signals for flight control during the main retro and vernier phases of terminal descent. The RADVS consists of a doppler velocity sensor (DVS), which computes velocity along the spacecraft *X*, *Y*, and Z axes, and a radar altimeter (RA), which computes slant range from 40,000 to 14 ft and generates 1000-ft and 14-ft mark signals. The RADVS comprises five assemblies: (1) klystron power supply/modulator (KPSM), which contains the RA and DVS klystrons, klystron power supplies, and altimeter modulator, (2) altimeter/velocity sensor antenna, which contains beams 1 and 4 transmitting and receiving antennas and preamplifiers, (3) velocity sensing antenna, which contains beams 2 and 3 transmitting antennas and preamplifiers, (4) RADVS signal data converter, which consists of the electronics to convert doppler shift signals into dc analog signals, and (5) interconnecting waveguide. The RADVS is turned on at about 50 miles above the lunar surface and is turned off at about 13 ft.

a. Doppler velocity sensor. The doppler velocity sensor (DVS) operates on the principle that a reflected signal has a doppler frequency shift proportional to the approaching velocity. The reflected signal frequency is higher than the transmitted frequency for the closing condition. Three beams directed toward the lunar surface enable velocities in an orthogonal coordinate system to be determined.

The KPSM provides an unmodulated DVS klystron output at a frequency of 13.3 kmc. This output is fed equally to the DVS1, DVS2, and DVS3 antennas. The RADVS velocity sensor antenna unit and the altimeter velocity sensor antenna unit provide both transmitting and receiving antennas for all three beams. The reflected signals are mixed with a small portion of the transmitted frequency at two points ¾ wavelength apart for phase determination, detected, and amplified by variable-gain amplifiers providing 40, 65, or 90 db of amplification, depending on received signal strength. The preamp output signals consist of two doppler frequencies, shifted by ¾ transmitted wavelength, and preamp gain-state signals for each beam. The signals are routed to the trackers in the RADVS signal data converter.

The D1 through D3 trackers in the signal data converter are similar in their operation. Each provides an output which is 600 kc plus the doppler frequency for approaching doppler shifts. If no doppler signal is present, the tracker will operate in search mode, scanning frequencies between 82 kc and 800 cps before retro burnout, or between 22 kc and 800 cps after retro burnout. When a doppler shift is obtained, the tracker will operate as described above and initiate a lock-on signal. The tracker also determines amplitude of the reflected signal and routes this information to the signal processing electronics for telemetry.

The velocity converter combines tracker output signals D_1 through D_3 to obtain dc analog signals corresponding to the spacecraft *X*, *Y*, and *Z* velocities; $D_1 + D_3$ is also sent to the altimeter converter to compute range.

Range mark, reliability, and reference circuits produce a *reliable operate* signal if D_1 through D_3 lock-on signals are present, or if any of these signals are present 3 sec after retro burnout. The *reliable operate DVS* signal is routed to the flight control electronics and to the signal processing electronics telemetry.

b. Radar altimeter. Slant range is determined by measuring the reflection time delay between the transmitted and received signals. The transmitted signal is frequency-modulated at a changing rate so that return signals can be identified.

The RF signal is radiated, and the reflected signal is received by the altimeter/velocity sensor antenna. The received signal is mixed with two samples of transmitted energy ¾ wavelength apart, detected, and amplified by 40, 60, or 80 db in the altimeter preamp, depending on signal strength. The signals produced are difference frequencies resulting from the time lag between transmitted and received signals of a known shift rate, coupled with an additional doppler frequency shift because of the spacecraft velocity.

The altimeter tracker in the signal data converter accepts doppler shift signals and gain-state signals from the altimeter/velocity sensor antenna and converts these into a signal which is 600 kc plus the range frequency plus the doppler frequency. This signal is routed to the altimeter converter for range dc analog signal generation.

The range mark, reliability, and reference circuits produce the *1000-ft mark* signal and the *14-ft mark* signal

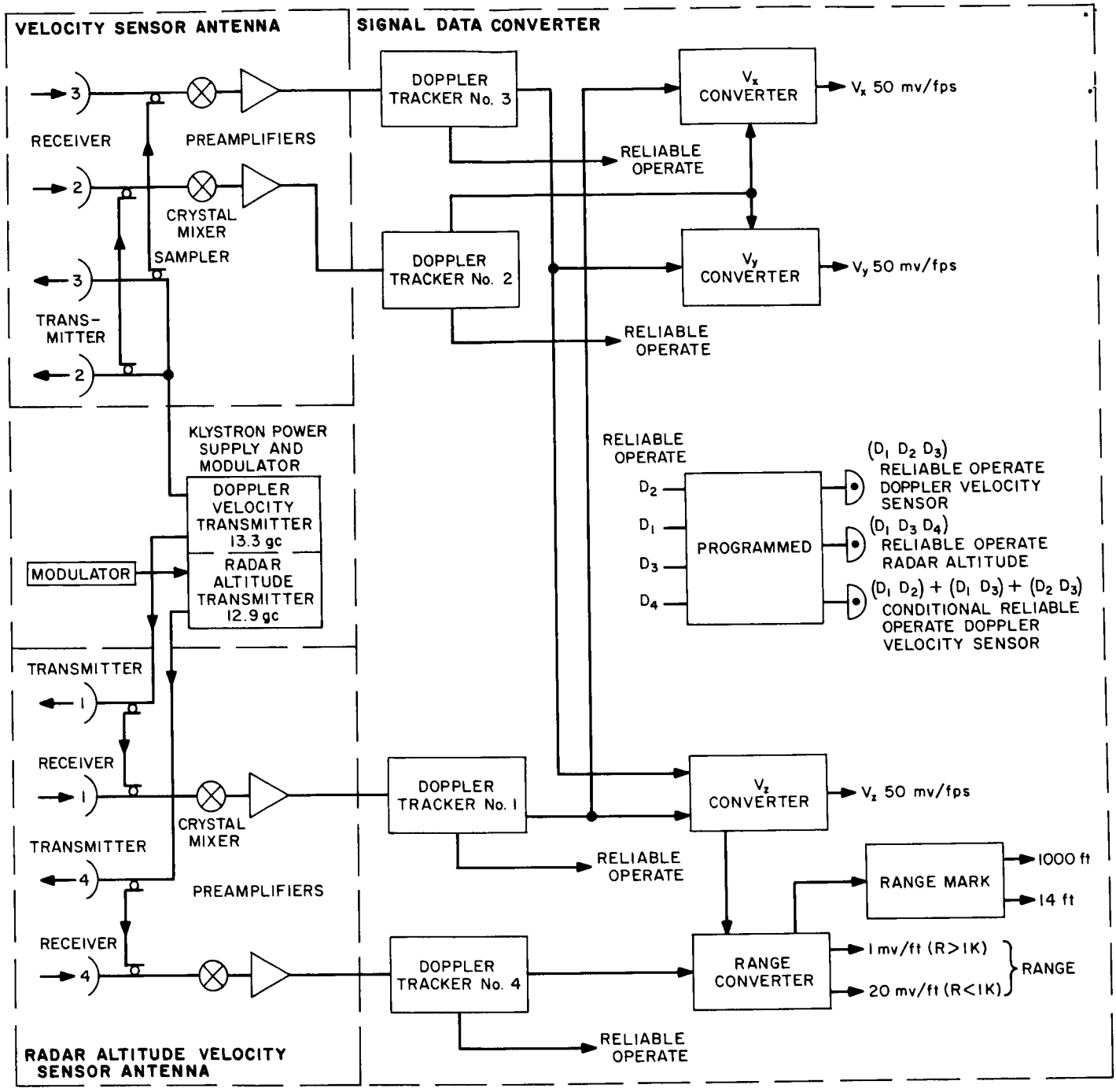

Fig. IV-40. Simplified RADVS functional block diagram

from the *range* signal generated by the altimeter converter where the doppler velocity V_z is subtracted giving the true range.

The *range mark* and *reliable* signals are routed to flight control electronics. The signals are used to rescale the *range* signal, for vernier engine shutoff and to indicate whether or not the *range* signal is reliable. The *reliable operate* signal is also routed to signal processing for transmission to DSIF.

c. RADVS performance. The RADVS was turned on prior to the main retro firing (near the end of the mission) for a battery load test. RADVS power was on for a total of 10 min 12 sec. Unfortunately, the telemetry mode was

not proper for RADVS operational data. The only data received were temperatures. Table IV-13 presents a listing of some of the RADVS temperatures during the mission. Figures IV-41 through IV-44 present the plots of the temperature rises during power on. The antennas and klystron power supply modulator (KPSM) starting temperatures were within the expected ranges. However, the signal data converter (SDC) temperature (−84°F) was much too low for reliable operation. Normally, the lowest expected starting temperature is −21°F. Since data other than temperatures is not available, an analysis of SDC operation cannot be made. The temperature rise does indicate that at least the power supply in the SDC operated.

Surveyors I and *II* unit temperature data was used to predict the maximum temperature attained on the *Surveyor I* KPSM as shown in Fig. IV-41. This prediction was based on a parallel temperature rise for both units.

Table IV-13. *Surveyor II* RADVS temperature data

Time, GMT (September 22)	AMR electronics, °F	AMR antenna, °F	KPSM, °F	SDC, °F	DVS, °F	RADVS, °F	Comments
03:57:39	97.58	149.5	40.11	−81.25	63.0	18.0	Last Goldstone pass
09:13:00	36.30	137.3	33.50	−84.00	36.1	98.1	
09:19:57							RADVS on
09:26:00	96.30	138.7	103.00	−33.28	48.0	95.7	
09:30:09	96.30	138.7	128.30	1.00	50.1	101.0	RADVS off
09:31:19	96.30	138.7	123.80	2.70	51.9	102.7	

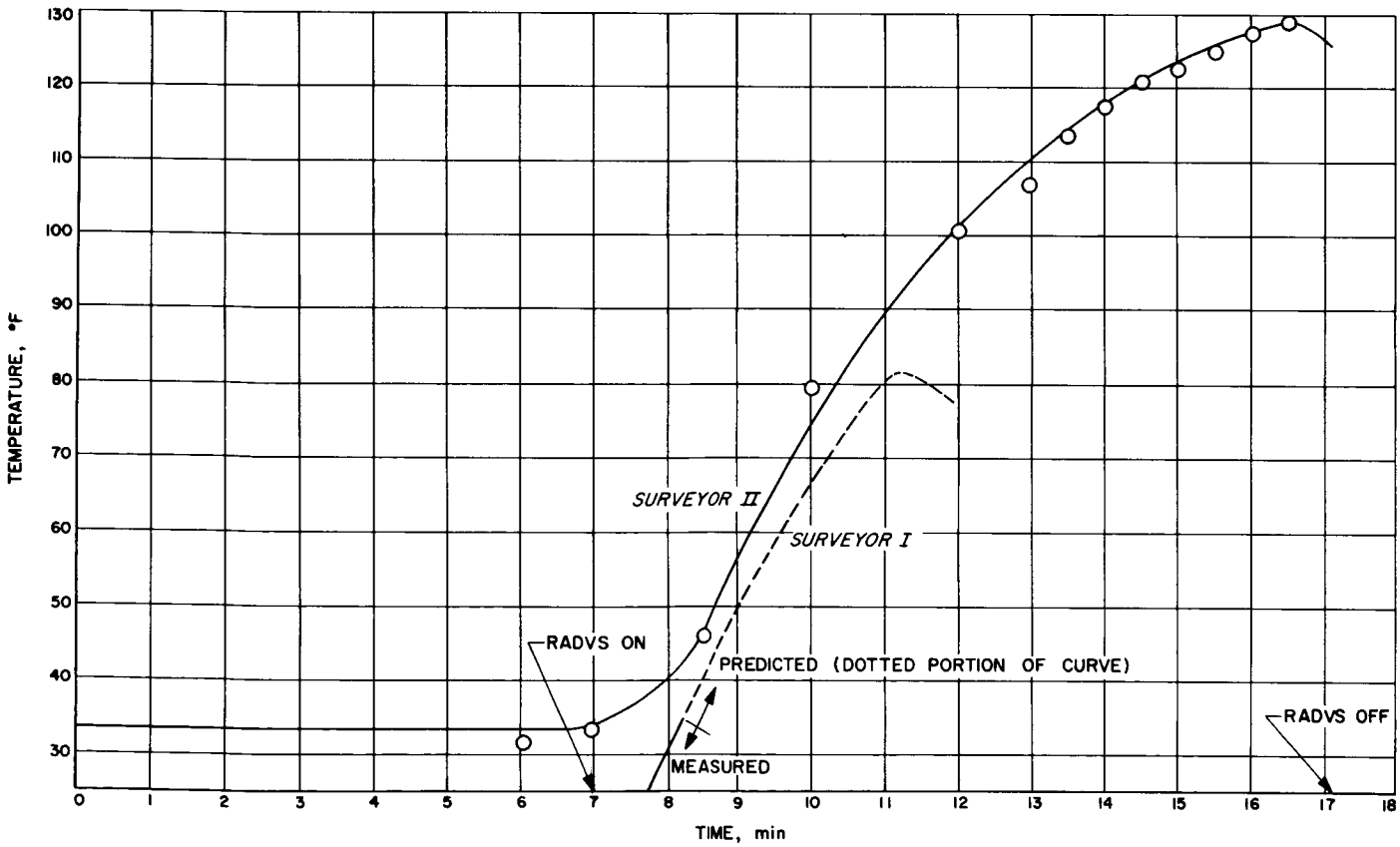

Fig. IV-41. Klystron power supply modulator temperature

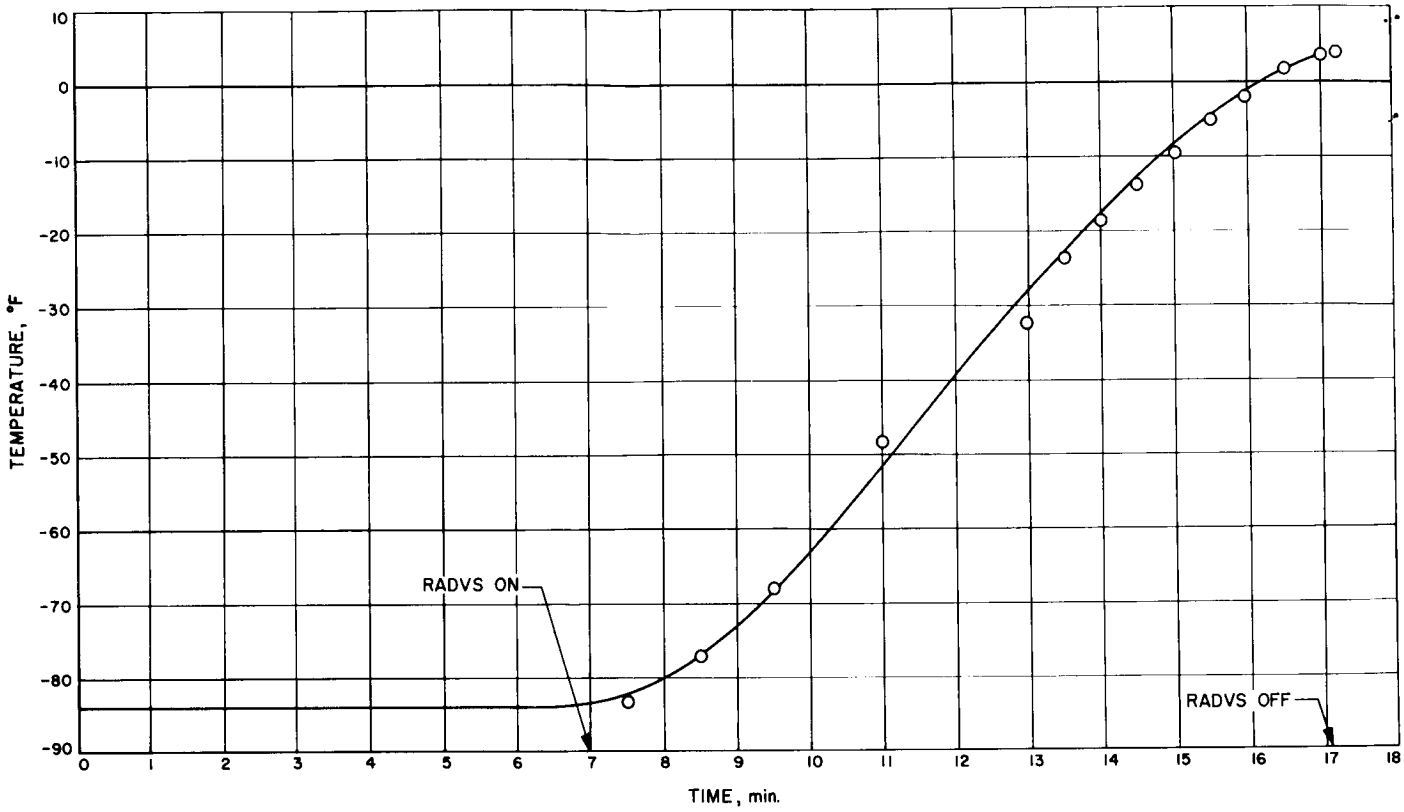

Fig. IV-42. Signal data converter temperature

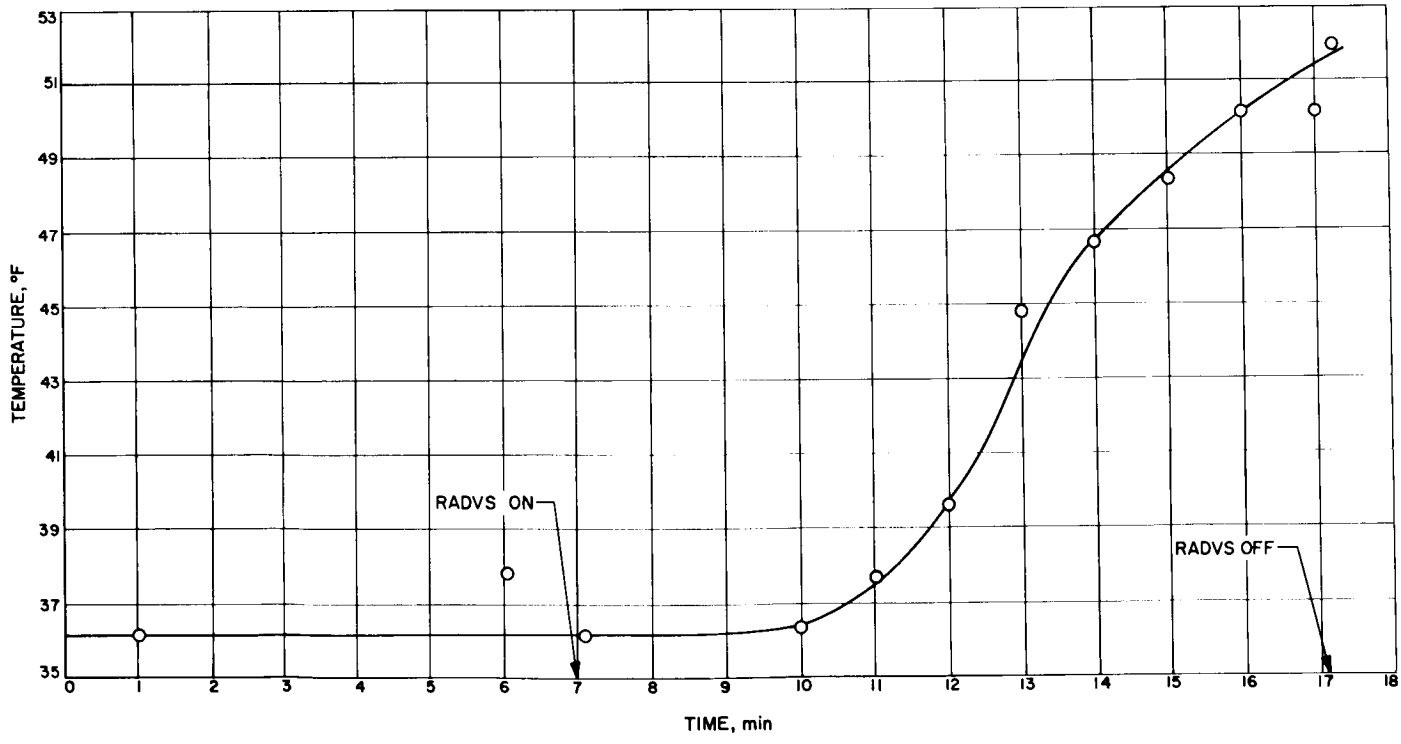

Fig. IV-43. Doppler velocity sensor temperature

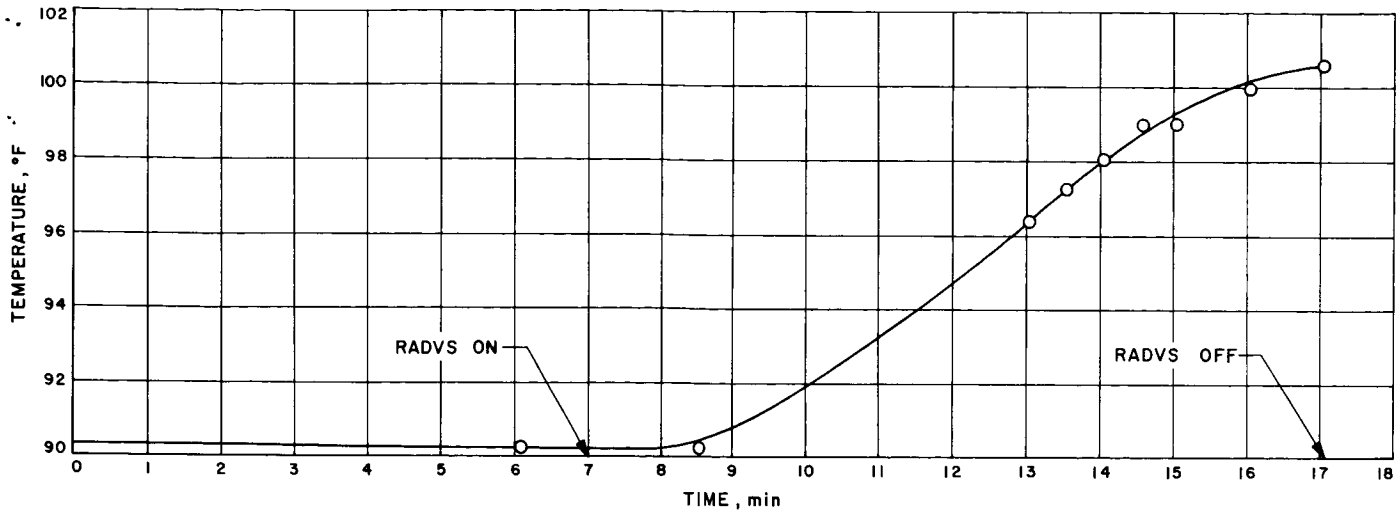

Fig. IV-44. Altitude marking radar temperature

Prediction variations of ±10 deg are expected since the klystron-to-heat-sink transfer characteristics differ for each unit. An attempt to predict the temperature rise in the SDC of *Surveyor I* was not made, owing to the vastly different starting temperatures.

H. Telecommunications

The *Surveyor* telecommunications subsystem contains radio, signal processing, and command decoding equipment, to provide (1) a method of telemetering information

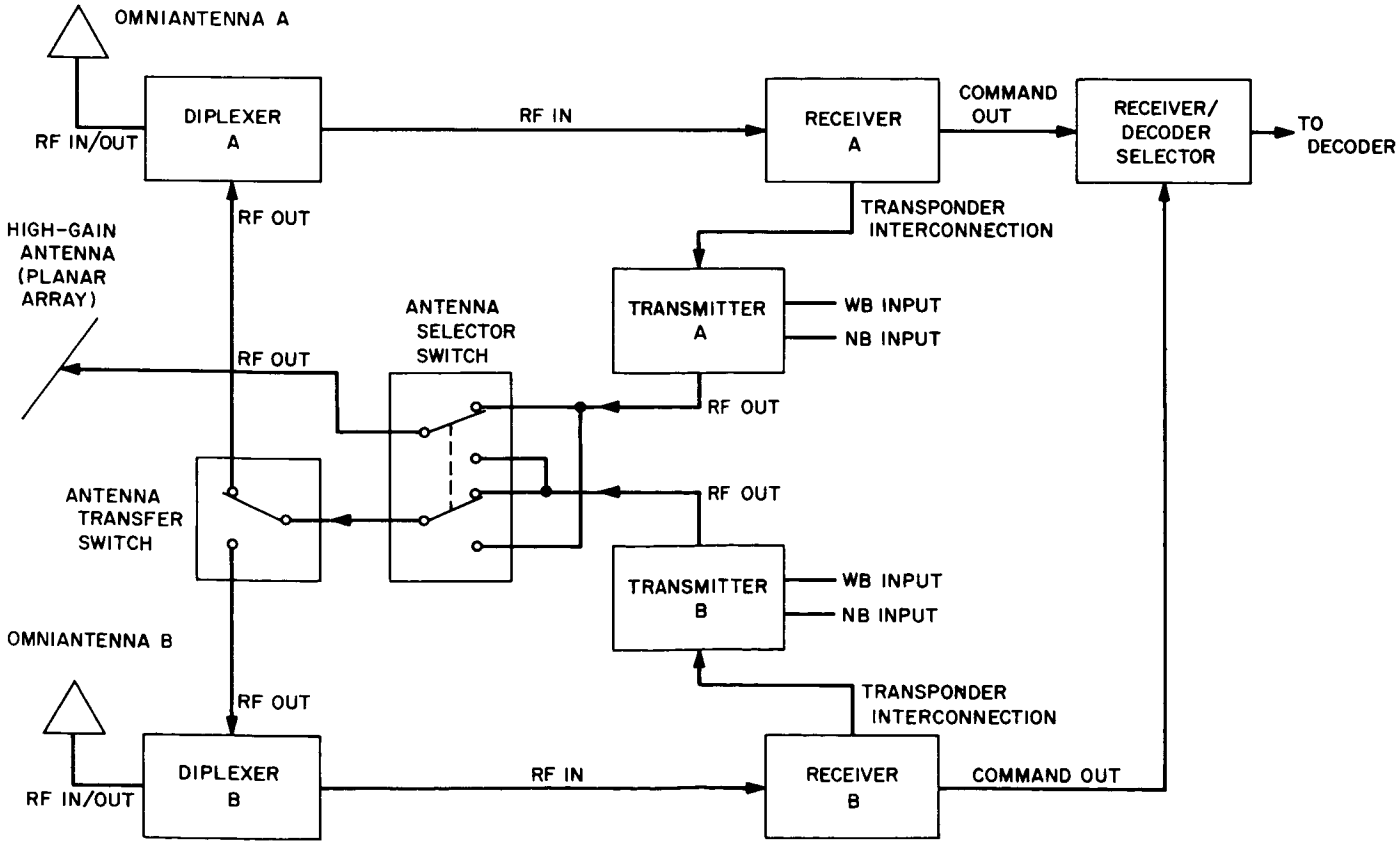

Fig. IV-45. Radio subsystem block diagram

to the earth, (2) the capability of receiving and processing commands to the spacecraft, and (3) angle-tracking one- or two-way doppler for orbit determination.

1. Radio Subsystem

The radio subsystem utilized on the *Surveyor* spacecraft is as shown in Fig. IV-45. Dual receivers, transmitters, and antennas were originally meant to provide redundancy for added reliability, although as arranged this is not completely true because of switching limitations. Each receiver is permanently connected to its corresponding antenna and transmitter.

Both receivers are identical crystal-controlled double-conversion units which operate continuously (cannot be commanded off). Each unit is capable of operation in an automatic frequency control (AFC) mode or an automatic phase control (APC) mode. The receivers provide two necessary spacecraft functions: the detection and processing of commands from the ground stations for spacecraft control (AFC and APC modes), and the phase-coherent spacecraft-to-earth signal required for doppler tracking (APC mode).

Transmitters A and B are identical units which provide the spacecraft-to-earth link for telemetry and doppler tracking information. The transmitters are commanded on (one at a time) from the ground stations. Each unit contains two crystal-controlled oscillators (wideband for TV data; narrowband for engineering data), which can be commanded on at will. The transmitters may also be commanded to operate at either 100 mw or 10 w of output power.

Two identical transponder interconnections permit each transmitter to be operated, on command, in a transponder mode. In the transponder mode, a transmitter

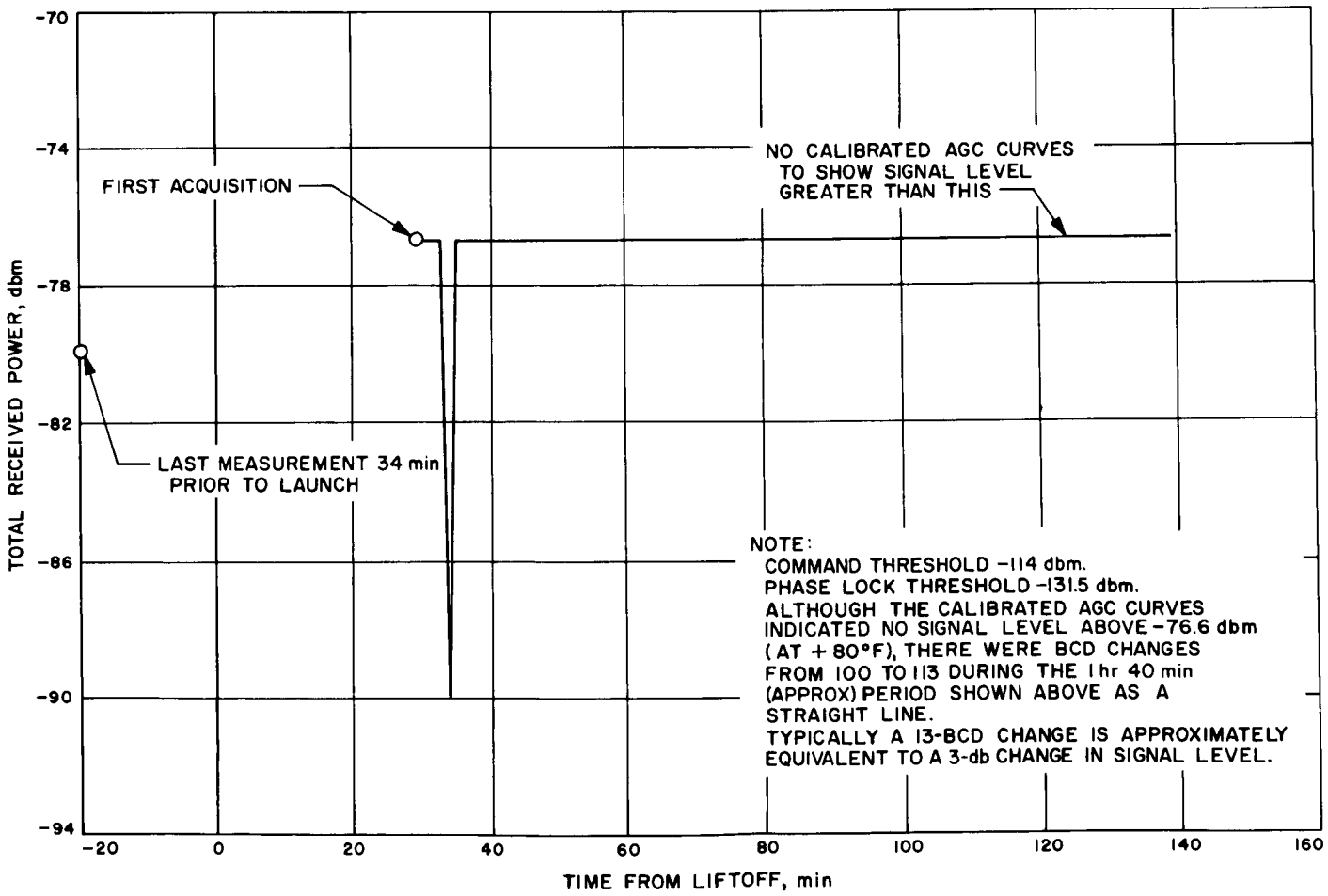

Fig. IV-46. Total received power, Receiver A

is operated with the corresponding receiver voltage-controlled oscillator to provide coherent signals when two-way doppler tracking data is required.

Three antennas are utilized on the *Surveyor* spacecraft. Two antennas are omnidirectional units which provide receive-transmit capability for the spacecraft. The third antenna is a high-gain (27-db) directional unit which is used primarily for transmission of wideband information. Either transmitter may be commanded to operate through any one of the spacecraft antennas as desired.

The radio subsystem on *Surveyor II* performed well during flight, except for Receiver B AGC telemetry. Receiver B was used as the prime spacecraft command receiver, and in conjunction with Transmitter B provided the necessary spacecraft doppler information. There was no evidence of malfunction in the receiver command or doppler performance during the flight.

The amplitudes of RF signals received at both spacecraft receivers and the DSIF stations were examined over the period of standard flight. The results are presented in Figs. IV-46 through IV-51 along with the predicted signal strengths. No attempts were made to correct for Receiver B AGC errors in that preflight calibration data was used. The AGC error becomes very evident in Fig. IV-49.

Three hours prior to launch, the receiver AGC problem was first questioned but not identified. Spacecraft telemetry indicated that Receiver A was receiving 25-db more signal than Receiver B. Previous data recorded 9 hr prior to launch indicated only a 9-db difference. The fact that

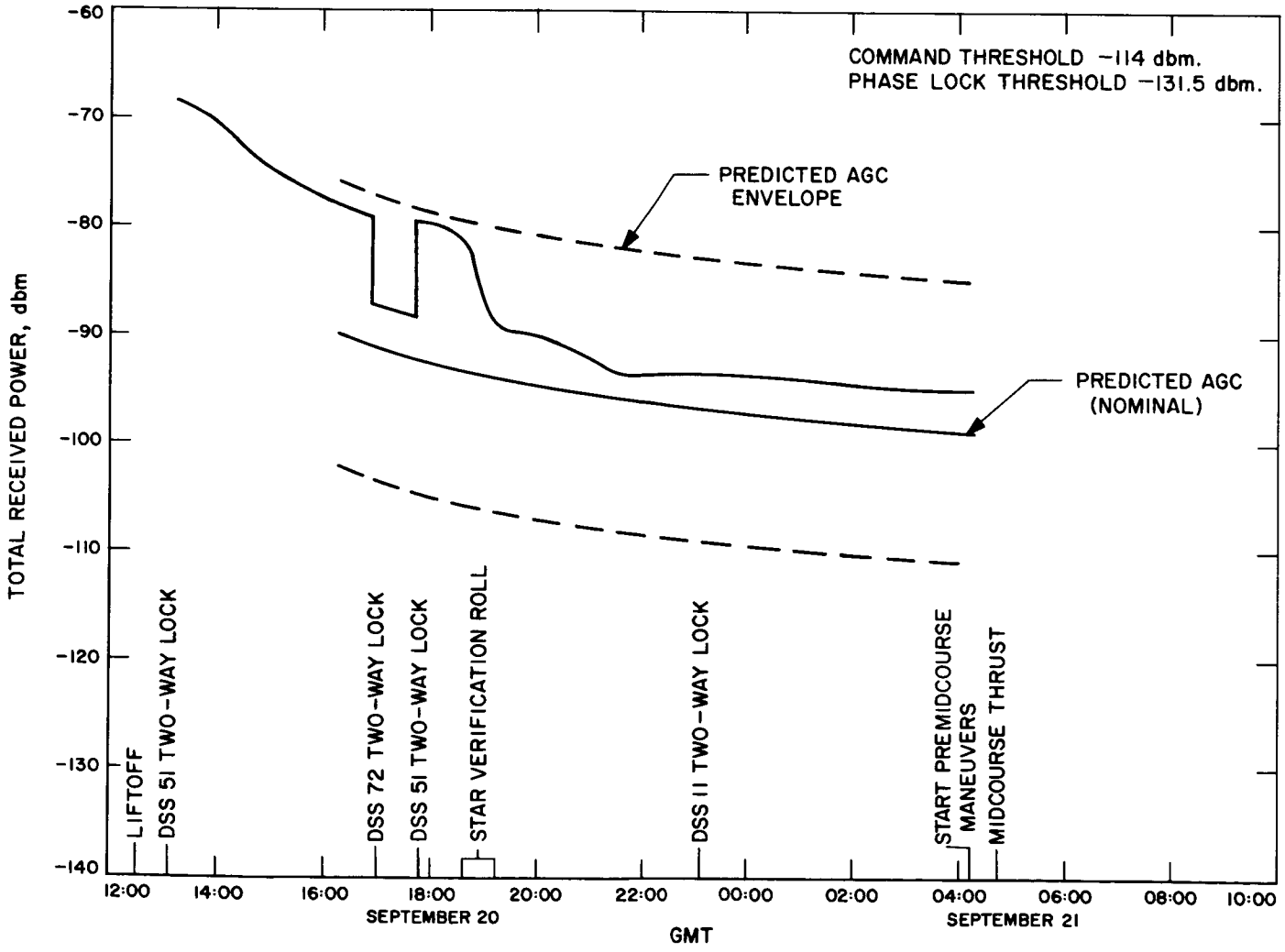

Fig. IV-47. Receiver A AGC vs GMT

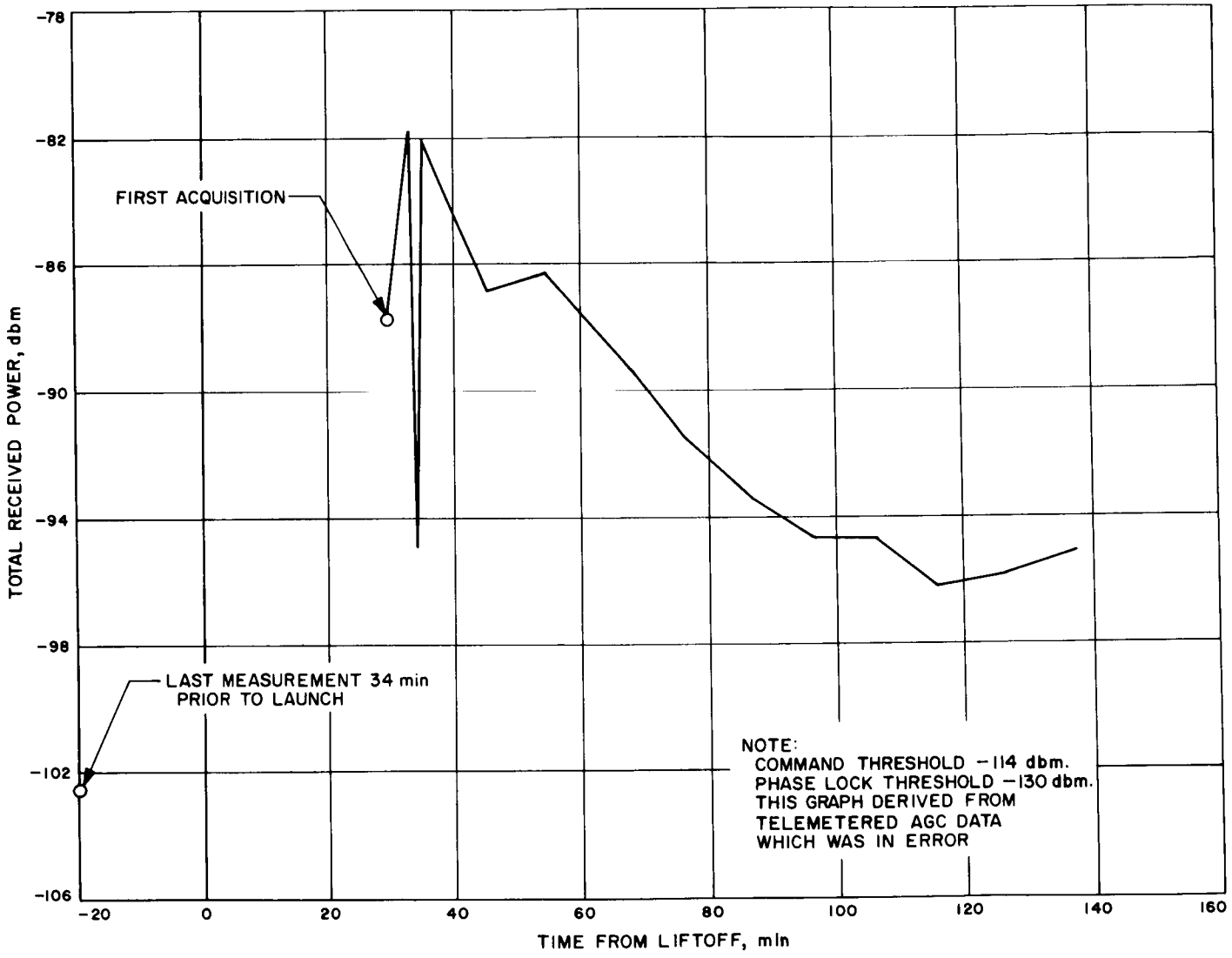

Fig. IV-48. Total received power, Receiver B

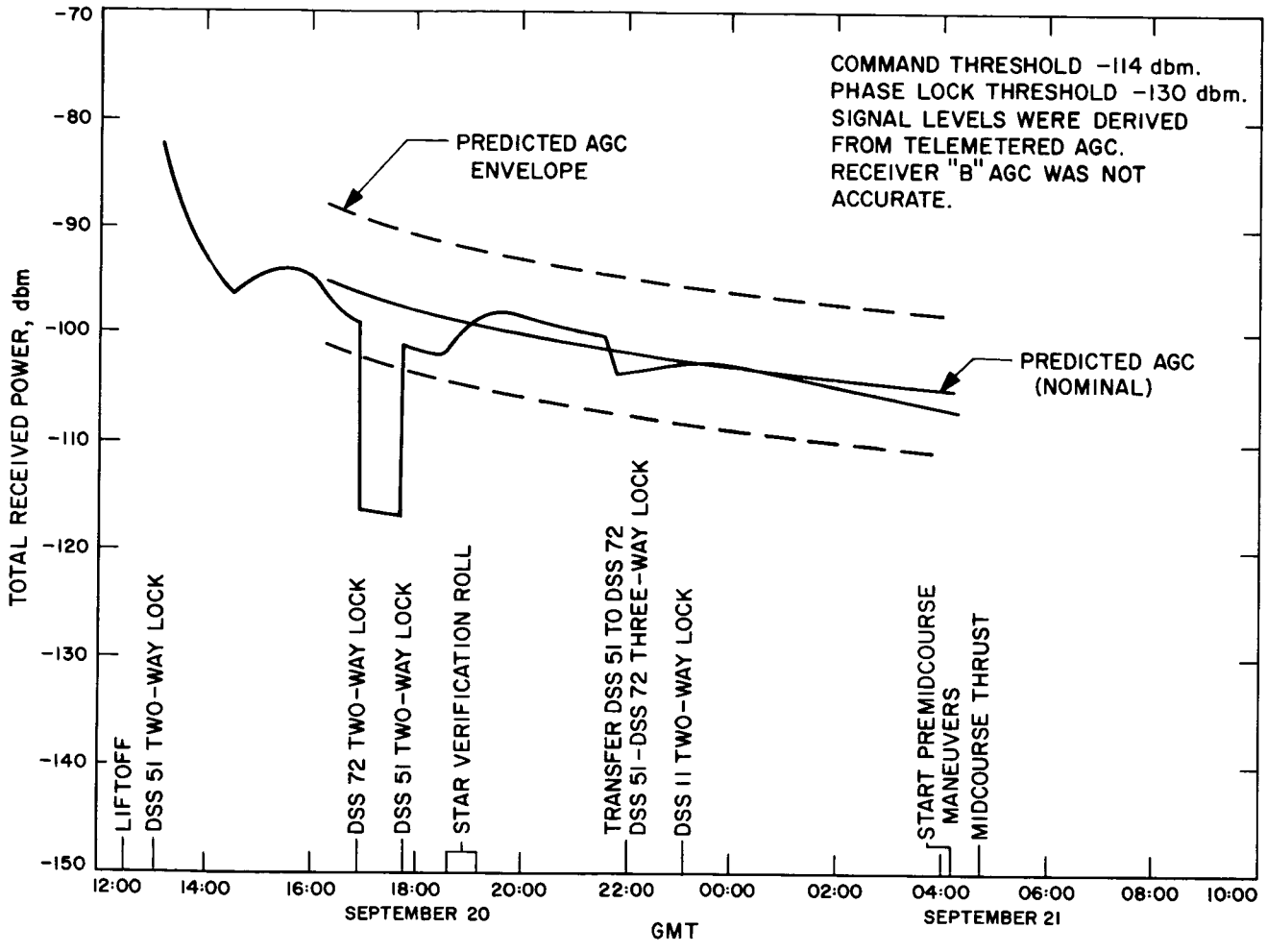

Fig. IV-49. Receiver B AGC vs GMT

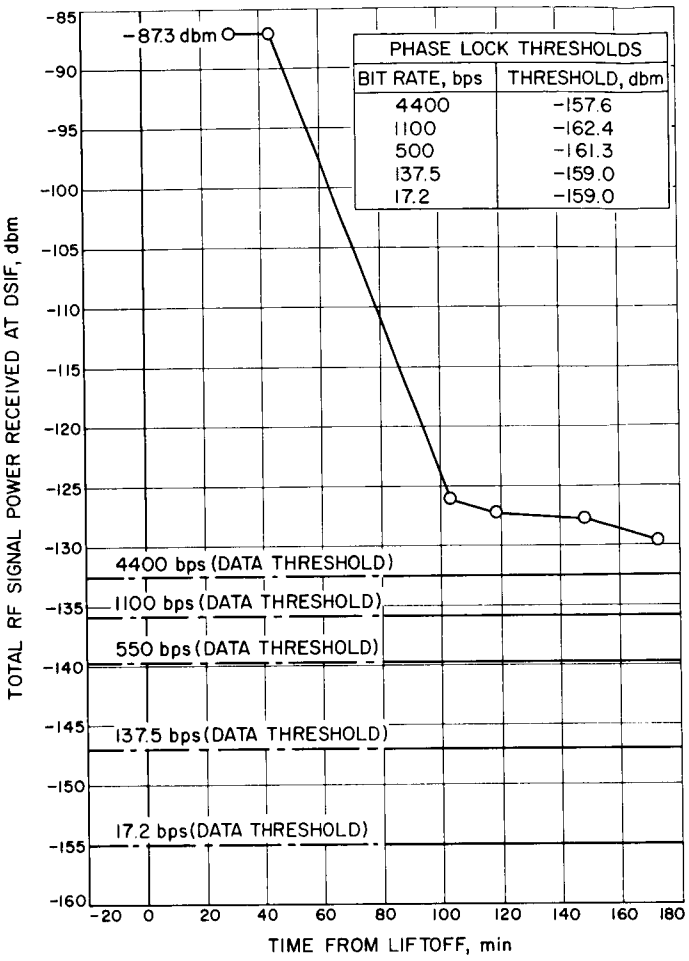

Fig. IV-50. DSS 51 received RF power vs time

the gantry was removed between the times of the two measurements leads to the conclusion that a null in the Receiver B antenna pattern produced the 25-db difference.

After launch, the lack of information on spacecraft orientation concealed the problem until Canopus was acquired (some 6 or 7 hr after liftoff). During the Canopus search, Receiver B never indicated signal levels as high as expected. After Canopus acquisition, the signal level to Receiver B was 11 db less than the signal to Receiver A. Omniantenna patterns were reviewed, and they indicated that during Canopus lock the signal to Receiver B should be stronger than the signal to Receiver A by greater than 10 db. Antenna contour maps are presented in Figs. IV-52 through IV-54. The results of the Canopus search are plotted in Figs. IV-55 through IV-57.

About 13 hr after launch, a special test was performed on the spacecraft receivers by lowering the DSIF station up-link power in 2-db steps while monitoring spacecraft telemetry. The results are presented in Table IV-14 and indicate the inadequacy of calibration data on Receiver B AGC. The first eight 2-db steps resulted in Receiver B telemetry changes of about 3 db. Telemetry information was further invalidated by the fact that receiver indexing did not occur until Receiver B telemetry indicated a signal level of −138 dbm.

(Preflight data indicated that Receiver B should index with a signal of −124 dbm.) It was not clear whether Receiver A or Receiver B actually produced the indexing, since the signal to Receiver A was close to its indexing level, and the telemetry data for Receiver B AGC was in error.

Preliminary investigations indicated that the signal processing equipment functioned normally and that the problem was in the receiver itself. If the spacecraft failure had not occurred at midcourse, further tests on Receiver B would have been performed and could have determined if its performance was actually degraded or only misrepresented by the telemetry.

The spacecraft radio system performed well during the nonstandard portion of the flight. When midcourse motor firing was initiated, the tumbling of the spacecraft was immediately apparent from the station receiver AGC. At the termination of firing the midcourse motors, the spacecraft rate of tumble was observed to be about 1.22 rev/sec, as indicated by receiver AGC. The gas stabilization jets reduced the tumbling rate to about 0.97 rev/sec in what appeared to be a fairly linear manner. The down-link signal amplitude initially varied as much as 17 dbm to as little as 3 dbm because the spacecraft rolled and tumbled in a periodic manner. The gas-jet firing stabilized the spacecraft antenna motion relative to the earth–spacecraft vector, thus producing fairly constant signal amplitude variations as the spacecraft tumbled. Typical signal amplitude variations during the early phase of the flight were 10 dbm with Omniantenna B and 15 dbm with Omniantenna A. As the tumbling rate increased with attempts to fire Engine 3, the station receiver AGC variations appeared to be less; the slow time constant of the AGC circuit would have damped out some of the variations.

Each time an attempt was made to fire Engine 3, an increased rate of AGC variation was noted. The lowest rate noted after midcourse was about 0.8 rev/sec and was recorded when the gas jets were inhibited prior to attempts at firing the malfunctioning engine. The many

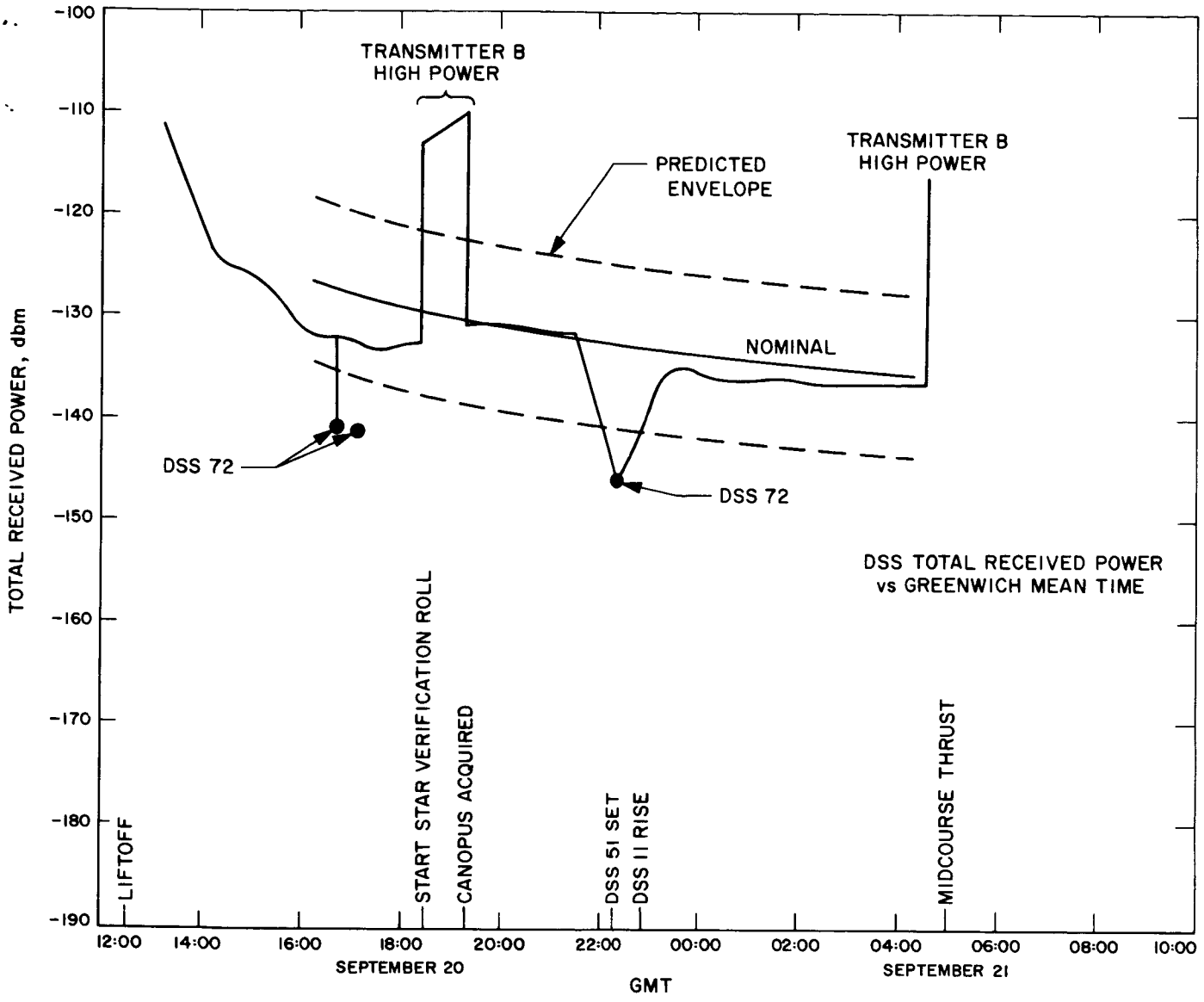

Fig. IV-51. DSS total received power vs GMT

attempts at short engine burns increased the AGC variations to a rate of about 1.5 rev/sec just prior to the long burn of 20 sec. The 20-sec burn increased the rate to about 2.3 rev/sec, which was slightly decreased when the helium was dumped. Firing of the retro engine reduced the AGC rate change to below 2 rev/sec just prior to loss of the down-link RF signal.

The ground stations experienced difficulty in maintaining decommutator lock until their receiver bandwidths were opened up. The bandwidths were first increased from about 76 cps to the desired 152 cps when in the 152-cps loop noise bandwidth position. The increased bandwidth was accomplished by physically modifying one of the receiver modules at the DSIF stations. Later in the flight, as the spacecraft tumbling rate increased (due to repeated engine firings) decommutator lock again became erratic. Further receiver modifications which increased the loop bandwidth to 300 cps reestablished firm decommutator lock.

2. Signal Processing Subsystem

The *Surveyor* signal processing subsystem accepts, encodes, and prepares for transmission the voltages, currents, and resistance changes corresponding to various spacecraft parameters such as events, voltages, temperatures, accelerations, etc.

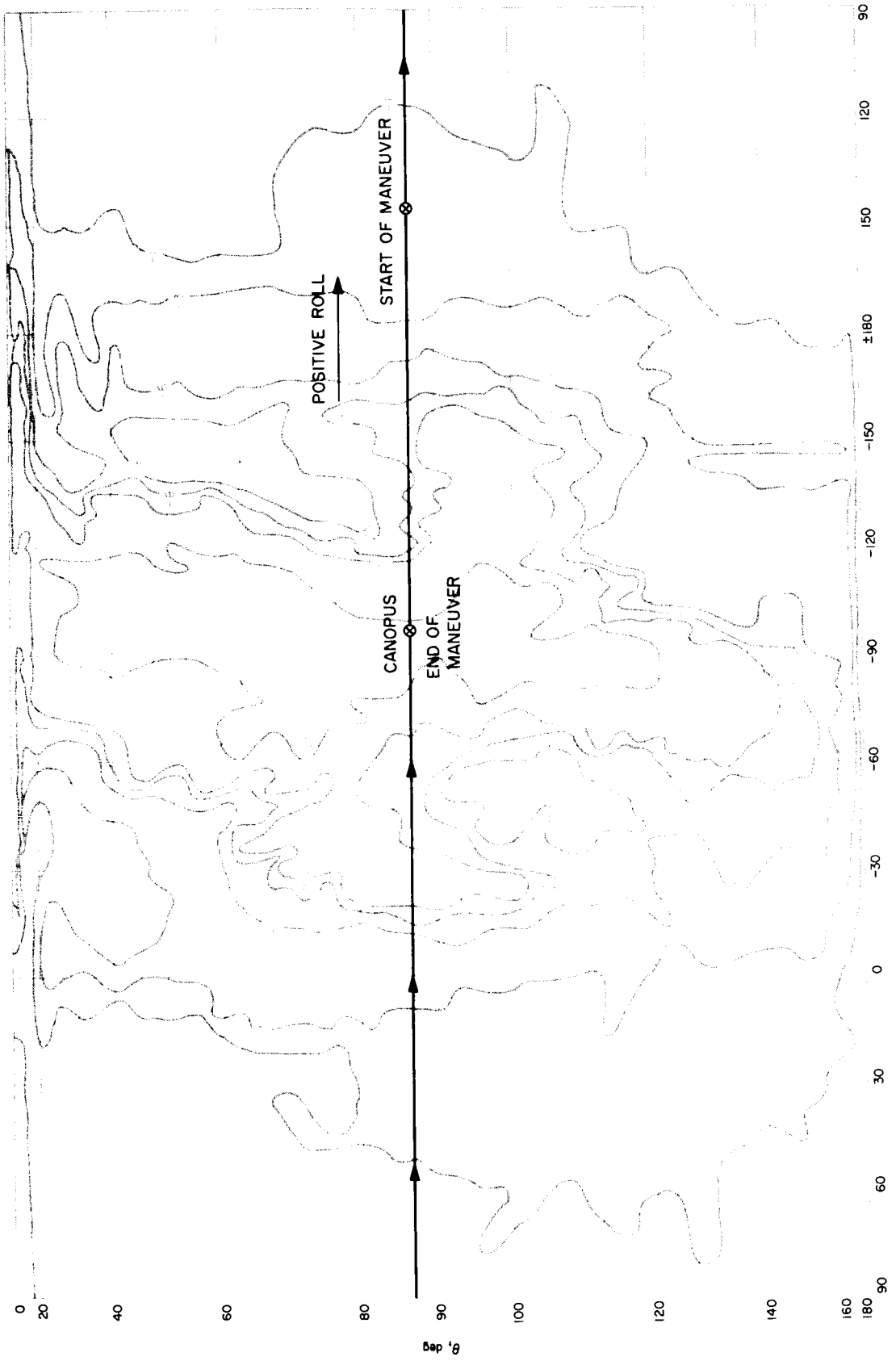

Fig. IV-52. Omniantenna A contour map, down-link

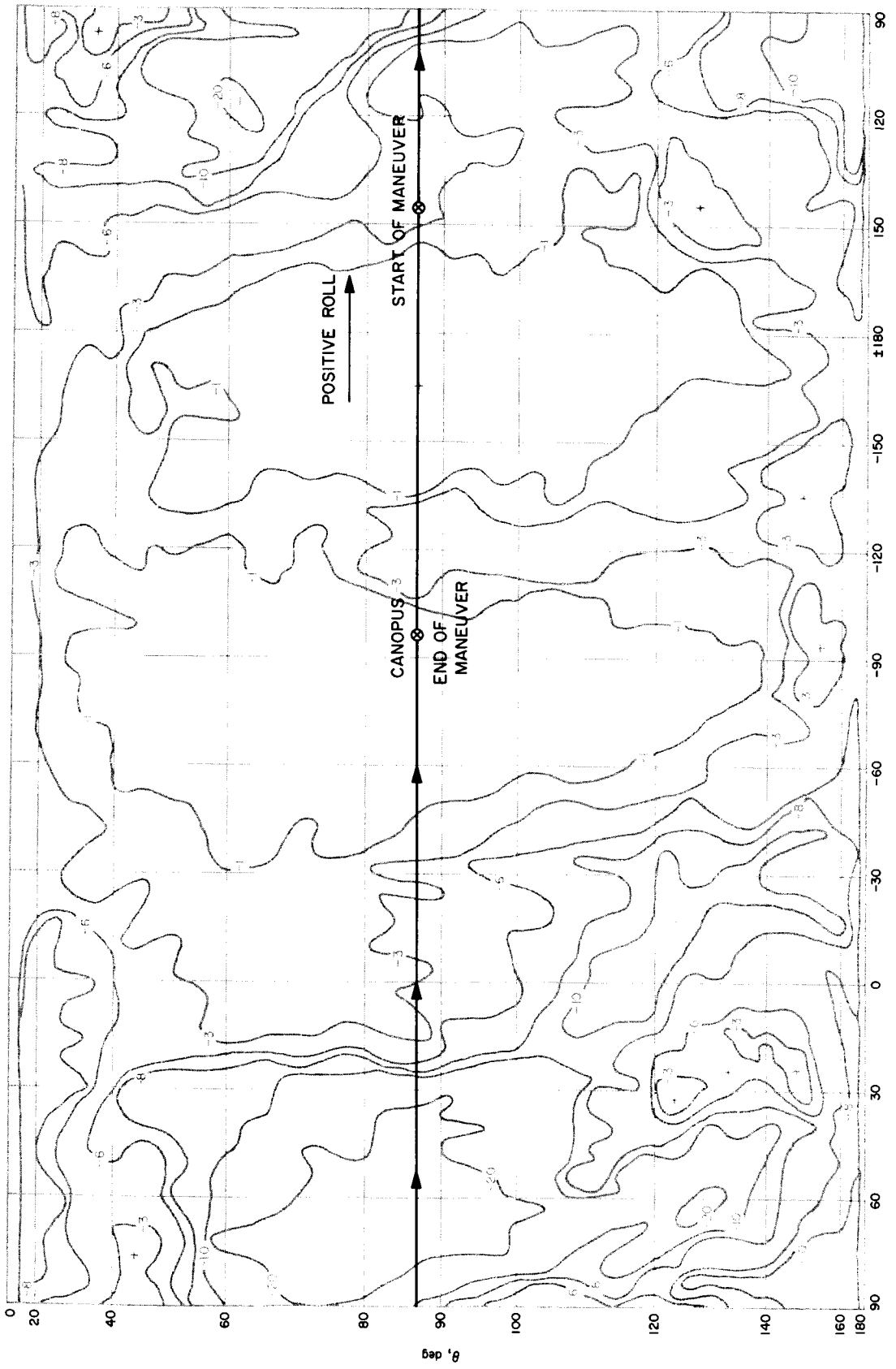

Fig. IV-53. Omniantenna B contour map, up link

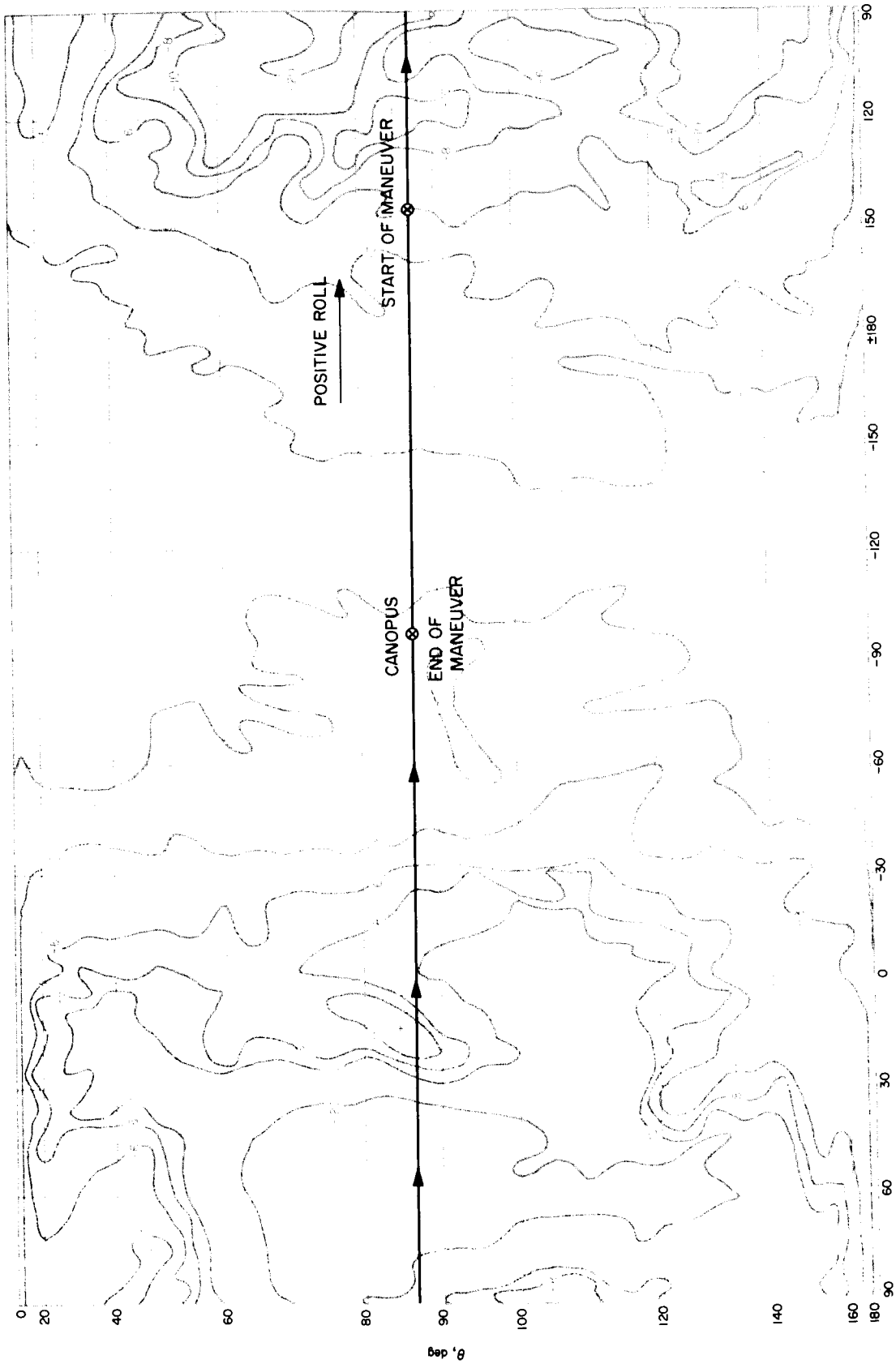

Fig. IV-54. Omniantenna B contour map, down link

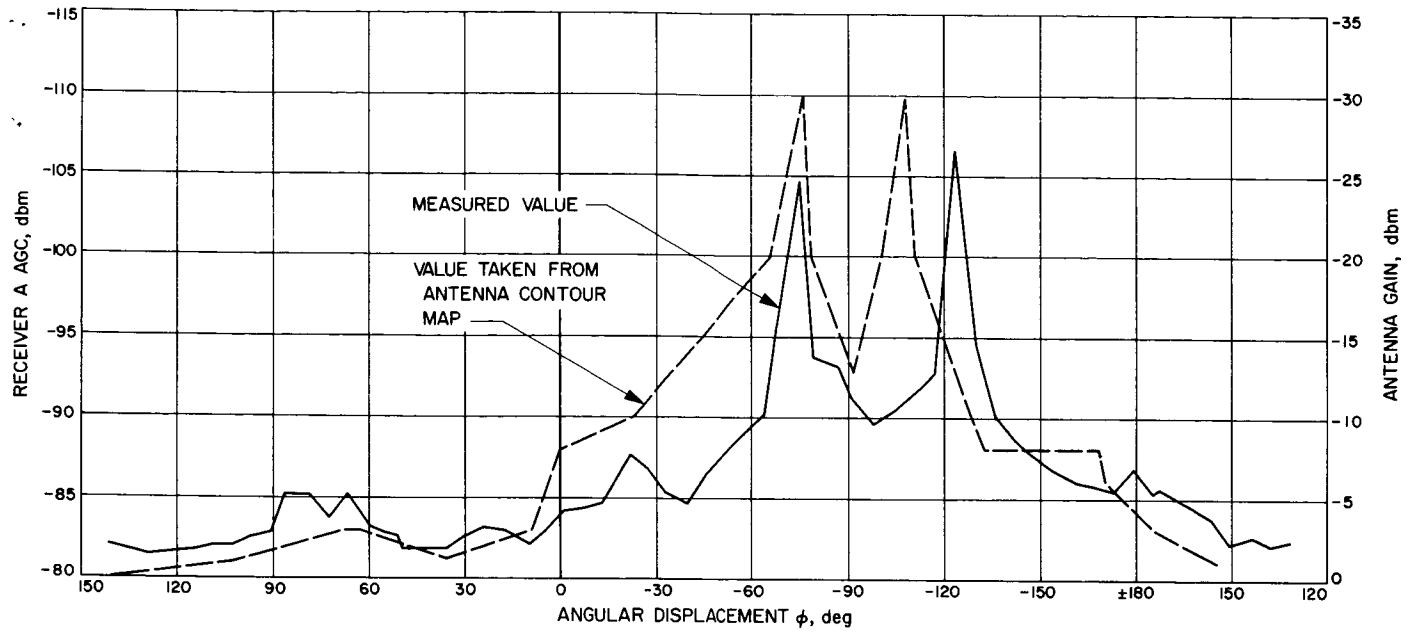

Fig. IV-55. Omniantenna A, Receiver A signal level vs angular displacement

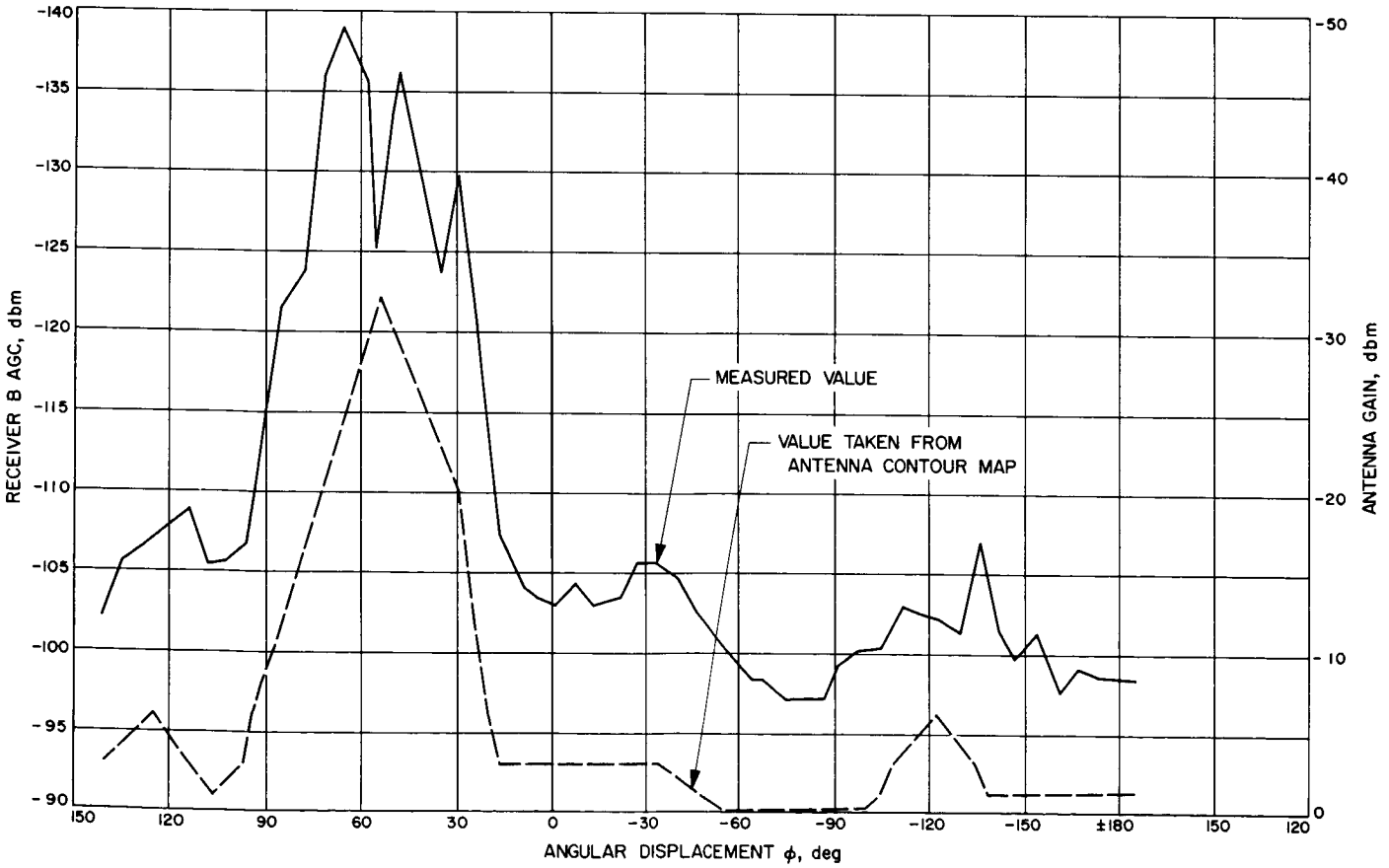

Fig. IV-56. Omniantenna B, Receiver B signal level vs angular displacement

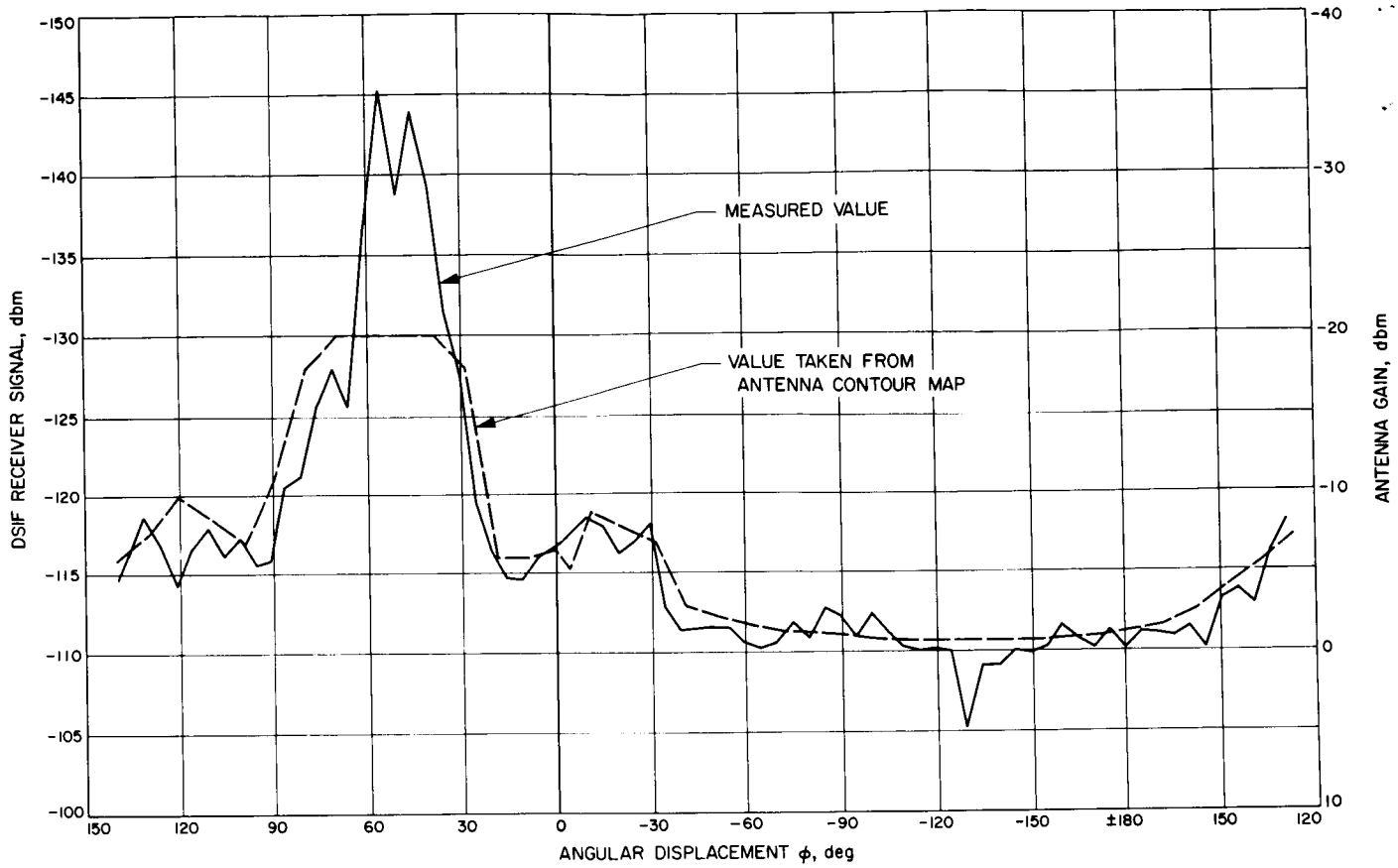

Fig. IV-57. Omniantenna B, Transmitter B signal level vs angular displacement

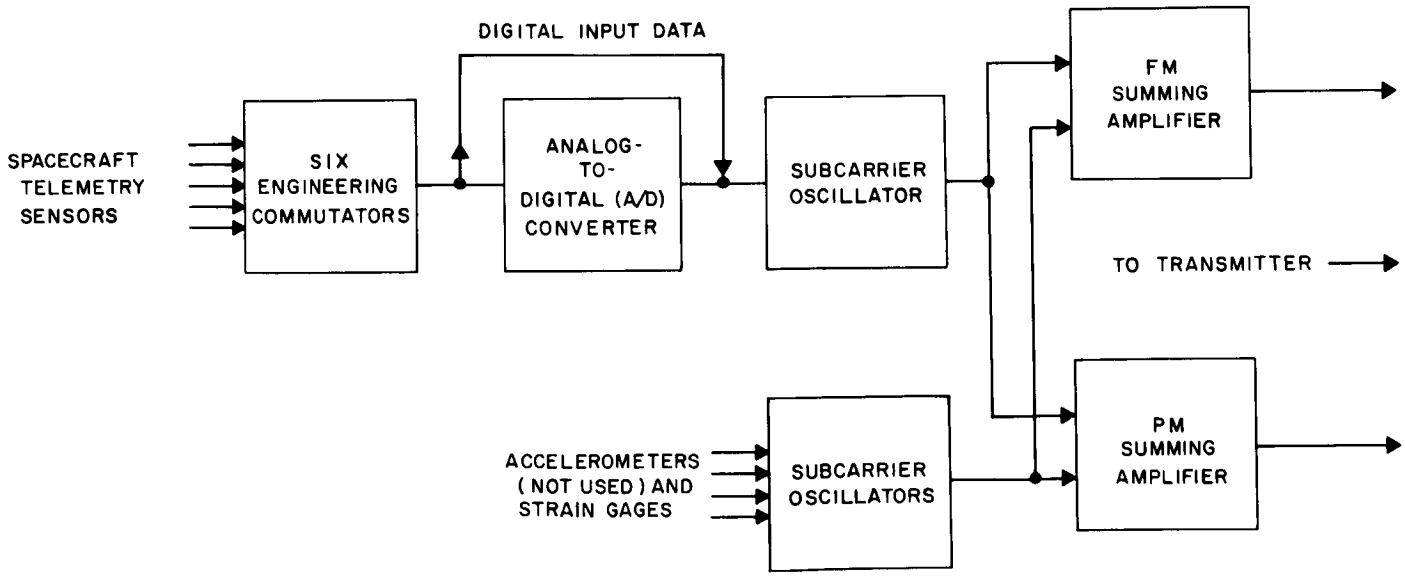

Fig. IV-58. Simplified signal processing subsystem block diagram

Table IV-14. Data from in-flight calibration of spacecraft receiver AGC

Time, GMT September 21	Change in DSIF signal level, dbm	Receiver A				Receiver B			
		BCD[a]	dbm	Receiver AGC change, dbm		BCD[a]	dbm	Receiver AGC change, dbm	
				Total	Last step			Total	Last step
01:36:39	0	207	−94.0	0	0	215	−104.9	0	0
01:37:15	− 2	223	−95.6	1.6	1.6	234	−108.3	3.4	3.4
01:39:48	− 4	242	−97.5	3.4	1.8	255	−112	7.1	3.7
01:42:04	− 6	258	−99.1	5.1	1.7	279	−115.9	11.0	3.9
01:44:21	− 8	278	−101.1	7.1	2.0	301	−119.1	14.2	3.2
01:47:15	−10	299	−103.3	9.3	2.2	321	−122.1	17.2	3.0
01:50:00	−12	318	−105.3	11.3	2.0	338	−124.9	20.0	2.8
01:51:28	−14	336	−107.4	13.4	2.1	353	−128.2	23.3	3.3
01:53:30	−16	356	−110.0	16.0	2.6	364	−131.3	26.4	3.1
01:56:24	−18	374	−113.0	19.0	3.0	371	−133.7	28.8	2.4
01:58:23	−20	388	−115.9	21.9	2.9	376	−135.7	30.8	2.0
02:00:12	−22	399	−118.7	24.7	2.8	379	−137	32.1	1.3
02:04:22	−24[b]	410	−122.2	28.2	3.5	381	−138	33.1	1.0

[a] Binary conversion data.

[b] Indexing occurred when DSIF signal was decreased by 24 dbm.

The signal processor (Fig. IV-58) employs both pulse code modulation and amplitude-to-frequency-modulation telemetry techniques to encode spacecraft signals for frequency- or phase-modulating the spacecraft transmitters.

The input signals to the signal processor are derived from various voltage or current pickoff points within the other subsystems as well as from standard telemetry transducing devices such as strain gages, accelerometers, temperature transducers, and pressure transducers. These signals generally are conditioned to standard ranges by the originating subsystem so that a minimum amount of signal conditioning is required by the signal processor.

As illustrated in Fig. IV-58, some of the signal inputs are commutated to the input of the analog-digital converter while others are applied directly to subcarrier oscillators. The measurements applied directly are accelerometer (not used) and strain gage measurements which require continuous monitoring over the short intervals in which they are active.

The commutators apply the majority of telemetry input signals to the analog-to-digital converter, where they are converted to a digital word. Binary measurements such as switch closures or contents of a digital register already exist in digital form and are therefore routed around the analog-to-digital converter. In these cases, the commutator supplies an inhibit signal to the analog-to-digital converter and, by sampling, assembles the digital input information into 10-bit digital words. The commutators are comprised of transistor switches and logic circuits which select the sequence and number of switch closures. There are six commutator configurations (or modes) used to satisfy the telemetry requirements other than television data for different phases of the mission.

The analog-to-digital converter generates an 11-bit digital word for each input signal applied to it. Ten bits of this word describe the voltage level of the input signal and one bit position is used to introduce a bit for parity checking by the ground telemetry equipment. When processing digital input information, the first 10 bits are not generated; however, the parity bit is still supplied.

The analog-to-digital converter also supplies commutator advance signals to the commutators at one of six different rates. These rates enable the signal processor to supply telemetry information at 4400, 1100, 550, 137.5 and 17.2 bps. The bit rates and commutator modes are changed by ground commands.

The subcarrier oscillators are voltage controlled oscillators used to provide frequency multiplexing of the telemetry information. This technique is used to greatly increase the amount of information transmitted on the spacecraft carrier frequency.

The summing amplifiers sum the outputs of the subcarrier oscillators and apply the composite signal to the spacecraft transmitters. Two types of summing amplifiers are employed because of the transmitter's ability to transmit either a phase-modulated or a frequency-modulated signal.

The signal processing subsystem employs a high degree of redundancy to insure against loss of vital spacecraft data. Two analog-to-digital converters, two independent commutators—the engineering signal processor (ESP) and auxiliary engineering signal processor (AESP)—and a wide selection of bit rate (each with the analog-to-digital converter (ADC) driving a different subcarrier oscillator) provide a high reliability of the signal processing subsystem in performing its function.

During the mission, 445 commands effecting changes in telemetry were received and properly executed by the signal processor. Of these, 106 were commutator mode changes and 37 were bit rate changes. This number of commands is far in excess of what would occur in a nominal transit sequence. They were executed to obtain additional data in support of the vernier propulsion failure. There is no evidence of any abnormal signal processing behavior due to this increased command density. In Table IV-15, a comparison of prelaunch and typical flight data is presented for the signal processing telemetered functions. These subsystem parameters were very stable throughout flight. From a review of the time plots of these channels there is no indication that anything abnormal occurred in the subsystem. The temperature in Compartment B stayed at all times within the 0–125°F range required for proper signal processing performance.

Approximately 80% of the subsystem was exercised during the abbreviated mission without the occurrence of any problems. The only major elements not checked out were ADC No. 2, Telemetry Commutator Mode 3, and accelerometer and touchdown strain gage channels.

Table IV-15. Typical signal processing parameter values

Parameter	Prelaunch	Flight
ESP reference volts, v	4.877	4.882
ESP reference return, v	0.0	0.0
ESP unbalance current, μa	−1.55	−1.35
ESP full-scale current calibration, % error from nominal	0.4	0.3
ESP mid-scale current calibration, % error from nominal	0.4	0.4
ESP zero-scale current calibration, % error from nominal	0.8	0.5
AESP full-scale current calibration, % error from nominal	0.7	0.8
AESP mid-scale current calibration, % error from nominal	0.5	0.6
AESP zero-scale current calibration, % error from nominal	0.5	0.6
AESP unbalance current, μa	−1.82	−1.82

3. Command Decoding Subsystem

Commands are received, detected, and decoded by one of the four receiver/central command decoder (CCD) combinations possible in the *Surveyor* command subsystem. The selection of the combination is accomplished by stopping the command information from modulating the up-link radio carrier for ½ sec. Once the selection is made, the link must be kept locked up continuously by either sending serial command words or unaddressable command words (referred to as fill-ins) at the maximum command rate of 2 words per sec.

The command information is formed into a 24-bit Manchester-coded digital train and is transmitted in a PCM/FM/PM modulation scheme to the spacecraft. When picked up by the spacecraft omniantennas, the radio carrier wave is stripped of the command PCM information by two series FM discriminators and a Schmitt digitizer. This digital output is then decoded by the CCD for word sync, bit sync, the 5-bit address and its complement, and the 5-bit command and its complement (this latter only for direct commands since the DC's contain 10 bits of information rather than 5 command bits and their complements). The CCD then compares the address with its complement and the command with its

complement on a bit-by-bit basis. If the comparisons are satisfactory, the CCD then selects that one of the eight subsystem decoders (SSD's) having the decoded address bits as its address, applies power to its command matrix, and then selects that one of the 32 matrix inputs having the decoded command bits as its address to issue a 20-msec pulse which initiates the desired single action.

Those DC commands that are irreversible or extremely critical are interlocked with a unique command word. Ten of the DC's and all of the quantitative commands are in this special category. None of these commands can be initiated if the interlock command word is not received immediately prior to the critical command.

The QC's, besides being interlocked, are also treated somewhat differently by the command subsystem. The only differences between the DC and QC are: (1) a unique address is assigned the QC words; (2) the QC word contains 10 bits of quantitative information in place of the 5 command and 5 command complement bits. Therefore, when this unique QC address is recognized, the CCD selects the flight control sensor group (FCSG) SSD and shifts the 10 bits of quantitative information into the FCSG magnitude register. Hence, the QC quantitative bits are loaded as they are decoded.

The command subsystem processed approximately 1330 commands during the mission. There were a few cases where commands had to be repeated, but this was due to having an improper up-link RF lock at the time. All commands were executed properly.

I. Television

The television subsystem is designed to obtain photographs of the lunar surface, lunar sky, and portions of the landed spacecraft. For the *Surveyor II* mission, the subsystem consisted of a downward-looking approach camera, a survey camera capable of panoramic viewing, and a television auxiliary for processing commands and telemetry data.

1. Approach Camera

The approach camera was designed to be turned on at a nominal distance of 1000 km above the lunar surface to provide overlapping photographs of the surface during the terminal descent phase. Although an approach camera was installed on the *Surveyor II* spacecraft, it was planned not to operate the approach camera on the mission because it was desired to minimize spacecraft operational requirements during the complex and critical descent phase.

2. Survey Camera

The survey television camera is shown in Fig. IV-59. The camera provides images over a 360-deg panorama and from +40 deg above the plane normal to the camera Z-axis to −60 deg below this same plane. The camera Z-axis is inclined 16 deg from the spacecraft Z-axis. Each picture, or frame, is imaged through an optical system onto a vidicon image sensor whose electron beam scans a photoconductive surface, thus producing an electrical output proportional to the conductivity changes resulting from the varying receipt of photons from the subject. The camera is designed to accommodate scene luminance levels from approximately 0.008 ft-lamberts to 2600 ft-lamberts, employing both electromechanical mode changes and iris control. Camera operation is totally dependent upon receipt of the proper commands from earth. Commandable operation allows each frame to be generated by shutter sequencing preceded by appropriate lens settings and mirror azimuth and elevation positioning to obtain adjacent views of the subject. Functionally, the camera provides a resolution capability of approximately 1mm at 4 meters and can focus from 1.23 meters to infinity.

Figure IV-60 depicts a functional block diagram of the survey camera and television auxiliary. Commands for the camera are processed by the telecommunications command decoder, with further processing by the television auxiliary decoder. Identification signals, in analog form, from the camera are commutated by the television auxiliary, with analog-to-digital conversion being performed within the signal processing equipment of the telecommunications subsystem. The ID data in PCM form is mixed in proper time relationship with the video signal in the TV auxiliary and subsequently sent to the telecommunications system for transmission to earth.

The survey camera contains a mirror, filters, lens, shutter, vidicon, and the attendant electronic circuitry.

The mirror assembly is comprised of a 10.5×15 cm elliptical mirror supported at its minor axis by trunnions. This mirror is formed by vacuum-depositing a Kanogen surface on a beryllium blank, followed by a deposition of aluminum with an overcoat of silicon monoxide. The mirrored surface is flat over the entire surface to less than ¼ wavelength at $\lambda = 550$ mμ and exhibits an average

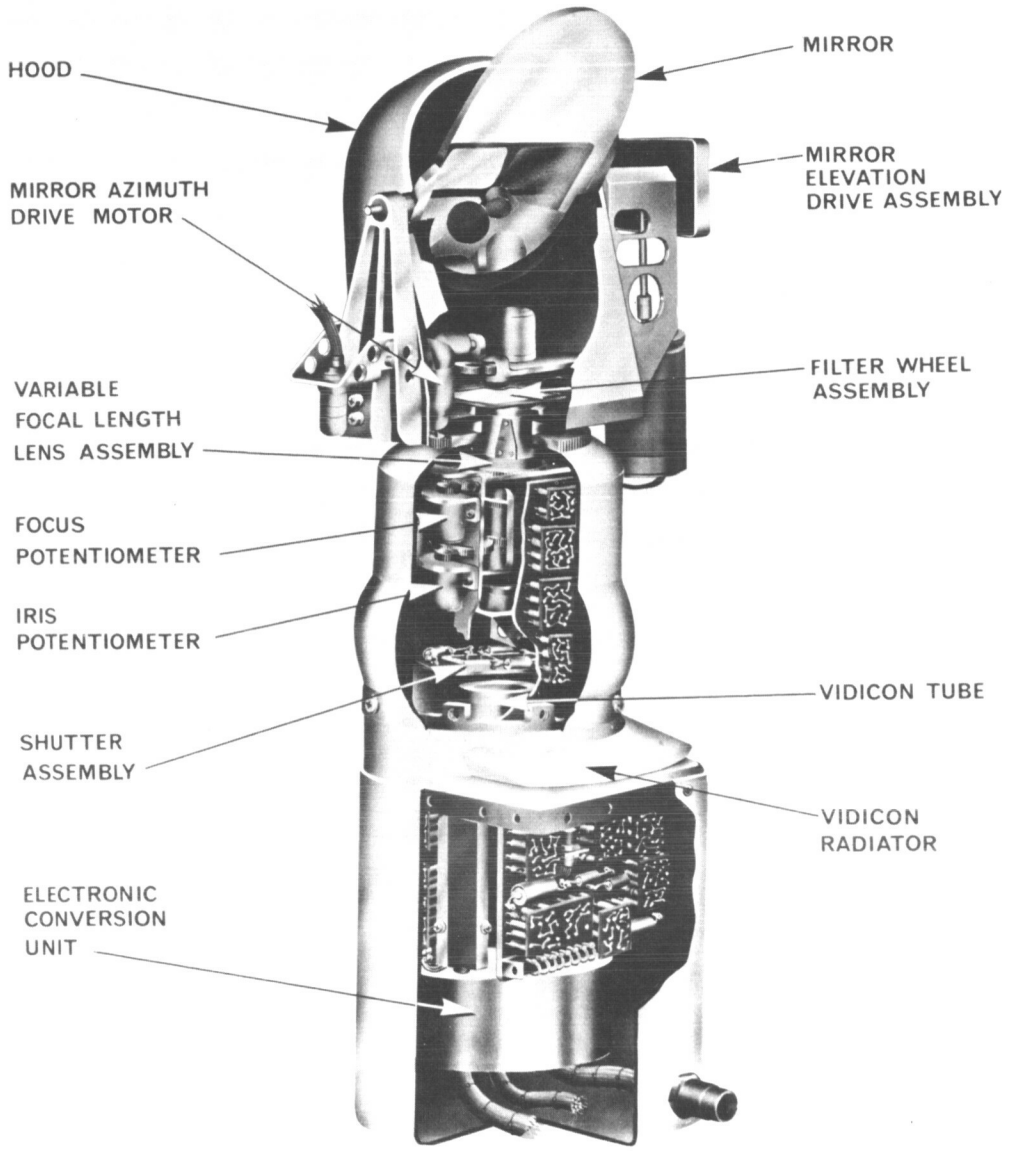

Fig. IV-59. Survey TV camera

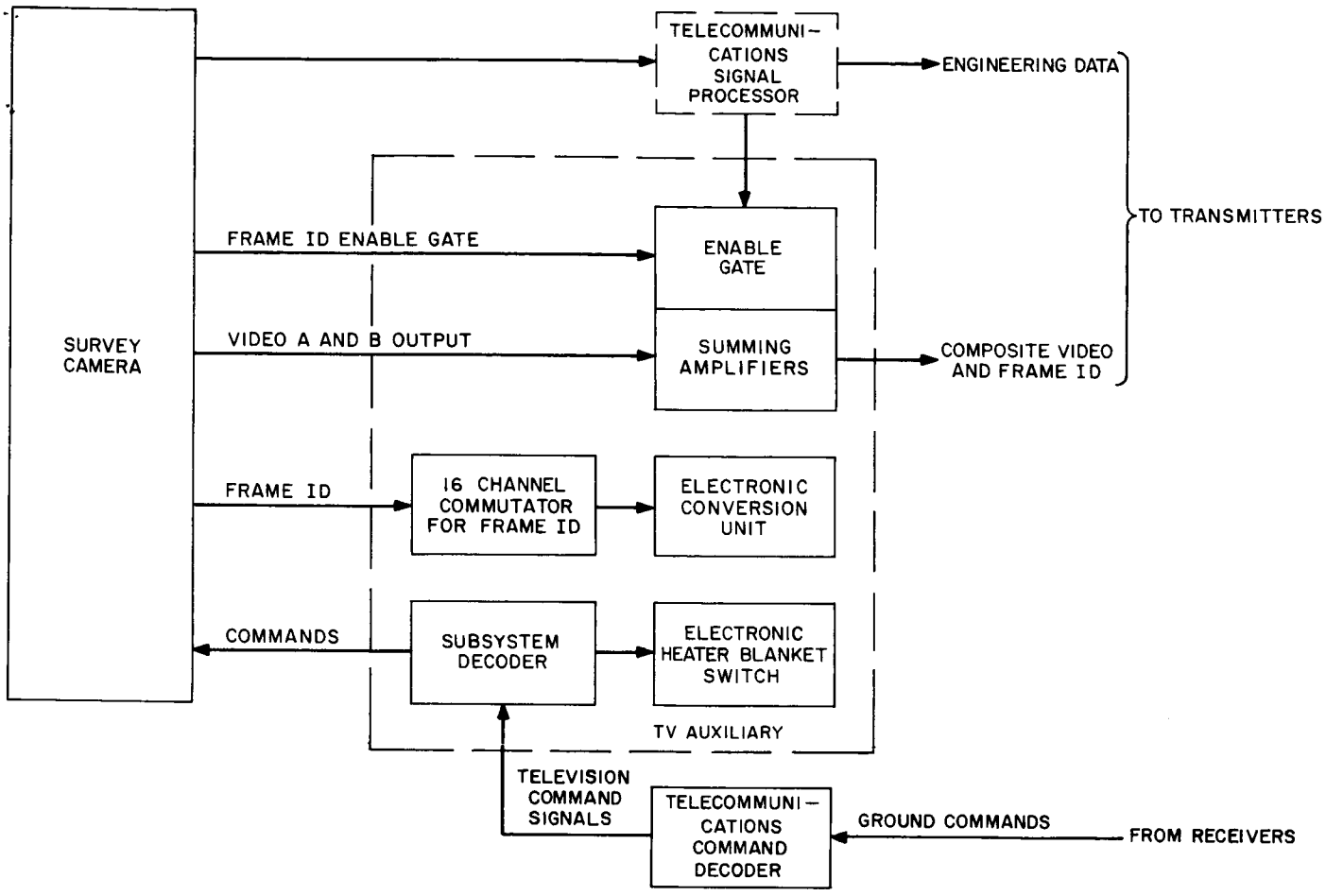

Fig. IV-60. Simplified survey TV camera functional block diagram

specular reflectivity in excess of 86%. The mirror is positioned by means of two drive mechanisms, one for azimuth and the other for elevation.

The mirror assembly contains three filters (red, green, and blue), in addition to a fourth section containing a clear element for nonmonochromatic observations. The filter characteristics are tailored such that the camera responses, including the spectral response of the image sensor, the lens, and the mirror match as nearly as possible the standard CIE tristimulus value curves (Fig. IV-61). Color photographs of any given lunar scene can be reproduced on earth by combining three video photographs, each made with a different monochromatic filter element in the field of view.

The optical formation of the image is performed by means of a variable-focal-length lens assembly placed between the vidicon image sensor and the mirror assembly. Each lens is capable of providing a focal length of either 100 or 25 mm, which results in an optical field of view of approximately 6.43 and 25.3 deg, respectively. Additionally, the lens assembly may vary its focus by means of a rotating focus cell from near 1.23 meters to infinity, while an adjustable iris provides effective aperture changes of from $f/4$ to $f/22$, in increments which result in an aperture area change of 0.5. While the most effective iris control is accomplished by means of command operation, a servo-type automatic iris is available to control the aperture area in proportion to the average scene luminance. As in the mirror assembly, potentiometers are geared to the iris, focal length, and focus elements to allow ground determination of these functions. A beam splitter integral to the lens assembly provides the necessary light sample (10% of incident light) for operation of the automatic iris.

Two modes of operation are afforded the camera by means of a mechanical focal plane shutter located between the lens assembly and the vidicon image sensor.

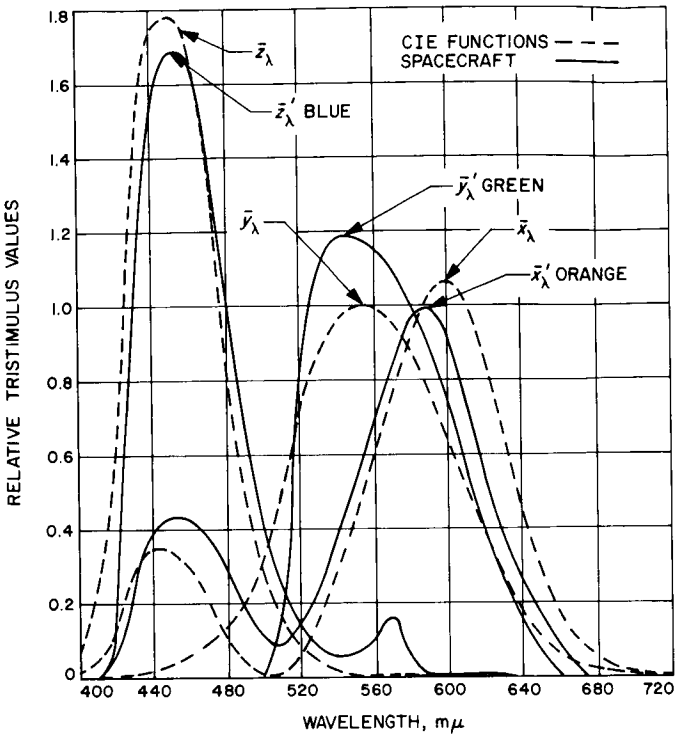

Fig. IV-61. Relative tristimulus values of the color filter elements

Upon earth command, the shutter blades are sequentially driven by solenoids across an aperture in the shutter base plate, thereby allowing light energy to reach the image sensor. The time interval between the initiation of each blade determines the exposure interval, nominally 150 millisec. An additional shutter mode allows the blades to be positioned to leave the aperture

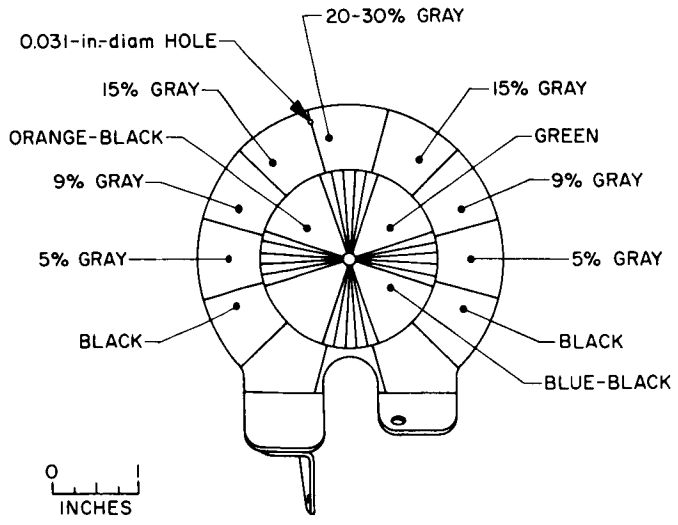

Fig. IV-62. TV photometric/colormetric reference chart

open, thereby providing continuous light energy to the image sensor. This mode of operation is useful in the imaging of scenes exhibiting extremely low luminance levels, including star patterns.

The transducing process of converting light energy from the object space to an equivalent electrical signal in the image plane is accomplished by the vidicon tube. A reference mark is included in each corner of the scanned format, which provides, in the video signal, an electronic level of the scanned image. In the normal, or 600-line mode of operation, the camera provides one 600-TV-line frame every 3.6 sec. Each frame requires nominally 1 sec to be read from the vidicon. A second mode of operation provides one 200-line frame every 61.8 sec. Each frame requires 20 sec to complete the video transmission and utilizes a bandwidth of 1.2 kc in contrast to the 220 kc used for the 600-line mode. This 200-line mode is used for omnidirectional antenna transmission from the spacecraft.

A third operational mode, used for stellar observations and lunar surface observation under earthshine illumination conditions, is referred to as an integrate mode. This mode may be applied, by earth command, to either the 200- or 600-line scan mode. Scene luminances on the order of 0.008 ft-lamberts are reproduced in this mode of operation, thereby permitting photographs under earthshine conditions.

Integral to the spacecraft and within the viewing capability of the camera are two photometric/colorimetric reference charts (Fig. IV-62). These charts, one on Omniantenna B and the other on a spacecraft leg adjacent to Footpad 3, are located such that the line of sight of the camera when viewing the chart is normal to the plane of the chart. Each chart is identical and contains a series of 13 gray wedges arranged circumferentially around the chart. In addition, three color wedges, whose CIE chromaticity coordinates are known, are located radially from the chart center. A series of radial lines is incorporated to provide a gross estimate of camera resolution. Finally, the chart contains a centerpost which aids in determining the solar angles after lunar landing by means of the shadow information. Each chart, prior to launch, is calibrated goniophotometrically to allow an estimation of post-landing camera dynamic range and to aid photometric and colorimetric data reduction.

The survey camera incorporates a total of four heaters to maintain proper thermal control and to provide a thermal environment in which the camera components

operate. The elements are designed to provide a sustaining operating temperature during the lunar night if energized. These consume 36 w of power when initiated. A temperature of −20°F must be achieved prior to camera turn-on.

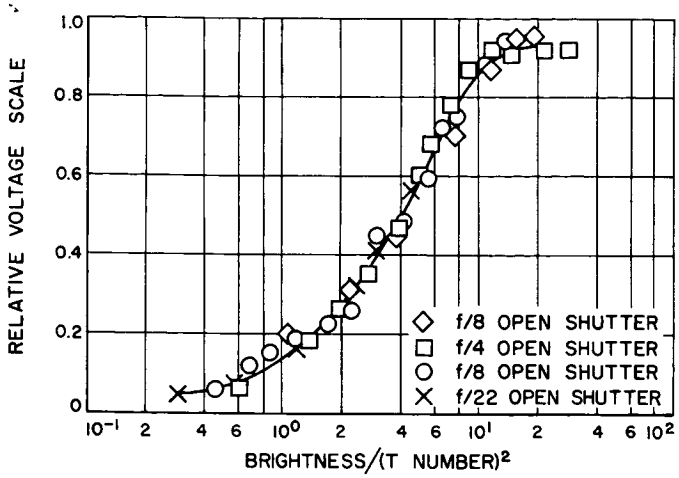

Fig. IV-63. Camera 600-line light transfer characteristic as a function of brightness (T No.)

3. Performance

A premission calibration was performed on the survey camera with the camera mounted on the spacecraft. Each calibration utilized the entire telecommunication system of the spacecraft, thereby including those factors of the modulator, transmitter, etc., which influence the overall image transfer characteristics. The calibration data was FM-recorded on magnetic tape for playback through the ground support equipment (GSE) at Goldstone and Pasadena. Thus the final calibration data recorded on the real-time mission film and tape represents a complete system calibration.

The calibration results, at the point of initial FM recording (i.e., not including the GSE), are shown in Figs. IV-63 through IV-68. Figure IV-63 represents a

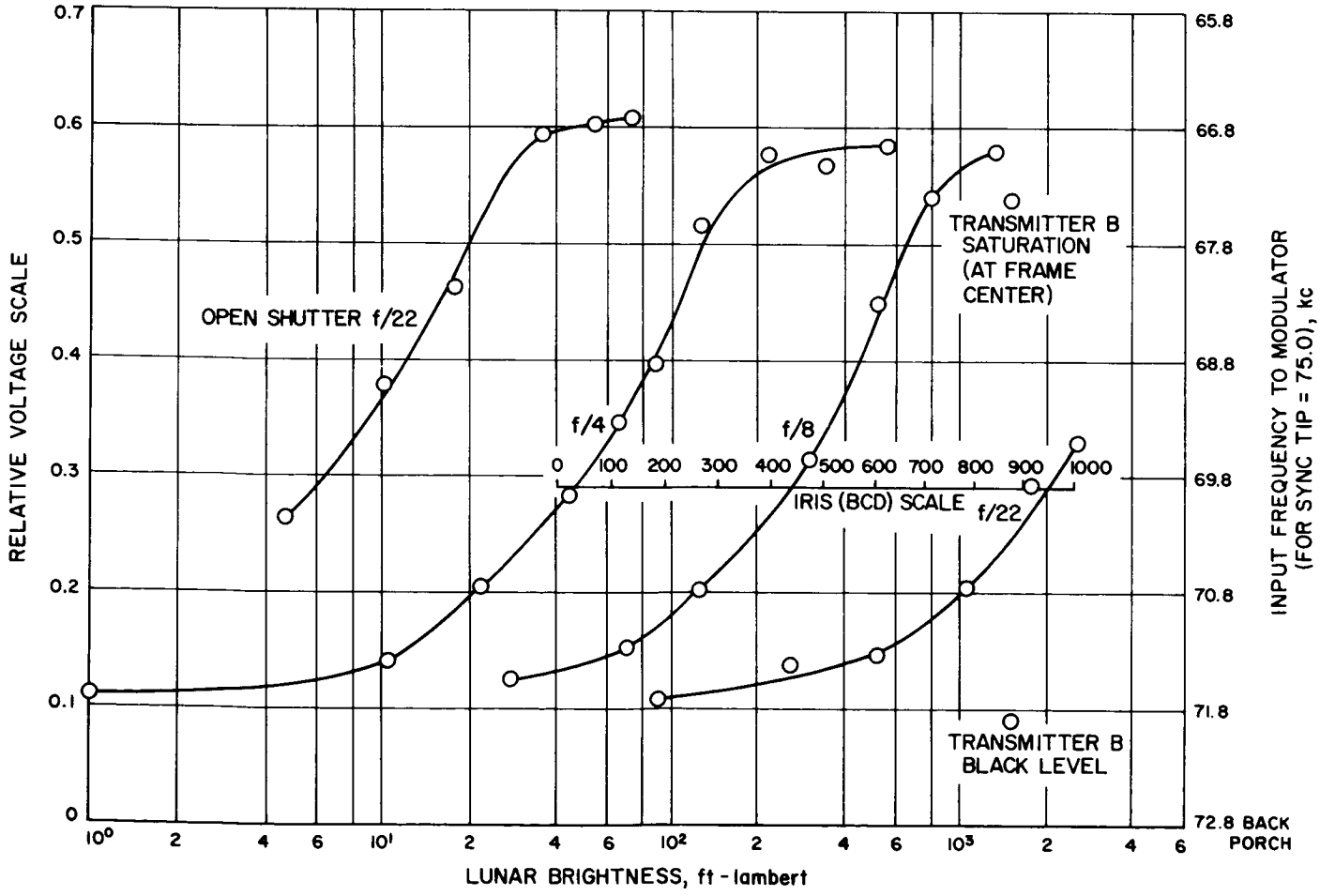

Fig. IV-64. Camera 200-line light transfer characteristic as a function of lunar brightness

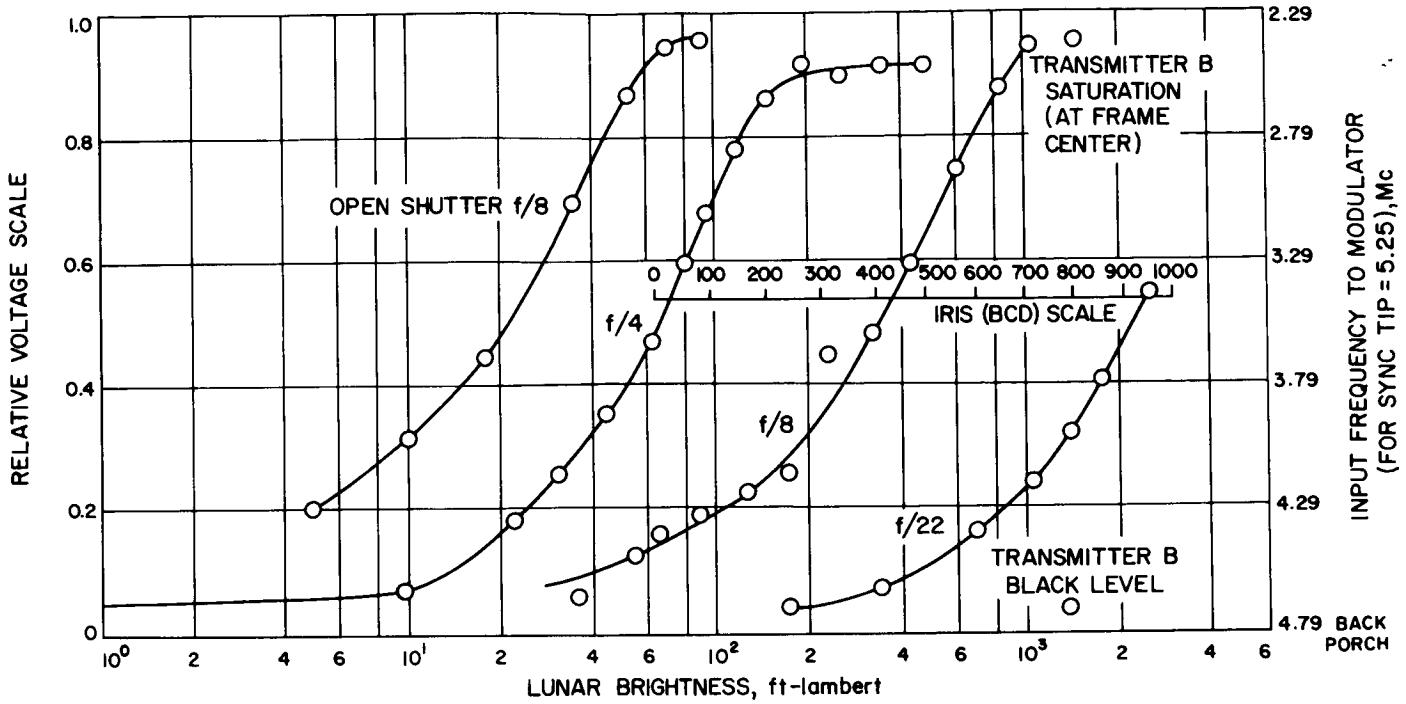

Fig. IV-65. Camera 600-line light transfer characteristic as a function of lunar brightness

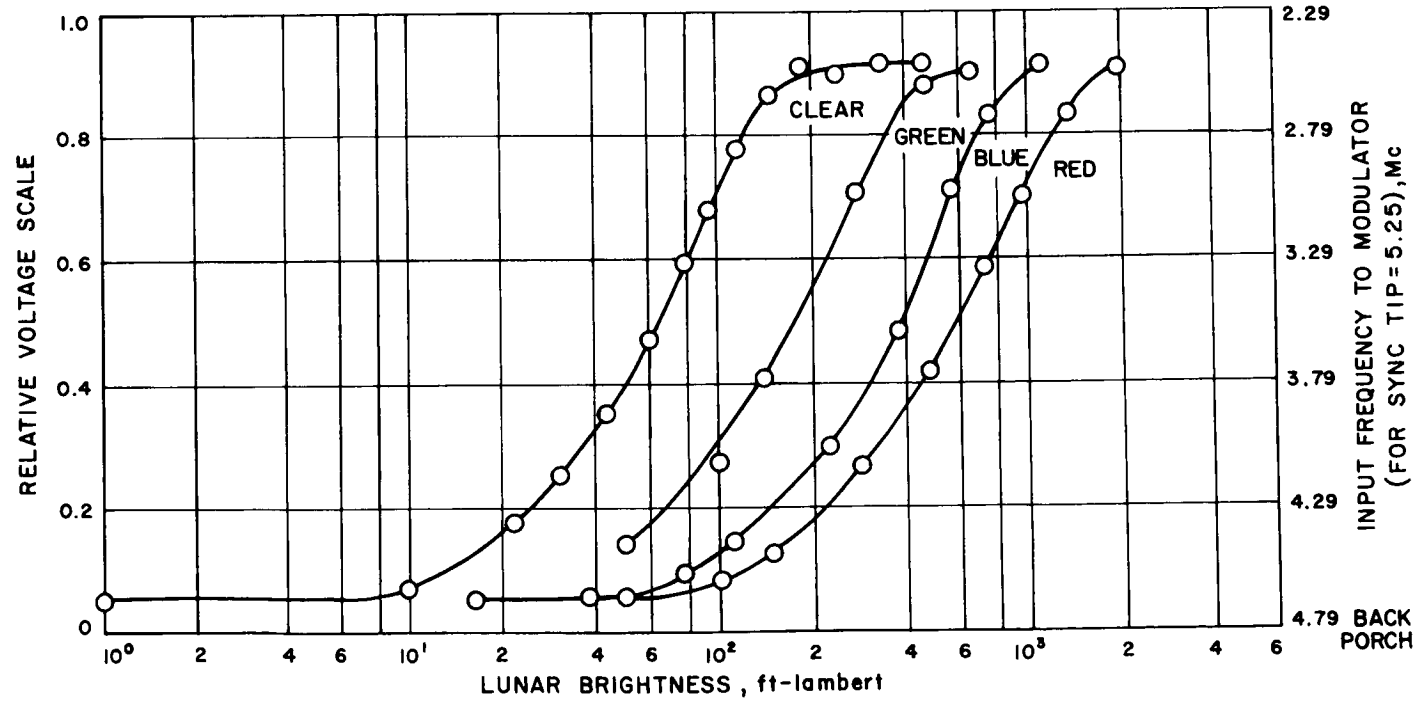

Fig. IV-66. Camera 600-line transfer characteristic as a function of color filter position for the f/4 iris stop

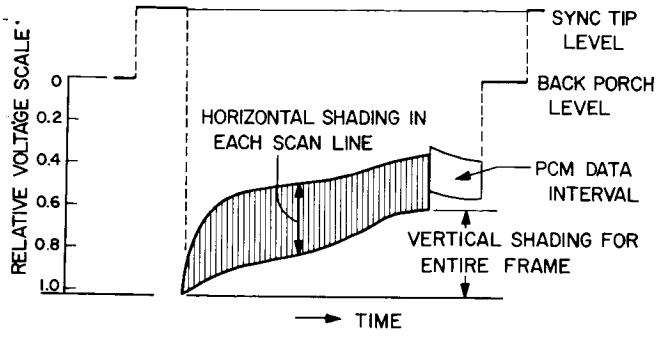

Fig. IV-67. Camera shading near saturation

composite of the 600-line mode light transfer characteristic data for various f/stops (T number), thus illustrating the data scatter. Figures IV-64 through IV-66 show the individual curves that were obtained for various f/stops and color filters for the 200- and 600-line scan modes. The curves depict the sensitivity of the camera system at the central portion of the frame to scenes of constant or static light level. The camera system, however, did not respond the same over the entire frame. This nonuniform response, called "shading," is depicted in Fig. IV-67.

The response of the spacecraft camera system to sinusoidally varying brightness scenes is shown by Fig. IV-68. Here, the sinusoidal nature of the test scene is given by

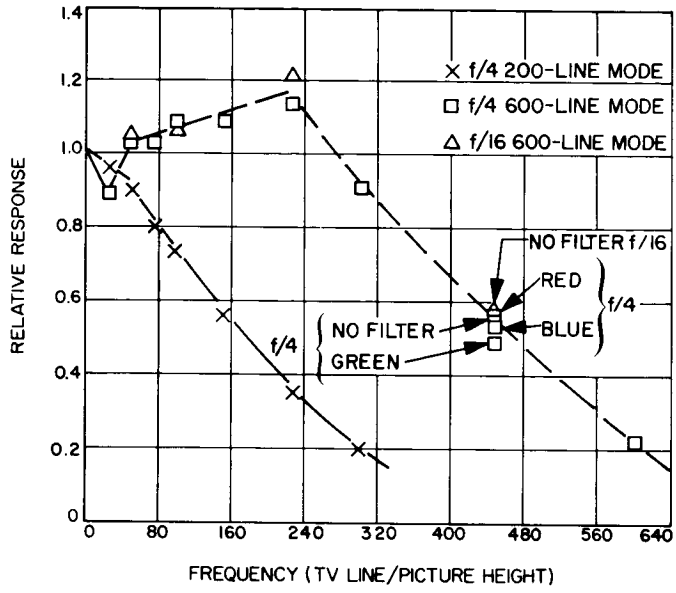

Fig. IV-68. Camera sine-wave response characteristic

the abscissa in terms of frequency, and the relative attenuation of the sine wave amplitude by the camera system is given at the ordinate. The "peaking" of the response curve of the 600-line modes is due to high peaking electronics and would be compensated by the GSE frequency response characteristic. From this curve it is seen that the spacecraft system has a 22% horizontal response at about 600 TV lines in the 600-line scan mode.

V. Tracking and Data Acquisition System

The Tracking and Data Acquisition (T&DA) System for the *Surveyor* Project consists of facilities of the Air Force Eastern Test Range (AFETR), Goddard Space Flight Center (GSFC), and the Deep Space Network (DSN). This section summarizes the mission preparation, flight support, and performance evaluation of each facility within the T&DA System.

The T&DA System support for the *Surveyor II* mission was considered excellent: some minor problems were experienced during operations but had no effect on required performance coverage. All requirements were met and in most cases exceeded. When this mission became nonstandard following the attempted midcourse correction, the DSIF performed very well, providing unanticipated support under difficult conditions.

A. Air Force Eastern Test Range

The AFETR performs T&DA supporting functions for *Surveyor* missions during the countdown and launch phase of the flight.

The *Surveyor* Mission requirements for launch phase tracking and telemetry coverage are classified as follows in accordance with their relative importance to successful mission accomplishment:

Class I requirements consist of the minimum essential needs to ensure accomplishment of first-priority flight test objectives. These are mandatory requirements which, if not met, may result in a decision not to launch.

Class II requirements define the needs to accomplish all stated flight test objectives.

Class III requirements define the ultimate in desired support, and would enable the range user to achieve the flight test objectives earlier in the test program.

The AFETR configuration for the *Surveyor II* Mission is listed in Table V-1. The configuration is similar to the *Surveyor I* configuration except for the deletion of the Range Instrumentation Ship (RIS) *General Arnold.*

Table V-1. AFETR configuration

Station	Radar	VHF telemetry	S-band telemetry
Merritt Island	X		
Cape Kennedy	X	X	X
Patrick AFB	X		
Grand Bahama Island	X	X	X
Grand Turk	X		
Antigua	X	X	X
Coastal Crusader (RIS 1)		X	X
Sword Knot (RIS 2)		X	X
Ascension	X	X	X
Pretoria	X	X	X

Figure V-1 illustrates the disposition of the range instrumentation ships and planned coverage for *Surveyor II* launch day. Except in the case of S-band telemetry facilities, AFETR preparations for *Surveyor II* consisted of routine testing of individual facilities, followed by several Operational Readiness Tests. All requirements were met by AFETR for the *Surveyor II* mission.

1. Tracking (Metric) Data

The AFETR tracks the C-band beacon of the *Centaur* stage to provide metric data. This data is required during intervals of time before and after separation of the spacecraft for use in calculating the *Centaur* orbit, which can be used as a close approximation of the post-separation spacecraft orbit. The *Centaur* orbit calculations were used to provide DSN acquisition information (in-flight predicts).

The significance of the lack of a metric RIS to augment the downrange land-based radars was recognized by both the *Surveyor* Project and AFETR. The resulting restriction in the launch window was such that a scrub would have resulted if any additional hold had been required over that actually experienced. The fact that the Project elected to launch without metric RIS support is not to be considered a precedent for future launches.

Estimated and actual radar coverages are shown in Figs. V-2 and V-3. The combined coverage of all stations is represented by the top set of bars in each figure. The Class I requirements were met and exceeded with AFETR stations downrange to Antigua (including Trinidad radar) providing continuous coverage to $L + 938$ sec. The Trinidad radar operated in the expected skin track mode. Since spacecraft separation occurred near the end of Trinidad track, and in view of the small separation rates between the spacecraft and *Centaur*, separation distance was not great enough to be observed with radar in the 1-mc fine resolution tracking (FRT) mode. This mode improves range resolution through pulse compression to about 470 ft. Rough track was experienced by Grand Turk as radar approached the loss-of-signal (LOS) point. At this time AFETR had no indication of occurrence of balance point shift. Later evaluation of data tended to confirm that the balance point shift did not occur owing to the roll attitude of the *Centaur*, which is not roll-attitude-stabilized. Farther downrange, Ascension and Pretoria experienced intermittent tracking conditions due to the lobing of the C-band beacon caused by vehicle roll.

2. *Atlas/Centaur* Telemetry (VHF)

To meet the Class I telemetry requirements, the AFETR must continuously receive and record *Atlas* telemetry (229.9-mc link) until shortly after *Atlas/Centaur* separation and *Centaur* telemetry (225.7-mc link) until shortly after spacecraft separation. Thereafter, *Centaur* telemetry is to be recorded, as station coverage permits, until completion of the *Centaur* retro maneuver. In addition to the land stations, the AFETR provided RIS *Sword Knot* and RIS *Coastal Crusader* and one range telemetry aircraft to cover the gap between Antigua and Ascension.

Estimated and actual VHF telemetry coverage is shown in Fig. V-4. All Class I, II, and III requirements were met since continuous and substantially redundant VHF telemetry data was received beginning with the countdown and through Pretoria LOS at $L + 3805$ sec. Coverage was more than predicted. However, since the *Centaur* stage is not designed for roll stabilization, the expected coverage was based on a specified minimum db level at the antenna null to allow for uncertainty in the antenna gain.

3. *Surveyor* Telemetry (S-band)

The AFETR also is required to receive, record and retransmit *Surveyor* S-band (2295-mc) telemetry in real-time after the spacecraft transmitter high power is turned on until 15 min after DSIF rise.

The S-band telemetry resources assigned to meet this requirement were the two Range Instrumentation Ships, the 85-ft antenna system at Grand Bahama Island, and the 30-ft S-band (TAA-3A) antenna systems located at Antigua and Ascension Islands. All primary S-band systems were used on a limited commitment basis since the

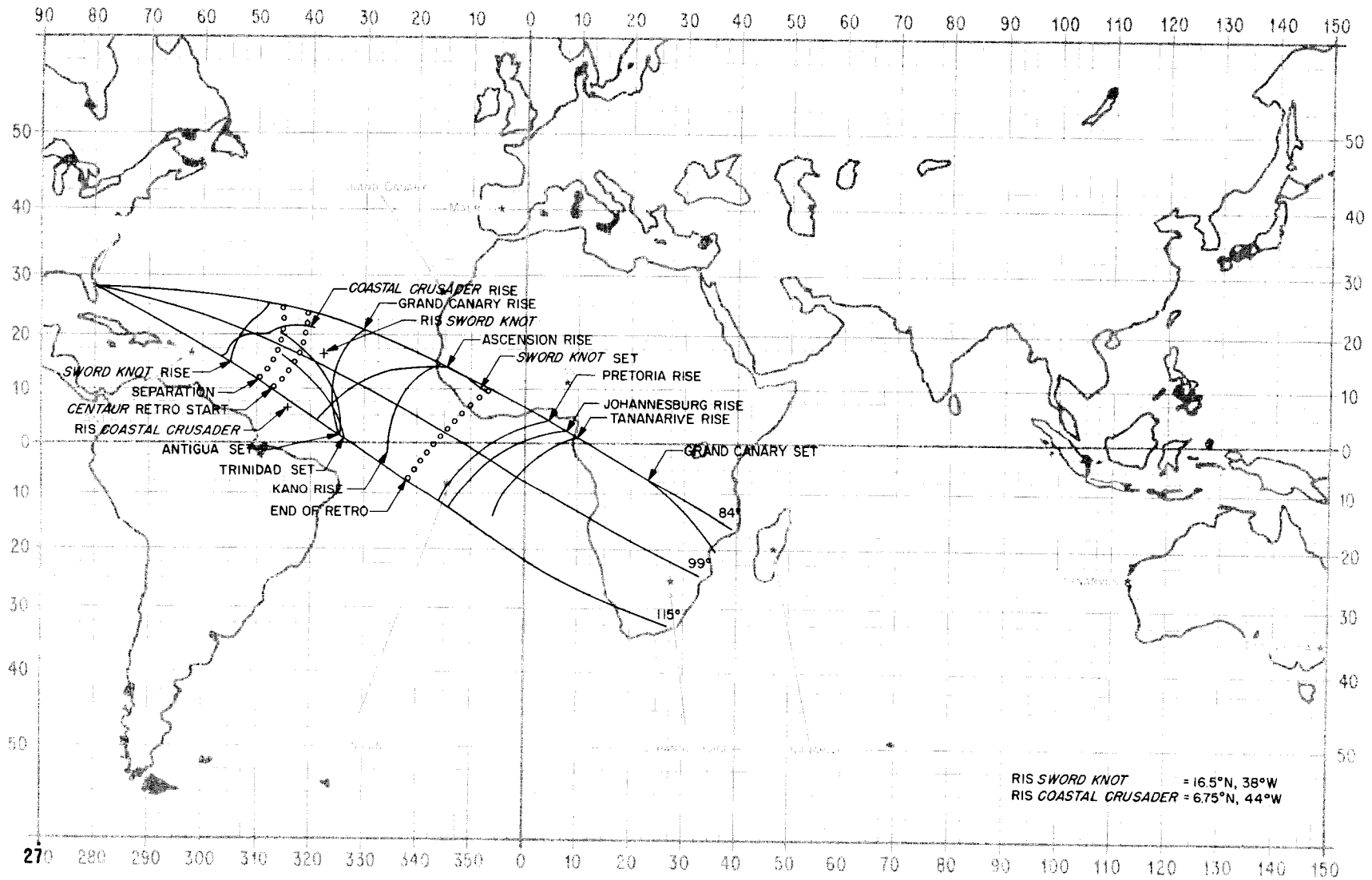

Fig. V-1. Planned launch phase coverage for September 20, 1966

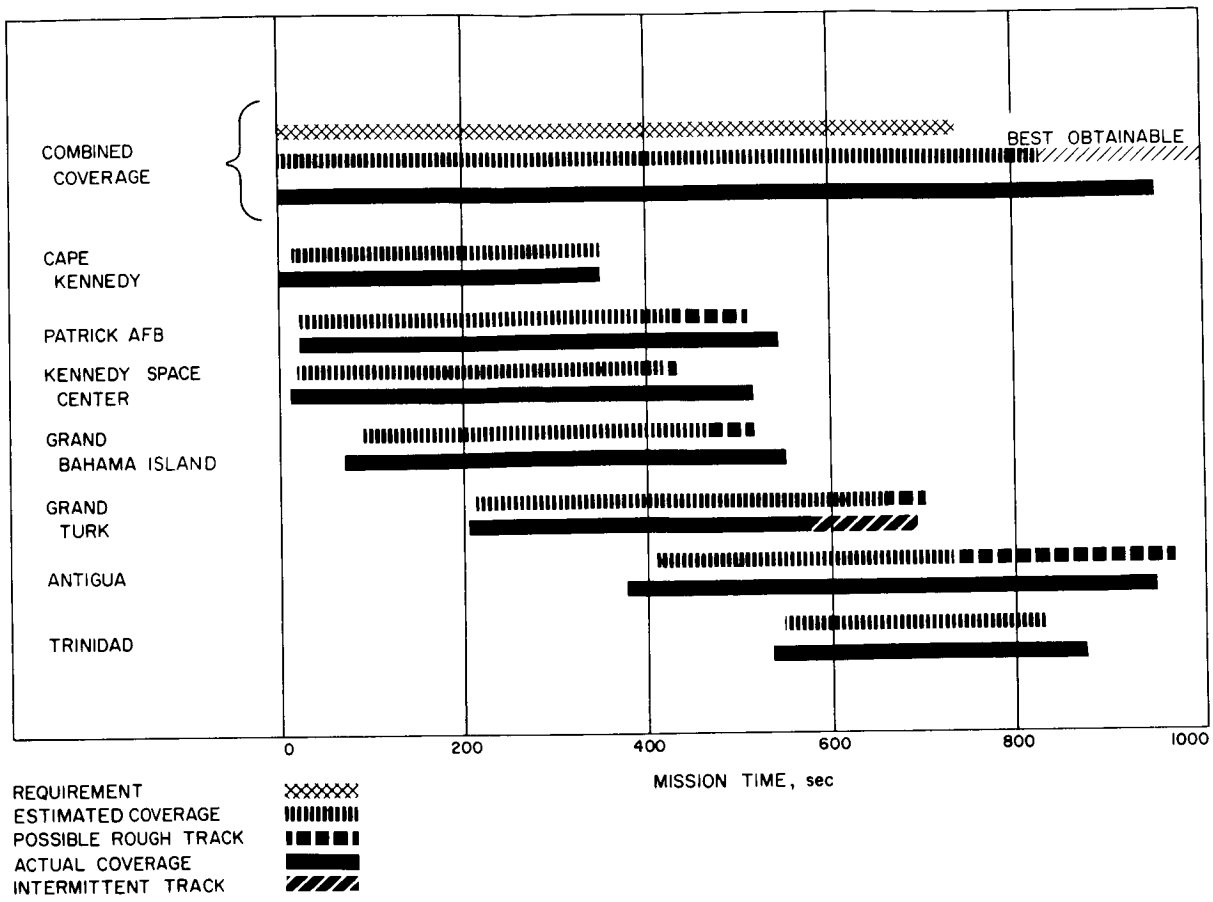

Fig. V-2. AFETR radar coverage: liftoff through Antigua

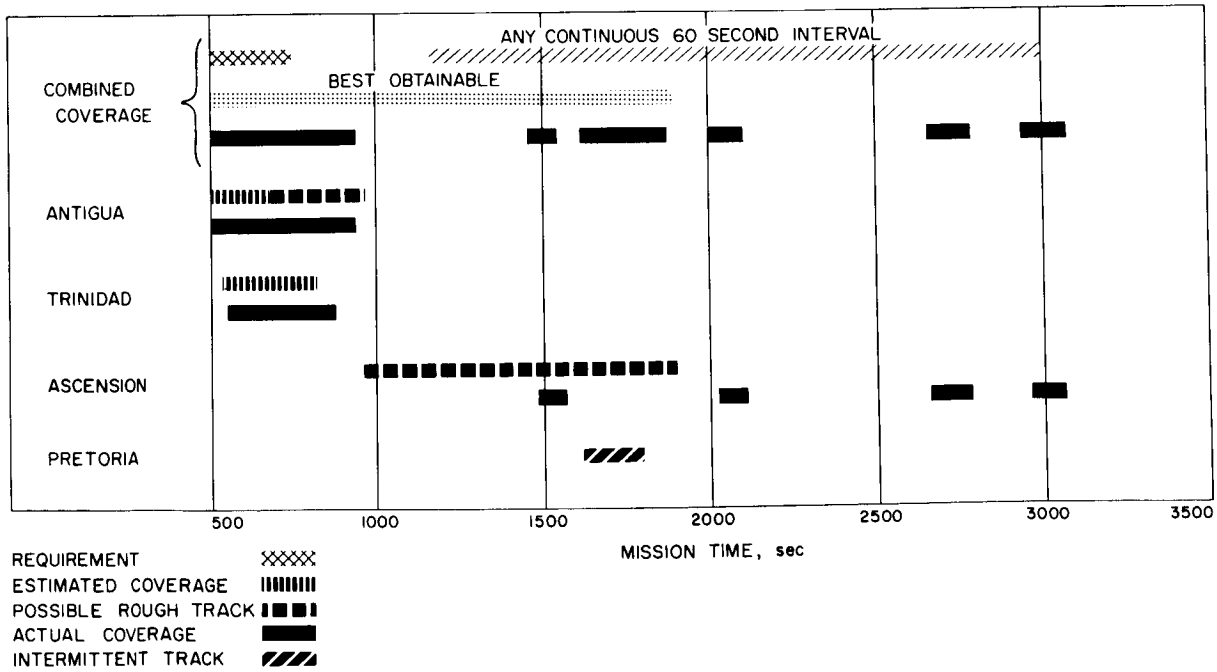

Fig. V-3. AFETR radar coverage: Antigua through Pretoria

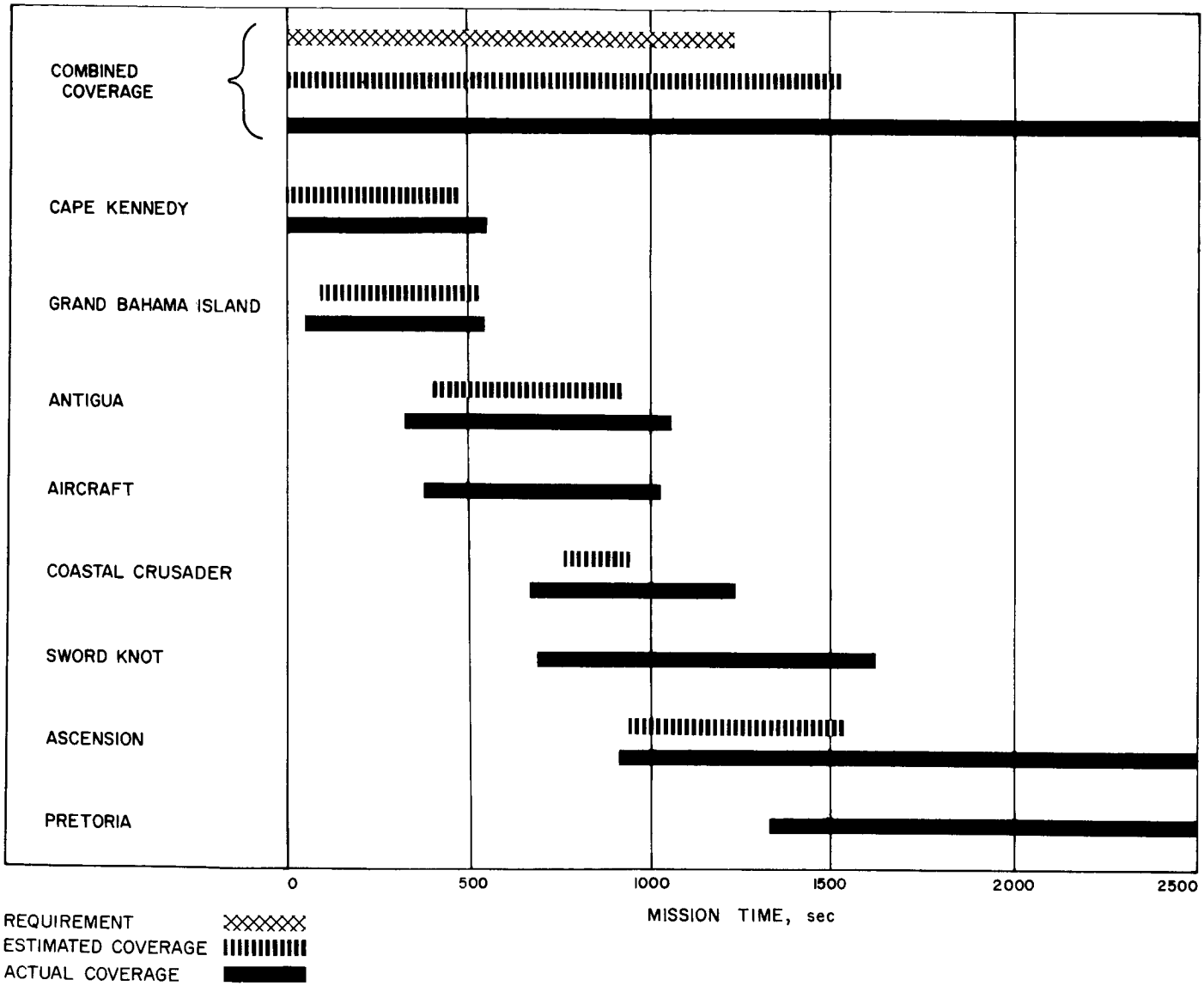

Fig. V-4. AFETR VHF telemetry coverage

Centaur vehicle is not roll-attitude-stabilized. Confidence in these systems was fairly high because of the successful S-band coverage provided by RIS *Sword Knot* for the two previous *Centaur* launches and the S-band support provided by RIS *Coastal Crusader* for *Pioneer* and *Surveyor I*.

A three-ft S-band antenna, with its associated down-converter, receiver, and communications equipment, was in place at Ascension. This system provided S-band data for the two previous *Centaur* launches and was used to back up the TAA-3A antenna system. A similar backup system was provided at Antigua.

With the exception of a 10-sec gap at $L+380$ sec, AFETR land stations and ships obtained continuous S-band telemetry coverage from liftoff through Ascension LOS at $L+2675$ sec. Although Ascension experienced a dropout between $L+1742$ and $L+1790$ sec, the interval was adequately covered by Pretoria. Estimated and actual S-band telemetry coverages are shown in Fig. V-5. All Class I, II, and III requirements were met.

4. Surveyor Real-Time Data

The AFETR retransmits *Surveyor* data (VHF or S-band) to Building AO, Cape Kennedy, for display and for re-

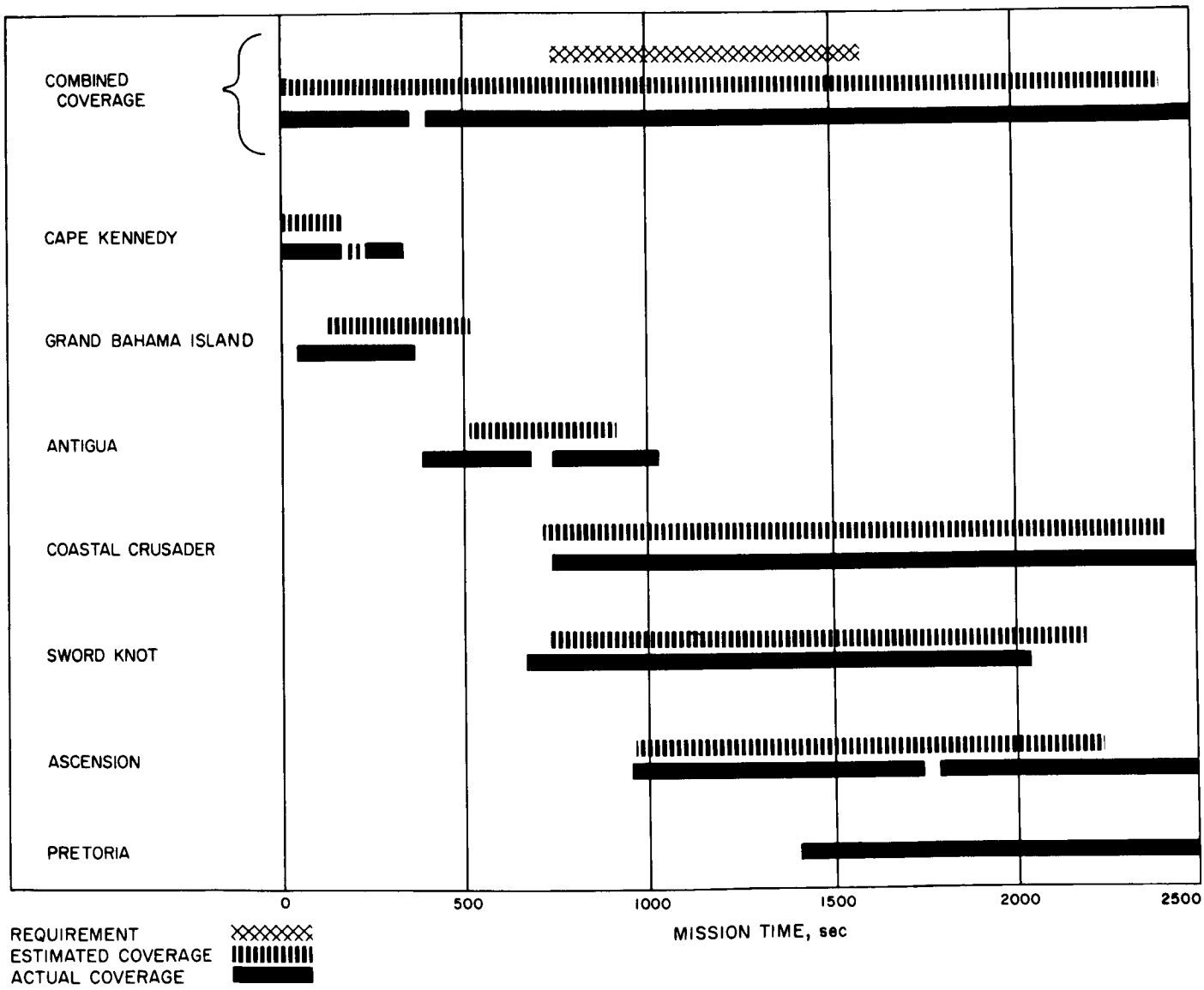

Fig. V-5. AFETR S-band telemetry coverage

transmission to the SFOF. In addition, downrange stations monitor specific channels and report events via voice communication.

For the *Surveyor II* mission, existing hardware and software facilities were utilized to meet the real-time data requirements.

All requirements were met. VHF telemetry data, including spacecraft data, were transmitted in real-time to the user from liftoff to spacecraft high power on. At high power on, AFETR switched as planned to real-time transmission of spacecraft S-band telemetry data to Building AO. Real-time data flow was very good. In addition, all Mark Events were read out and reported.

5. Real-Time Computer System (RTCS)

For the launch phase of the mission, the RTCS provides trajectory computations based on tracking data and vehicle guidance data. The RTCS output includes:

(1) The interrange vector (IRV), the standard orbital parameter message (SOPM), and orbital elements.

(2) Predicts, look angles, and frequencies for acquisition use by downrange stations.

(3) I-matrix and moon map for mapping injection conditions and estimating trajectory accuracy. Provides for early orbit evaluation prior to orbital data generated by Flight Path Analysis and Command (FPAC).

The RTCS computed a total of six orbits (five transfer orbits and one *Centaur* post-retro orbit) using different data sources. The first orbit, based on Antigua data, and the related acquisition look angles and frequencies for downrange stations were generated and transmitted on schedule. The RTCS computed the second orbit based on real-time *Centaur* guidance data, but some delay occurred because of errors in the initial guidance data provided to the RTCS by Kennedy Space Center (KSC). The third orbit was a recursive solution using Antigua data which improved the first orbit. The fourth orbit involved a multistation solution using Antigua C-band data and Trinidad skin-track data. The third and fourth orbits were computed on the RTCS Computer B while Computer A was attempting to process the Ascension and Pretoria post-retro data to compute the fifth orbit. However, the Ascension and Pretoria data was difficult to process because many points were "off-track." (The intermittent tracking by Ascension and Pretoria was attributed to a weak C-band beacon.) After completing the fifth orbit, the RTCS computed a final orbit based upon data from Antigua and DSS 51.

B. Goddard Space Flight Center

The Manned Space Flight Network (MSFN), managed by GSFC, supports *Surveyor* missions by performing the following functions:

(1) Tracking of the *Centaur* beacon (C-band) for approximately 3.5 hr.

(2) Receiving and recording *Centaur*-link telemetry from Bermuda acquisition until loss of signal at Kano.

(3) Providing real-time confirmation of certain Mark Events (see Appendix A).

(4) Providing real-time reformatting of Carnarvon radar data from the hexidecimal system to the 38-character octal format and retransmitting these data to the RTCF at AFETR.

(5) Providing NASCOM support to all NASA elements for simulations and launch and extending this communications support as necessary to interface with the combined worldwide network.

The GSFC supported the *Surveyor II* mission with the tracking facilities and equipment listed in Table V-2. However, GSFC did not support the Operational Readiness Test (ORT) prior to launch.

1. Acquisition Aids

Stations at Bermuda, Canary Island, and Kano are equipped with acquisition aids to track the vehicle and provide RF inputs to the telemetry receivers. Performance recorders are used to record AGC and angle errors for post-mission analysis. The acquisition aids provide telemetry RF inputs from Bermuda acquisition through loss of signal at Kano. All MSFN acquisition aid systems performed their required functions during the *Surveyor II* mission.

2. Telemetry Data

Bermuda, Canary Island, and Kano were also equipped to decommutate, receive, and record telemetry. Capability for coverage was provided from Bermuda acquisition through loss of signal at Kano. Mark Event readouts

Table V-2. GSFC Network configuration

Location	Acquisition aid	VHF Telemetry	C-band radar	SCAMA	Radar high-speed data	Real-time readouts
Bermuda	X	X	X	X	X	X
Canary Island	X	X		X		X
Kano	X	X		X		X
Carnarvon				X		
GSFC					X	
Cape Kennedy				X	X	

were required from all stations in real-time or as near real-time as possible when the vehicle was in view of a station.

MSFN telemetry support was good. There were no equipment failures or discrepancies during the operation.

Only Mark Events 6 and 7 were confirmed by Bermuda.

3. Tracking Data (C-Band)

Bermuda provided radar beacon tracking, magnetic tape recording (at a minimum of 10 points/sec), and real-time data transmission to GSFC and AFETR.

4. Computer Support, Data Handling, and Ground Communications

The GSFC Data Operations Branch provided computer support during the prelaunch, launch, and orbital phases of the mission. Data was provided by MSFN stations at Bermuda, Canary Island, Kano, and Carnarvon in accordance with the requirements of the Network Operations Plan. Existing NASCOM and DOD Network facility voice and teletype circuits provided ground communications to all participating stations.

C. Deep Space Network

The DSN supports *Surveyor* missions with the integrated facilities of the Deep Space Instrumentation Facility (DSIF), the Ground Communication System (GCS), and the DSN facilities in the Space Flight Operations Facility (SFOF).

1. The DSIF

The following Deep Space Stations were committed as prime stations for the support of the *Surveyor II* mission:

DSS 11 Pioneer, Goldstone Deep Space Communications Complex (DSCC), Barstow, California

DSS 42 Tidbinbilla, Australia, near Canberra (Fig. V-6)

DSS 51 Johannesburg, South Africa

DSS 72 Ascension Island (first pass only)

DSS 11, 42, and 51 are equipped with 85-ft-diameter, polar-mount antennas. DSS 72 is equipped with a 30-ft azimuth-elevation antenna. These prime stations were committed to provide tracking coverage on a 24-hr/day basis, from launch to lunar landing, and for the first lunar day and night. For succeeding lunar days and nights, the commitment was for 24-hr/day coverage during the first three and last two earth days and for 10-hr/earth day in between.

In addition to the basic support provided by prime stations, the following facilities support was provided for the *Surveyor II* mission:

(1) DSS 71, Cape Kennedy, provided facilities for spacecraft/DSIF compatibility testing, and also received telemetry after liftoff for engineering evaluation of its new Command and Data Handling Console (CDC) equipment.

Fig. V-6. DSS 42, Tidbinbilla, Australia

(2) DSS 61, Robledo, Madrid DSCC, was designated a training station during the *Surveyor II* mission and was committed to provide tracking capability within a 1- to 1.5-hr callup. During Pass 2, DSS 61 provided emergency telemetry and command coverage when communications problems with DSS 51 were encountered.

(3) DSS 12, Echo, Goldstone DSCC, provided a backup transmitter capability during midcourse maneuver. This support, however, was not required.

(4) DSS 14, Mars, Goldstone DSCC, provided backup telemetry coverage using the 210-ft antenna during both Goldstone passes. The Mars station assisted with accurate measurement of spacecraft tumbling rates during Pass 2.

Data is handled by the prime DSIF stations as follows:

(1) Tracking data, consisting of antenna pointing angles and doppler (radial velocity) data, is supplied in near-real-time via teletype to the SFOF and postflight in the form of punched paper tape. Two- and three-way doppler data is supplied full-time during the lunar flight, and also during lunar operations when requested by the *Surveyor* Project Office. The two-way doppler function implies a transmit capability at the prime stations.

(2) Spacecraft telemetry data is received and recorded on magnetic tape. Baseband telemetry data is supplied to the CDC for decommutation and real-time readout. The DSIF also performs precommunication processing of the decommutated data, using an on-site data processing (OSDP) computer. The data is then transmitted to the SFOF in near real-time over high-speed data lines (HSDL).

(3) Video data is received and recorded on magnetic tape. This data is sent to the CDC and, at DSS 11 only, to the TV Ground Data Handling System

(TV-GDHS, TV-11) for photographic recording. In addition, video data from DSS 11 is sent in real-time to the SFOF for magnetic and photographic recording by the TV-GDHS (TV-1). Since a soft landing could not be achieved on the *Surveyor II* mission, no video data was received. After lunar landing on a standard mission, DSS 11 performs a special function. Two receivers are used for different functions. One provides a signal to the CDC, the other to the TV-GDHS. (Signals for the latter system are the prime *Surveyor* Project requirement during this phase of a mission.)

(4) Command transmission is another function provided by the DSIF. Approximately 280 commands are sent to the spacecraft during the nominal sequence from launch to touchdown. Confirmation of the commands sent is processed by the OSDP computer and transmitted by teletype to the SFOF.

The characteristics for the S-band and L/S-band tracking systems are given in Table V-3. The L/S-band conversion is located at DSS 51, the Johannesburg station, and consists of a hybrid, interim arrangement of L-band

Table V-3. Characteristics for S-band and L/S-band tracking systems

Antenna, tracking		Transmitter	
Type	85-ft parabolic	Frequency (nominal)	2113 mc
Mount	Polar (HA-Dec)	Frequency channel	14b
Beamwidth ±3 db	−0.4 deg	Power	10 kw, max
Gain, receiving	53.0 db, + 1.0, −0.5	Tuning range	±100 kc
Gain, transmitting	51.0 db, + 1.0, 0.5	Modulator	
Feed	Cassegrain	Phase input impedance	≥ 50 Ω
Polarization	LH[b] or RH circular	Input voltage	≤ 2.5 v peak
Max. angle tracking rate[a]	51 deg/min 0.85 deg/sec	Frequency response (3 db)	DC to 100 kc
Max. angular acceleration	5.0 deg/sec/sec	Sensitivity at carrier output frequency	1.0 rad peak/v peak
Tracking accuracy (1σ)	0.14 deg	Peak deviation	2.5 rad peak
Antenna, acquisition		Modulation deviation stability	±5%
Type	2 × 2-ft horn	Frequency, standard	Rubidium
Gain, receiving	21.0 db ±1.0	Stability, short-term (1σ)	1×10^{-11}
Gain, transmitting	20.0 db ±2.0	Stability, long-term (1σ)	5×10^{-11}
Beamwidth ±3 db	−16 deg	Doppler accuracy at $F_{r,r}$ (1σ)	0.2 cps ≈ 0.03 m/sec
Polarization	RH circular	Data transmission	TTY and HSDL
Receiver	S-band		
Typical system temperature			
With paramp	270 ±50°K		
With maser	55 ±10°K		
Loop noise bandwidth threshold ($2B_{L,th}$)	12, 48 or 152 cps + 0, −10%		
Strong signal ($2B_{L,th}$)	120, 255, or 550 cps + 0, −10%		
Frequency (nominal)	2295 mc		
Frequency channel	14a		

[a] Both axes.
[b] Goldstone only.

and S-band components configured to operate at the S-band frequency. Differences are in the hardware and operational techniques rather than in performance characteristics. The essential differences are as follows: The L/S-band receiver subsystem consists of standard L-band receiver elements with modification equipment added to permit acceptance of the nominal S-band receive frequency of 2295 mc. Where the S-band stations are equipped with two standard receivers, the L/S-band conversion consists of only one receiver suitable for tracking functions (two angles and radial velocity) and a second, "suitcase" receiver which is used for telemetry reception. Telemetry bandwidths and loop noise bandwidths are restrictive compared to the S-band system.

The angle-tracking parameters for stations equipped with 85-ft antennas are as follows:

(1) Maximum angle tracking rate (both axes): 51 deg/min = 0.85 deg/sec.

(2) Maximum angular acceleration: 5.0 deg/sec/sec.

(3) Tracking accuracy (one standard deviation): $\alpha = 0.14$ deg.

(4) The system doppler tracking accuracy at the receiver carrier frequency for one standard deviation is 0.2 cps = 0.03 m/sec.

The maximum doppler tracking rate depends on the loop noise bandwidth. For phase error of less than 30 deg and strong signal (−100 dbm), tracking rates are as follows:

Loop noise bandwidths, cps	Maximum tracking rate, cps/sec
12	100
48	920
152	5000

The angle tracking parameters for the DSS 72 30-ft antenna are as follows:

(1) Maximum azimuth tracking rate: 6 deg/sec.

(2) Maximum elevation angle tracking: 3 deg/sec.

(3) Tracking accuracy: 0.01 deg.

(4) The system doppler tracking accuracy and doppler tracking rates are the same as for 85-ft antennas.

The receiver characteristics for S-band and L/S-band stations are as follows:

(1) *Noise temperature.* The total effective system noise temperature including circuit losses when looking at or near the galactic pole is:
Traveling-wave maser, 55 ±10°K
Parametric amplifier, 270 ±50°K

(2) *Loop noise bandwidth.* The closed-loop noise bandwidth for various signal conditions is:
Threshold $2B_{Lo}$, 12, 48, or 152 cps +0, −20%
Strong signals $2B_4$, 132, 274 or 518 cps +0, −20%

(3) *Threshold.* Carrier lock will be maintained with an rms phase error due to noise of less than 30 deg when the ratio of carrier power to noise power in the closed-loop noise bandwidth is 6 db or greater. Owing to the nature of the operation of the phase-lock loop, this condition requires the carrier power at the receiver input to be 9 db greater than the value at threshold, which is defined as a carrier-to-noise power ratio of zero db in the threshold loop noise bandwidth $2B_{Lo}$.

a. DSIF preparation testing. Operational Tests (C-Tests) are conducted for each mission to verify that all prime stations, communication lines, and the SFOF are fully prepared to meet Mission responsibility. Selected portions of the Sequence of Events are followed rigidly, using both standard and nonstandard procedures.

The operational test schedule is presented in Table V-4. DSS 11, 42, 51, and 72 participated in the Operational Readiness Test (ORT) C-5.0 Phase 1, which was conducted a week prior to launch. An evaluation of station and Net Control support during the ORT indicated the

Table V-4. Operational test schedule

Test	Stations	Date, 1966
C-1.5	DSS 72	8/21
C-1.6	DSS 72 and AFETR	8/25
C-3.0 Phase 1	DSS 11, 42, 51, 72 and AFETR	8/30
C-3.0 Phase 2	DSS 11	9/1
C-5.0 Phase 1	DSS 11, 42, 51, and 72	9/13
C-5.0 Phase 2	DSS 11	9/15

readiness of the T&DA System. Although the operational tests were minimal, each station was adequately manned and trained to properly support the *Surveyor II* mission.

Surveyor on-site computer program (SOCP) integration tests are conducted to check out the SOCP and to verify that data can be transmitted from a DSIF station to the SFOF and then processed. Such tests were run on a regular basis with each prime station (DSS 11, 42, and 51). These tests were concluded with a checkout of the final SOCP program in April 1966. Operational tests continued up until three weeks prior to launch to provide additional training for operational personnel.

b. DSIF flight support. All of the DSIF prime and engineering practice stations reported "go" status during the countdown. All measured station parameters were within nominal performance specifications, and communications circuits were up.

Figure V-7 is a profile of the DSIF mission activity from launch until mission termination. This figure contains the periods each station tracked the spacecraft plotted against mission time. Table V-5 is a tabulation of all commands sent during the *Surveyor II* Mission.

The DSIF stations operated very well, providing continuous tracking and telemetry coverage from $L+00:17$

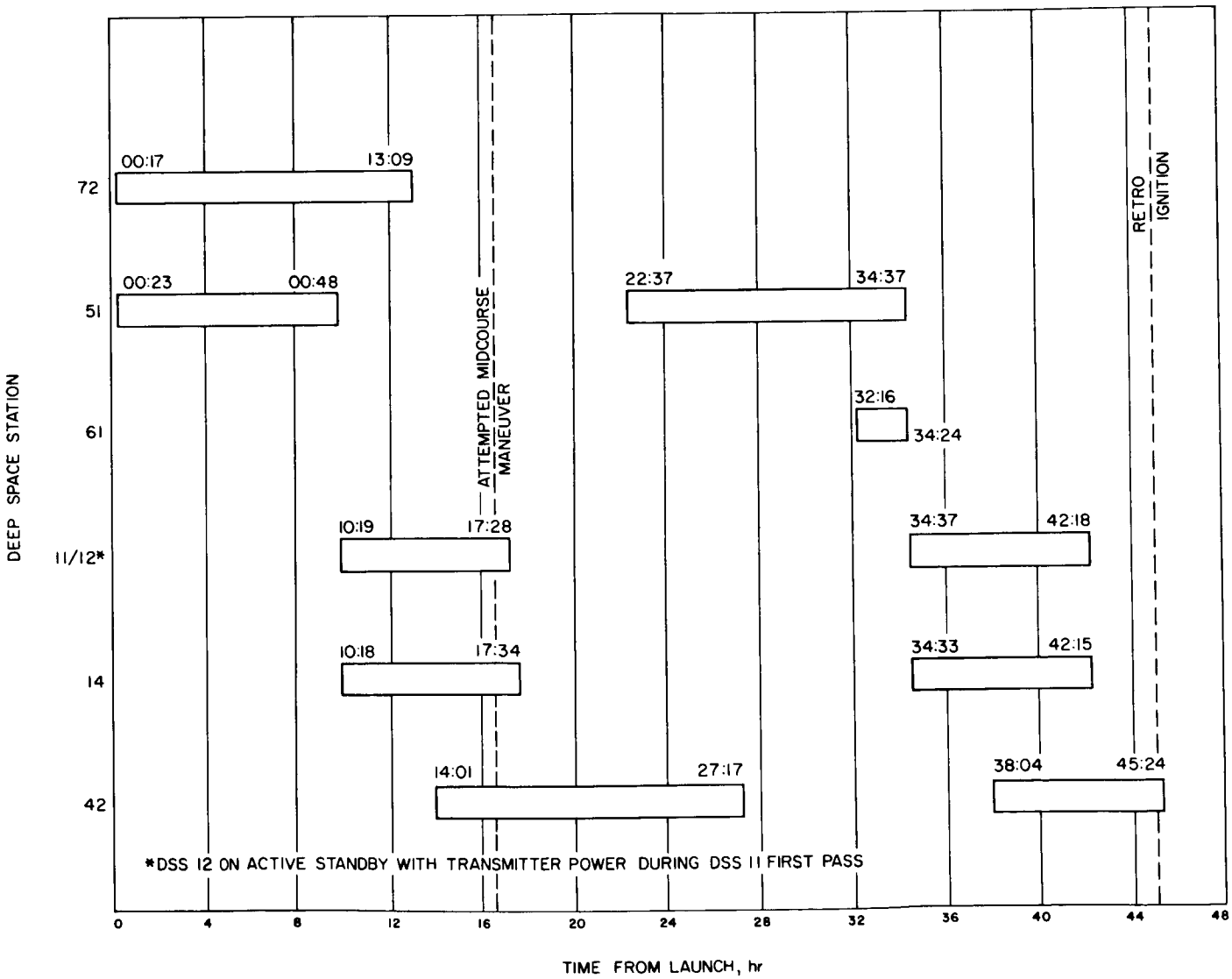

Fig. V-7. Station tracking periods

Table V-5. Commands transmitted by DSIF stations

Pass No.	Date, 1966 GMT	Event	Commands transmitted					
			DSS 71	DSS 72	DSS 51	DSS 11	DSS 42	DSS 61
Launch	9/20		0					
Launch	9/20			0				
Launch/01	9/20				85	8		
01	9/21	Midcourse correction commanded				102		
01	9/21						86	
02	9/21				102			
02	9/22					744		3
02	9/22	Retro ignition commanded					449	
		Station Total	0	0	187	854	535	3
		Grand Total	1579					

(DSS 72 rise) to end of mission at $L+45{:}24$. This was the first use of DSS 72 as a committed *Surveyor* station, and the two-way tracking data supplied was quite useful in the initial orbit calculations. This station was also used to fill a gap in station coverage between first pass set at DSS 51 and first pass rise at DSS 11. The gap had a duration of 31 min and was a result of launching late in the window on a more southerly azimuth. Because of the lower antenna gain (30-ft antenna) and higher system noise temperature (paramp instead of maser), it was necessary to reduce the spacecraft data rate to 17.2 bit/sec in order to obtain usable telemetry data. This was done, and DSS 72 was able to obtain telemetry data during the gap period.

DSS 42 experienced some difficulty obtaining lock during its initial tracking period because of inaccurate pointing angle data in the received predicts. This was caused by an outdated set of antenna angle correction coefficients for DSS 42 in the predict program.

The signal levels received at the DSIF stations are shown in Fig. V-8. They compare favorably with the predicted values. Only the portion of the mission before the midcourse maneuver is shown because the post-midcourse data is very inaccurate owing to spacecraft tumbling. A 2-db discrepancy between DSS 11 signal levels and other stations (notably DSS 42) is apparent. This discrepancy is a result of the AGC calibration method used and is consistent with results obtained in the *Surveyor I* mission. The 7-db drop in signal level recorded by DSS 51 between 16:00 and 18:00 is due to a 3-db increase in carrier suppression of the 137.5 bit/sec data rate and a 4-db spacecraft antenna loss due to spacecraft orientation. Note that this occurred prior to star acquisition. Because of its larger reflector (210 ft), the received level of DSS 14 is 8 db above the received signal levels of other prime stations. Since DSS 72 uses a smaller reflector (30 ft), its received signal levels are 10 db less than the other stations. These levels were consistent during the respective station tracking periods. The variations in the DSS 72 signal level data are due to the increased carrier suppression at 17.2 bit/sec coupled with a loss of calibration accuracy at low signal levels.

When the attempted midcourse maneuver caused a nonstandard spacecraft tumbling condition, low spacecraft signal strength coupled with S-band frequency variation of 200 to 300 cps resulted in difficult tracking. In order to continue tracking the tumbling spacecraft, DSS 51 and 42 modified their DSIF standard (Goldstone duplicate standard: GSDS) receivers in real-time during the second pass at each station. These modifications extended the tracking loop bandwidths of DSS 51 and 42 by factors of 2 and 4, respectively.

During the second pass at DSS 51, when severe communications problems existed, DSS 61 (designated a training station) was called up. DSS 61 was able to interrupt a Pioneer track, reconfigure for *Surveyor*, and was in two-way lock ready for commanding in approximately 13 min. This operation was accomplished with a very limited crew in the middle of the night. No high-speed data was obtained from DSS 61 during this pass because of a manning problem complicated by an OSDP hardware problem.

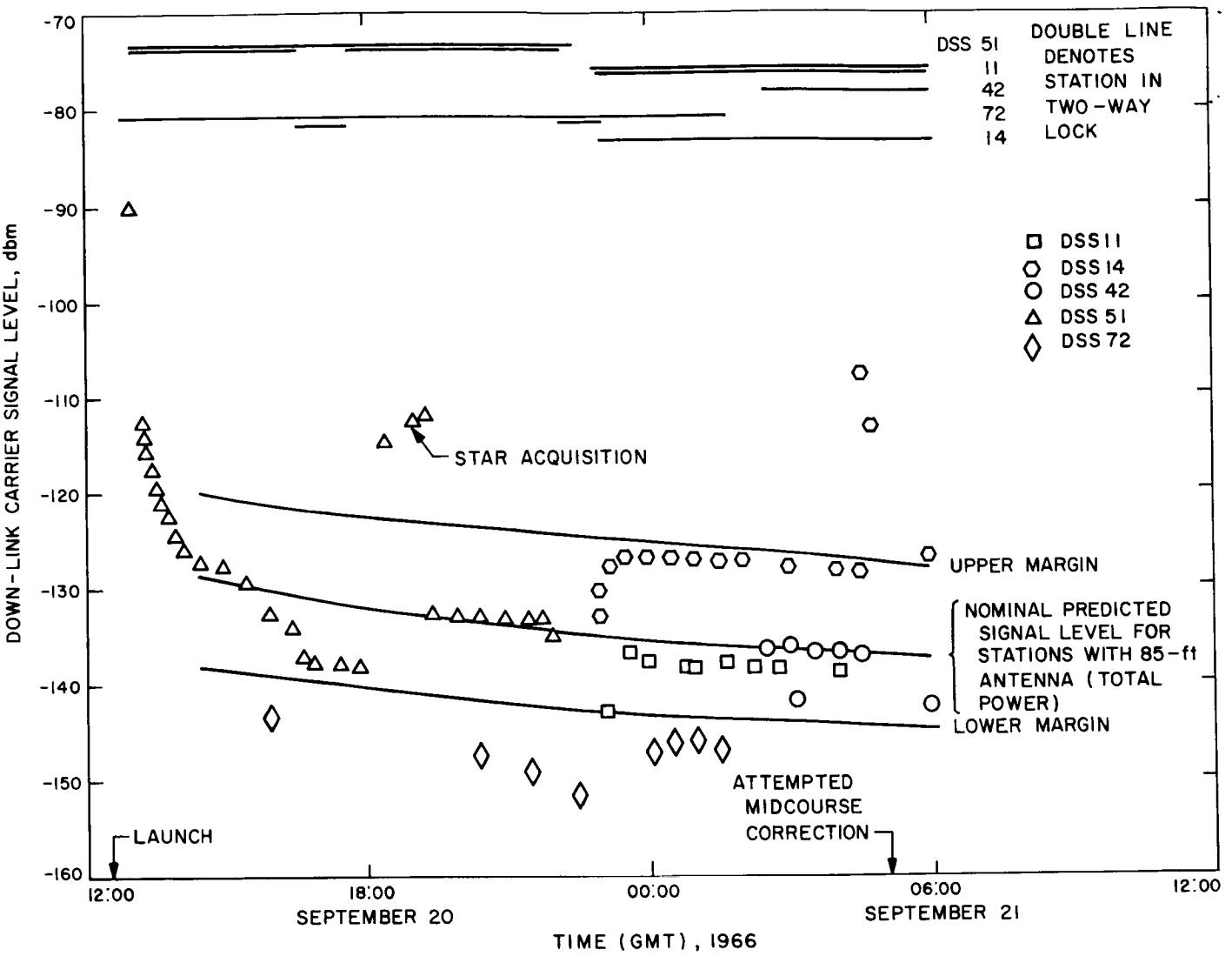

Fig. V-8. DSS received signal level

A number of minor equipment anomalies and procedural problems occurred but were readily corrected by station personnel without affecting the mission.

Although the masers at all stations performed well during this mission, the prelaunch experience caused some concern about their reliability. The low angle rate and high signal level performance of DSS 51 require investigation and possibly some engineering action or replacement with a standard S-band system.

2. GCS/NASCOM

For *Surveyor* missions, the Ground Communications System (GCS) transmits tracking, telemetry, and command data from the DSIF to the SFOF and control and command functions from the SFOF to the DSIF by means of NASCOM facilities. The GCS also transmits simulated tracking data to the DSIF and video data and base-band telemetry from DSS 11, Goldstone DSCC, to the SFOF. The links involved in the system are shown in Fig. V-9.

a. Teletype (TTY) circuits. Teletype circuits (four available to prime stations) are used for tracking data, telemetry, commands, and administrative traffic. The teletype circuits were exceptionally reliable, the weakest circuits (DSS 51) showing approximately 97% reliability. The most serious problem associated with teletype circuits developed at Goldstone, where the total number of teletype lines available in support of *Surveyor II, Lunar*

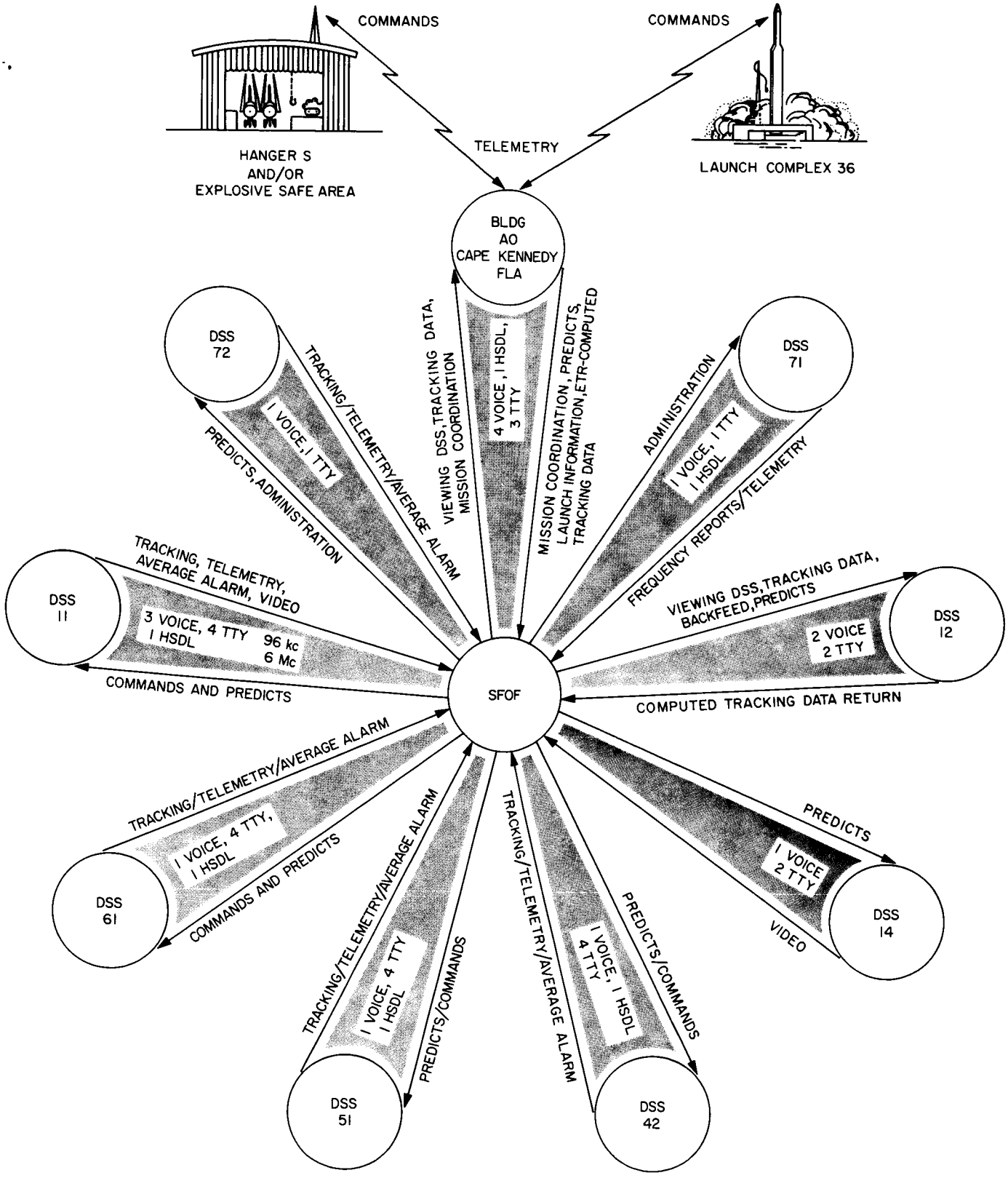

Fig. V-9. DSN/GCS communications links

Orbiter, and *Pioneer* Missions was inadequate. The lack of circuits to Goldstone was a constraint during the August–September testing periods. However, during launch and midcourse, the system operated faultlessly. JPL communication engineers added one additional TTY circuit to the Goldstone Microwave System, increasing the total to nine prior to the *Surveyor II* Mission. This number, however, is still insufficient during SFOF multimission periods. NASCOM provided two additional temporary TTY circuits from JPL to Goddard to assure sufficient lines during the launch phase of the mission.

b. Voice circuits. The voice circuits are shared between the DSIF and the *Surveyor* Project for administrative, control, and commanding functions. The NASCOM voice circuits provided for the *Surveyor II* mission performed perfectly except for failures which occurred in the circuits to the South Africa station (DSS 51) and the Ascension Island station (DSS 72).

The DSS 51 voice circuit was above average during the prelaunch phase. Just after launch, however, this circuit failed because of expected high-frequency propagation conditions.

The "backdoor" circuit via Australia was also interrupted during this same critical period. A commercial telephone link was established with DSS 51 via the New York Overseas Operator, and voice operation was transferred to this temporary circuit. The commercial circuit also failed periodically, though at different time intervals from the NASCOM circuits. This additional capability was maintained for approximately two hours after launch and proved quite helpful. On September 21, the same high-frequency radio propagation condition occurred during certain critical portions of the DSS 51 view period following the midcourse phase. Activation of the Commercial Overseas Operator circuit was again required for a period of approximately two hours. NASCOM provided all possible support in attempting to restore DSS 51 circuits during the mission critical launch phase and during emergency operations following midcourse.

Because of high-frequency radio propagation, the DSS 72 voice circuit was continually up and down, as were most of the DSS 72 circuits during both premission tests and the mission.

The *Surveyor* Control Net within the SFOF was overloaded during prelaunch tests and mission operations, causing much slower voice communication. The problem developed because of insufficient and limited configuration of the Operational Voice Communication System (OVCS). The intercom portion of the OVCS has since been reconfigured to allow point-to-point coordination of prepass events and to overcome the communications overload.

c. High-speed data line (HSDL). One HSDL is provided to each prime site for telemetry data transmission to the SFOF in real-time. This part of the communications system performed well during the mission, providing better-quality high-speed data with less downtime than during the *Surveyor I* mission. Crossed lines at GSFC were responsible for a 10-min loss of data from AFETR, and a mispatch in the JPL Communications Center resulted in the loss of some data from Goldstone. Both modem* types (NASCOM and Hallicrafter) were required during the *Surveyor II* mission, since the Johannesburg station is not equipped with NASCOM modems.

Modem 1A, one of the two Hallicrafter modem receivers, was again found to be considerably less reliable during testing than was Receiver 1B (as was the case during the *Surveyor I* mission) and was not used during the *Surveyor II* mission.

Hallicrafter Modem Receiver 1B was used exclusively for DSS 41 high-speed data. Reliability was considered high, and much superior to that of the previous mission. The changeover from Hallicrafter to NASCOM modems at DSS 51 is still highly desirable, but it is doubtful that this can be accomplished prior to the next mission, as change of modems will be required at RCA New York, Tangier, and Pretoria, South Africa, as well as at DSS 51.

The use of NASCOM modems in the *Surveyor II* mission proved to be highly successful, with fewer line outages and with higher quality data received from all stations.

d. Wideband microwave system. The wideband microwave link between DSS 11, Goldstone DSCC, and the SFOF consists of two 6-Mc lines for video, and one 96-kc duplex line. The microwave link between Goldstone and the SFOF performed with nearly 100% reliability on the *Surveyor II* Mission. The microwave circuits were involved, however, in numerous line level and patching discrepancies during the August–September testing periods. Most patching problems experienced during testing involved patching of mission nonstandard simulated data

*A modem (modulator-demodulator) is a device for converting a digital signal to a signal which is compatible with telephone line transmission (e.g., a frequency-modulated tone).

through station tracking and video systems and return to SFOF. After JPL communications engineers and Western Union personnel had succeeded in obtaining proper equalization on these circuits, most of the problems disappeared during the mission.

3. DSN in SFOF and DSN/AFETR Interface

The DSN supports the *Surveyor* missions by providing mission control facilities and performing special functions within the SFOF. The DSN also provides an interface with the AFETR for real-time transmission of downrange spacecraft telemetry data from Building AO at Cape Kennedy to the SFOF.

a. Data Processing System (DPS). The SFOF Data Processing System performs the following functions for *Surveyor* missions:

(1) Computation of acquisition predictions for DSIF stations (antenna pointing angles and receiver and transmitter frequencies).

(2) Orbit determinations.

(3) Midcourse maneuver computations and analysis.

(4) On-line telemetry processing.

(5) Command tape generation.

(6) Simulated data generation (telemetry and tracking data).

The DPS general configuration for the *Surveyor II* mission is shown in Fig. V-10 and consists of two PDP-7 computers* in the telemetry processing station (TPS), two strings of IBM 7044/7094 computers in the Central Computing Complex (CCC), and a sublet of the input/output (I/O) system.

The DPS performed in a nominal manner, with only minor hardware problems which did not detract from

*Manufactured by Digital Equipment Corp.

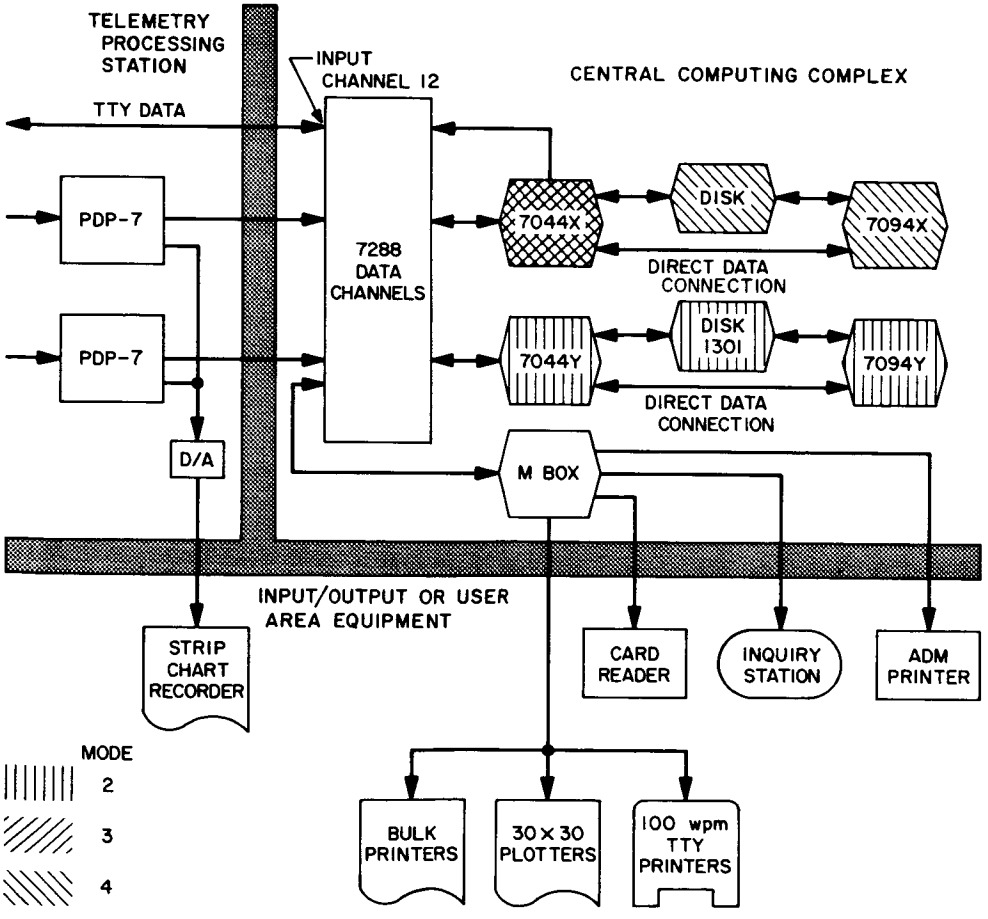

Fig. V-10. General configuration of SFOF data processing system

mission support. The two PDP-7 computers were used extensively to process high-speed telemetry data for the *Surveyor II* mission. This processing consisted of decommutating and transferring the data to the 7044 computer via the 7288 data channels, generating a digital tape for non-real-time processing, and supplying digital-to-analog converters with discrete data parameters to drive analog recorders in both the Spacecraft Analysis Area and the Space Science Analysis Area. Two PDP-7 problems occurred when the telemetry modes were changed. From all indications, the computer appeared to be functioning properly. However, data was not being supplied to the 7288 data channels. The problem was quickly resolved by switching to the second PDP-7 as the prime processor. It has not been determined if this was a hardware or software problem.

The IBM 7044/7094 computer string dual configuration successfully processed all high-speed data received from the TPS and all teletype data received from the communications center, as well as all input/output requests from the user areas. A dual Mode 2 string was utilized by the *Surveyor* Project until 00:00 GMT on September 22.

The problems experienced in the Central Computing Complex were quite easily remedied and had little or no effect on the mission.

The Input/Output System provides the capability for entering data control parameters into the 7044/7094 computers and also for displaying computed data in the user areas via the various display devices. The Input/Output System performed quite adequately with only a few reported problems.

b. DSN Intracommunications System (DSN/ICS). The DSN/ICS provides the capability of receiving, switching, and distributing all types of information required for spaceflight operations to designated areas or users within the SFOF. The system includes facilities for handling all voice communications, closed circuit television, teletype, high-speed data, and data received over the microwave channels.

In general, the DSN/ICS performance was well within the expected reliability parameters. There were some problems but these were not of a critical nature. During the ORT's and *Surveyor II* mission, the communications status display in the SFOF proved to be inadequate to support multimissions. Fewer voice line patching errors occurred during this mission than during the previous mission. Seventeen tie lines were available from the communications center to the telemetry processing station during the *Surveyor II* mission.

c. DSN/AFETR interface. The DSN/AFETR interface provides real-time data transmission capability for both VHF and S-band downrange telemetry. The nominal switchover time is after the spacecraft S-band transmitter is turned to high power. The interface with the *Surveyor* Project is at the input to the Command and Data Handling Console in Building AO. The output of the CDC is then interfaced with the Ground Communications System for transmission to the SFOF. It is also possible to go directly from the range data output to the GCS, bypassing the CDC.

This real-time telemetry transmission interface performed quite well. Good data was received at the SFOF whenever good data was received at Building AO.

VI. Mission Operations System

A. Functions and Organization

The basic functions of the Mission Operations System (MOS) are the following:

(1) Continual assessment and evaluation of mission status and performance, utilizing the tracking and telemetry data received and processed.

(2) Determination and implementation of appropriate command sequences required to maintain spacecraft control and to carry out desired spacecraft operations during transit and on the lunar surface.

The *Surveyor* command system philosophy introduces a major change in the concept of unmanned spacecraft control: virtually all in-flight and lunar operations of the spacecraft must be initiated from earth. In previous space missions, spacecraft were directed by a minimum of earth-based commands. Most in-flight functions of those spacecraft were automatically controlled by an on-board sequencer which stored preprogrammed instructions. These instructions were initiated by either an on-board timer or by single direct commands from earth. For example, during the *Ranger VIII* 67-hr mission, only 11 commands were sent to the spacecraft; whereas for a standard *Surveyor* mission, approximately 280 commands must be sent to the spacecraft during the transit phase, out of a command vocabulary of 256 different direct commands. For *Surveyor I*, 288 commands were sent during transit and over 100,000 commands were sent following touchdown.

Throughout the space-flight operations of each *Surveyor* mission, the command link between earth and spacecraft is in continuous use, transmitting either fill-in or real commands every 0.5 sec. The *Surveyor* commands are controlled from the SFOF and are transmitted to the spacecraft by a DSIF station.

The equipment utilized to perform MOS functions falls into two categories: mission-independent and mission-dependent equipment. The former is composed chiefly of the *Surveyor* T&DA system equipment and has been described in Section V. It is referred to as mission-independent because it is general-purpose equipment which can be utilized by more than one NASA project when used with the appropriate project computer programs. Selected parts of this equipment have been assigned to perform the functions necessary to the *Surveyor* Project. The mission-dependent equipment (described in Section VI-B, following) consists of special equipment which has been installed at DSN facilities for specific functions peculiar to the project.

The *Surveyor* Project Manager, in his capacity as Mission Director, is in full charge of all mission operations. The Mission Director is aided by the Assistant Mission Director and a staff of mission advisors. During the mission, the MOS organization is as shown in Fig. VI-1.

Mission operations are under the immediate, primary control of the Space Flight Operations Director (SFOD) and supporting *Surveyor* personnel. Other members of the team are the T&DA personnel who perform services for the *Surveyor* Project.

During space-flight and lunar surface operations, all commands are issued by the SFOD or his specifically delegated authority. Three groups of specialists provide technical support to the SFOD. These groups are specialists in the flight path, spacecraft performance, and scientific experiments, respectively.

1. Flight Path Analysis and Command Group

The Flight Path Analysis and Command (FPAC) group handles those space-flight functions that relate to the location of the spacecraft. The FPAC Director maintains control of the activities of the group and makes specific recommendations for maneuvers to the SFOD in accordance with the flight plan. In making these recommendations, the FPAC Director relies on five subgroups of specialists within the FPAC Group.

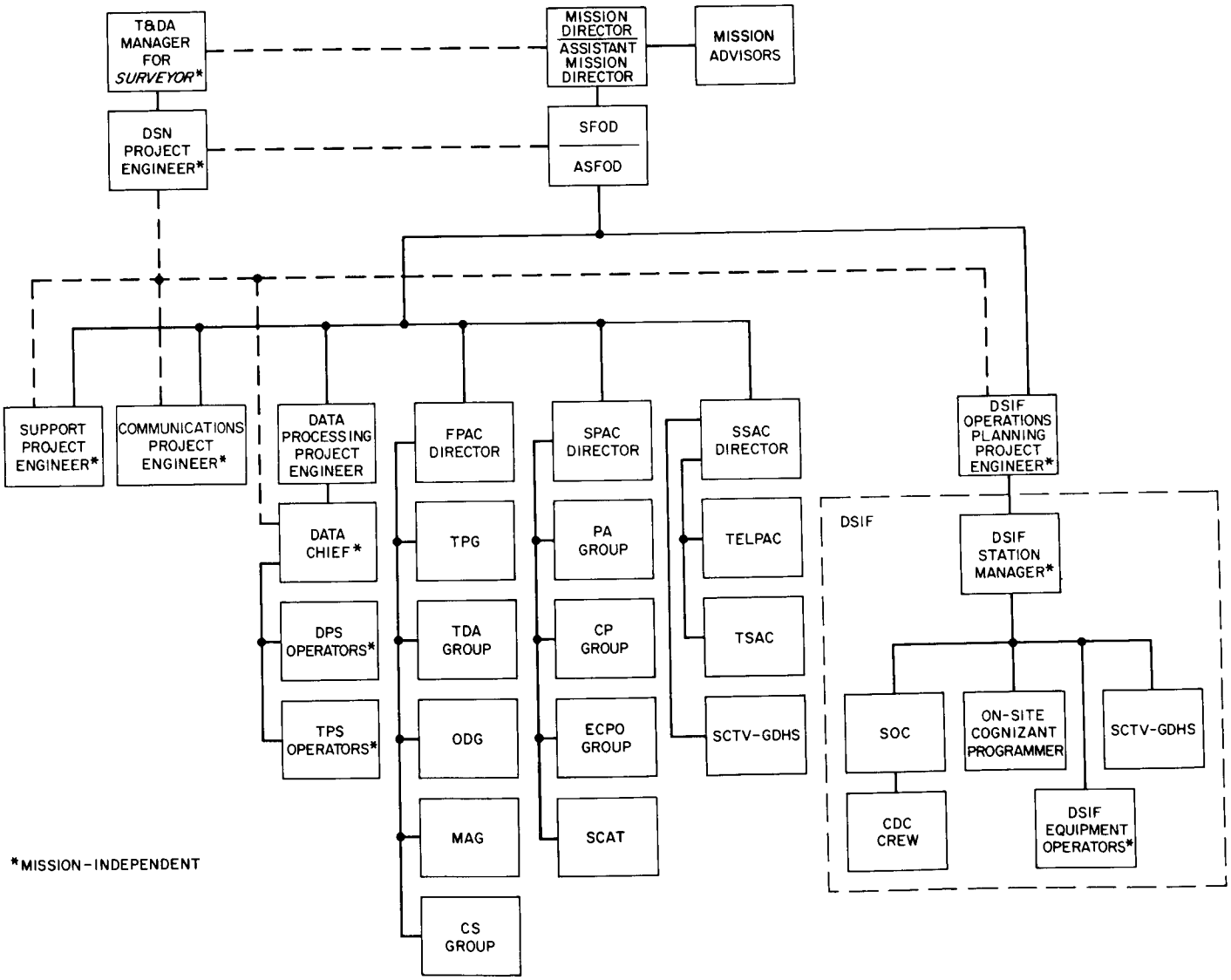

Fig. VI-1. Organization of MOS

(1) The Trajectory Prediction Group (TPG) determines the nominal conditions of spacecraft injection and generates lunar encounter conditions based on injection conditions as reported by AFETR and computed from tracking data by the Orbit Determination Group. The actual trajectory determinations are made by computer.

(2) The Tracking Data Analysis (TDA) group makes a quantitative and descriptive evaluation of tracking data received from the DSIF stations. The TDA group provides 24-hr/day monitoring of incoming tracking data. To perform these functions the TDA group takes advantage of the Data Processing System (DPS) and of computer programs generated for their use. The TDA acts as direct liaison between the data users (the orbit determination group) and the DSIF and provides predicts to the DSIF.

(3) The Orbit Determination Group (ODG), during mission operations, determines the actual orbit of the spacecraft by processing the tracking data received from the DSN tracking stations by way of the TDA group. Also, statistics on various parameters are generated so that maneuver situations can be evaluated. The ODG generates tracking predictions for the DSIF stations and recomputes the orbit of the spacecraft after maneuvers to determine the success of the maneuver.

(4) The Maneuver Analysis Group (MAG) is the subgroup of FPAC responsible for describing possible midcourse and terminal maneuvers for both standard and nonstandard missions in real-time during the actual flight. In addition, once the decision has been made as to what maneuver should be performed, the MAG generates the proper spacecraft commands to effect these maneuvers. These commands are then relayed to the Spacecraft Performance Analysis and Command Group to be included with other spacecraft commands. Once the command message has been generated, the MAG must verify that the calculated commands are correct.

(5) The Computing Support Group acts in a service capacity to the other FPAC subgroups, and is responsible for ensuring that all computer programs used in space operations are fully checked out before mission operations begin and that optimum use is made of the Data Processing System facilities.

2. Spacecraft Performance Analysis and Command Group

The Spacecraft Performance Analysis and Command (SPAC) Group, operating under the SPAC Director, is basically responsible for the operation of the spacecraft itself. The SPAC Group is divided into three subgroups:

(1) The Performance Analysis (PA) group monitors incoming engineering data telemetered from the spacecraft, determines the status of the spacecraft, and maintains spacecraft status displays throughout the mission. The PA group also determines the results of all commands sent to the spacecraft. In the event of a failure aboard the spacecraft, as indicated by telemetry data, the PA group analyzes the cause and recommends appropriate nonstandard procedures.

(2) The Command Preparation (CP) group is basically responsible for preparing command sequences to be sent to the spacecraft. In so doing they provide inputs for computer programs used in generating the sequences, verify that the commands for the spacecraft have been correctly received at the DSS, and then ascertain that the commands have been correctly transmitted to the spacecraft. If nonstandard operations become necessary, the CP group also generates the required command sequences.

(3) The Engineering Computer Program Operations (ECPO) group includes the operators for the DPS input/output (I/O) console and related card punch, card reader, page printers, and plotters in the spacecraft performance analysis area (SPAA). The ECPO group handles all computing functions for the rest of the SPAC group, including the maintenance of an up-to-date list of parameters for each program.

In order to take maximum advantage during the mission of the knowledge and experience of the various personnel who are not a part of the "hard-core" operations teams (FPAC, SPAC, and SSAC) but have been engaged in detail design, analysis, or testing of the spacecraft, a Spacecraft Analysis Team (SCAT) has been established. The SCAT group, located in a building adjacent to the SFOF, has appropriate data displays showing the current status of the mission. The SCAT is available upon request for immediate consultation and detailed analysis in support of the SPAC.

3. Space Science Analysis and Command Group

The Space Science Analysis and Command (SSAC) group performs those space-flight functions related to the operation of the survey TV camera. SSAC is divided into two operating sub-groups:

(1) The Television Performance Analysis and Command (TelPAC) group analyzes the performance of the TV equipment and is responsible for generating standard and nonstandard command sequences for the survey TV cameras.

(2) The Television Science Analysis and Command (TSAC) group analyzes and interprets the TV pictures for the purpose of ensuring that the mission objectives are being met. The TSAC group is under the direction of the Project Scientist and performs the scientific analysis and evaluation of the TV pictures.

The portion of the spacecraft TV Ground Data Handling System (TV-GDHS) in the SFOF provides direct support to the SSAC group in the form of processed electrical video signals and finished photographic prints. The TV-GDHS operates as a service organization within the MOS structure. Documentation, system checkout, and quality control within the system are the responsibility of the TV-GDHS Operations Manager. During operations support the TV-GDHS Operations Manager reports to the SSAC Director.

4. Data Processing Personnel

The use of the Data Processing System (DPS) by *Surveyor* is under the direction of the Assistant Space Flight Operations Director (ASFOD) for Computer Programming. His job is to direct the use of the DPS from the viewpoint of the MOS. He communicates directly with the Data Chief, who is in direct charge of DPS personnel and equipment. Included among these personnel are the I/O console operators throughout the SFOF, as well as the equipment operators in the DPS and Telemetry Processing Station (TPS) areas.

Computer programs are the means of selecting and combining the extensive data processing capabilities of electronic computers. By means of electronic data processing, the vast quantities of mission-produced data are assembled, identified, categorized, processed and displayed in the various areas of the SFOF where the data are used. Their most significant service to the MOS is providing knowledge in real-time of the current state of the spacecraft throughout the entire mission. This service is particularly important to engineers and scientists of the technical support groups since, by use of the computer programs, they can select, organize, compare and process current-status data urgently needed to form their time-critical recommendations to the SFOD. (See Section V-C-3 for a description of the DPS.)

5. Other Personnel

The Communications Project Engineer (PE) controls the operational communications personnel and equipment within the SFOF, as well as the DSN/GCS lines to the DSIF stations throughout the world.

The Support PE is responsible for ensuring the availability of all SFOF support functions, including air conditioning and electric power; for monitoring the display of *Surveyor* information on the Mission Status Board and throughout the facility; for directing the handling, distribution, and storage of data being derived from the mission; and for ensuring that only those personnel necessary for mission operations are allowed to enter the operational areas.

The DSIF Operations Planning PE is in overall control of the DSIF Stations at Goldstone, Johannesburg, and Tidbinbilla; his post of duty is in the SFOF in Pasadena. At each station, there is a local DSIF station manager, who is in charge of all aspects of his DSIF station and its operation during a mission. The *Surveyor* personnel located at each station report to the station manager.

B. Mission-Dependent Equipment

Mission-dependent equipment consists of special hardware provided exclusively for the *Surveyor* Project to support the Mission Operations System. Most of the equipment in this category is contained in the Command and Data Handling Consoles and Spacecraft Television Ground Data Handling System, which are described below.

1. Command and Data Handling Console

The Command and Data Handling Console (CDC) comprises that mission-dependent equipment, located at the participating Deep Space Stations, that is used to:

(1) Generate commands for control of the *Surveyor* spacecraft by modulation of the DSS transmitter.

(2) Process and display telemetered spacecraft data and relay telemetry signals to the on-site data processor (OSDP) for transmission to the SFOF.

(3) Process, display, and record television pictures taken by the spacecraft.

The CDC consists of four major subsystems:

(1) The command subsystem generates FM digital command signals from punched tape or manual inputs for the DSS transmitter, and prints a permanent record of the commands sent. The major units of the command subsystem, which can accommodate 1024 different commands, are the command generator, the command subcarrier oscillator, the punched tape reader, and the command printer. Outgoing commands are relayed to the SFOF and logged on magnetic tape by the DSS.

(2) The FM demodulator subsystem accepts the FM intermediate-frequency signal of the DSS receiver and derives from it a baseband signal. The baseband signal consists of either video data or a composite of engineering subcarrier signals. Depending upon the type of data constituting the baseband signal, the CDC processes the data in either the TV data subsystem or the telemetry data subsystem.

(3) The TV data subsystem receives video data from the FM demodulator and processes it for real-time display at the CDC and for 35-mm photographic recording. In addition, telemetered frame-identification data is displayed and photorecorded. A long-persistence-screen TV monitor is mounted in the CDC. The operator, when requested, can thus evaluate the picture and, upon the SFOD's direction, initiate corrective commands during lunar television surveys.

(4) The telemetry data subsystem of the CDC separates the various data channels from the baseband signal coming from either the FM demodulator or the DSS receiver phase-detected output and displays the desired data to the operators. Discriminators are provided for each subcarrier channel contained in the baseband signal. The output of each discriminator, in the case of time-multiplexed data, is sent to the pulse code modulation (PCM) decommutator and then relayed to both the OSDP computer for subsequent transmission to the SFOF and to meters for evaluation of spacecraft performance. In the case of continuous data transmissions, the output of the discriminator is sent to an oscillograph for recording and evaluation.

The CDC contains built-in test equipment to ensure normal operation of its subsystems. A CDC tester, consisting of a spacecraft transponder with the necessary modulation and demodulation equipment, ensures day-to-day compatibility of the CDC and DSIF stations.

a. Network configuration. Table VI-1 lists the CDC mission-dependent equipment provided for support of *Surveyor II* at the DSIF stations. CDC's were located at DSS 11, 42, 51, 61, 71, and 72. Stations 11, 42, 51, and 72 were the prime *Surveyor* stations. However, Station 61, at Madrid, was used for some command transmissions. DSS 12, the Echo site at Goldstone, was configured and checked out to provide command backup to DSS 11. The Echo Station transmitter was set to the *Surveyor* frequency and a patchable interface established via the intersite microwave link for the command subcarrier from the CDC at DSS 11. A return link was also established from the DSS 12 receiver back to the DSS 11 CDC for purposes of checking the command transmission. DSS 14, the Mars site at Goldstone, was configured to record both pre- and post-detection signals on magnetic tape. The added capability of this station was used to increase the probability of obtaining data during critical mission phases. DSS 71, the Cape Kennedy spacecraft monitoring station, was provided for a DSIF compatibility test with the *Surveyor II* spacecraft several weeks prior to launch. DSS 71 was also used to obtain spacecraft telemetry data during the prelaunch countdown and immediately after launch.

Table VI-1. CDC mission-dependent equipment support of *Surveyor II* at DSIF stations

DSS 11, Goldstone	Prime station with command, telemetry, and TV
DSS 42, Canberra	Prime station with command, telemetry, and TV
DSS 51, Johannesburg	Prime station with command and telemetry
DSS 61, Madrid	Backup station with command, telemetry, and TV
DSS 71, Cape Kennedy	Station used for spacecraft compatibility tests and pre- and post-launch telemetry monitoring
DSS 72, Ascension	Prime station with command and telemetry
DSS 12, Goldstone	Station configured for command backup
DSS 14, Goldstone	Station configured to record critical mission phases

Table VI-2. *Surveyor II* command activity

Station	Commands transmitted
DSS 11	854
DSS 42	535
DSS 51	187
DSS 61	3
DSS 71	0
DSS 72	0
	1579

b. CDC operations. During the mission, CDC operations were conducted at six of the DSIF stations. Table VI-2 lists the number of commands transmitted by each station during the mission. Only seven CDC anomalies occurred during the *Surveyor II* Mission (countdown and flight operations). No detrimental effects on the mission resulted from these anomalies.

(1) *DSS 11, Goldstone.* The Pioneer Station, at Goldstone, participated in two passes. This station used a full CDC with command, telemetry, and TV equipment. Three additional interfaces identical to those used for *Surveyor I* were established, as follows:

(a) During telemetry sequences, the received telemetry subcarriers were transmitted to the SFOF from the CDC via the "96-kc" line. Signal-limiting and level adjustments were provided by the CDC.

(b) As mentioned earlier, an interface was established with DSS 12, Echo Station, for command backup. If necessary, the CDC command subcarrier oscillator could be patched to the intersite microwave link for transmission to the Echo site, where the S-band transmitter would be modulated. A detected signal from the Station 12 transmitter was fed back to the Pioneer Station CDC via another microwave channel for checking command transmissions in the CDC.

(c) Two dataphone links were established with Hughes Aircraft Company (HAC), El Segundo, California. One line carried the reconstructed telemetry PCM waveform to HAC from the CDC's decommutator; the second line carried the command waveform obtained at the CDC system tester.

(2) *DSS 42, Canberra.* This station participated in two passes. The CDC configuration was standard with full capability available, except that the spare TV monitor was connected in parallel with the prime monitor for better on-site TV monitoring. DSS 42 commanded RADVS turn-on and retro firing.

(3) *DSS 51, Johannesburg.* This station participated in two passes. The CDC configuration was standard although the interface with the DSIF was modified to use the L/S-band receiver during the second pass. Because of the tumbling spacecraft, the *Surveyor* suitcase receiver (S-band receiver for *Surveyor* telemetry) was unable to lock onto the spacecraft signal since the suitcase receiver tracking loop bandwidth of 12 cps was too narrow to track the doppler rate caused by tumbling. The L/S receiver, with a bandwidth of 152 cps (later changed to about 300 cps), was able to maintain lock most of the time. Thus, telemetry data reception was possible.

(4) *DSS 61, Madrid.* This station participated on a backup basis during two separate periods of the second view period. No station countdown was performed prior to the tracking periods, but two-way lock with the spacecraft was achieved and several commands transmitted.

(5) *DSS 71, Cape Kennedy.* This station was equipped with a CDC in the period between *Surveyor I* and *II* missions and includes only command and telemetry equipment. A DSIF compatibility test with *Surveyor II* spacecraft was conducted in mid-August to establish RF, command, and telemetry compatibility. During the final portion of the prelaunch countdown and the first several minutes after liftoff, spacecraft telemetry data was processed by this station and sent to the SFOF via one high-speed data line and one teletype line.

(6) *DSS 72, Ascension.* The CDC at DSS 72 is limited to pulse code modulation telemetry operation and manual command transmission. No television or analog telemetry equipment is provided. This station acquired the spacecraft signal on the first pass and started processing telemetry data and transferring the data to SFOF via high-speed data and teletype lines. It also monitored the spacecraft two-way acquisition by DSS 51. The station again acquired the spacecraft during the loss-of-view period between DSS 51 and DSS 11. After transferring the spacecraft to DSS 11, DSS 72 terminated participation in the *Surveyor II* mission.

2. Spacecraft Television Ground Data Handling System

The Spacecraft Television Ground Data Handling System (TV-GDHS) was designed to record on film the television images received from *Surveyor* spacecraft. The principal guiding criterion was photometric and photogrammetric accuracy with negligible loss of information. The system was also designed to provide display information for the conduct of mission operations and for the production of user products such as prints, enlargements, duplicate negatives, and catalogs of ID information.

The system is divided into two major parts which are located at DSS 11, Goldstone, and at the SFOF, Pasadena. At DSS 11 is an on-site data recovery (OSDR) subsystem, and an on-site film recorder (OSFR) subsystem. These subsystems are duplicated in the media conversion data recovery (MCDR) subsystem and in the media conversion film recorder (MCRF) subsystem which are located at the SFOF along with additional equipment making up the complete system.

The complete TV-GDHS was committed for the *Surveyor II* mission. For the *Surveyor I* mission, only portions of the system at the SFOF had been committed because of implementation constraints.

a. Equipment at Pioneer Site, Goldstone (TV-11). Data for the TV-GDHS is injected into the system at the interface between the Station 11 receiver and the OSDR. At this point, the signal from *Surveyor* has been down-converted to a 10-Mc FM-modulated signal. The OSDR further down-converts it to 4 Mc* for the 600-line TV mode (500 kc, and 70 kc from the CDC, for the 200-line mode), inputs this signal into the station's FR-800 videotape recorder, and provides an output signal to the Microwave Communication Link for transmission to the SFOF. The station's FR-1400 records the baseband video signal only during 600-line mode and the 500- and 70-kc during 200-line mode. The OSDR further processes signals to obtain television image synchronization, telemetry synchronization, and the baseband video signal. This information is then used by the OSFR to record the video image and the raw ID telemetry in bit form on 70-mm film, together with an internally generated electrical gray scale and "human readable" time and record number.

Prior to the *Surveyor II* mission, replacement of the cathode ray tube in the OSFR required an additional final calibration of the film recorder. No new major problems occurred during the mission. Since the mission was terminated prior to spacecraft landing, no results were obtained from TV-11.

b. Equipment at the SFOF (TV-1). The signal presented to the Microwave Terminal at DSS 11 is transmitted to the SFOF where it is distributed to the MCDR. The MCDR processes the signal in the same manner as the OSDR. An FR-700 video magnetic tape recorder records the predetection signal in the same manner as the FR-800 at DSS 11. In addition, the MCDR passes the raw ID information to the media conversion (MC) computer, which converts the data to engineering units. This converted data is passed to (1) the film recorder, where it is recorded as "human readable" ID, (2) the ID wall display board in the SSAC area, (3) the disc file, where the film chip index file is kept, and (4) the history tape.

The scan converter accepts the slow-scan image information from the film recorder and converts it to the standard RETMA television signal for use by the SFOF closed-circuit television and the public TV broadcast stations.

The MC film recorder provides two films. One of these films is passed directly to the bimat processor; the other is accumulated in a magazine and is wet-processed off-line.

The bimat processor laminates the exposed film with the bimat imbibed material, producing a developed negative and a positive transparency. The negative is used to make strip contact prints, which are delivered to the users. The negative is then cut into chips and entered into the chip file, where they are available for use in making additional contact prints and enlargements.

No major problems associated with the TV-GDHS occurred during the *Surveyor II* mission. Prior to the mission, a hardware malfunction in the disc file and its interface to the MC computer prevented the Real-Time System Program from working. Another problem, a nonlinear demodulated video signal in the MCDR, prevented expeditious video verification and produced degraded output recordings. The problems with these two subsystems were corrected, and the total system was operational prior to launch. However, since the mission was terminated before spacecraft landing, there were no results from TV-1 at the SFOF.

*For the *Surveyor I* mission, the center frequency of the FM signal was 5 Mc.

C. Mission Operations Chronology

Inasmuch as mission operations functions were carried out on an essentially continuous basis throughout the *Surveyor II* mission, only the more significant and special, or nonstandard, operations are described in this chronicle. Refer also to the sequence of mission events presented in Table A-1 of Appendix A.

1. Countdown and Launch Phase

No significant problems were reported in the early phases of the countdown, and the spacecraft operations were ahead of schedule at times during this period, which included the Spacecraft Readiness Test. During the countdown, MSFN and AFETR encountered only temporary difficulties with Bermuda and Trinidad radars and the communication links with the RIS *Coastal Crusader*.

Approximately one hour prior to scheduled launch, SPAC reported spacecraft Receiver B AGC indication was 26 db below that of Receiver A. Launch Operations personnel at Cape Kennedy indicated that this anomaly was not due to spacecraft receiver failure as it had been observed before owing to gantry movement, although *Surveyor I* showed only a 5-db drop as a result of gantry movement. On the basis of this report, the countdown was continued. (Later, during the early cruise phase of the mission, a Receiver B threshold test was conducted which revealed that the anomaly was due to a faulty telemetry indication.)

After proceeding normally to the built-in hold at T-5 min, additional unscheduled holds were required because of launch vehicle problems associated with a low *Centaur* hydrogen peroxide temperature indication, failure of the *Atlas* liquid oxygen boil-off valve to close at the start of flight pressurization, and failure of the *Atlas* automatic topping system to maintain satisfactory liquid oxygen level while holding for the preceding problem. As a result of these problems, which are described in greater detail in Section II, liftoff was not achieved until the final seconds of the available launch window.

Liftoff occurred at 12:31:59.824 GMT on September 20, 1966, with all systems reported in a "go" condition. All "mark event" times were received from AFETR, although the reports were somewhat late. Launch vehicle performance appeared to be nominal, with no significant anomalies on either the *Atlas* or *Centaur*. Injection of the spacecraft into the prescribed lunar transfer orbit was well within established limits, and the required retro maneuver was successfully performed by the *Centaur*. A description of launch vehicle performance and sequence of events from launch through injection is contained in Section III.

Spacecraft performance during the launch-to-injection phase appeared nominal. The *Centaur*-commanded spacecraft events just prior to separation were monitored as they occurred by observing spacecraft telemetry transmitted to Cape Kennedy from downrange in real time.

With the exception of a 1-min (approx) transmission dropout at L + 1 min due to a Cape-wide power failure, a total of 44 min of in-flight spacecraft telemetry was received at the SFOF from Cape Kennedy, including data retransmitted from downrange stations in real time.

Following separation at 12:44:32 GMT, the spacecraft executed the planned automatic sequences as follows. By using its cold-gas jets, which were enabled at separation, the Flight Control Subsystem nulled out the small rotational rates imparted by the separation springs, and initiated a roll–yaw sequence to acquire the sun. After a minus roll of approximately 72 deg and a plus yaw of 16.5 deg, acquisition and lock-on to the sun by the spacecraft sun sensors were completed at 12:48:13 GMT. Concurrently with the sun acquisition sequence, the A/SPP stepping sequence was initiated to deploy the solar panel axis and roll axis 85 and 60 deg, respectively. At 12:54:46 GMT, the solar panel was in its proper transit position. All of these operations were confirmed in real-time from the spacecraft telemetry.

Following sun lock-on, the spacecraft coasted, with its pitch and yaw axes controlled to track the sun and with its roll axis held inertially fixed.

2. DSIF and Canopus Acquisition Phase

DSS 72 (Ascension) was the first DSIF tracking station to "see" the spacecraft, and it achieved one-way lock with the spacecraft at approximately L + 00:16:50. However, by prior mission operations planning, initial two-way acquisition was reserved for DSS 51 (Johannesburg).

Approximately 23 min after launch, the spacecraft became visible to DSS 51, and the initial DSIF acquisition procedure was initiated to establish the communication and tracking link between the spacecraft and the ground station. DSS 51 acquired one-way lock at L + 00:25:00 and, less than 10 min later, confirmed that two-way lock had been established with the spacecraft at L +00:32:58.

The first ground-controlled sequence ("Initial Spacecraft Operations") was initiated at L +00:45 (13:17 GMT) and consisted of commands for (1) turning off spacecraft equipment required only until DSIF acquisition, such as high-power transmitter and accelerometer amplifiers, (2) seating the solar panel and roll axis locking pins securely, (3) increasing the telemetry sampling rate to 1100 bit/sec, and (4) performing the initial interrogation of all telemetry commutator modes. All spacecraft responses to the commands were normal. As a result of assessment of the data, it was determined from the star intensity telemetry signal that an object (which was believed to be the earth) was in the field of view of the Canopus sensor. Therefore, it was recommended that the roll axis be held in the inertial mode and the *cruise mode* command (which would have caused the spacecraft roll attitude to be slaved to the position of the earth) not be sent to the spacecraft. It was also recommended that Transponder A not be turned on, since the Receiver A AFC indicated that this receiver was tracking the ground-station signal.

The spacecraft continued to coast normally, with its pitch-yaw attitude controlled to track the sun and with its roll axis held inertially fixed. Tracking and telemetry data was obtained by use of Transponder B and Transmitter B operating in low power. The spacecraft telemetry bit rate/mode profile for the complete mission is shown in Fig. IV-5.

Approximately four and one half hours after launch, control of the spacecraft was transferred to DSS 72 to provide additional tracking data for FPAC. The additional tracking data from DSS 72 was important in that it provided confirmation of the DSS 51 data and greater confidence in the premidcourse orbit determination. Transfer to DSS 72 necessitated a decrease in telemetry rate from 1100 bit/sec to 137.5 bit/sec owing to the lower antenna gain available at DSS 72. At approximately L + 05:13, control of the spacecraft was returned to DSS 51, and shortly thereafter the telemetry rate was increased to 1100 bit/sec.

At about L + 06:06, a spacecraft roll maneuver was initiated for making a star map and then acquiring the star Canopus in order to fix the roll attitude of the spacecraft to a precise position from which the midcourse maneuvers could be initiated. At the recommendation of SPAC, the maneuver was made with the spacecraft transmitting Mode 5 data* at 1100 bit/sec by means of Transmitter B high power via Omniantenna B with the transponder off. Two complete revolutions (one using Omniantenna B and one using Omniantenna A) were used to generate the star map. The earth, moon, and stars Shaula and Ras Alhague were identified on the map in addition to Canopus, which appeared after 240 degrees of roll. However, for reasons unknown at the time, the relative intensities of the stars were not as had been expected. (It was later determined that reflected earthlight caused the abnormal intensities.) As was the case in the *Surveyor I* mission, a Canopus lock-on signal was *not* generated as the star sensor swept past Canopus, because the Canopus intensity signal was above the upper threshold of the lock-on range. As the vehicle continued to roll, the time for sending the proper command to achieve manned lock-on to Canopus was computed. Manual lock-on was achieved successfully at approximately L +06:40. In this mode the spacecraft roll attitude is controlled so that the Canopus sensor remains locked on the star.

*See Section IV-A for data content of telemetry modes.

3. Premidcourse Coast Phase

About 15 min after Canopus lock-on, a gyro drift check was initiated by commanding the spacecraft to inertial mode. The vehicle continued to coast as before, but with its attitude held inertially so that the sun and star sensors continued to point at the sun and Canopus, respectively. At L + 09:03, the gyro drift check was terminated by commanding the return to Canopus lock-on.

DSS 51 lost visibility of the spacecraft at L + 09:46. A gap of about 40 min would have occurred in spacecraft visibility before spacecraft rise at DSS 11 owing to the geometry of the trajectory which resulted from the high value of launch azimuth (114.361 deg). In order to cover this period, a deviation was made in the Standard Sequence of Events, permitting transfer of control to DSS 72 and reduction of telemetry rate again to 17.2 bit/sec. After acquisition, DSS 72 had considerable difficulty in providing good data (SPAC estimated that 80% of the data was bad). After the spacecraft became visible to DSS 11 at L + 10:12, transfer was made to this station and the bit rate was commanded back to 1100 bit/sec.

The first of two premidcourse maneuver conferences was convened about 7 hours after launch to present to the project managers a preliminary set of maneuver alternatives and a comprehensive spacecraft status report. The maneuver alternatives are discussed in Section VII with summary data presented in Table VII-2. All subsystems

of the spacecraft were reported as performing well with two exceptions.

(1) The spacecraft Receiver B up-link sensitivity was found to be approximately 18 db lower than expected.

(2) During Canopus acquisition the star intensities did not agree with predicted values, causing intermittent lock-on of the star sensor and requiring, as with *Surveyor I*, the transmission of the *manual Canopus lock-on* command. Star positions did appear as predicted.

The SPAC director indicated that the spacecraft would be capable of supporting any maneuver choice selected from among the alternatives presented by FPAC.

The second premidcourse maneuver conference was held about 12 hours after launch. The Mission Director approved the following recommendations made by the SFOD and Project Scientist relative to the midcourse maneuver plan and target site selection, respectively:

(1) The maneuver to be a roll-yaw maneuver. Such a maneuver was favored over the possible pitch-yaw or yaw-pitch maneuvers because of reduced execution errors, and over the possible roll-pitch maneuver because of a somewhat better antenna profile and improved gain margins.

(2) Spacecraft transmission during the maneuver to be over Omniantenna B exclusively.

(3) Spacecraft transmission during the maneuvers to be in the one-way mode. (This recommendation was based on the as yet unresolved problem of reduced spacecraft Receiver B sensitivity. It was subsequently determined by means of an up-link sensitivity threshold test, described below, that the malfunction was caused by a telemetry anomaly, and the maneuvers were actually executed in the transponder mode.)

(4) Spacecraft transmission rate to be 4400 bit/sec throughout the maneuver sequence.

(5) The maneuver execution time to be at approximately launch plus 16½ hr (05:00 GMT, September 21), leaving open the possibility of a launch-plus-40-hr maneuver if the necessity should arise.

(6) The target site to be shifted slightly to 0.55 deg latitude, 359.17 deg longitude.

Final computation of midcourse parameters was conducted following approval of the above plan and target site selection. (Refer to Section VII for a discussion of the factors considered in selecting the midcourse correction magnitude and final aiming point.)

Because analysis of Receiver B AGC telemetry data obtained during star verification and acquisition indicated a signal strength which was approximately 18 db below the predicted value, a special test for performing an in-flight calibration of this data channel was recommended to determine whether the receiver had a malfunction or the telemetry calibration had shifted. This test was required to establish the feasibility of utilizing the transponder for two-way tracking during the midcourse correction, inasmuch as a degradation of 16 db in Receiver B sensitivity would be indicative of a receiver malfunction and would preclude such utilization. Following satisfactory completion of the scheduled premidcourse low-power engineering interrogation, the special calibration test was conducted. During this sequence, the DSS 11 transmitter power was reduced in 2-db steps until the command threshold level, as indicated by an indexing of the receiver-decoder-select unit, was reached. This occurred after a total reduction of 24 db at telemetry-indicated signal strengths of −133 dbm for Receiver B and −121 dbm for Receiver A. The conclusion reached was that the calibration of Receiver B had changed from the pre-mission data, and that the signal strength could be lowered by 24 db without causing a receiver index, and by 30 db without causing a loss of carrier signal in Receiver B. Therefore, it was recommended that the midcourse correction be done in two-way lock.

At approximately L +14:19, the scheduled premidcourse engineering interrogation was initiated. This sequence was executed using low-power transmitter operation since this mode permitted a data rate of 1100 bit/sec to be obtained. As part of this sequence, the gyro speeds were measured and were found to be exactly nominal at 50 cps.

4. Midcourse Maneuver Phase

The midcourse correction sequence was initiated at L + 15:42 with an engineering interrogation which indicated that the spacecraft was in satisfactory condition for the midcourse operations. This was followed by commands to turn on transmitter high power and increase the telemetry sampling rate from 1100 to 4400 bit/sec. Starting at L +16:12, the required roll-attitude (+75.4 deg) and yaw-attitude (+110.6 deg) maneuvers were executed satisfactorily, thereby aligning the spacecraft axes in the desired direction for applying the midcourse thrust. Next the spacecraft was prepared for midcourse

thrusting by sending commands to (1) turn on strain gages, (2) pressurize the vernier propulsion system, and (3) load the desired thrust time in the flight-control programmer magnitude register. Then, at L + 16:28:02, the command was sent to thrust the vernier engines for applying the midcourse velocity correction. Following this command, the strain gage of Vernier Engine 3 indicated that this engine was not thrusting properly, and the gyro error signals became saturated (pitch error negative, yaw error positive, and roll error negative). Based upon the previously commanded time increment, the vernier engines shut off after a thrust duration of 9.8 sec. However, a check of the DSIF receiver AGC recording in the SPAC area showed that the vehicle was rotating at a rate of approximately 1.22 rev/sec, with a secondary motion having a period of approximately 12 sec.

The spacecraft was in the inertial mode for the midcourse firing but, about 4 min after midcourse firing, it was commanded to the rate mode. The gas-jet system is active in both modes and was operating to reduce the spin rate. However, the rate mode was preferred under the existing conditions because in that mode the gyros are less likely to be damaged because of the tumbling motion, and angular rate data can be obtained more directly from telemetry.

Approximately 14 min after midcourse firing, when it became evident that the gas jets could not stop the spinning (approximately 60% of the gas had been used, and the spin rate was still 0.97 rev/sec), the gas jets were inhibited to conserve the remaining gas supply.

A 2-sec firing was recommended to attempt to clear the Vernier Engine 3 problem and determine if the spacecraft could be stabilized by firing the vernier engines. This sequence, using the midcourse thrust level, was attempted at L +18:56 and again at L +19:18 without success.

5. Post-Midcourse Phase

Since the spacecraft was rotating such that solar panel output was zero, the only sources of electrical power for spacecraft loads were the main and auxiliary batteries. In an attempt to conserve energy, a sequence was initiated in which the flight control coast phase power was cycled on and off periodically. Power was left on for approximately 40 min, then off for approximately 90 min, the cycle being based on the gyro and electronic temperatures of the flight control system having reached limits of +70°F and 0°F, respectively.

An interrogation of Modes 2 and 4 at hourly intervals was also initiated. In addition, the auxiliary battery mode was commanded on when the auxiliary battery temperature dropped to +35°F to utilize the energy of this battery and to keep it above its lower operational limit.

At L + 28:40, a special post-midcourse conference was convened by the Mission Operations System Manager to consider current spacecraft and trajectory status and to formulate specific plans directed towards attainment of the primary mission objectives. The FPAC director first reported that the spacecraft unbraked target coordinates were computed to be approximately 7 deg latitude, 353 deg longitude. It was also stated that good two-way doppler tracking data was received during the abortive maneuver attempt and throughout the period following it. Ground receiver lock had not been lost during the unbalanced thrusting of the spacecraft. The SPAC Director then reported the following major spacecraft status items:

(1) Present spacecraft tumbling rate was approximately 0.95 rev/sec with the flight control system in the rate mode. All gyros were saturated.

(2) Cold gas jets were inhibited and nitrogen gas remaining was 2.16 lb, about 50% of normal.

(3) The spacecraft was operating in the phase-lock mode over Omniantenna/Receiver B and transmitting in the low-power mode at a telemetry rate of 137.5 bit/sec.

(4) The spacecraft was operating in the auxiliary battery mode and flight control power was on. Estimated battery life remaining was approximately 25 hr at L + 27:54.

(5) Spacecraft temperatures were within acceptable limits with the following exceptions:

  (a) Compartment B was out of the sun and was showing a constant loss of heat through the radiator.

  (b) The lower part of the spacecraft was absorbing considerable amounts of energy as manifested by much higher than normal temperatures of the AMR nozzle (+150°F vs −190°F) and retro attach points (+140°F vs −120°F for Attach Point 2).

  (c) The RADVS temperature was abnormally low and out of tolerance.

  (d) All shock absorber temperatures were low (No. 2 was at −15°F, and Nos. 1 and 3 were at −30°F).

After presentation, by HAC, of a detailed analysis of the Vernier Engine 3 anomaly, the Mission Director placed highest priority on attempts to restore the vernier engine system to normal operation and assigned Mission Operations system personnel with the task of detailed design and execution of a vernier engine remedial command sequence.

The sequence which was prepared provided for pulse-firing the engine five times (0.2-sec duration per firing, 5-min intervals between firings), followed by firing of engines for a 2-sec period. This sequence was initiated at approximately L + 31:12 with the result that there appeared to be no firing of Engine 3.

At L + 35:15, a final post-midcourse conference was convened by the Mission Operations System Manager to present a general plan for the further conduct of the mission. This plan had been formulated by the Mission Operations System Manager and SFOD and was concurred in by the Mission Director. Primary elements of the general plan were as follows:

(1) Because of continued spacecraft abnormal behavior, DSS 42 and 51 were to assume the mission control function during their respective visibility periods. The level of mission control organization staffing at the SFOF was to be reduced during these periods commensurate with the shift in responsibility.

(2) A vernier engine thrust sequence consisting of five short thrusts, 0.2 sec duration and 5 min apart, followed by a 2-sec thrust, was to be executed in 1-hr intervals until the spacecraft either recovered or failed entirely.

(3) If, upon evaluation of telemetry data at the remote DSIF stations, it was determined that all three vernier engines had ignited as a result of command sequence execution, the Mission Director, Mission Operations System Manager, SFOD, and Technical Analysis Area Directors were to be notified immediately to assume full control from the SFOF as soon as possible.

(4) Under such circumstances, the spacecraft would be stabilized as soon as possible and normal spacecraft transit orientation would be accomplished. Spacecraft power would be conserved to the extent feasible. Providing there was sufficient time for a trajectory correction before the spacecraft reached the moon, another maneuver would be prepared and executed. Detailed maneuver requirements would be established, depending on the circumstances existing at the time.

Using this plan, four additional attempts to achieve Vernier Engine 3 thrusting were made, beginning at L+36:28, but all proved to be ineffective. Between the second and third vernier engine firings, two attempts were made to command the deployment of the planar array upward from its launch position so that the solar panel would be lowered to a position where some illumination of the solar panel would occur. Solar panel illumination was desirable for two reasons:

(1) To obtain energy for the spacecraft.

(2) To achieve illumination of one or more of the secondary sun sensor cells, which are mounted on the face of the solar panel, so that the actual orientation of the spacecraft could be established. The two attempts to move the planar array were unsuccessful, apparently because of the opposing force created by the spacecraft rotation.

Following these unsuccessful attempts, the Project Management replaced the above plan with one designed to achieve a higher thrust level with less rise time by placing the flight control system in the post-retro-eject condition. The objective was to be accomplished by commanding *retro sequence mode* on and *emergency retro eject* prior to turning on the flight control thrust power. This would prevent the ejection of the main retro engine while placing the flight control programmer in the desired state. The sequence was completed at L+41:11 with the commanding of a vernier engine firing of about 2.5-sec duration. Engine ignition and shutoff were both effected by ground command. Again the results were negative. With each attempt to fire the engines, the rotation rate of the spacecraft continued to increase so that, at completion of the post-retro-eject thrusting, the spin rate was approximately 1.54 rev/sec as determined from the DSS AGC variation.

After the failure of these attempts to salvage the mission, a final four-part plan was implemented. The necessary sequences were prepared in order to:

(1) Attempt to step the solar panel in an effort to illuminate its active face and the secondary sun sensor cells.

(2) Dump the helium to obtain a curve of pressure decay as a function of time in order to determine whether a zero-shift had occurred in the helium pressure telemetry signal.

(3) Perform an evaluation of the capability of the main battery to continue to supply power reliably under the heavy terminal descent load conditions (flight control thrust phase power on, high-power transmitter on, RADVS on, etc.) when the remaining battery energy is on the order of only 15 to 30 amp-hr.

(4) Fire the main retro motor in the normal terminal descent mode.

At $L+42:22$, a squib was "blown" by ground command to unlock the solar panel. The solar-panel position telemetry signal showed a change of approximately 23 deg, indicating that the force on the panel created by the spacecraft spin had caused the panel to move. Further attempts to step the panel were unsuccessful.

Beginning at $L+43:13$, a sequence was executed for pulse-firing the engine 5 times (0.2 sec for each firing, with 1 min between firings) followed by a 20-sec firing in the post-retro-eject mode. Although the temperature of Vernier Engine 3 rose approximately 24°F during the 20-sec firing compared to about 100°F for Engines 1 and 2, the strain gage on Engine 3 indicated no thrust.

The helium dumping sequence was initiated at $L+44:41$, and appeared to confirm that a zero-shift in the helium pressure telemetry had occurred. The observed zero-shift would account for the relatively large decrease in pressure which was noted when the system was pressurized prior to execution of midcourse thrusting.

Flight control thrust phase power and RADVS were turned on at $L+44:47$ when the energy remaining in the main battery was estimated to be 10 amp-hr. The bus voltage dropped from 19.4 to 17.3 v when this load of 47 amps was placed on the battery. The RADVS was then turned off at the direction of the acting SFOD. At this time, the spacecraft spin rate was approximately 2.3 rev/sec. A profile of the spacecraft spin rate following attempted midcourse correction is presented in Fig. IV-11.

The Emergency AMR signal was sent to the spacecraft to initiate the retro engine firing sequence at $L+45:02:17$ (09:34 GMT, September 22, 1966). Ignition of Vernier Engines 1 and 2 as well as the main retro motor was verified. Approximately 30 sec after the retro motor ignited, contact with the spacecraft was lost, terminating the *Surveyor II* Mission.

VII. Flight Path and Events

For *Surveyor II*, the landing site selected prior to launch for targeting of the launch vehicle ascent trajectory was near the center of the Apollo zone of interest at 0.0 deg latitude, 359.33 longitude (0.67 deg west longitude). The following factors influenced the selection of this site: predicted terrain smoothness, desire to land within the Apollo zone, off-vertical approach angle of near 25 deg, and good post-landing lighting. An unbraked impact speed was selected so that the Goldstone arrival visibility constraints would be satisfied for all launch days in the launch period.

A. Launch Phase

The *Surveyor II* spacecraft was launched from AFETR launch site 36A at Cape Kennedy, Florida, on Tuesday, September 20, 1966. The launch was held until almost the close of the launch window owing to difficulties experienced with the *Atlas* (see Section II). Liftoff occurred at 12:31:59.824 GMT. At 2 sec after liftoff, the *Atlas/Centaur* launch vehicle began a 13-sec programmed roll that oriented the vehicle from a pad-aligned azimuth of 105 deg to a launch azimuth of 114.361 deg. At 15 sec, a programmed pitch maneuver was initiated. All event times for the launch phase were nominal or within the 3-σ tolerance. The launch phase sequence is discussed in greater detail in Section III. Nominal and actual event times for all phases of the mission are summarized in Table A-1 of Appendix A.

B. Cruise Phase

Separation of *Surveyor* from the *Centaur* occurred at 12:44:32.4 GMT on September 20, 1966, at a geocentric latitude and longitude of 12.9 and 309.8 deg, respectively. The spacecraft was in the sunlight at separation and never entered the earth's shadow during the transit trajectory.

The Johannesburg station (DSS 51) reported good one-way data at 12:55:17, only seconds after predicted rise over the station horizon mask. Good two-way data was reported by DSS 51 at 13:05:07. The DSIF stations provided continuous tracking data coverage from this initial acquisition until loss of signal occurred at approximately 09:35 GMT on September 22, 1966. The station tracking periods are presented in Fig. V-7.

The nominal earth-moon transfer trajectory and events are shown in Fig. VII-1. A plot of the actual *Surveyor II* trajectory projected on the earth's equatorial plane is provided in Fig. VII-2. The earth track traced by *Surveyor II* appears in Fig. VII-3. Specific events such as sun and Canopus acquisition and rise and set times for the DSIF stations are also noted.

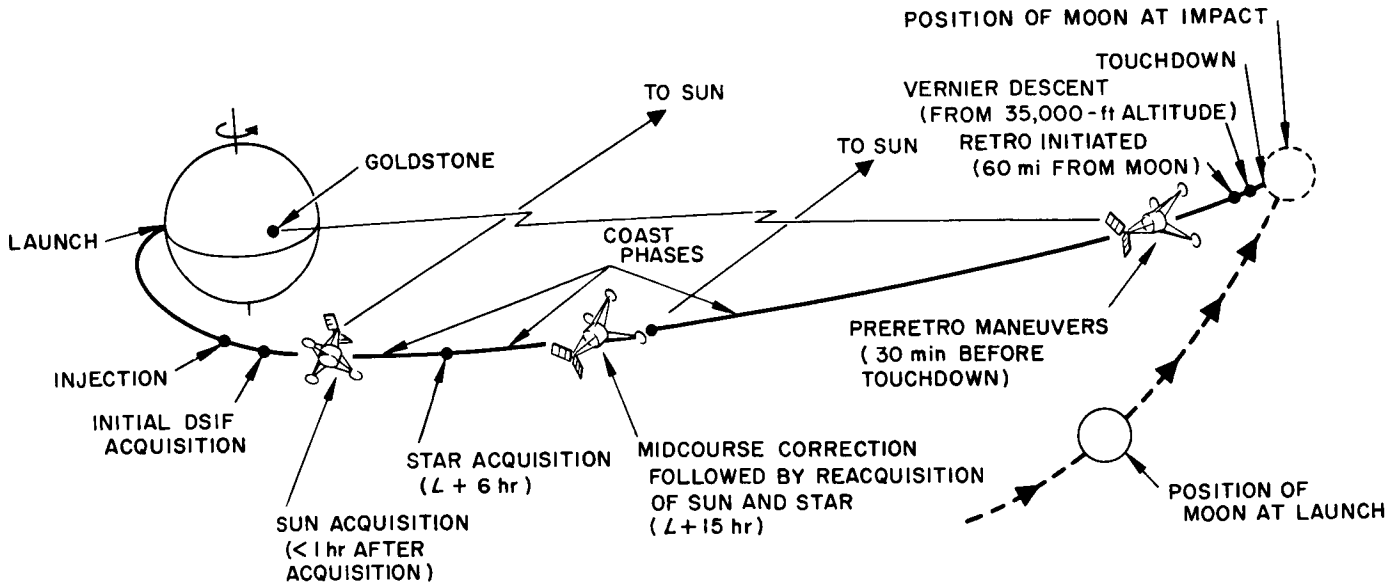

Fig. VII-1. Earth-moon trajectory and nominal events

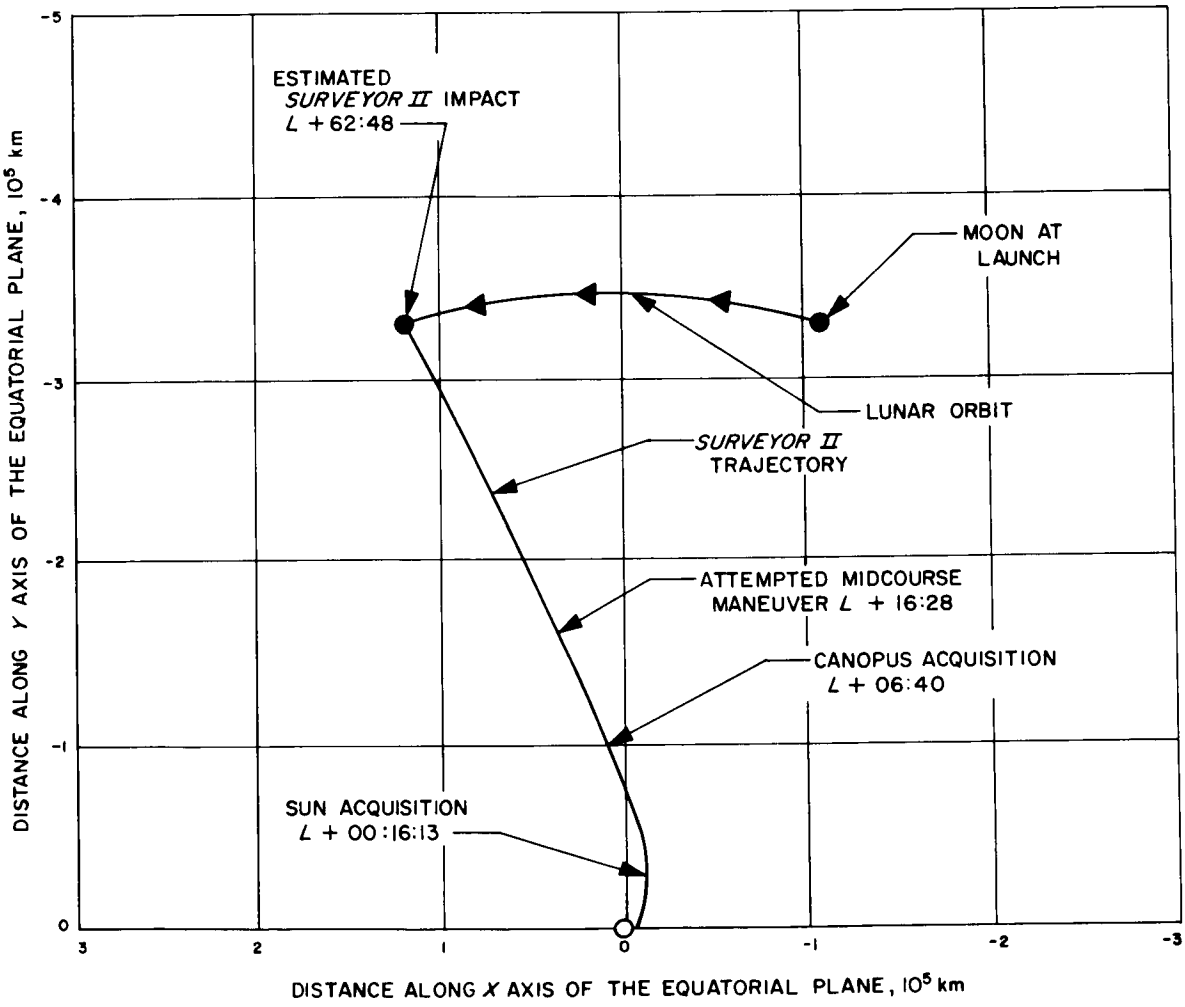

Fig. VII-2. *Surveyor II* trajectory in earth's equatorial plane

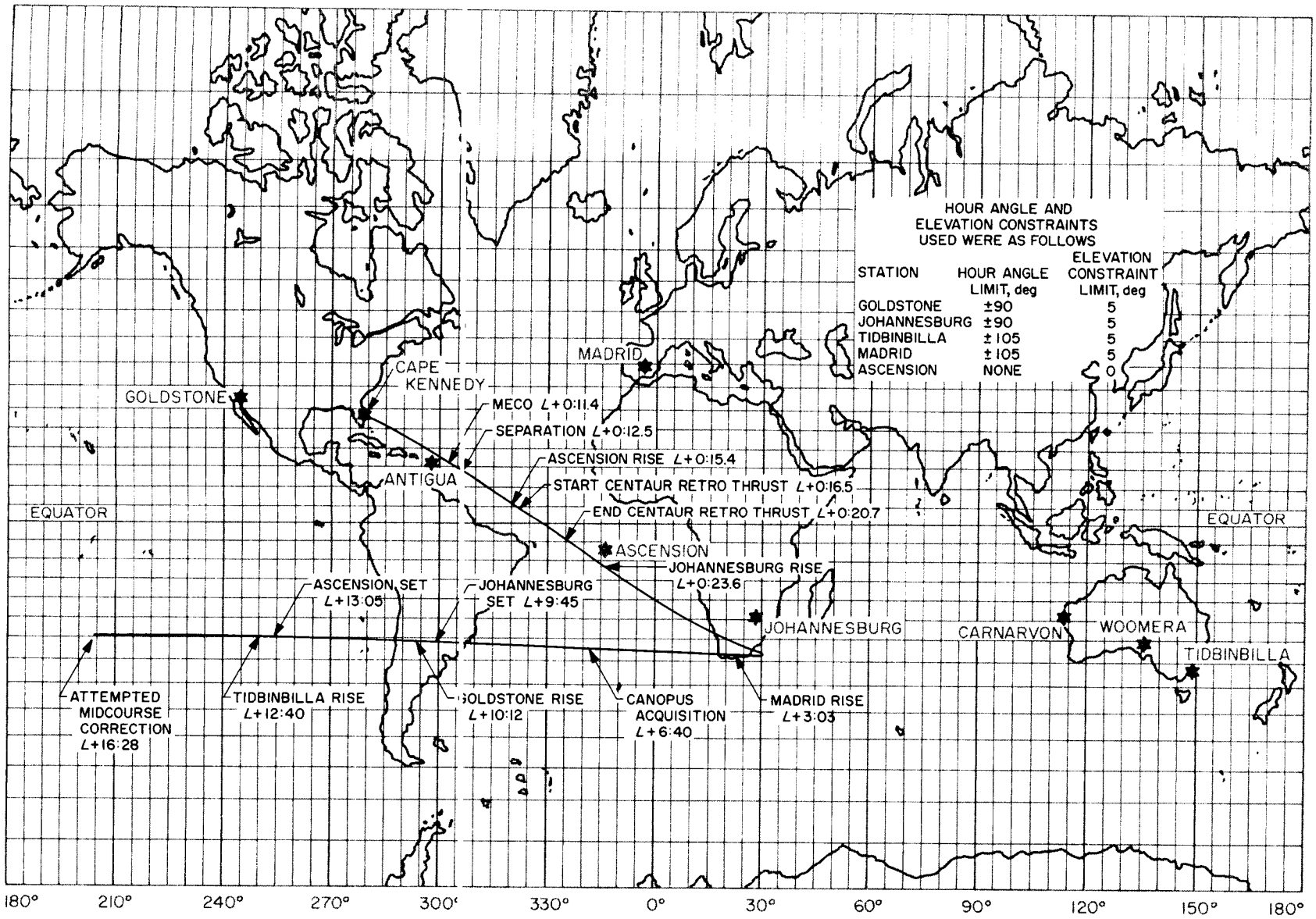

Fig. VII-3. *Surveyor II* earth track

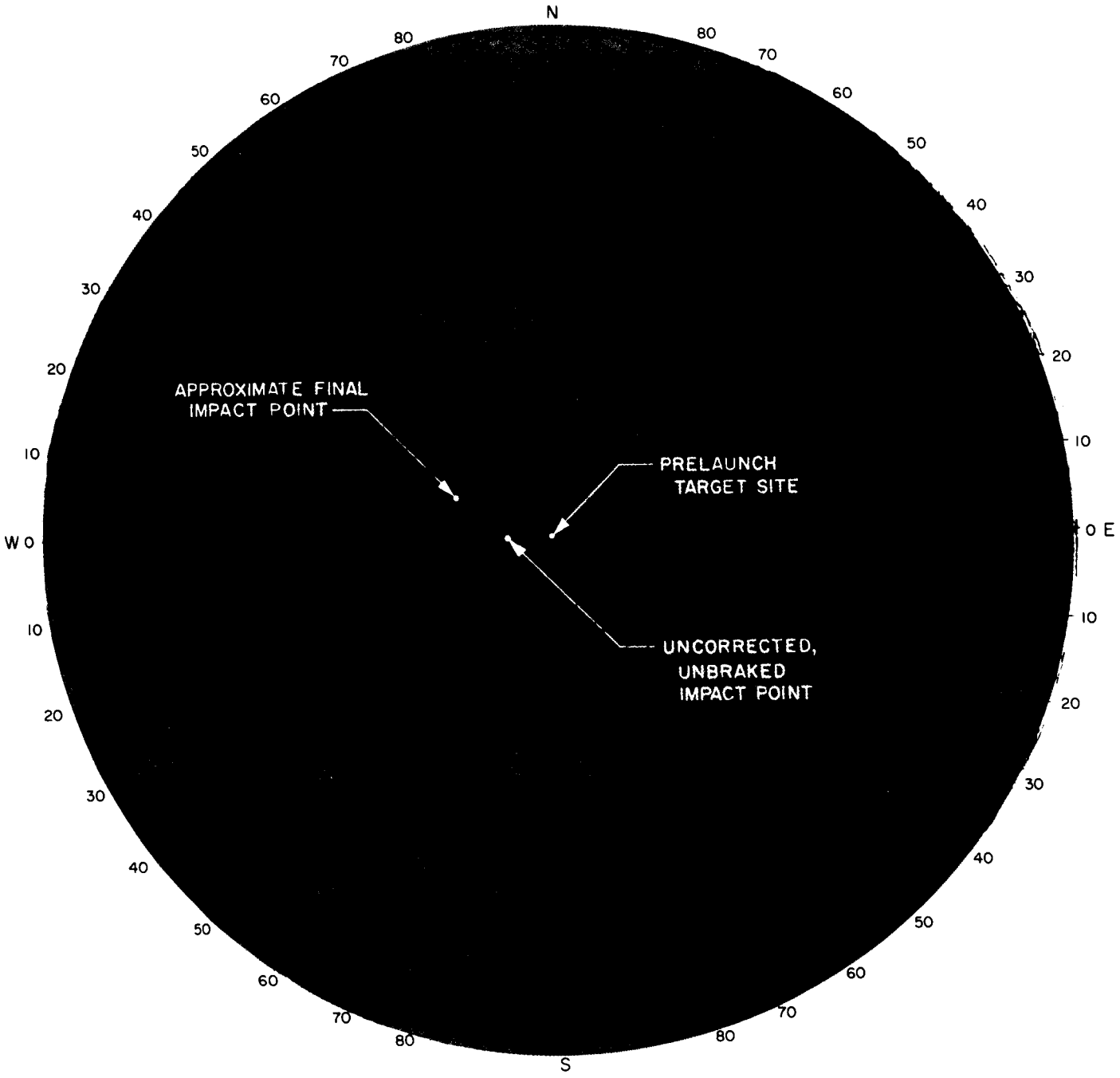

Fig. VII-4. *Surveyor II* target, uncorrected impact, and final impact points

The proximity of the uncorrected, unbraked impact point (−0.0837 deg latitude, 354.658 deg longitude) and the original aiming point (0.0 deg latitude, 359.33 deg longitude) is shown in Fig. VII-4. The uncorrected, unbraked impact point is located on the western edge of Sinus Medii just northeast of the crater Mösting. The two points are approximately 142 km (88 mi) apart on the surface of the moon. Also shown in Fig. VII-4 is the approximate final impact site of the spacecraft.

C. Midcourse Maneuver Phase

The original aim point was selected assuming the 99% landing dispersions to be a 50-km-radius circle on the lunar surface. However, primarily because of the small midcourse correction which was determined to be required, the 99% dispersion computed in-flight was found to be an ellipse when mapped on the moon's surface with a semimajor axis of 53.9 km and a semiminor axis of 17.17 km. Because of this smaller dispersion and based upon a detailed examination of *Lunar Orbiter I* photographs, it was decided to bias the aiming point a little to the north northwest to maximize the probability of soft landing. The enlarged area of the moon shown in Fig. VII-5 illustrates the initial aim point, the final aim point, the 99% dispersion associated with premidcourse tracking and execution errors, and the approximate final impact site. The latitude and longitude for these locations as well as for the uncorrected impact point are given below:

	Longitude, deg	Latitude, deg
Original aim point	0.0	359.33
Uncorrected impact point		
Computed in-flight	−0.0837	354.658
Computed post-flight	−0.0519	354.710
Final aim point	0.55	359.17
Final impact point (approx)	4.0	349.0

Table VII-1 presents the injection and uncorrected encounter conditions. These are the results of the final post-flight calculations.

Table VII-1. Injection and uncorrected encounter conditions

Coordinate system	Injection conditions September 20, 1966, 12:43:13.670 GMT					
Inertial cartesian	X = −4360.9041 km	Y = 4616.8513 km	Z = 1896.4001 km	DX = −8.7282187 km/sec	DY = −4.5253066 km/sec	DZ = −4.7559824 km/sec
Inertial spherical	RAD = 6627.9056 km	DEC = 16.626021 deg	RA = 133.36699 deg	VI = 10.921519 km/sec	PTI = 6.4654237 deg	AZI = 119.42063 deg
Earth-fixed spherical	RAD = 6627.9056 km	LAT = 16.626021 deg	LON = 303.60264 deg	VE = 10.523257 km/sec	PTE = 6.7112166 deg	AZE = 120.66787 deg
Orbital elements	C3 = −1.0001392 km²/sec²	ECC = 0.98358240	INC = 33.423575 deg	TA = 13.039233 deg	LAN = 340.26840 deg	APF = 135.66564 deg
	Uncorrected encounter conditions September 23, 1966, 03:19:54.426 GMT					
Selenocentric	RAD = 1738.5 km	LAT = −.051930781 deg	LON = 354.70985 deg	VP = 2.6614642 km/sec	PTP = −69.779146 deg	AZP = 90.222833 deg
Miss parameter earth equator	BTQ = 1321.7977 km	BRQ = −1793.8803 km	B = 1333.9151 km			
Miss parameter moon equator	BTT = 1333.9064 km	BRT = 5.1242575 km	B = 1333.9162 km			

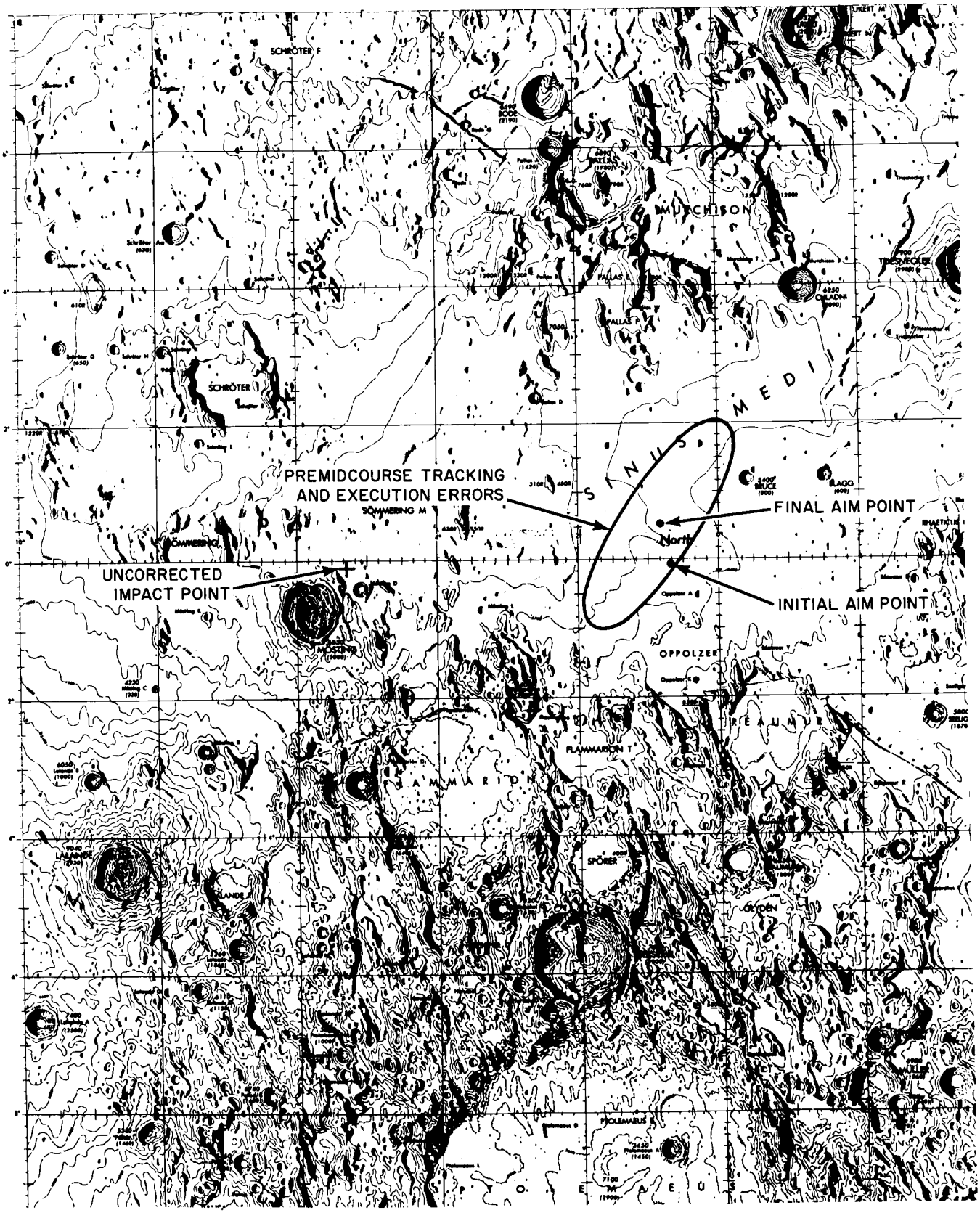

Fig. VII-5. *Surveyor II* impact locations

The maximum midcourse correction capability is shown in Fig. VII-6 for three values of unbraked impact speed, V_{imp}. Also shown are the expected 3σ *Centaur* injection guidance dispersions, the effective lunar radius, and the maximum maneuver which could have been executed if thrusting had been terminated automatically by a spacecraft timer signal. The midcourse capability contours are in the conventional R-S-T coordinate system.*

*Kizner, W. A., *A Method of Describing Miss Distances for Lunar and Interplanetary Trajectories*, External Publication 674, Jet Propulsion Laboratory, Pasadena, August 1, 1959.

A midcourse correction of 9.587 m/sec was selected for execution by the spacecraft. The velocity component in the critical plane, to correct "miss only," was 1.185 m/sec. This component is referred to as the critical component. The velocity component normal to the critical component is referred to as the noncritical component since it does not affect the miss to first order. Figure VII-7 presents the variations in flight time, main retro burnout velocity, and vernier propellant margin with the noncritical velocity component $\dot{U}_3$. The propellant margin and flight time were acceptable within the limits shown. However, it was desirable to (1) provide backup midcourse correction

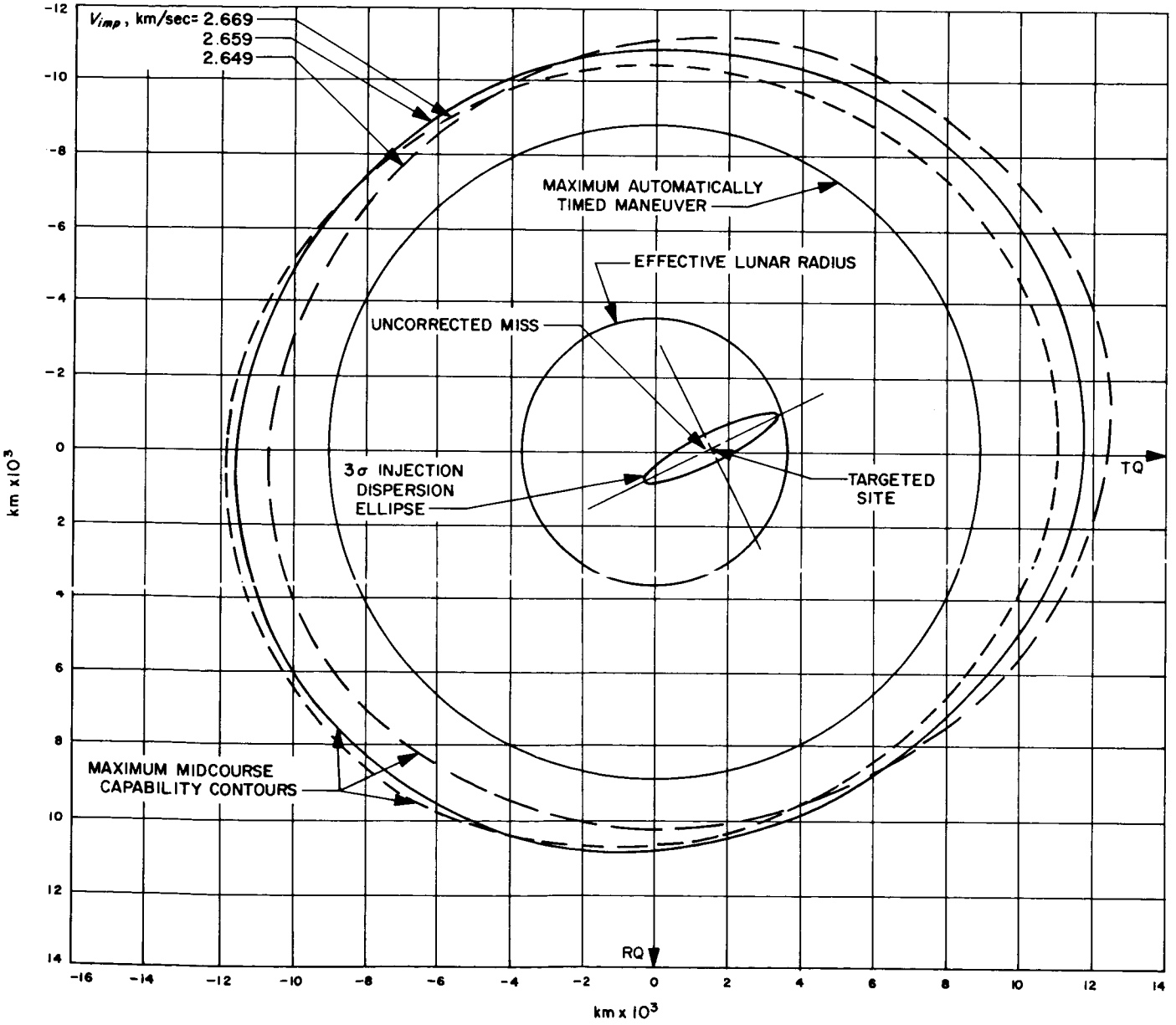

Fig. VII-6. Midcourse capability contours for September 20 launch

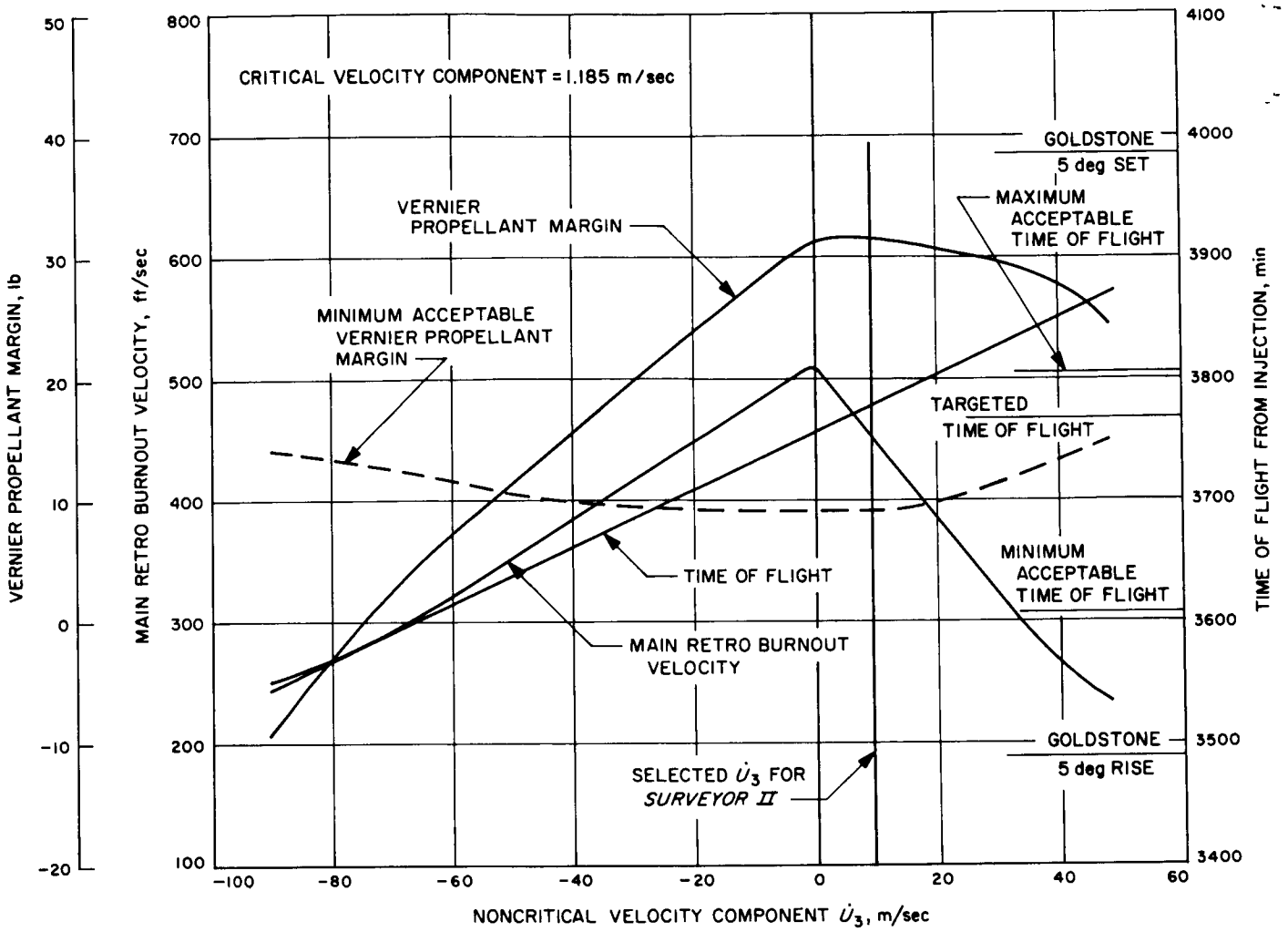

Fig. VII-7. Effect of noncritical velocity component on terminal descent parameters

capability in the event the first midcourse correction was unsatisfactory, (2) not exceed a main retro burnout velocity of 450 ft/sec for flight control stability considerations, and (3) keep the midcourse maneuver small in order to reduce the execution errors, which are proportional to the magnitude. Consideration of these factors led to the selection of a value of 9.5 m/sec for the noncritical component. The predicted results of the selected midcourse correction and alternatives considered are given in Table VII-2.

If the maneuver strategy had been simply to correct miss and flight time to the new aim point, the required noncritical component would have been 4.325 m/sec, giving a total correction of approximately 4.48 m/sec. However, to properly evaluate the performance of the *Centaur* guidance system, the original aiming point must be used in computing the correction, in which case the "miss only" correction is 1.015 m/sec and the "miss-plus-flight-time" correction is 4.44 m/sec.

Execution of the midcourse correction was initiated at 05:00 GMT on September 21, 1966. Owing to failure of Vernier Engine 3 to produce thrust during the midcourse maneuver, a major, nonstandard flight condition developed wherein the spacecraft entered a tumbling mode.

D. Post-Midcourse and Mission Termination

The nonstandard condition which resulted from the attempted midcourse correction precluded a normal soft landing since the tumbling rate was too great to be overcome with the attitude control gas-jet system, and repeated attempts to resolve the vernier system anomaly by commanding short thrust bursts were unsuccessful.

Table VII-2. Midcourse maneuver alternatives

	Selected midcourse	Alternate considerations				
	Execution time from launch, hr					
	16.5	No midcourse	14.5	14.5	14.5	38.8	38.8
Critical component, m/sec	1.18		0.51	0.51	0.51	1.0	2.24
Noncritical component, m/sec	9.50		2.0	15.0	−33.4	1.7	17.0
Total correction, m/sec	9.59		2.1	15.0	33.4	2.0	17.2
Propellant required, lb	7.96		1.6	12.0	26.4	1.6	14.26
Unbraked impact velocity, km/sec	2.658	2.663	2.662	2.654	2.681	2.662	2.656
Main retro burnout velocity, ft/sec	450	515	505	400	400	505	408
Vernier propellant margin, lb	30.5	31	31	31	33.4	31	30.0
Arrival time 9/23/66, GMT	03:42	03:20	03:25	03:57	03:42	03:22	03:38
Visibility							
Time before landing	04:41	04:19	04:24	04:56	04:41	04:21	04:37
Time after landing	03:25	03:47	03:42	03:10	03:25	03:45	03:29
Landing errors (3σ)							
Semimajor axis, km	53.9	20	20	33.5	63	5.5	16.3
Semiminor axis, km	17.7	5	5	27	55	3.7	15.6
Orientation angle, deg	−57	−56	−56	−55	−60	−46	−52

The spacecraft batteries could not provide sufficient power for the full duration of the transit phase since the spacecraft was unable to obtain solar power in the unstable mode. Before power failure would have occurred, a final command to ignite the retrorocket was transmitted to the spacecraft at 09:34 GMT, September 22, 1966. Mission termination resulted about 30 sec later with loss of spacecraft signal. The best estimate of the impact location of the *Surveyor II* spacecraft is 4 deg latitude, 349 deg longitude.

Appendix A

Surveyor II Flight Events

Table A-1. Mission flight events

Event	Mark No.	Mission time (predicted)[a]	Mission time (actual)	GMT (actual)
Liftoff to DSIF acquisition				
				(September 20, 1966)
Liftoff (2-in. rise)		L + 00:00:00.00	L + 00:00:00.00	12:31:59.824
Initiate roll program		L + 00:00:02		
Terminate roll, initiate pitch program		L + 00:00:15		
Mach 1			L + 00:00:58	12:32:58
Max. aerodynamic loading			L + 00:01:15.7	12:33:15.5
Booster engine cutoff (BECO)	1	L + 00:02:22.72	L + 00:02:22.2	12:34:22.0
Jettison booster package	2	L + 00:02:25.82	L + 00:02:25.3	12:34:25.1
Admit guidance steering		L + 00:02:31		
Jettison *Centaur* insulation panels	3		L + 00:02:56.0	12:34:55.8
Jettison nose fairing	4		L + 00:03:22.9	12:35:22.7
Start *Centaur* boost pumps		L + 00:03:36		
Sustainer engine cutoff (SECO)	5	L + 00:03:55.35	L + 00:03:55.1	12:35:54.9
Atlas/Centaur separation	6		L + 00:03:57.0	12:35:56.8
Centaur main engine ignition (MEIG)	7	L + 00:04:06.85	L + 00:04:06.6	12:36:06.4
Centaur main engine cutoff (MECO)	8	L + 00:11:23.44	L + 00:11:26.3	12:43:26.1
Vehicle destruct system safed by ground command			L + 00:11:36.2	12:43:36.0
Extend *Surveyor* landing legs command	9	L + 00:11:50.85	L + 00:11:51	12:43.51
Extend *Surveyor* antennas command	10	L + 00:12:01.35	L + 00:12:01	12:44:01
Surveyor transmitter high power on command	11	L +00:12:21.85	L + 00:12:21	12:44:21
Surveyor/Centaur electrical disconnect	12	L + 00:12:27.30	L + 00:12:27	12:44:27
Surveyor/Centaur separation	13	L + 00:12:32.85	L + 00:12:32.6	12:44:32.4
Solar panel unlocked and start stepping			L + 00:12:34	12:44:34
Start *Centaur* 180 deg turn	14	L + 00:12:37.85	L + 00:12:38	12:44:37
Start *Centaur* lateral thrust	15	L + 00:13:17.85	L + 00:13:18	12:45:17
Start sun acquisition roll			L + 00:13:18	12:45:18
Cutoff *Centaur* lateral thrust	16	L + 00:13:37.85	L + 00:13:38	12:45:37
Primary sun sensor lock-on			L + 00:16:13	12:48:13
Start *Centaur* retro (blowdown tanks)	17	L + 00:16:32.85	L + 00:16:33	12:48:32
Solar axis locked; start roll axis stepping			L + 00:18:34	12:50:34
Cutoff *Centaur* retro and power off	18, 19	L + 00:20:42.85	L + 00:20:43	12:52:42
Roll axis locked in transit position			L + 00:22:46	12:54:46
Initial DSIF acquisition (two-way lock) completed			L + 00:32:58	13:04:58
DSIF acquisition to star acquisition				
Initial commanded spacecraft operations				
1. Command transmitter from high to low power			L + 00:44:33	13:16:33
2. Command off accelerometer amplifiers, solar panel deployment logic, and strain gage power			L + 00:46:45	13:18:45
3. Command rock solar panel back and forth to seat locking pin			L + 00:48:16	13:20:16
4. Command rock roll axis back and forth to seat locking pin			L + 00:49:44	13:21:44

[a] The predicted values were computed postflight utilizing actual launch azimuth, tanked propellant weights, and atmospheric data which depend on day and time of liftoff.

Table A-1 (contd)

Event	Mission time (actual)	GMT (actual)
DSIF acquisition to star acquisition (contd)		
		(September 20, 1966)
5. Perform engineering interrogation at 1100 bit/sec	L + 00:54:19 to L + 01:07:24	13:26:19 to 13:39:24
6. Command transfer to Transmitter A low pwr	L + 01:09:19	13:41:19
Command telemetry rate reduction from 1100 to 137.5 bit/sec	L + 04:06:38	16:38:38
Star verification/acquisition		
1. 1100-bit/sec engineering interrogation over Transmitter A	L + 05:29:26 to L + 05:52:35	18:01.26 to 18:24:35
2. Command Transmitter B high power turn on prior to star verification	L + 05:56:59	18:28:59
3. Command transponder power off and flight control preparation	L + 06:01:01	18:33:01
4. Command execution of positive roll	L + 06:05:34	18:37:34
5. Command transfer to Omniantenna A during roll	L + 06:22:45	18:54:45
6. Command return to Omniantenna B during roll	L + 06:34:37	19:06:37
7. Manual (commanded) star lock achieved	L + 06:39:57	19:11:57
8. Command transponder power on and return to low-power operation	L + 06:42:21	19:14:21
Premidcourse coast phase		
Command gyro drift check	L + 06:54:24 to L + 09:03:22	19:26:24 to 21:35:22
Command telemetry rate reduction from 1100 to 17.2 bit/sec	L + 09:11:54	21:47:54
Command return to 1100 bit/sec	L + 10:35:54	23:11:54
Low-power engineering interrogation at 1100 bit/sec	L + 11:04:31 to L + 11:11:46	23:40:31 to 23:47:46
		(September 21, 1966)
Low-power engineering interrogation at 1100 bit/sec	L + 14:18:44 to L + 14:29:41	02:54:44 to 03:05:41
Command gyro speed check	L + 14:35:43 to L + 14:41:18	03:07:43 to 03:13:18
Midcourse correction		
Midcourse correction sequence		
1. Low-power engineering interrogation at 1100 bit/sec	L + 15:42:00 to L + 15:46:10	04:14:00 to 04:18:10
2. Command transmitter high-power on	L + 16:04:43	04:36:43
3. Command increase telemetry rate from 1100 to 4400 bit/sec	L + 16:05:36	04:37:36
4. Command roll maneuver magnitude and direction (positive roll of 75.4 deg)	L + 16:09:16	04:41:16
5. Command roll execution	L + 16:12:00	04:44:00
6. Command yaw maneuver magnitude (positive yaw of 110.6 deg)	L + 16:15:16	04:47:16
7. Command yaw execution	L + 16:16:05	04:48:05

Table A-1 (contd)

Event	Mission time (actual)	GMT (actual)
Midcourse correction (contd)		
		(September 21, 1966)
8. Command propulsion strain gage power on	L + 16:20:22	04:52:22
9. Command pressurization of vernier system (helium) and unlock Engine 1 to permit roll control	L + 16:21:38	04:53:38
10. Command thrust phase power on	L + 16:22:20	04:54:20
11. Command desired thrust duration (9.8 sec)	L + 16:22:47	04:54:47
12. Command midcourse thrust execution	L + 16:28:02	05:00:02
13. Turn off thrust phase power	L + 16:28:41	05:00:41
14. Command off power for propulsion strain gage auxiliary acceleration amplifiers, and touchdown strain gages	L + 16:28:53	05:00:53
15. Command return to 1100 bit/sec	L + 16:28:55	05:00:55
Nonstandard post-midcourse phase		
		(September 21, 1966)
Command flight control rate mode on	L + 16:31:48	05:03:48
Command gas jet system off	L + 16:42:29	05:14:29
Command telemetry rate reduction from 1100 to 550 bit/sec	L + 16:47:23	05:19:23
Command transmitter high-power off	L + 16:51:02	05:23:02
Command telemetry rate reduction from 550 to 137.5 bit/sec	L + 16:57:20	05:29:20
Low-power engineering interrogation at 137.5 bit/sec	L + 16:59:46 to L + 17:16:43	05:31:46 to 05:48:43
Postmidcourse vernier Firings 1 and 2		
1. Command transmitter high-power on	L + 18:46:28	07:18:28
2. Command telemetry rate increase from 137.5 to 1100 bit/sec	L + 18:49:08	07:21:08
3. Command postmidcourse vernier Firing 1 (1.975-sec duration)	L + 18:56:25	07:28:25
4. Command telemetry rate reduction from 1100 to 550 to 137.5 bit/sec	L + 18:57:53	07:29:53
5. Command transmitter high-power off	L + 19:02:47	07:34:47
6. Command transmitter high-power on	L + 19:14:36	07:46:36
7. Command telemetry rate increase from 137.5 to 1100 bit/sec	L + 19:15:31	07:47:31
8. Command post-midcourse vernier Firing 2 (1.975-sec duration)	L + 19:18:03	07:50:03
9. Command telemetry rate reduction from 1100 to 550 to 137.5 bit/sec	L + 19:19:00	07:51:00
10. Command transmitter high-power off	L + 19:26:16	07:58:16
Command flight control power off	L + 21:47:43	10:19:43
Low-power engineering interrogation initiated at 137.5 bit/sec	L + 21:49:05	10:21:05
Command auxiliary battery mode on	L + 23:09:09	11:41:09
Low-power engineering interrogation initiated at 137.5 bit/sec	L + 23:09:34	11:41:34
Command flight control power on	L + 23:33:57	12:05:57
Command transfer to Omniantenna A followed by return to Omniantenna B	L + 23:40:12	12:12:12
Low-power engineering interrogation initiated at 137.5 bit/sec	L + 24:50:14	13:22:14
Command flight control power off	L + 25:15:16	13:47:16
Command flight control power on	L + 26:37:24	15:09:24
High-power engineering interrogation at 1100 bit/sec	L + 26:58:48 to L + 27:16:51	15:30:48 to 15:48:51

Table A-1 (contd)

Event	Mission time (actual)	GMT (actual)
Nonstandard post-midcourse phase (contd)		
		(September 21, 1966)
Command flight control power off for 24-min period	L + 28:56:08	17:28:08
Post-midcourse vernier Firings 3 through 8		
1. Command post-midcourse vernier Firing 3 (0.225-sec duration)	L + 31:12:59	19:44:59
2. Command post-midcourse vernier Firing 4 (0.225-sec duration)	L + 31:35:05	20:07:05
3. Command post-midcourse vernier Firing 5 (0.225-sec duration)	L + 32:03:20	20:35:20
4. Command post-midcourse vernier Firing 6 (0.225-sec duration)	L + 32:23:06	20:55:06
5. Command post-midcourse vernier Firing 7 (0.225-sec duration)	L + 32:43:12	21:15:12
6. Command return to main battery mode	L + 32:55:44	21:27:44
7. Command transmitter high-power on	L + 34:48:02	23:20:02
8. Command telemetry rate increase to 4400 bit/sec	L + 34:50:35	23:22:35
9. Command telemetry rate decrease to 1100 bit/sec	L + 34:56:08	23:28:08
10. Command postmidcourse vernier Firing 8 (1.975-sec duration)	L + 35:01:23	23:33:23
11. High-power engineering interrogation of Modes 4 and 5 initiated	L + 35:02:33	23:34:33
12. Command telemetry rate reduction from 1100 to 137.5 bit/sec	L + 35:08:42	23:40:42
13. Command transmitter high-power off	L + 35:11:31	23:43:31
Post-midcourse vernier Firings 9 through 14		(September 22, 1966)
1. Command postmidcourse vernier Firing 9 (0.225-sec duration)	L + 36:28:34	01:00:34
2. Command postmidcourse vernier Firing 10 (0.225-sec duration)	L + 36:33:42	01:05:42
3. Command postmidcourse vernier Firing 11 (0.225-sec duration)	L + 36:37:23	01:09:23
4. Command postmidcourse vernier Firing 12 (0.225-sec duration)	L + 36:42:41	01:14:41
5. Command postmidcourse vernier Firing 13 (0.225-sec duration)	L + 36:47:46	01:19:46
6. Command transmitter high-power on	L + 36:52:02	01:24:02
7. Command telemetry rate increase from 137.5 to 1100 bit/sec	L + 36:53:06	01:25:06
8. Command post-midcourse vernier Firing 14 (1.975-sec duration)	L + 36:56:11	01:28:11
9. Command telemetry rate reduction from 1100 to 137.5 bit/sec	L + 36:57:38	01:29:38
10. Command transmitter high-power off	L + 36:58:24	01:30:24
Low-power engineering interrogation of Modes 4 and 5 initiated	L + 37:08:09	01:40:09
Post-midcourse vernier Firings 15 through 20		
1. Command post-midcourse vernier Firing 15 (0.225-sec duration)	L + 37:29:19	02:01:19
2. Command post-midcourse vernier Firing 16 (0.225-sec duration)	L + 37:36:11	02:08:11
3. Command post-midcourse vernier Firing 17 (0.225-sec duration)	L + 37:41:34	02:13:34
4. Command post-midcourse vernier Firing 18 (0.225-sec duration)	L + 37:47:37	02:19:37
5. Command post-midcourse vernier Firing 19 (0.225-sec duration)	L + 37:54:06	02:26:06
6. Command transmitter high-power on	L + 38:02:07	02:34:07
7. Command telemetry rate increase from 137.5 to 1100 bit/sec	L + 38:03:54	02:35:54
8. Command postmidcourse vernier Firing 20 (1.975-sec duration)	L + 38:07:14	02:39:14
9. Command telemetry rate reduction from 1100 to 137.5 bit/sec	L + 38:09:16	02:41:16
10. Command transmitter high-power off	L + 38:10:21	02:42:21
Unsuccessful attempts to command A/SPP polar axis to step positive (240 times)	L + 38:12:58	02:44:58
Post-midcourse vernier Firings 21 through 26		
1. Command postmidcourse vernier Firing 21 (0.225-sec duration)	L + 38:45:24	03:17:24
2. Command postmidcourse vernier Firing 22 (0.225-sec duration)	L + 38:51:53	03:23:53
3. Command postmidcourse vernier Firing 23 (0.225-sec duration)	L + 38:57:07	03:29:07

Table A-1 (contd)

Event	Mission time (actual)	GMT (actual)
Nonstandard post-midcourse phase (contd)		
		(September 22, 1966)
4. Command postmidcourse vernier Firing 24 (0.225-sec duration)	L + 39:02:33	03:34:33
5. Command postmidcourse vernier Firing 25 (0.225-sec duration)	L + 39:07:07	03:39:07
6. Command transmitter high-power on	L + 39:11:52	03:43:52
7. Command telemetry rate increase from 137.5 to 1100 bit/sec	L + 39:13:03	03:45:03
8. Command postmidcourse vernier Firing 26 (1.975-sec duration)	L + 39:15:56	03:47:56
9. Command telemetry rate reduction from 1100 to 137.5 bit/sec	L + 39:17:22	03:49:22
10. Command transmitter high-power off	L + 39:18:06	03:50:06
Command flight control power off for 24-min period	L + 39:19:34	03:51:34
Post-midcourse vernier Firings 27 through 32		
1. Command post-midcourse vernier Firing 27 (0.225-sec duration)	L + 39:45:31	04:17:31
2. Command post-midcourse vernier Firing 28 (0.225-sec duration)	L + 39:51:53	04:23:53
3. Command post-midcourse vernier Firing 29 (0.225-sec duration)	L + 39:57:51	04:29:51
4. Command post-midcourse vernier Firing 30 (0.225-sec duration)	L + 40:03:34	04:35:34
5. Command post-midcourse vernier Firing 31 (0.225-sec duration)	L + 40:09:20	04:41:20
6. Command transmitter high-power on	L + 40:20:46	04:52:46
7. Command telemetry rate increase from 137.5 to 1100 bit/sec	L + 40:21:47	04:53:47
8. Command post-midcourse vernier Firing 32 (1.975-sec duration)	L + 40:24:12	04:56:12
9. Command telemetry rate reduction from 1100 to 137.5 bit/sec	L + 40:25:15	04:57:15
10. Command transmitter high-power off	L + 40:26:19	04:58:19
Command flight control power off for 31 min period	L + 40:27:16	04:59:16
Postmidcourse vernier Firing 33		
1. Command transmitter high-power on	L + 41:00:59	05:32:59
2. Command telemetry rate increase from 137.5 to 1100 bit/sec	L + 41:02:11	05:34:11
3. Command retro sequence mode on (to obtain high thrust level)	L + 41:06:58	05:38:58
4. Command post-midcourse vernier Firing 33 (2.5-sec duration)	L + 41:11:19	05:43:19
5. Command telemetry rate decrease from 1100 to 137.5 bit/sec	L + 41:14:08	05:46:08
6. Command transmitter high-power off	L + 41:15:01	05:47:01
Command flight control power off for 1 hr 46 min period	L + 41:16:51	05:48:51
Attempt to step solar panel in transit locked position		
1. Command transmitter high-power on	L + 42:00:45	06:32:45
2. Command telemetry rate increase from 137.5 to 1100 bit/sec	L + 42:02:38	06:34:38
3. Command unlock of solar panel launch lock (5 times)	L + 42:03:18	06:35:18
4. Command solar panel in multiple steps, alternating plus and minus	L + 42:09:39 to L + 42:17:24	06:41:39 to 06:49:24
5. Command telemetry rate reduction from 1100 to 137.5 bit/sec	L + 42:18:33	06:50:33
Unlocking of solar panel transit lock		
1. Command telemetry rate increase from 137.5 to 1100 bit/sec	L + 42:21:54	06:53:54
2. Command unlock of solar panel transit lock (panel slips 20 deg)	L + 42:22:33	06:54:33
3. Command solar panel to step minus (87 times)	L + 42:23:06	06:55:06
4. Command telemetry rate decrease from 1100 to 137.5 bit/sec	L + 42:26:02	06:58:02
5. Command transmitter high-power off	L + 42:27:12	06:59:12

Table A-1 (contd)

Event	Mission time (actual)	GMT (actual)
Nonstandard post-midcourse phase (contd)		
		(September 22, 1966)
Post-midcourse vernier Firings 34 through 39		
1. Command transmitter high-power on	L + 43:09:49	07:41:49
2. Command telemetry rate increase from 137.5 to 1100 bit/sec	L + 43:10:50	07:42:50
3. Command post-midcourse vernier Firing 34 (0.225-sec duration)	L + 43:13:00	07:45:00
4. Command post-midcourse vernier Firing 35 (0.225-sec duration)	L + 43:14:12	07:46:12
5. Command post-midcourse vernier Firing 36 (0.225-sec duration)	L + 43:15:15	07:47:15
6. Command post-midcourse vernier Firing 37 (0.225-sec duration)	L + 43:16:18	07:48:18
7. Command post-midcourse vernier Firing 38 (0.225-sec duration)	L + 43:17:25	07:49:25
8. Command telemetry rate reduction from 1100 to 137.5 bit/sec	L + 43:18:23	07:50:23
9. Command transmitter high-power off	L + 43:19:17	07:51:17
10. Command transmitter high-power on	L + 43:28:52	08:00:52
11. Command telemetry rate increase from 137.5 to 1100 bit/sec	L + 43:30:11	08:02:11
12. Command retro sequence mode on (to obtain high thrust level)	L + 43:31:09	08:03:09
13. Command post-midcourse vernier Firing 39 (21.5-sec duration)	L + 43:33:12	08:05:12
14. Command telemetry rate reduction from 1100 to 137.5 bit/sec	L + 43:36:33	08:08:33
15. Command transmitter high-power off	L + 43:37:19	08:09:19
Command flight control power off for 1 hr 2 min period	L + 43:38:28	08:10:28
Helium dump sequence		
1. Command on telemetry Mode 2	L + 44:39:44	09:11:44
2. Command transmitter high-power on	L + 44:39:50	09:11:50
3. Command telemetry rate increase from 137.5 to 1100 bit/sec	L + 44:40:34	09:12:34
4. Command helium dump	L +44:41:16	09:13:16
Battery power check under load		
1. Command battery pressure logic off	L + 44:46:42	09:18:42
2. Command flight control thrust phase power on	L + 44:47:06	09:19:06
3. Command RADVS power on	L + 44:47:57	09:19:57
4. Command power mode switching	L + 44:50:16 to L + 44:56:01	09:22:16 to 09:28:01
5. Command RADVS power off	L + 44:58:09	09:30:09
Main retromotor firing		
1. Command on telemetry Mode 2	L + 45:00:19	09:32:19
2. Command retro sequence mode on	L + 45:01:14	09:33:14
3. Transmit emergency AMR signal to initiate retro engine firing sequence	L + 45:02:17	09:34:17
4. Vernier engine ignition	L + 45:02:27	09:34:27.2
5. Retro motor ignition	L + 45:02:09	09:34:28.6
6. Loss of spacecraft telemetry signal	L + 45:03:00	09:35:00

Appendix B

Surveyor Spacecraft Configuration

POSTLANDING CONFIGURATION

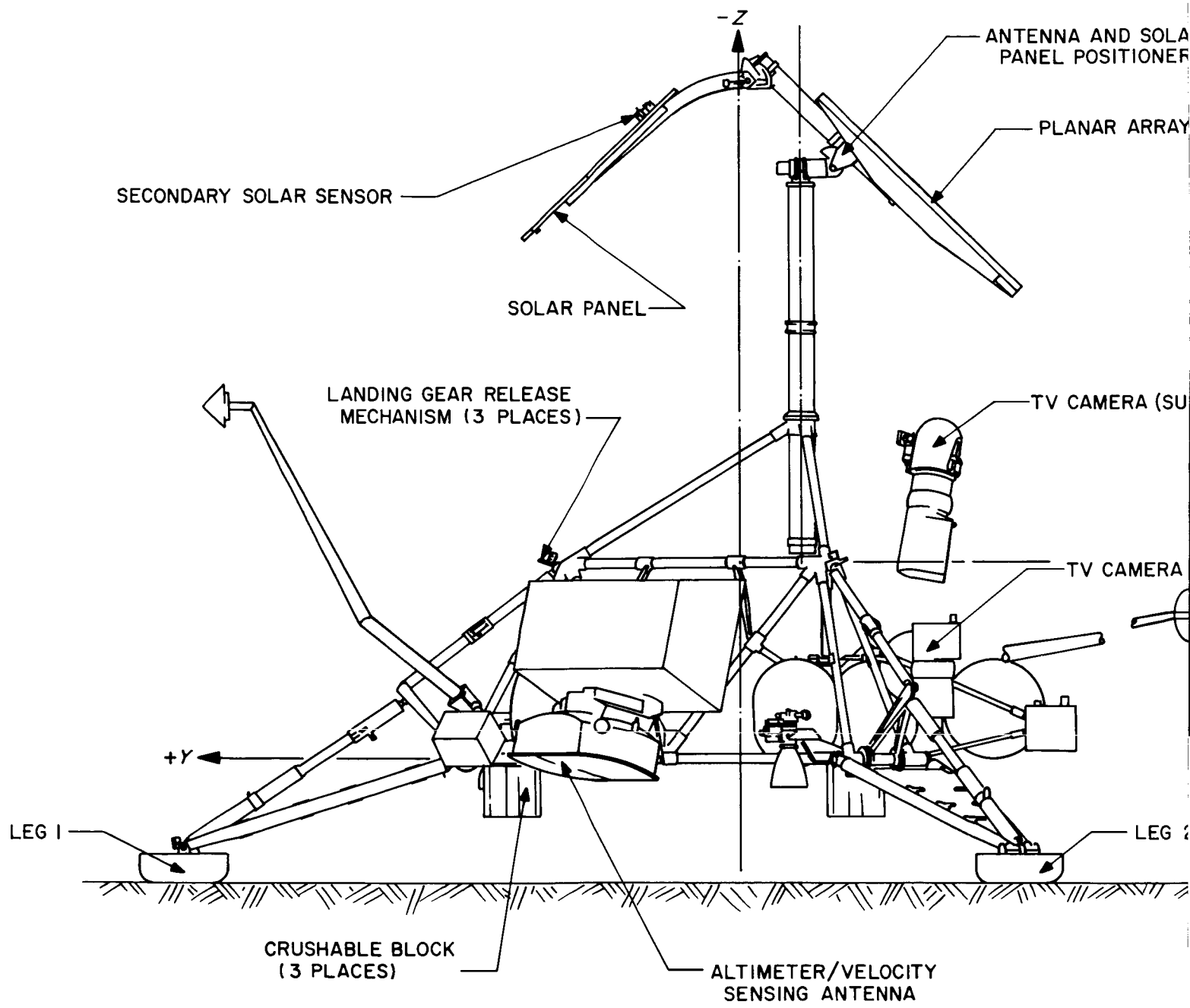

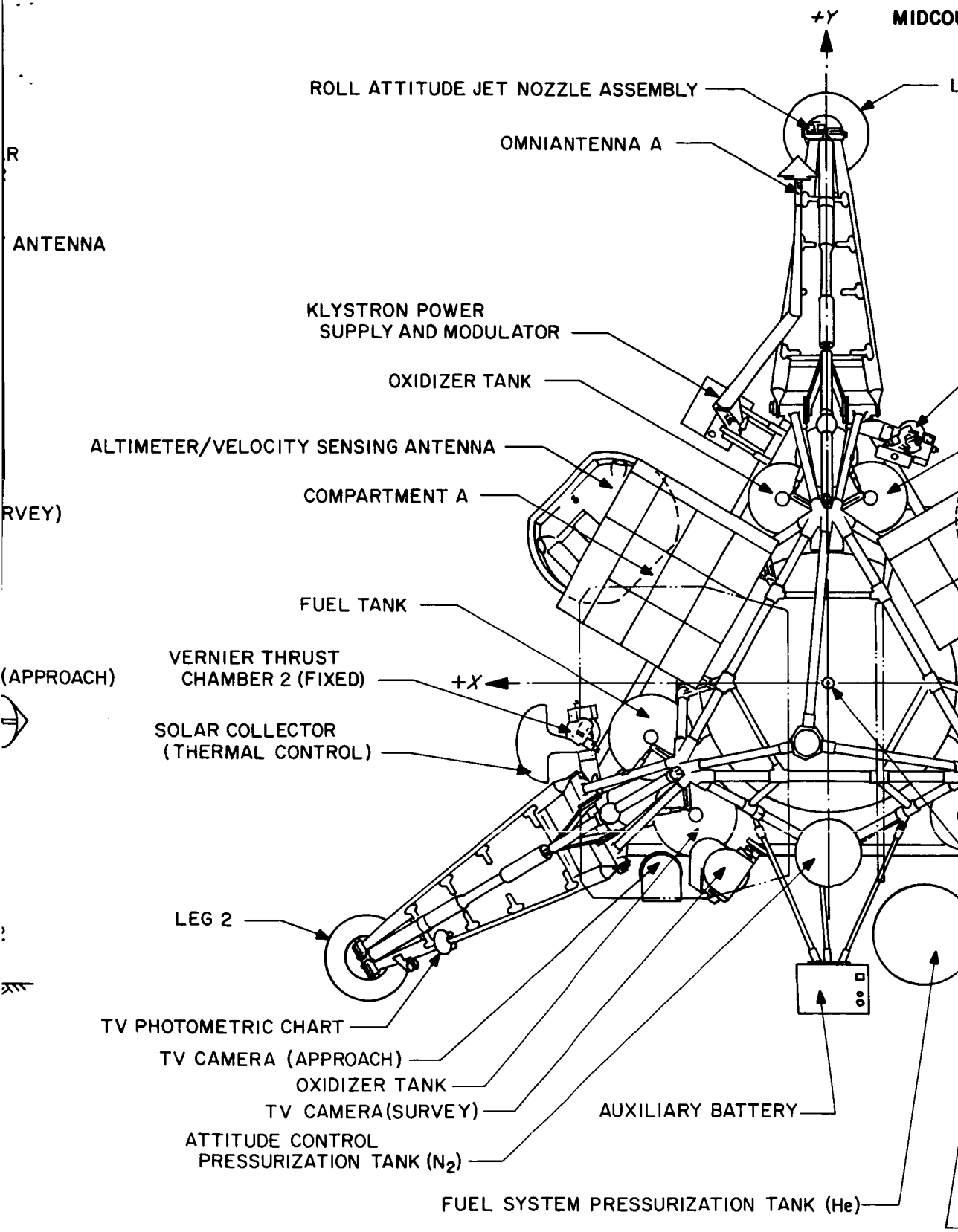
+Y
MIDCOU
ROLL ATTITUDE JET NOZZLE ASSEMBLY
OMNIANTENNA A
KLYSTRON POWER SUPPLY AND MODULATOR
OXIDIZER TANK
ALTIMETER/VELOCITY SENSING ANTENNA
COMPARTMENT A
FUEL TANK
VERNIER THRUST CHAMBER 2 (FIXED)
+X
SOLAR COLLECTOR (THERMAL CONTROL)
LEG 2
TV PHOTOMETRIC CHART
TV CAMERA (APPROACH)
OXIDIZER TANK
TV CAMERA(SURVEY)
ATTITUDE CONTROL PRESSURIZATION TANK (N_2)
AUXILIARY BATTERY
FUEL SYSTEM PRESSURIZATION TANK (He)

URSE CONFIGURATION

EG I

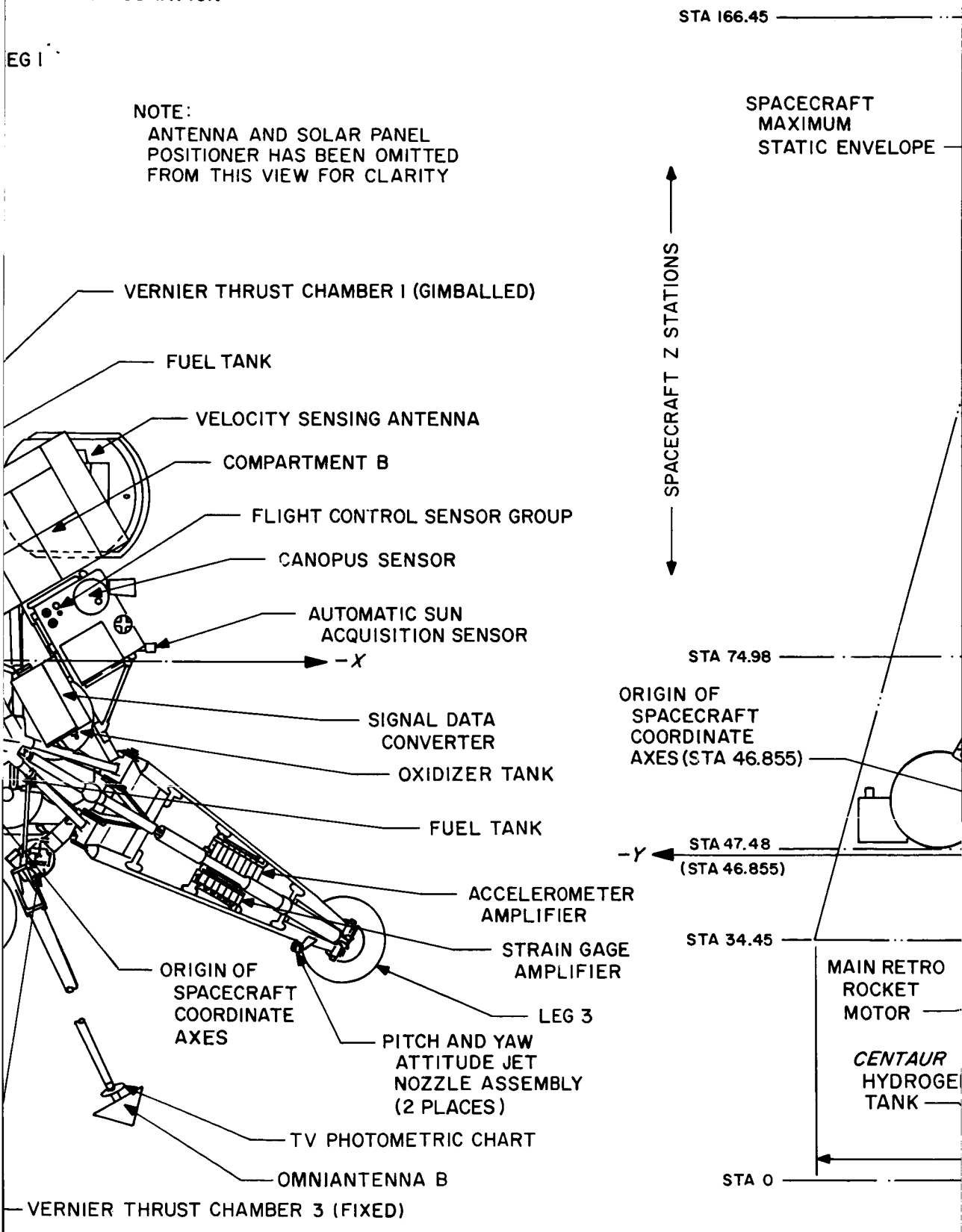

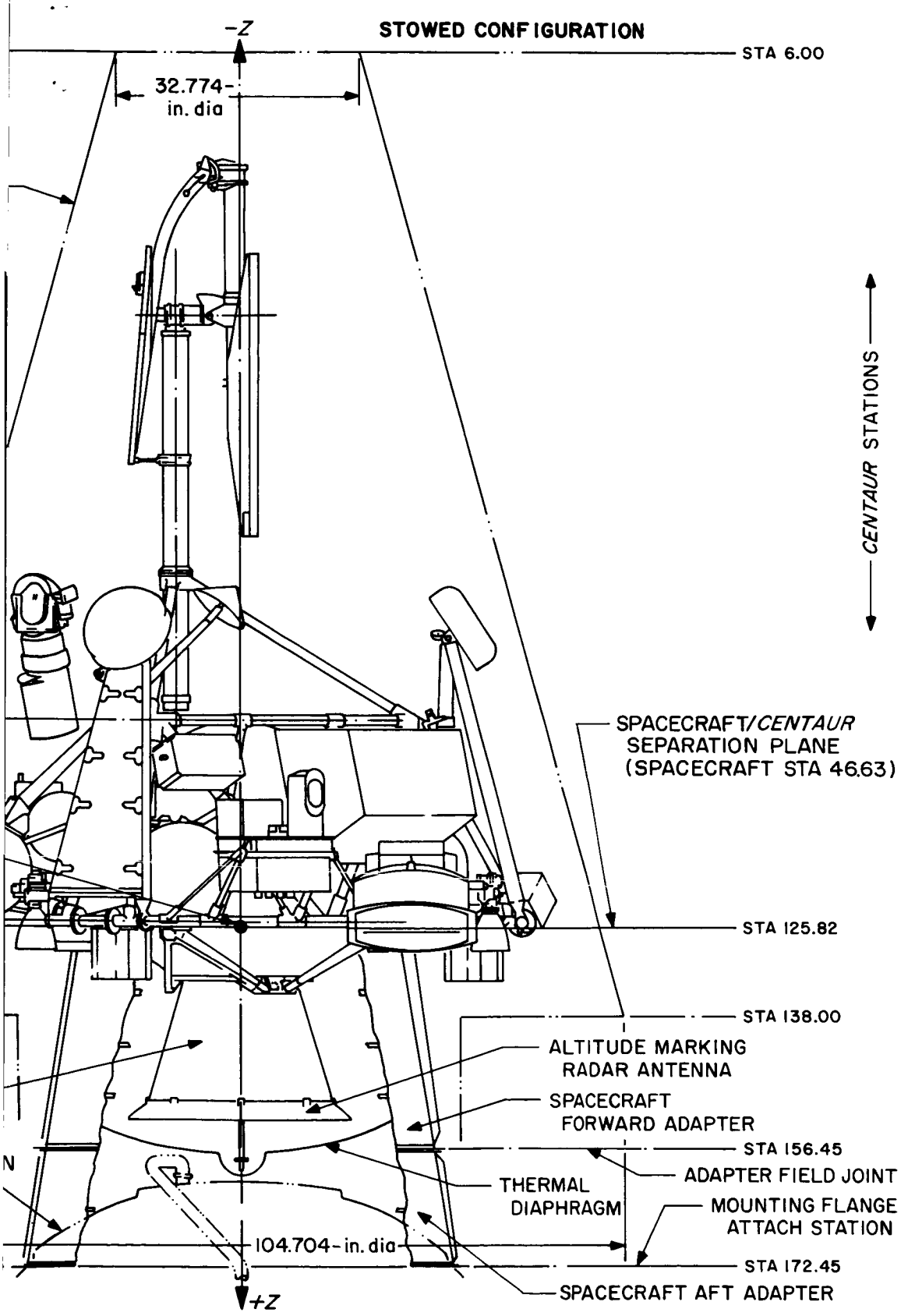
-Z
STOWED CONFIGURATION
STA 6.00
32.774-in. dia
CENTAUR STATIONS
SPACECRAFT/CENTAUR SEPARATION PLANE (SPACECRAFT STA 46.63)
STA 125.82
STA 138.00
ALTITUDE MARKING RADAR ANTENNA
SPACECRAFT FORWARD ADAPTER
STA 156.45
ADAPTER FIELD JOINT
THERMAL DIAPHRAGM
MOUNTING FLANGE ATTACH STATION
104.704-in. dia
STA 172.45
SPACECRAFT AFT ADAPTER
+Z

Appendix C

Surveyor II Failure Review Board Recommendations

Recommendations herein are the result of observations made by the Failure Review Board (FRB) during its investigations.

The Board has been unable to determine the exact cause of the *Surveyor II* spacecraft (SC-2) failure. In its search for a single failure mode that would explain the anomalies observed at all three legs of the vernier propulsion system, the Board defined to the best of its ability all possible single-failure-mode causes. This search required the Board to consider (for commonality to the three legs) all potential failure causes that could be defined, although most of these were later assessed by the Board to be incapable of explaining all observed anomalies. Thus this search for a failure cause resulted in the consideration of potential causes that singly or collectively could explain observed anomalies when occurring either simultaneously or sequentially. Inasmuch as the Board was unable to determine whether single or multiple failures were involved, its recommendations are based on consideration of all potential causes that were defined—regardless of how they would have had to occur to produce the SC-2 failure.

Recommendations resulting from considerations of potential causes of the SC-2 failure are primarily associated with improved test procedures designed to provide confidence that the potential failures will not occur on future *Surveyors*. Some of these recommended procedure changes are required because the Board considered previous procedures to be inadequate. Others might not ordinarily be required, but are recommended because of the unknown nature of the SC-2 failure.

The Board experienced considerable difficulty in interpreting much flight telemetry data and preflight test data. In addition, certain flight data that would have been useful to the Board was either not telemetered or was not telemetered in commutator modes used during critical flight events. Further, the Board found that the preflight characterization of several data channels was inadequate to serve as a standard for comparison with flight data. Therefore, several recommendations framed by the Board are directed at providing a capability for improved diagnostics.

Recommendations 1 through 5 are directed at assuring a proper electrical interface between the vernier propulsion system and the remainder of the spacecraft.

Recommendations 6 through 25 are intended to ensure cleanliness and integrity of the vernier propulsion system.

Recommendations 26 through 40 should provide improved diagnostics, or generate basic data with which test or flight data can be compared.

Recommendations 41 through 46 are directed at additional improvements in test procedures.

Additional recommendations, resulting from observations of the FRB, are included as Recommendations 47 through 51.

The Board has placed each recommendation in a class of "Mandatory," "Desirable," or "Consider," as an indication to project management of the importance attached thereto.

Recommendation 1 (Mandatory)

During each flow bench check of each vernier thrust chamber assembly (TCA) at ETR, the waveforms of TCA solenoid current shall be recorded over a range of voltages as the voltage is turned on and off. These measurements shall be made under flight pressure conditions. The corresponding liquid flow response times shall also be recorded at one throttle-valve position.

Reason: These measurements will ensure that the solenoid operated valve (SOV) on each TCA is operating consistently within specification. Such data, when compared with drive current supplied by the spacecraft flight control system, will ensure an ample margin in each solenoid circuit.

Recommendation 2 (Mandatory)

At the flight control sensor group level, a test shall be performed to ensure an adequate margin in the current supplied to the TCA solenoids. The current waveform shall be recorded. Flight-type solenoids shall be used as loads during this test. Dummy resistors shall not be used.

Reason: Improper current to the TCA solenoids can produce erratic engine responses. This test will ensure current that is proper at the unit level, and will provide information against which spacecraft-level data can be compared.

Recommendation 3 (Mandatory)

Spacecraft testing at ETR, and also at HAC, El Segundo, as a control, should include the measurement and recording of waveforms of the current to each SOV solenoid. This current should be compared with Engineering Processor 4 (EP-4) telemetry data, with flight control sensor group level data, and with calculations to ensure that it is correct. Testing should be performed at simulated minimum-specification unregulated bus voltage to determine whether circuitry up to the solenoids provides adequate margin; and the minimum acceptable current under these conditions shall be specified to be sufficiently higher than SOV pull-in current to provide margin in the solenoids.

Reason: Improper current to the SOV solenoids can produce erratic engine responses. In the past, there has been only qualitative checking of current to the flight SOV solenoids.

Recommendation 4 (Mandatory)

Provisions shall be incorporated on the spacecraft to permit assuring—by means of a low-current resistance measurement—that electrical continuity exists through all three SOV solenoids after the last mating of the three SOV connectors.

Reason: The SOV connectors are last mated after propellant loading, and safety precautions preclude a check of the mating by energizing the solenoids in a normal manner. The recommended check will provide confidence that proper mating has been accomplished.

Recommendation 5 (Mandatory)

Throttle valve current at each TCA shall be measured by means of a clamp-on ammeter following the final mating of each throttle valve connector.

Reason: This will ensure proper mating and confirm circuit integrity.

Recommendation 6 (Mandatory)

Each TCA shall be flow-bench-checked at ETR prior to the first mating with a spacecraft at HAC, El Segundo, and again prior to final mating at ETR.

Reason: This procedure will provide a historical record of TCA performance, and ensure proper operation of the TCA immediately prior to final installation aboard the spacecraft.

Recommendation 7 (Mandatory)

Prior to TCA installation on the spacecraft, the TCA lines and fittings shall be X-rayed.

Reason: X-rays will detect large pieces of foreign material that would not be detected in fluid contaminant checks. This procedure will help establish confidence in TCA cleanliness.

Recommendation 8 (Mandatory)

At each flow bench check of a TCA at ETR, the first liquid that flows through each side of the TCA shall be drawn off and checked for contamination.

Reason: This procedure will provide a historical record of TCA cleanliness and ensure cleanliness shortly prior to installation of the TCA aboard the spacecraft.

Recommendation 9 (Mandatory)

A vacuum bell jar shall be employed during the TCA drying operation at ETR following each TCA flow check, or following any test in which liquids are allowed to come in contact with TCA flow passages downstream of the shutoff valve.

Reason: Aluminum oxide was found in engines that were not properly dried after removal from SC-3. This improved procedure (already used successfully at Reaction Motors Division, Thiokol) will ensure that all parts of the TCA are thoroughly dried.

Recommendation 10 (Mandatory)

The last TCA flow bench check at ETR shall be performed two weeks prior to required installation on the spacecraft, and the TCA installation shall be as late as practicable before propellant loading.

Reason: Previously, the TCA's were installed on the spacecraft during the first two weeks the spacecraft was at ETR. This recommended change will confirm proper TCA performance at the latest practicable time, and reduce the opportunity for unnecessary handling while on the spacecraft—thereby providing increased confidence.

Recommendation 11 (Mandatory)

Filters shall be added in the hoses used to load propellants and gas on board the spacecraft at points as close to the spacecraft as practicable.

Reason: Filters are presently installed in the ground support equipment (GSE) upstream of the hoses. Contaminents within the hoses are not presently prevented from entering the spacecraft vernier propulsion system.

Recommendation 12 (Mandatory)

Propellants and solvents loaded into any future spacecraft shall be sampled from the GSE and checked for contamination before and after the loading is completed.

Reason: This procedure will ensure that the contamination level has not changed during the filling operation as a result of flow through various lines and fittings, and will help provide confidence in the cleanliness of the vernier propulsion system.

Recommendation 13 (Mandatory)

Each time solvents are down-loaded, off-loaded, or overflowed from the spacecraft, samples shall be checked for contamination. In addition, samples of propellants shall be taken from the overflow lines during propellant loading and checked for contamination. The last solvent and propellant samples for the spacecraft and all GSE Millipore filters shall be preserved for post-mission analysis.

Reason: This procedure will ensure the cleanliness of the major portions of the vernier propulsion system at the time of each off-loading, down-loading, or overflow operation.

Recommendation 14 (Mandatory)

The two check valves in the helium pressurization system shall be tested individually, rather than in parallel.

Reason: The present test procedure results in an indication of proper flow, even if one of the two check valves does not open.

Recommendation 15 (Mandatory)

A test for blockage or contamination of helium inlet lines shall be made before each attachment to a TCA.

Reason: Helium line blockage would prevent SOV actuation. Contamination might prevent proper SOV operation by obstructing motion of the helium solenoid-actuated piston, by closing an inlet or exit port, or by forming deposits on the nylon seats at inlet and exit ports.

Recommendation 16 (Mandatory)

A final helium gas leak check of the solenoid helium pilot valve seat shall be performed after the last solenoid actuation is completed.

Reason: The TCA solenoid is not presently checked for leakage after it is assembled to the spacecraft and after "click" tests are performed.

Recommendation 17 (Mandatory)

A low-level (2 to 5 psi) gas leak test of all propellant bladders shall be performed immediately prior to propellant loading at ETR.

Reason: This test has been performed in the past at various times during the spacecraft test cycle, but not immediately prior to propellant loading. Performance of the test immediately prior to propellant loading will ensure bladder integrity later.

Recommendation 18 (Mandatory*)

A bladder integrity check shall be conducted after final propellant loading to ensure that no bladder damage has been incurred during loading.

Reason: Large amounts of fuel in the helium system could affect SOV operation.

Recommendation 19 (Mandatory)

Procedures between the start of propellant loading and encapsulation shall be formalized to require continuous monitoring for propellant leaks by means of probes inserted in the TCA throats. A vacuum shall be drawn in an optimum fashion to sense any leakage and eliminate traces of propellants that may have seeped through the shutoff valve. This is in addition to monitoring requirements already in existence for external vernier propulsion system (VPS) leak detection and personnel safety.

Reason: This type of testing was done periodically on SC-2 after loading, but the procedure was not formalized and resultant data was not recorded. Excessive oxidizer leakage could result in injector salting, and excessive fuel leakage could result in gumming of the fuel regulator.

*If feasible, FRB unable to suggest technique.

Recommendation 20 (Mandatory)

An improved method of propellant leak detection after encapsulation is required. This method would preferably draw samples from within the TCA throats, and alternately draw a vacuum in an optimum fashion to sense any leakage and eliminate traces of propellants that may have seeped through the shutoff valve. In addition, the present monitoring system shall be retained.

Reason: The monitoring system used in the past has adequate sensitivity to detect leak rates that are potentially hazardous to personnel, but does not have sufficient sensitivity to detect lower-level leak rates that might produce injector salting or otherwise result in abnormal vernier propulsion system performance.

Recommendation 21 (Desirable)

In addition to the vernier system pressure-decay test performed at half of flight pressure, a brief test shall be performed at flight pressure to ensure system integrity. In addition, a gas-vs-liquid leak test shall be evaluated to finalize a test procedure that provides the best evidence of system integrity and demonstrates that adequate margins exist prior to launch.

Reason: The liquid pressure-decay test that has been run in the past is performed at half flight pressure for reasons of safety. Liquid leaks that might occur at flight pressure may not thus be detected. The Board recognizes that special safety precautions will be required to perform this test.

Recommendation 22 (Desirable)

The flow time required to load or unload solvents or propellants on the spacecraft during each loading or unloading operation shall be recorded and compared with calculated values.

Reason: This will provide flow rate data, and has the potential of detecting gross line blockages that might otherwise be undetected.

Recommendation 23 (Desirable)

A filter shall be provided at the output of the helium inlet line to each TCA.

Reason: Contaminants in the helium might affect SOV operation.

Recommendation 24 (Desirable)

Acceptable levels of propellant leakage at various joints in the liquid portion of the vernier propulsion system shall be established after final propellant loading.

Reason: In the past, the significance of any leak has been assessed, but no formal criteria have existed.

Recommendation 25 (Desirable)

Corrosion protection shall be applied to the threads of TCA fill and vent valves.

Reason: Aluminum oxide was found on these threads after removal of TCA's from SC-3. (Removed TCA's were not properly dried.)

Recommendation 26 (Mandatory)

Telemetry channels in the several commutator modes shall be reassigned, so that data from sensors in the vernier propulsion system will be present in commutator modes during thrusting phases.

Reason: Engine temperatures were not present in SC-2 Commutator Mode 1, which was used during midcourse. As a result, the FRB was unable to completely assess the performance of the vernier engines during midcourse.

Recommendation 27 (Mandatory)

A filter shall be added between the unregulated current shunt EP-4 and the $\times 50$ amplifier to remove effects of ripple currents from telemetered current indications.

Reason: This channel is the primary indication of current flow to each TCA solenoid, gas jet, and several other items. The noise level on this channel often exceeds current demands of many loads, making it difficult (if not impossible) to determine whether the loads are properly energized. In addition, the telemetry system appears to respond to ripple currents through the EP-4 shunt in such a manner as to bias the current indication. The FRB devoted more time to interpreting this channel than it did to any other telemetry channel.

Recommendation 28 (Mandatory)

Existing strain gage instrumentation on the engine mounting brackets shall be revised or replaced with a system that will provide improved, more reliable thrust measurements at each TCA. The instrumentation should be calibrated dynamically as well as statically.

Reason: The existing strain-gage instrumentation system does not provide quantitative data. Gages are sensitive to forces in directions not parallel to the thrust axes and exhibit considerable zero shift. In addition, the gages are temperature-sensitive and respond to radiative heating from the TCA's. Dynamic response characteristics of the strain-gage mounting-bracket combination have not been available in the past.

Recommendation 29 (Mandatory)

A dynamic calibration of flight-type engine thermal sensors shall be performed over the expected range of temperatures and for room and high-temperature sensor bondings to be used.

Reason: This will permit a better interpretation of flight data.

Recommendation 30 (Desirable)

All future TCA acceptance testing for any reason shall include continuous recording of thermal-sensor resistance during all hot firings and for a period of 5 min (continuously) immediately subsequent to engine shutdown. Each recording shall be included in the TCA Flight Acceptance Test (FAT) log.

Reason: This will provide a standard for comparisons of flight data.

Recommendation 31 (Desirable)

The dynamic thermal performance of the TCA shall be characterized as seen by the flight-jacket temperature sensor.

Reason: This will result in a better understanding of TCA flight data.

Recommendation 32 (Desirable)

The maximum duty cycle of the vernier propulsion system line and tank heaters shall be determined for every sun level during the solar-thermal-vacuum (STV) test.

Reason: This will provide data for more thorough diagnosis of the VPS heater system performance.

Recommendation 33 (Desirable)

Gas jets shall be inhibited during vernier thrusting periods either by command or an interlock in flight control.

Reason: Uncertain conditions of gas jets during the *Surveyor II* midcourse thrusting period made unregulated-current (EP-4) telemetry data difficult to interpret.

Recommendation 34 (Desirable)

A study shall be performed to determine whether engineering, midcourse, or retro accelerometers might provide a useful indication of total vernier engine thrust if telemetered during midcourse.

Reason: This telemetry information would aid in the performance analysis of the vernier propulsion system.

Recommendation 35 (Desirable)

Telemetry of fuel-line temperatures and fuel-side pressure (either fuel or helium) shall be added for commutator modes used during thrusting periods.

Reason: Assessment of VPS performance on *Surveyor II* was hampered by a lack of data.

Recommendation 36 (Desirable)

Separate current shunts shall be provided for loads presently on the unregulated-current shunt (EP-4) in the following manner: one shunt for cyclic loads, one shunt for the gas jets and roll actuator, and one shunt for the SOV solenoids and continuous loads.

As an alternative, the following three steps could be taken: Inhibit gas jets during any thrusting period, telemeter yaw gyro heater on-off information (only pitch and roll were telemetered on *Surveyor II*), and return gyro heater currents directly to the EP-9 shunt without passing through the EP-4 shunt.

Reason: Either of these changes (the first being the most desirable) will permit more accurate determination of SOV solenoid current during both test and flight.

Recommendation 37 (Desirable)

A filter shall be added between the EP-14 current shunt and the $\times 50$ amplifier to remove effects of ripple from the telemetry of regulated current.

Reason: The EP-14 telemetry channel is very noisy, and it is difficult (if not impossible) to detect small current changes in noise resulting from the response of the telemetry system to ripple through the EP-14 shunt.

Recommendation 38 (Desirable)

The signal processing circuitry shall be modified to eliminate data inaccuracies that exist at 4400 bit/sec relative to other bit rates.

Reason: Various telemetry channels—primarily the temperature telemetry channels—provide data that varies as a function of the value of the preceding word in the telemetry format at 4400 bit/sec. The phenomenon is understood and often permits the correction of telemetry data in non-real-time, but leads to considerable uncertainty in real-time and lowers the confidence that can be placed in the data during post-flight analysis.

Recommendation 39 (Desirable)

Yaw gyro heater on-off information shall be telemetered (only pitch and roll have been telemetered in the past).

Reason: This will permit the more accurate correction of current telemetry data during both tests and flight.

Recommendation 40 (Consider)

A helium tank pressure indication that is not subject to zero shift shall be provided.

Reason: The helium pressure transducer on *Surveyor II* exhibited zero shift at pressurization and at helium dump. In addition, pressure indications were erratic at other times during the flight. It is believed that the erratic indications are related to the zero-shift phenomenon. The zero shift and the erratic behavior make it difficult to place high reliance on the helium-pressure data.

Recommendation 41 (Mandatory)

The power system current telemetry channels EP-4 and EP-14 shall be calibrated at all bit rates against hard-line measurements and compared with expected responses as each load is turned on and off, one at a time (in the case of the roll actuator, for null and saturated conditions). This procedure should be performed at ETR, and at HAC, El Segundo, as a control.

Reason: This will ensure that all loads are drawing proper currents, and that the telemetry is properly calibrated. This procedure — if followed on *Surveyor II* — would have guaranteed, for example, that proper current flowed to the SOV solenoids, and would have enabled EP-4 flight data to be more accurately corrected for the effects of several variable loads (e.g., roll actuator, gas jets, and gyro heaters). In addition, this procedure will generate power profile data for each spacecraft and assure that all connections and loads are proper.

Recommendation 42 (Mandatory)

Throughout the system test cycle, when the flight TCA's are not on board the spacecraft or not connected, flight-type TCA solenoids shall be used to simulate solenoids on the flight TCA's. Dummy resistors shall not be used.

Reason: *Surveyor II* test data suggests that the current flow may be different with dummy resistors than with inductive solenoids. This procedure will permit better simulation of flight loads.

Recommendation 43 (Mandatory)

In the event of loss of air conditioning between propellant loading and encapsulation, standby vacuum pumps shall be applied to each TCA within 20 min.

Reason: This will prevent injector salting that might result from high humidity. Using desiccants in place of a vacuum pump is not sufficient because the oxidizer itself is hygroscopic.

Recommendation 44 (Mandatory)

During final harness inspection, it shall be determined (and recorded) that there are adequate service loops for vehicle vibration.

Reason: Photographs of SC-2 prior to encapsulation indicate that the harness to the connector at the TCA 3 solenoid was taut.

Recommendation 45 (Desirable)

The resolution of the hard-line current measuring system used to monitor spacecraft heaters during STV shall be increased.

Reason: This will allow improved diagnosis of the spacecraft thermal control system. In the past, resolution was inadequate to monitor cycling of thermal heaters.

Recommendation 46 (Desirable)

Provisions shall be incorporated on the spacecraft to permit assuring, by means of a low-current resistance measurement, that electrical continuity exists in all VPS line and tank heater circuits.

Reason: These circuits cannot be checked functionally at ETR because their thermostats are not actuated by ambient temperatures.

Recommendation 47 (Desirable)

Consideration shall be given to reducing the level of oxidizer leakage at the TCA throttle-valve filters and bellows areas.

Reason: This could prevent damage to the TCA thermal finish.

Recommendation 48 (Desirable)

An appropriate filter shall be placed in the circuitry driving the roll actuator motor to eliminate harmonic components of the drive current.

Reason: The drive current to the roll actuator has a peaked waveform which derives from a square-wave error signal at the input to the servo amplifier. Large current peaks pass through regulated-current shunt EP-4, and produce "noisy" EP-4 telemetry.

Recommendation 49 (Desirable)

Wiring harness redundancy shall be added in critical circuits such as those to the TCA solenoids.

Reason: This will improve reliability.

Recommendation 50 (Desirable)

In the event of future in-flight failures, TV pictures of pertinent areas of the spacecraft shall be taken.

Reason: Structural damage remains an unclosed item in the *Surveyor II* failure investigation. Concern over damage in the area of Engine 3 is intensified by the recovery of the fragment of the nose cone with its peculiar hole. TV pictures would be invaluable in the assessment of such damage.

Recommendation 51 (Consider)

Operations personnel shall review criteria for transmission of the emergency thrust termination command during vernier engine thrusting periods. In addition, the chain of command associated with making the abort decision should be reviewed with the intent of shortening the chain.

Reason: *Surveyor II* midcourse thrusting was allowed to continue for 9.85 sec without termination. If the emergency termination command had been sent sufficiently early, the spacecraft tumbling rate could have been corrected by the cold-gas attitude control system. This probably would not have saved the mission in the case of *Surveyor II*; but for some failure modes, a more rapid response might permit the salvaging of a future mission.

Appendix D

Surveyor II Temperature Histories

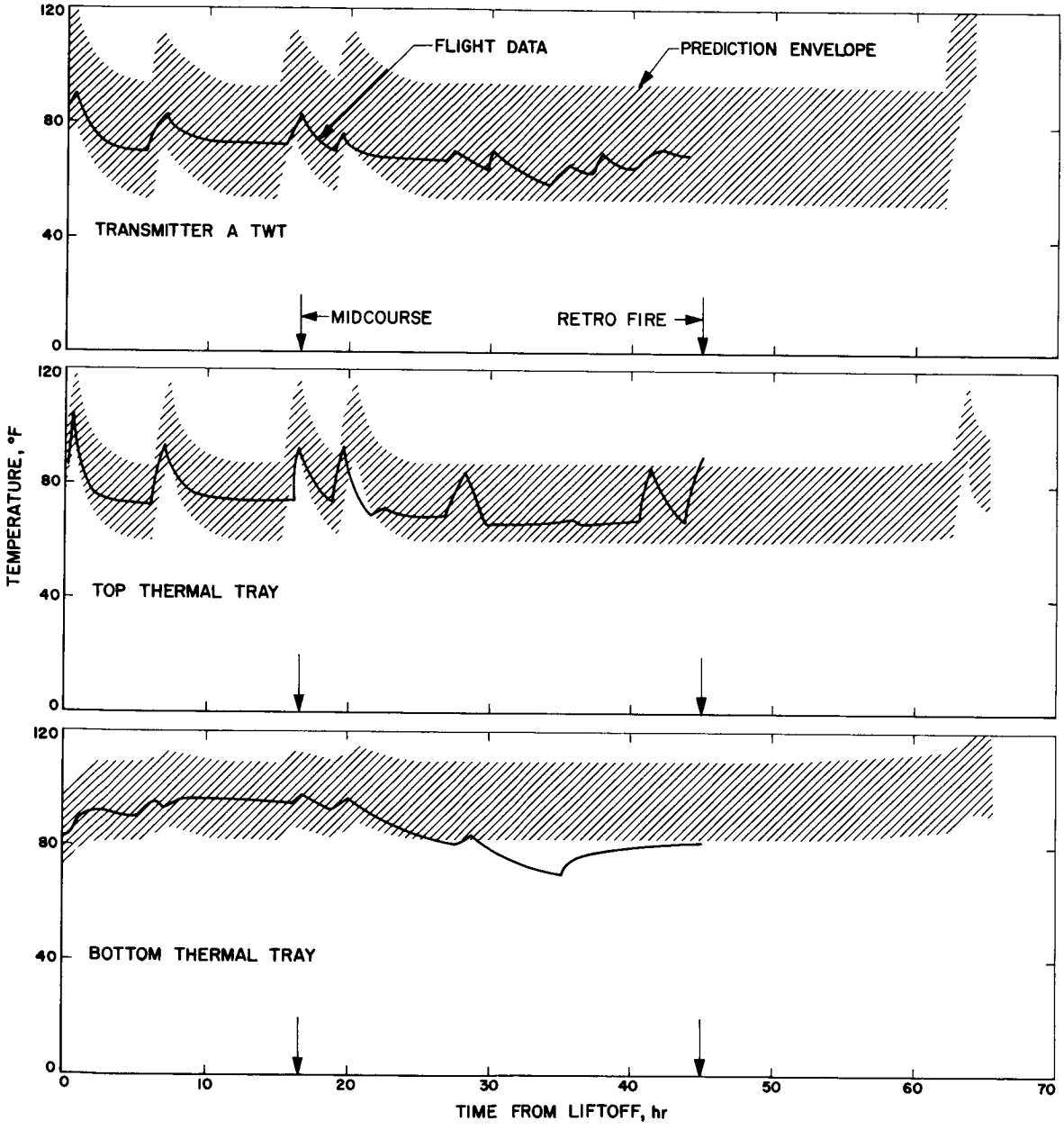

Fig. D-1. Compartment A transit temperatures

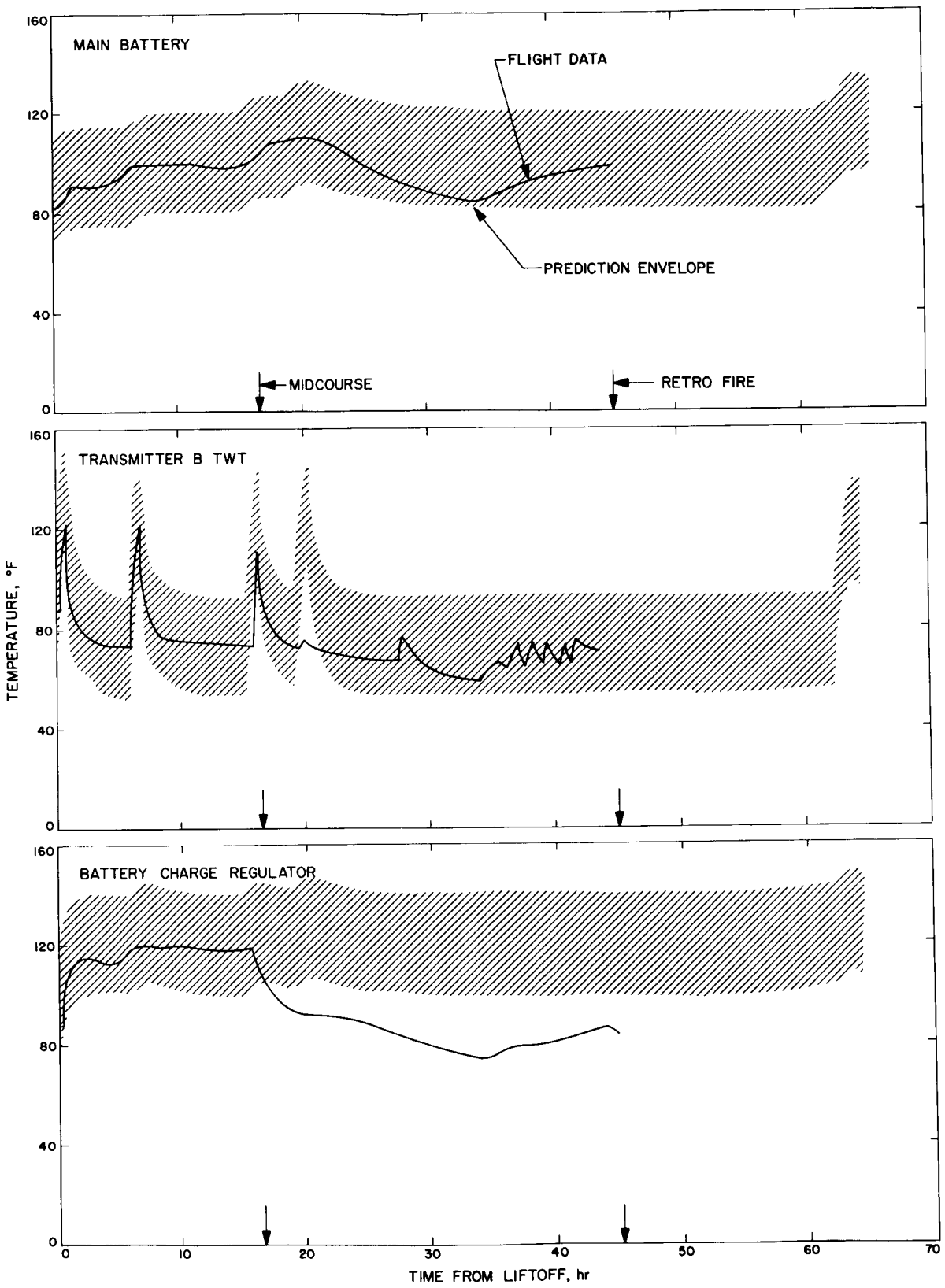
MAIN BATTERY
FLIGHT DATA
PREDICTION ENVELOPE
MIDCOURSE
RETRO FIRE
TRANSMITTER B TWT
BATTERY CHARGE REGULATOR
TEMPERATURE, °F
TIME FROM LIFTOFF, hr
160
120
80
40
0
10
20
30
40
50
60
70

Fig. D-1 (contd)

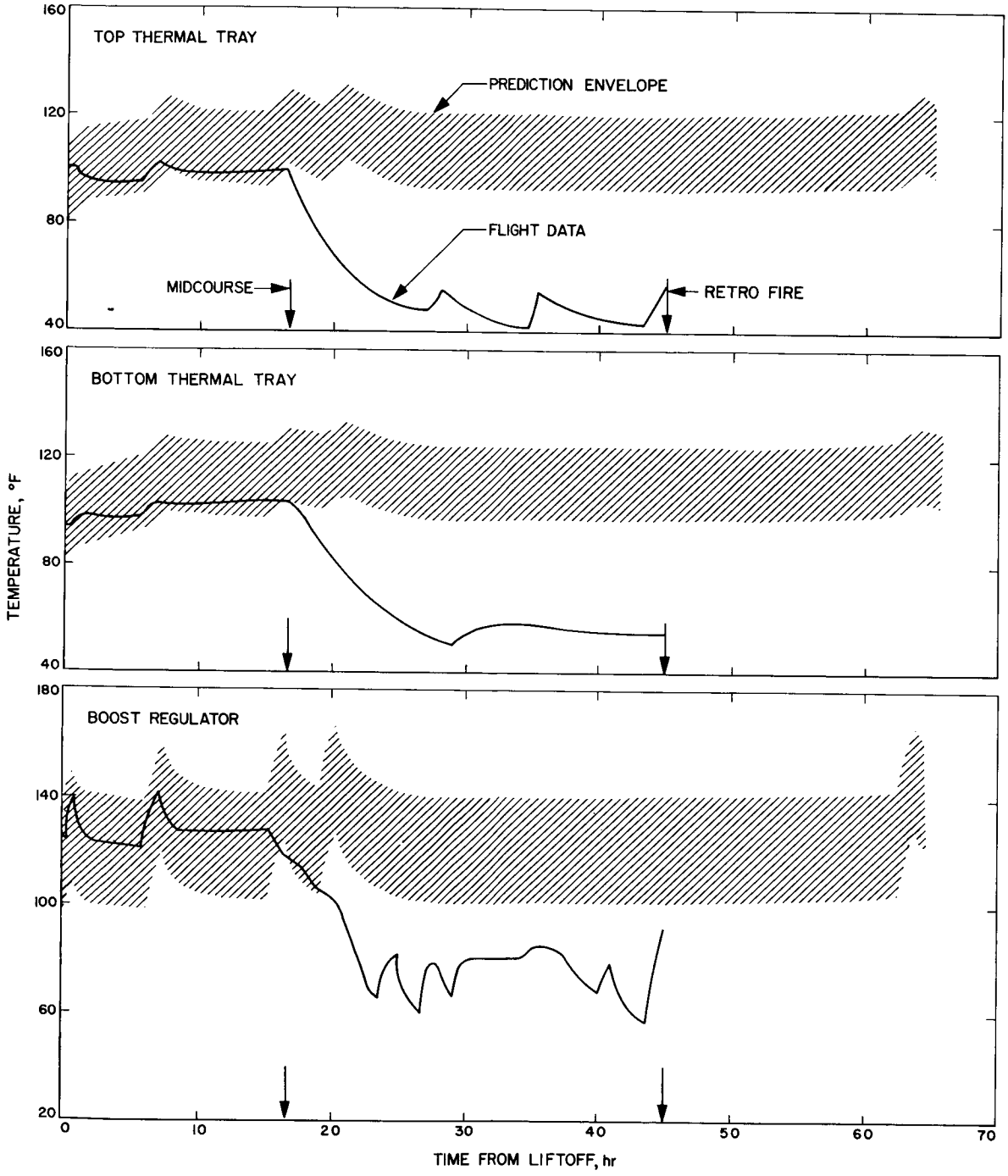

Fig. D-2. Compartment B transit temperatures

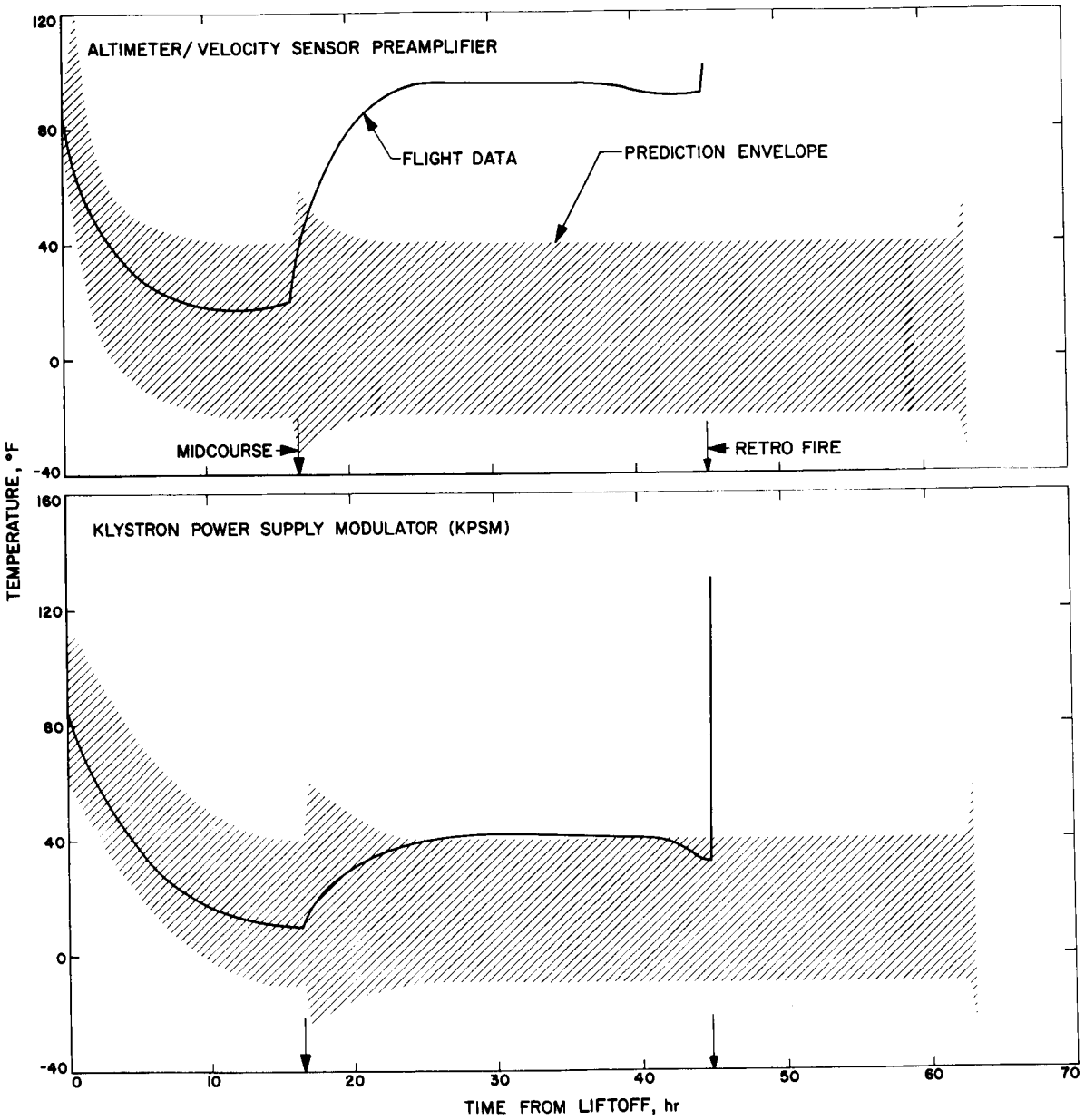

Fig. D-3. RADVS transit temperatures

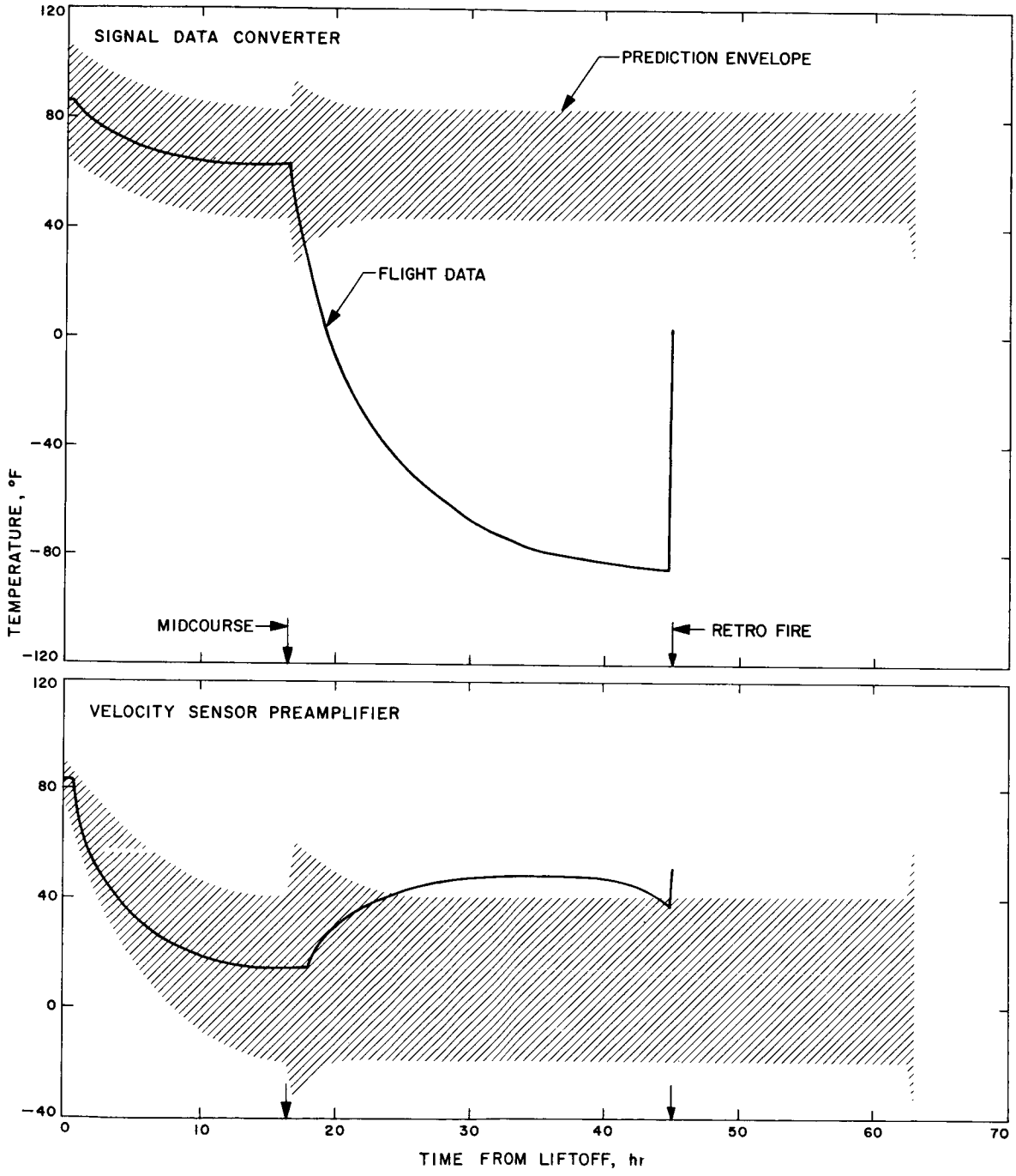
SIGNAL DATA CONVERTER
PREDICTION ENVELOPE
FLIGHT DATA
MIDCOURSE
RETRO FIRE
VELOCITY SENSOR PREAMPLIFIER
TEMPERATURE, °F
120
80
40
0
-40
-80
-120
0
10
20
30
40
50
60
70
TIME FROM LIFTOFF, hr

Fig. D-3 (contd)

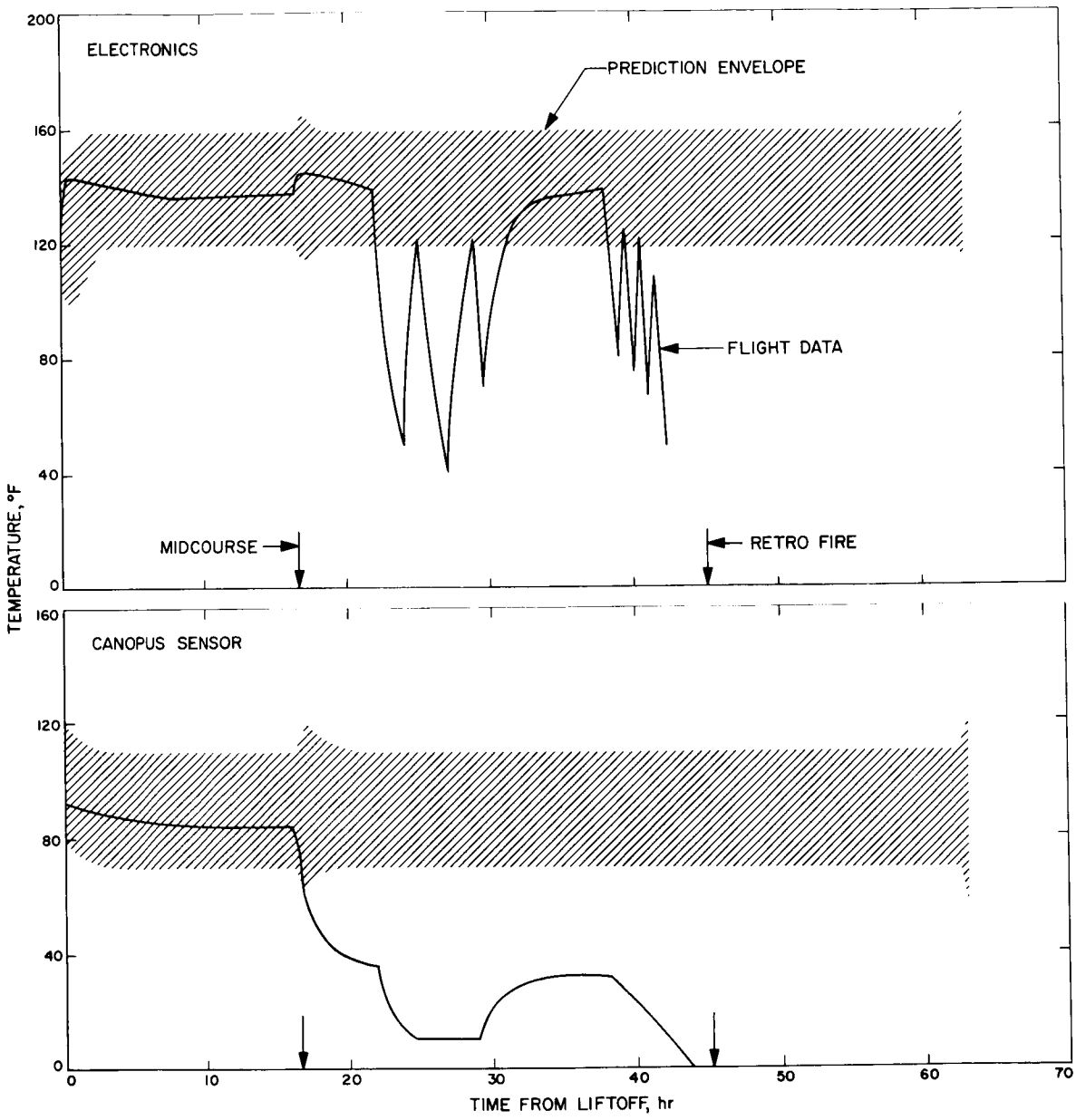

Fig. D-4. Flight control transit temperatures

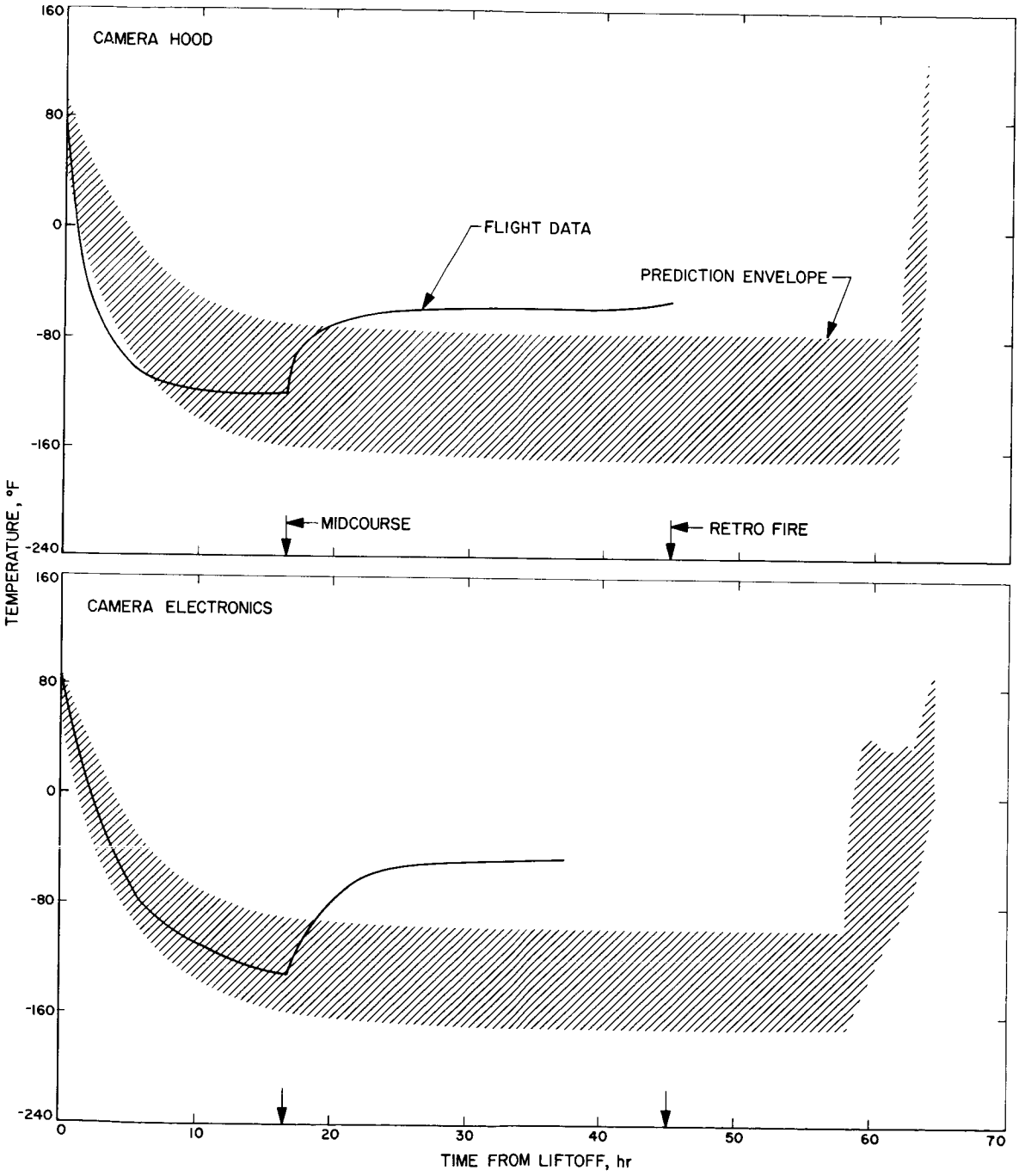

Fig. D-5. Survey TV camera transit temperatures

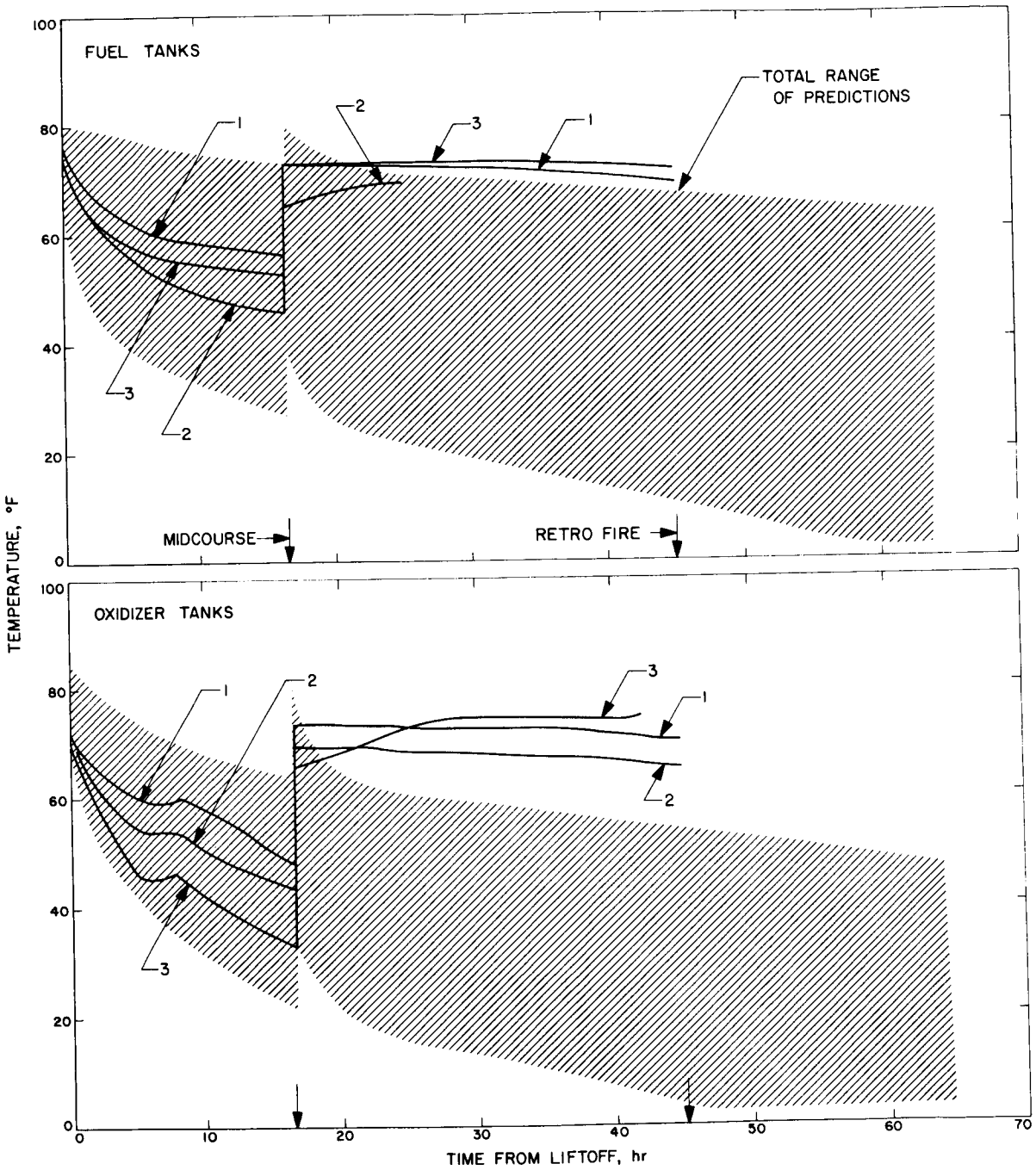

Fig. D-6. Vernier propulsion transit temperatures

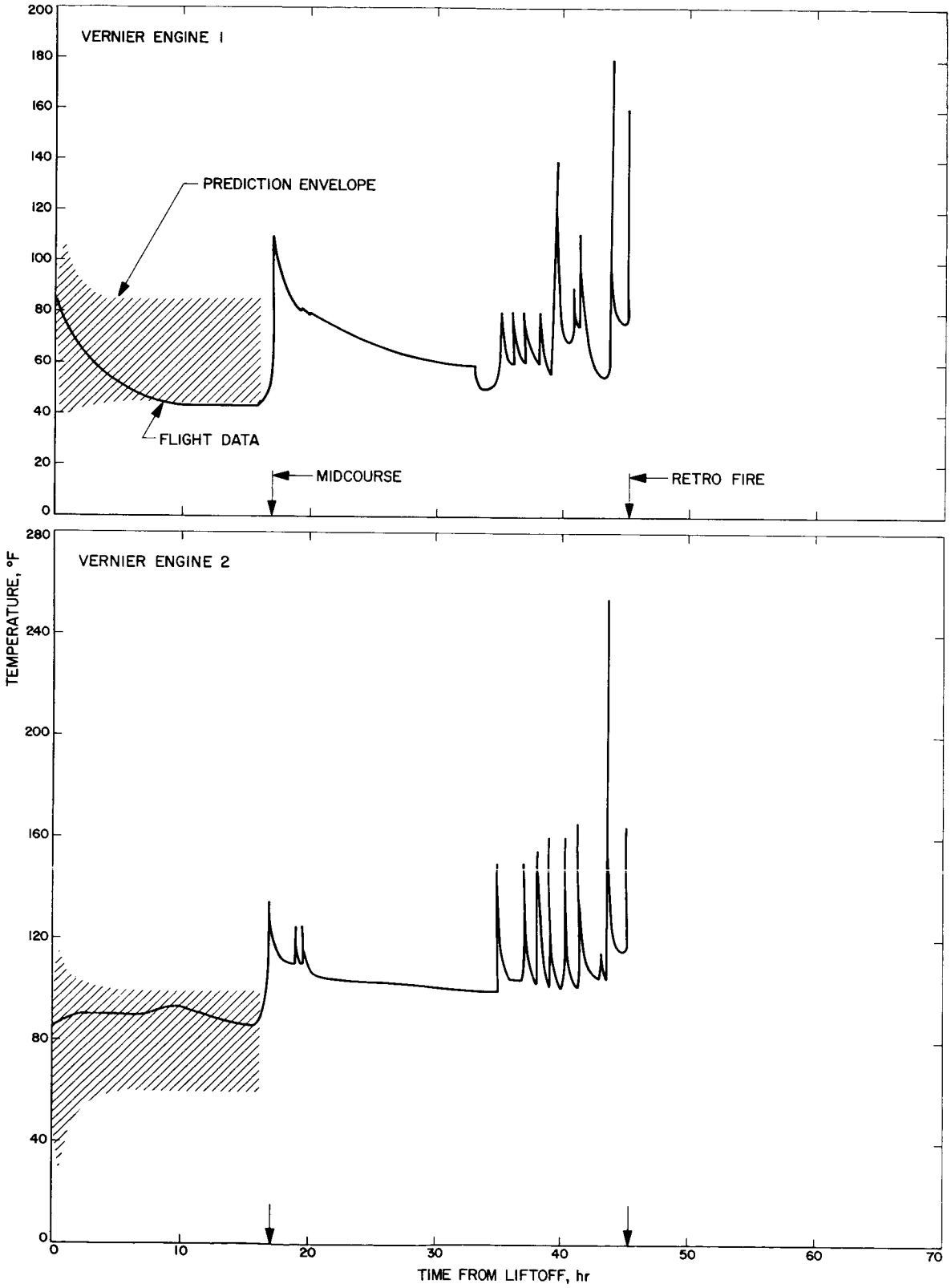
VERNIER ENGINE 1
PREDICTION ENVELOPE
FLIGHT DATA
MIDCOURSE
RETRO FIRE
VERNIER ENGINE 2
TEMPERATURE, °F
TIME FROM LIFTOFF, hr

Fig. D-6 (contd)

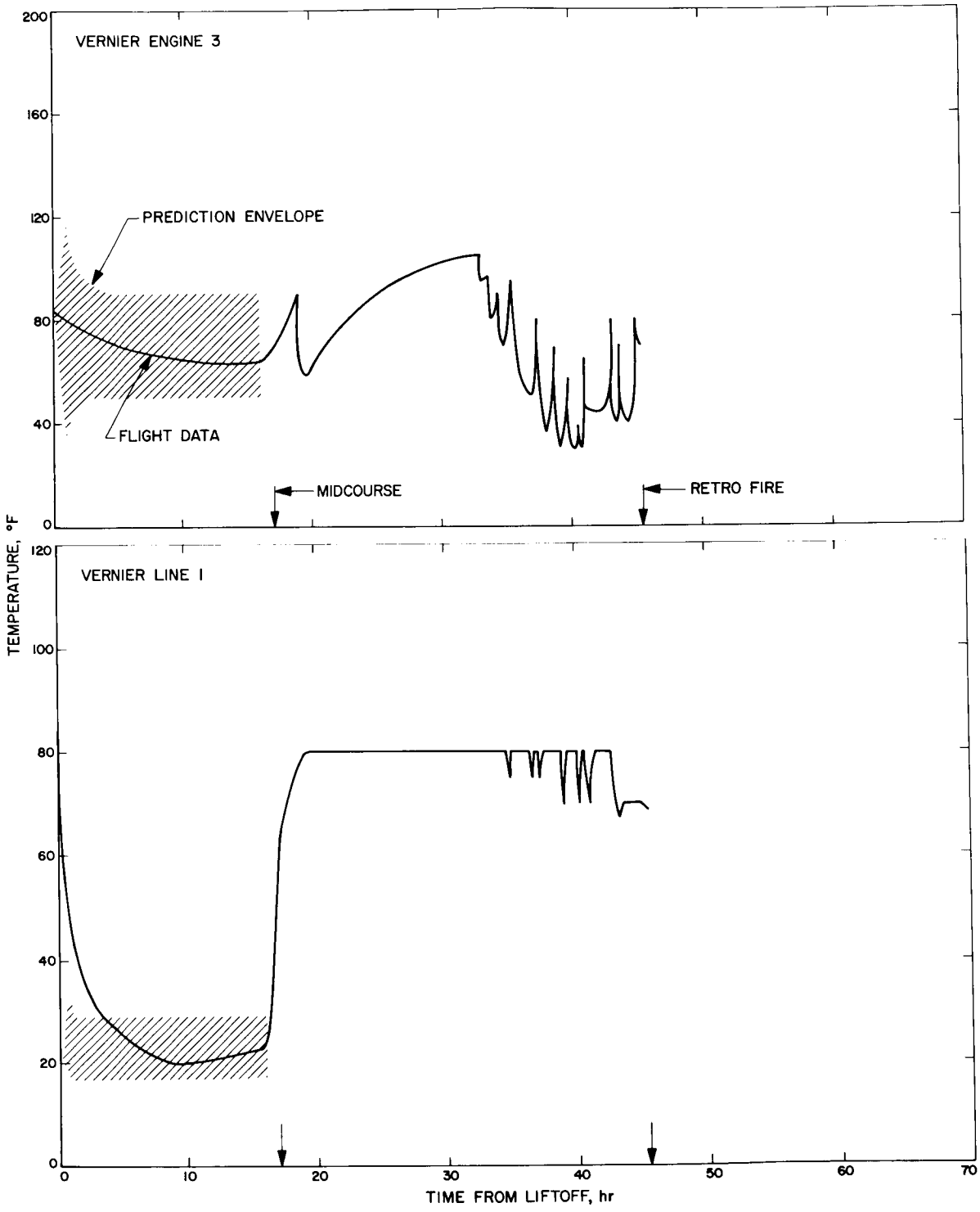
VERNIER ENGINE 3
PREDICTION ENVELOPE
FLIGHT DATA
MIDCOURSE
RETRO FIRE
VERNIER LINE I
TEMPERATURE, °F
TIME FROM LIFTOFF, hr
200
160
120
80
40
0
120
100
80
60
40
20
0
0
10
20
30
40
50
60
70

Fig. D-6 (contd)

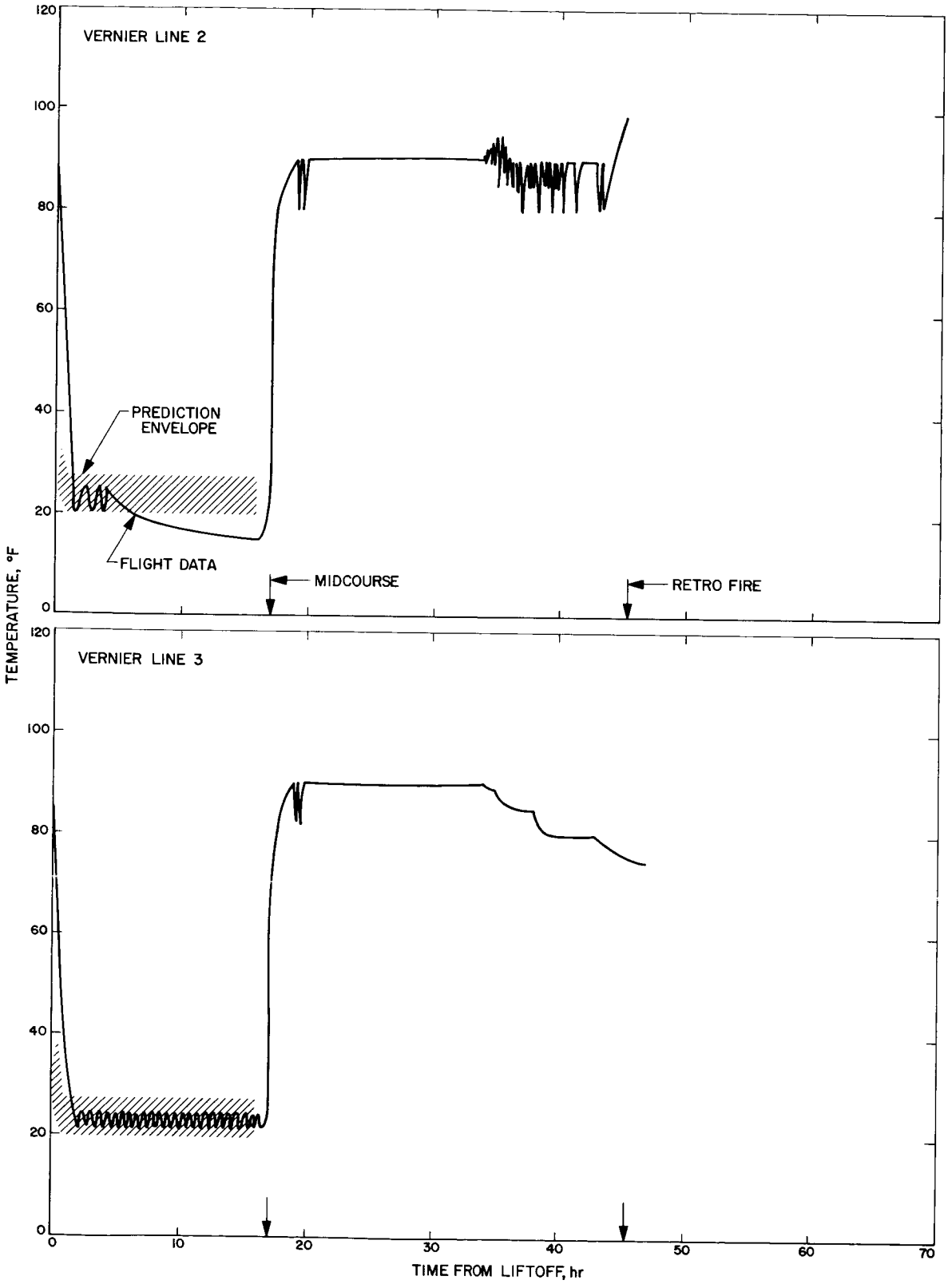
VERNIER LINE 2
VERNIER LINE 3
PREDICTION ENVELOPE
FLIGHT DATA
MIDCOURSE
RETRO FIRE
TEMPERATURE, °F
TIME FROM LIFTOFF, hr
0
20
40
60
80
100
120
0
10
20
30
40
50
60
70

Fig. D-6 (contd)

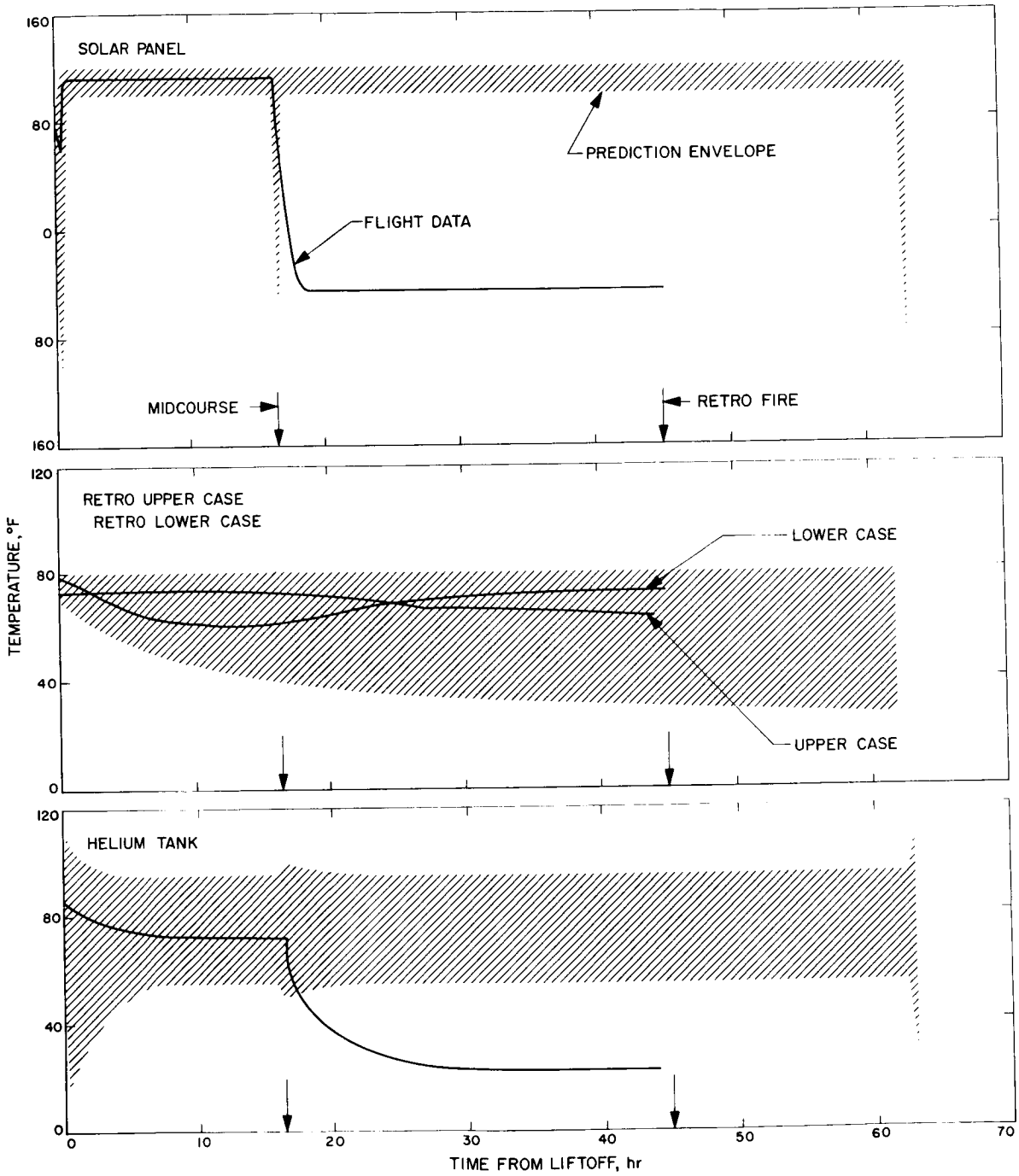

Fig. D-7. Miscellaneous transit temperatures

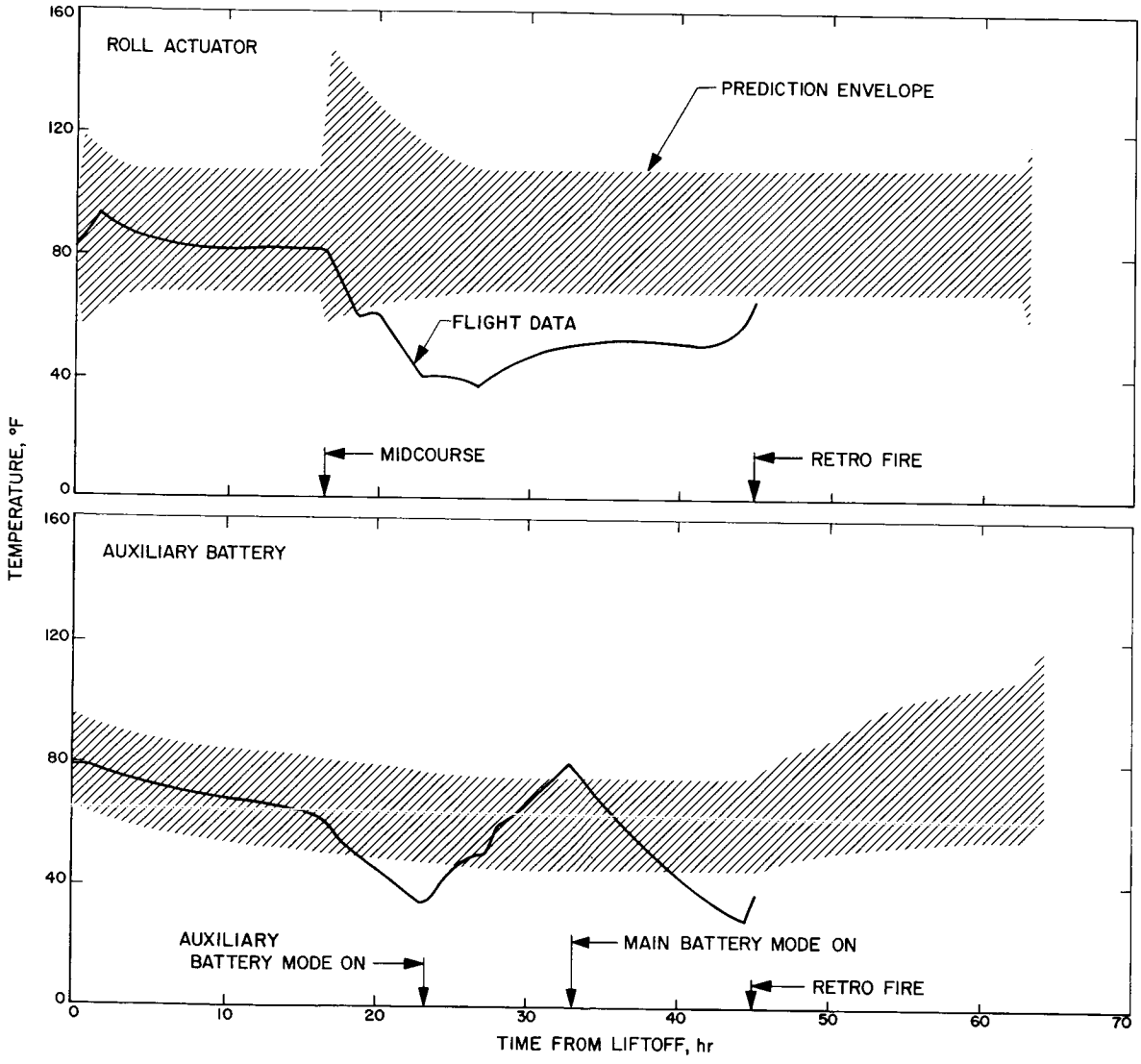
ROLL ACTUATOR
PREDICTION ENVELOPE
FLIGHT DATA
MIDCOURSE
RETRO FIRE
AUXILIARY BATTERY
AUXILIARY BATTERY MODE ON
MAIN BATTERY MODE ON
RETRO FIRE
TEMPERATURE, °F
TIME FROM LIFTOFF, hr
160
120
80
40
0
0
10
20
30
40
50
60
70

Fig. D-7 (contd)

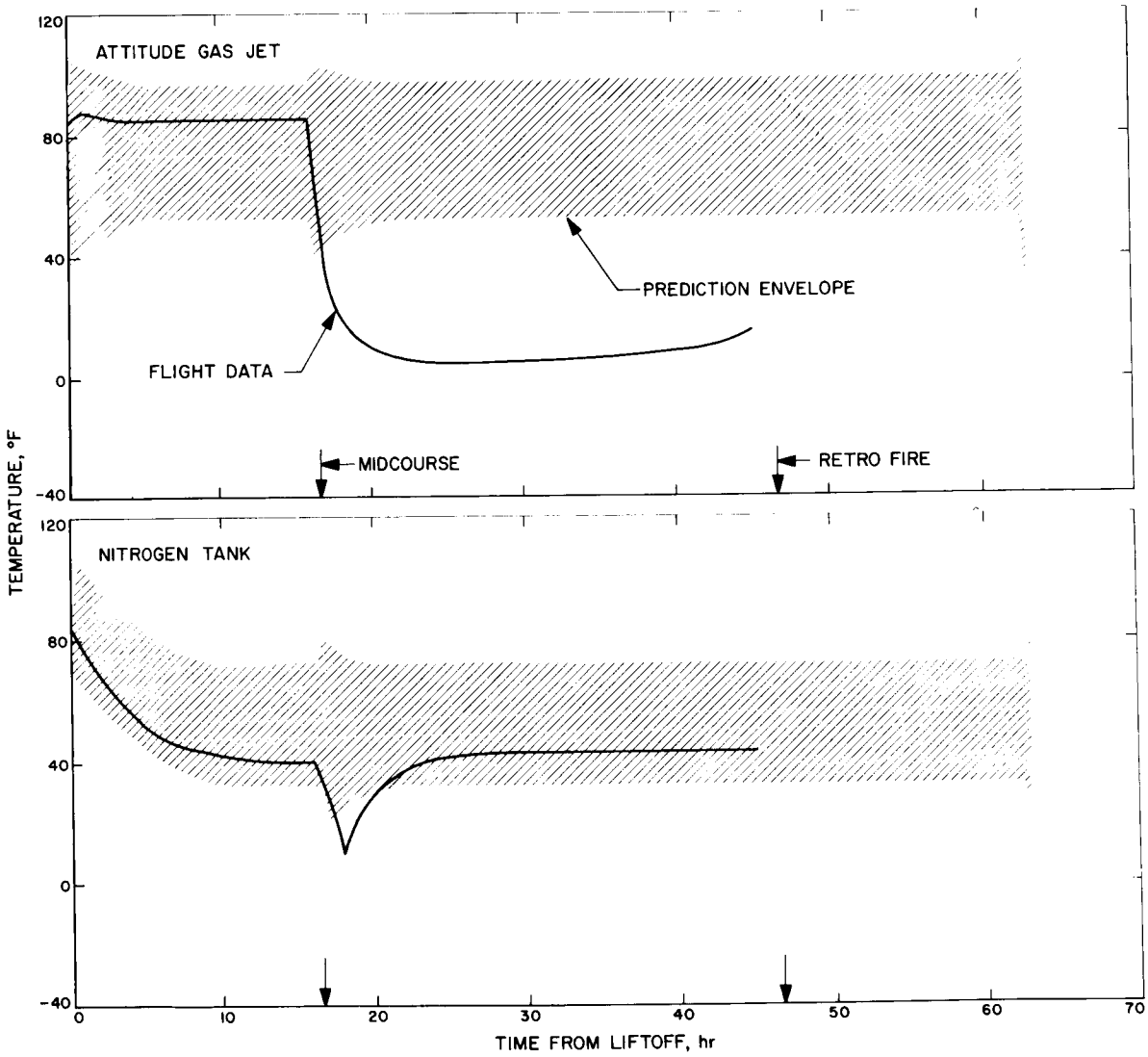
ATTITUDE GAS JET
PREDICTION ENVELOPE
FLIGHT DATA
MIDCOURSE
RETRO FIRE
NITROGEN TANK
TEMPERATURE, °F
TIME FROM LIFTOFF, hr
120
80
40
0
-40
0
10
20
30
40
50
60
70

Fig. D-7 (contd)

Glossary

AC	*Atlas/Centaur*
A/D	analog-to-digital
AESP	auxiliary engine signal processor
AFC	automatic frequency control
AFETR	Air Force Eastern Test Range
AGE	aerospace ground equipment
APC	automatic phase control
A/SPP	antenna and solar panel positioner
BCD	binary coded digital
BECO	booster engine cutoff
BR	boost regulator
CCC	Central Computing Complex
CDC	command and data (handling) console
CDS	computer data system
CP	Command Preparation (Group)
CRT	Composite Readiness Test
CSP	central signal processor
CSTS	Combined Systems Test Stand
DC	direct command
DOD	Department of Defense
DPS	Data Processing System
DSCC	Deep Space Communications Complex
DSIF	Deep Space Instrumentation Facility
DSS	Deep Space Station
DVS	doppler velocity sensor
ECPO	Engineering Computer Program Operations (Group)
EMA	engineering mechanism auxiliary
ESF	Explosive Safe Facility
ESP	engineering signal processor
FC	flight control
FCSG	Flight Control Sensor Group
FPAC	Flight Path Analysis and Command
FRB	Failure Review Board
FRT	fine resolution tracking
GCS	Ground Communication System
GSE	ground support equipment
GSFC	Goddard Space Flight Center
HSDL	high-speed data line
ICS	Intracommunications System
I/O	input/output
IRV	interrange vector
J-FACT	Joint Flight Acceptance Composite Test
KPSM	klystron power supply modulator
KSC	Kennedy Space Center
LOS	loss of signal
MAG	Maneuver Analysis Group
MCDR	media conversion data recovery (subsystem)
MCFR	media conversion film recorder (subsystem)
MECO	main engine cutoff
MEIG	main engine ignition
MSFN	Manned Space Flight Network
NASCOM	NASA World-Wide Communication Network
ODG	Orbit Determination Group
ORT	Operational Readiness Test
OSDP	on-site data processing
OSDR	on-site data recovery (subsystem)
OSFR	on-site film recorder (subsystem)
OTC	overload trip circuit
OVCS	operational voice communication system
PA	Performance Analysis (Group)
PCM	pulse code modulation
PU	propellant utilization
PVT	Performance Verification Tests
QC	quantitative command
RETMA	Radio Electronics Television Manufacturing Association
RFI	radio frequency interference
RIS	range instrumentation ship
RTCS	real-time computer system
SDC	signal data converter

Glossary (contd)

SECO	sustainer engine cutoff
SFOD	Space Flight Operations Director
SFOF	Space Flight Operations Facility
SOCP	*Surveyor* on-site computer program
SOPM	standard orbital parameter message
SOV	solenoid-operated valves
SRT	System Readiness Test
SCAT	Spacecraft Analysis Team
SPAC	Spacecraft Performance Analysis and Command (Group)
SSAC	Space Science Analysis and Command
SSD	subsystem decoder
SSE	Standard Sequence of Events
STEA	system test equipment assembly
STV	solar-thermal-vacuum
TDA	Tracking Data Analysis (Group)
T&DA	tracking and data acquisition
TelPAC	Television Performance Analysis and Command (Group)
TPS	telemetry processing system
TSAC	Television Science Analysis and Command (Group)
TTY	teletype
TV-GDHS	TV Ground Data Handling System
VECO	vernier engine cutoff
VPS	vernier propulsion system

Bibliography

Project and Mission

Surveyor A-G Project Development Plan, Project Document 13, Vol. 1, Jet Propulsion Laboratory, Pasadena, January 3, 1966.

Clarke, V. C., Jr., *Surveyor Project Objectives and Flight Objectives for Missions A through D*, Project Document 34, Jet Propulsion Laboratory, Pasadena, March 15, 1965.

Parks, R. J., *Flight Objectives for Surveyor Mission B*, Interoffice Memorandum MA&E 66-122, Jet Propulsion Laboratory, Pasadena, July 21, 1966.

"*Surveyor B* Post-flight Review Meeting," minutes of meeting held at JPL October 5, 1966.

"Space Exploration Programs and Space Sciences," *Space Programs Summary No. 37-42*, Vol. VI, for the period September 1 to October 31, 1966, Jet Propulsion Laboratory, Pasadena, November 30, 1966.

Surveyor I Mission Report. Part I. Mission Description and Performance, Technical Report 32-1023, Jet Propulsion Laboratory, Pasadena, August 31, 1966.

Launch Operations

Macomber, H. L., *Surveyor Block I Launch Constraints Document*, Project Document 43, Jet Propulsion Laboratory, Pasadena, June 11, 1965.

Macomber, H. L., and O'Neil, W. J., *Surveyor Launch Constraints Mission B–September 1966 Launch Opportunity*, Project Document 43, Addendum No. 2, Jet Propulsion Laboratory, Pasadena, September 13, 1966.

Macomber, H. L., *Surveyor A-G Mission Operations Plan (Launch Operations Phase) Mission A*, Project Document 58, Jet Propulsion Laboratory, Pasadena, May 16, 1966.

Centaur Unified Test Plan AC-7/SC-2 Launch Operations and Flight Plan (Surveyor Mission B), Section 8.7, Report AY62-0047, Rev. B, General Dynamics/Convair, San Diego, September 30, 1966.

Test Procedure Centaur/Surveyor Launch Countdown Operations AC-7/SC-2 Launch (CTP-INT-0004K), Report AA63-0500-004-03K, General Dynamics/Convair, San Diego, September 6, 1966.

Barnum, P. W., *JPL ETR Field Station Launch Operations Plan, Surveyor Mission B*, Engineering Planning Document 423, Jet Propulsion Laboratory, Pasadena, July 27, 1966.

Surveyor Mission B Centaur-7 Operations Summary, TR-432, *Centaur* Operations Branch, KSC/ULO, Cape Kennedy, September 12, 1966.

Surveyor B (AC-7) Flash Flight Report, Report TR-438, *Centaur* Operations Branch, KSC/ULO, Cape Kennedy, September 23, 1966.

Bibliography (contd)

Launch Vehicle System

Galleher, V. R., and Shaffer, J., Jr., *Surveyor Spacecraft/Launch Vehicle Interface Requirements*, Project Document 1, Rev. 2, Jet Propulsion Laboratory, Pasadena, December 14, 1965.

Atlas Space Launch Vehicle Familiarization Handbook, Report GD/C-BGJ66-002, General Dynamics/Convair, San Diego, February 15, 1966.

Centaur Technical Handbook, Convair Division, Report GD/C-BPM64-001-1, Rev. B, General Dynamics/Convair, San Diego, January 24, 1966.

Centaur Monthly Configuration, Performance and Weight Status Report, Report GDC63-0495-41, General Dynamics/Convair, San Diego, October 21, 1966.

Preliminary AC-7 Atlas-Centaur Flight Evaluation, (by staff of Lewis Research Center, Cleveland, Ohio), NASA Technical Memorandum X-52243, NASA, Washington, D.C., 1966.

Spacecraft System

Surveyor Spacecraft A-21 Functional Description, Document 239524 (HAC Pub. 70-93401), 3 Vols., Hughes Aircraft Co., El Segundo, Calif., November 1, 1964 (with revision sheets).

Surveyor Spacecraft A-21 Model Description, Document 224847B, Hughes Aircraft Co., El Segundo, Calif., March 1, 1965 (with revision sheets).

Surveyor Spacecraft Monthly Performance Assessment Report, SSD 68202R, Hughes Aircraft Co., El Segundo, Calif., September 21, 1966.

Surveyor Spacecraft System–Bimonthly Progress Report, mid-August through mid-October 1966, SSD 68218R, Hughes Aircraft Co., El Segundo, Calif., October 24, 1966.

Surveyor II Flight Performance Final Report, SSD 68189-2R, Hughes Aircraft Co., El Segundo, Calif., January 1967.

Tracking and Data Acquisition

Program Requirements Document No. 3400, Surveyor, Revision 10, Air Force Eastern Test Range, Patrick Air Force Base, Fla., July 22, 1966.

Operations Requirement 3400, Surveyor Launch, Revision 3, Air Force Eastern Test Range, Patrick Air Force Base, Fla., August 26, 1966.

Operations Directive 3400, Surveyor Launch, Revision 3, Air Force Eastern Test Range, Patrick Air Force Base, Fla., September 1, 1966.

Project Surveyor–Support Instrumentation Requirements Document, Revision 1, prepared by JPL for NASA, September 9, 1966.

Surveyor Project/Deep Space Network Interface Agreement, Engineering Planning Document 260, Rev. 2, Jet Propulsion Laboratory, Pasadena, November 22, 1965.

Bibliography (contd)

Tracking and Data Acquisition (contd)

DSIF Tracking Instruction Manual (TIM), Surveyor Mission B, (4 volumes), Engineering Planning Document 391, Jet Propulsion Laboratory, Pasadena, August 1966.

Tracking and Data-Acquisition System Pre-Flight and Post-Flight Review Surveyor Mission B, Engineering Planning Document 438, Jet Propulsion Laboratory, Pasadena, December 12, 1966.

Mission Operations System

Surveyor Mission Operations System, Technical Memorandum 33-264, Jet Propulsion Laboratory, Pasadena, April 4, 1966.

Space Flight Operations Plan–Surveyor Mission B, Engineering Planning Document 180-S/MB, Jet Propulsion Laboratory, Pasadena, August 4, 1966 (and revision sheets through September 16, 1966).

Final Report–Surveyor SC-2/Mission Operations System Compatibility Test, Engineering Planning Document 436, Jet Propulsion Laboratory, Pasadena, September 1966.

Surveyor Mission B Space Flight Operations Report, Report SSD 64257R (2 volumes), Hughes Aircraft Company, El Segundo, Calif., November 1966.

Flight Path

Surveyor Spacecraft/Launch Vehicle Guidance and Trajectory Interface Schedule, Project Document 14, Rev. 2, Jet Propulsion Laboratory, Pasadena, August 13, 1965.

"Design Specification–Performance Ground Rules and Launch Periods–*Surveyor* Mission B," Specification SAO-50504-DSN, Jet Propulsion Laboratory, Pasadena, February 24, 1966.

"Design Specification *Surveyor/Centaur* Target Criteria *Surveyor* Mission A," Specification SAO-50552-DSN-A, Jet Propulsion Laboratory, Pasadena, July 25, 1966.

Surveyor Station View Periods and Trajectory Coordinates–Launch Dates August, September, October, November, December 1966, SSD 68073R, Hughes Aircraft Co., El Segundo, Calif., March 1966.

Cheng, R. K., Meredith, C. M., and Conrad, D. A., "Design Considerations for *Surveyor* Guidance," IDC 2253.2/473, Hughes Aircraft Co., El Segundo, Calif., October 15, 1965.

Fisher, J. N., and Gillett, R. W., *Surveyor Direct Ascent Trajectory Characteristics,* SSD 56028R, Hughes Aircraft Co., El Segundo, Calif., December 1965.

Winkelman, C. H., *Surveyor Mission B Trajectory Design Report,* SSD 64144R, Hughes Aircraft Co., El Segundo, Calif., March 16, 1966.

Pre-Injection Trajectory Characteristics Report AC-7, GDC-BTD66-081, General Dynamics/Convair, San Diego, July 1966.

Bibliography (contd)

Flight Path (contd)

O'Brian, W. G., *Surveyor Mission B Post Injection Standard Trajectories*, SSD 68169R, SSD 68157R (Appendix A to SSD 68169R), and SSD 68184R (Addendum to SSD 68157R), Hughes Aircraft Co., El Segundo, Calif., August 1966.

Ribarich, J. J., *Surveyor Mission A Preflight Maneuver Analysis*, SSD 68163R and SSD 68164R (Appendix A of SSD 68163R), Hughes Aircraft Co., El Segundo, Calif., August 1966.

Davids, L., Meredith, C., and Ribarich, J., *Midcourse and Terminal Guidance Operations Programs*, SSD 4051R, Hughes Aircraft Co., El Segundo, Calif., April 1964.

AC-7 Guidance System Accuracy Analysis, GDC-BKM66-003, General Dynamics/Convair, San Diego, August 31, 1966.

AC-7 Firing Tables Data, September 1966 Launch Opportunity, GD/C-BTD66, General Dynamics/Convair, San Diego, 1966.

Surveyor II Flight Path Analysis and Command Operations Report, SSD 64260R, Hughes Aircraft Co., El Segundo, Calif., November 1, 1966.